ADVANCES IN PATHOGENESIS AND THERAPIES OF GOUT

EDITED BY: Lihua Duan, Ye Yang, Xiaoxia Zhu and Jixin Zhong
PUBLISHED IN: Frontiers in Immunology

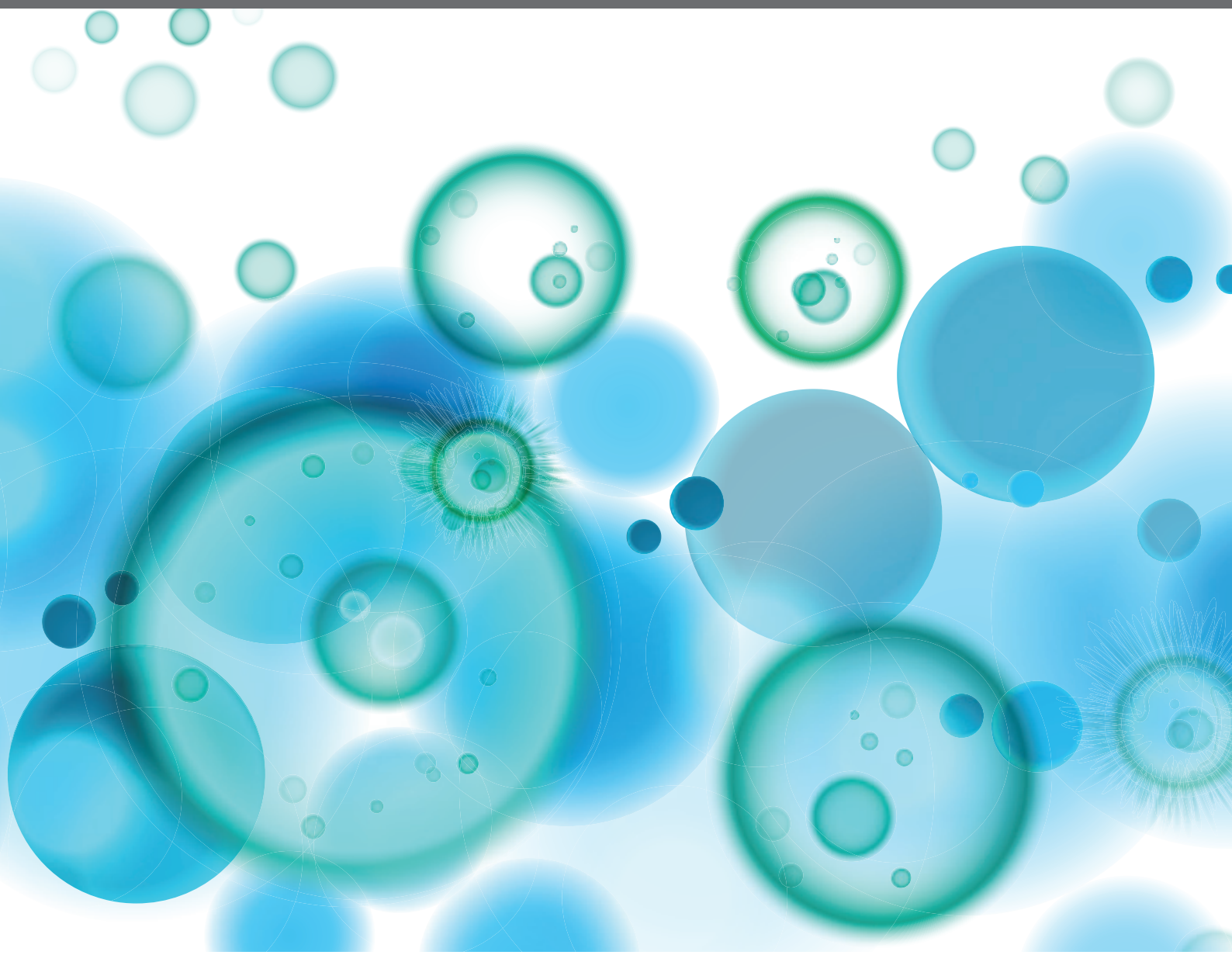

frontiers Research Topics

frontiers

ISSN 1664-8714
ISBN 978-2-88976-002-2
DOI 10.3389/978-2-88976-002-2

About Frontiers

Frontiers is more than just an open-access publisher of scholarly articles: it is a pioneering approach to the world of academia, radically improving the way scholarly research is managed. The grand vision of Frontiers is a world where all people have an equal opportunity to seek, share and generate knowledge. Frontiers provides immediate and permanent online open access to all its publications, but this alone is not enough to realize our grand goals.

Frontiers Journal Series

The Frontiers Journal Series is a multi-tier and interdisciplinary set of open-access, online journals, promising a paradigm shift from the current review, selection and dissemination processes in academic publishing. All Frontiers journals are driven by researchers for researchers; therefore, they constitute a service to the scholarly community. At the same time, the Frontiers Journal Series operates on a revolutionary invention, the tiered publishing system, initially addressing specific communities of scholars, and gradually climbing up to broader public understanding, thus serving the interests of the lay society, too.

Dedication to Quality

Each Frontiers article is a landmark of the highest quality, thanks to genuinely collaborative interactions between authors and review editors, who include some of the world's best academicians. Research must be certified by peers before entering a stream of knowledge that may eventually reach the public - and shape society; therefore, Frontiers only applies the most rigorous and unbiased reviews.
Frontiers revolutionizes research publishing by freely delivering the most outstanding research, evaluated with no bias from both the academic and social point of view. By applying the most advanced information technologies, Frontiers is catapulting scholarly publishing into a new generation.

What are Frontiers Research Topics?

Frontiers Research Topics are very popular trademarks of the Frontiers Journals Series: they are collections of at least ten articles, all centered on a particular subject. With their unique mix of varied contributions from Original Research to Review Articles, Frontiers Research Topics unify the most influential researchers, the latest key findings and historical advances in a hot research area! Find out more on how to host your own Frontiers Research Topic or contribute to one as an author by contacting the Frontiers Editorial Office: frontiersin.org/about/contact

ADVANCES IN PATHOGENESIS AND THERAPIES OF GOUT

Topic Editors:
Lihua Duan, Jiangxi Provincial People's Hospital, China
Ye Yang, University of Florida, United States
Xiaoxia Zhu, Fudan University, China
Jixin Zhong, Huazhong University of Science and Technology, China

Citation: Duan, L., Yang, Y., Zhu, X., Zhong, J., eds. (2022). Advances in Pathogenesis and Therapies of Gout. Lausanne: Frontiers Media SA. doi: 10.3389/978-2-88976-002-2

Table of Contents

frontiers | Frontiers in Immunology

EDITORIAL
published: 01 April 2022
doi: 10.3389/fimmu.2022.890204

Editorial: Advances in Pathogenesis and Therapies of Gout

Lihua Duan[1]*, *Jixin Zhong*[2], *Ye Yang*[3] and *Xiaoxia Zhu*[4]

[1] Department of Rheumatology and Clinical Immunology, Jiangxi Provincial People's Hospital, The First Affiliated Hospital of Nanchang Medical College, Nanchang, China, [2] Department of Rheumatology and Immunology, Tongji Hospital, Tongji Medical College, Huazhong University of Science and Technology, Wuhan, China, [3] Department of Medicine, University of Florida, FL, Gainesville, United States, [4] Division of Rheumatology, Huashan Hospital, Fudan University, Shanghai, China

Keywords: gout, inflammation, inflammasome, hyperuricemia, monosodium urate

Editorial on the Research Topic

Advances in Pathogenesis and Therapies of Gout

Gout is one of the most common metabolic disorders in human caused by inflammatory responses to the deposition of monosodium urate (MSU) crystals, which form in the presence of increased urate concentrations. The pathogenesis of gout is that MSU crystal triggers a strong inflammatory response by activating macrophages in tissues and promoting the collection of neutrophils to tissues or organs (1). It has been reported that many soluble mediators are implicated in the initiation and amplification of the gout flare, including pro-inflammatory cytokines, lipid mediators, and complement (2). However, activation of the NOD-, LRR- and pyrin domain-containing protein 3 (NLRP3) inflammasome by monosodium urate crystals with release of IL-1β plays a major role in the initiation of the gout flare (3). Interestingly, the gout flare is a self-limiting inflammation, and several mechanisms of resolution have been proposed, such as neutrophil extracellular traps (4), negative regulators of inflammasome and TLR signaling, and anti-inflammatory cytokines (5). It is noteworthy that gout is closely related to many comorbidities (6), especially cardiovascular diseases. To further our understanding of inflammatory regulation in the molecular pathophysiology of gout and to explore potential therapeutic approaches, this Research Topic exhibits a number of original research articles and review papers on the topic of advances in pathogenesis and therapies of gout.

In this Research Topic, Zhang et al. investigated the nationwide prevalence of hyperuricemia in China and evaluate its trends and associated risk factors. And significant escalating trends were observed between 2015-16 and 2018-19. Qiu et al. performed a series of bioinformatics analyses to identify molecular mechanisms related to gout, and found that pro-ADM can be used as a new inflammation related biomarker to predict and diagnose gout. Advanced imaging technology enables early gout diagnosis and can be used to evaluate the therapeutic effect. Li et al. summarized the role of ultrasonography, dual-energy computed tomography,and magnetic resonance imaging in the management of gout.

The activation of NLRP3 inflammasome and subsequent induction of the release of IL-1β exerts a central role in the initiation of gout flares. Besides MSU, various purine metabolites bind to different purine receptors for regulating IL-1β secretion implicated in the pathogenesis of gout flares (7). Given that the purine signaling pathway exerts different regulatory effects on inflammation, Tao et al. reviewed the role of purinergic receptor-mediated signaling pathways in the regulation of gout flare and resolution. The possibility that epigenetic mechanisms may contribute to gout pathogenesis offers the potential of a set of completely different therapeutic options (8). Georgel and Georgel reviewed the current mechanistic understanding of several components provided by

OPEN ACCESS

Edited and reviewed by:
Betty Diamond,
Feinstein Institute for Medical Research, United States

***Correspondence:**
Lihua Duan
lh-duan@163.com

Specialty section:
This article was submitted to Autoimmune and Autoinflammatory Disorders, a section of the journal Frontiers in Immunology

Received: *05 March 2022*
Accepted: *09 March 2022*
Published: *01 April 2022*

Citation:
Duan L, Zhong J, Yang Y and Zhu X (2022) Editorial: Advances in Pathogenesis and Therapies of Gout. Front. Immunol. 13:890204. doi: 10.3389/fimmu.2022.890204

food intake that are capable of modulating inflammation through epigenetic modification/reprogramming of innate cells.

Both psoriasis and gout are associated with increased risk of cardiovascular diseases (CVD) (9, 10), Chen et al. reported in this Research Topic that gout augments the risk of CVD independently of traditional risk factors in patients with psoriasis. This finding suggests that the management of gout/hyperuricemia may be beneficial in reducing the risk of developing CVD in patients with Psoriasis.

Galectin-9 (Gal-9) is a modulator of innate and adaptive immunity with both pro- and anti-inflammatory functions, dependent upon its expression and cellular location (11). Using mouse models of gout, Mansour et al. investigated the action of exogenous Gal-9 in MSU-gouty inflammation, which provide a new therapeutic strategy for preventing tissue damage in gouty arthritic inflammation. El Sayed et al. examined the anti-inflammatory mechanism of proteoglycan 4(rhPRG4) in MSU stimulated monocytes by animal model, Their work indicates that rhPRG4 exerts an anti-inflammatory activity in gout PBMCs, mediated by its ability to reduce urate crystal phagocytosis. Si-Miao-San (SMS)is a traditional Chinese medicine that has been reported to relieve the symptoms of gouty arthritis (12). A research by Cao et al. explored the anti-inflammatory mechanism of SMS on gout through animal and cellular experiments. Uric acid is excreted mainly through the kidneys and intestines. A mini review by Yin et al. summarized the effects of intestinal uric acid transporters and intestinal flora on uric acid excretion.

Collectively, the original research and review articles in this Research Topic cover a series of important aspects in the field of inflammatory regulation and clinical management in gout which may provide new insights into the diagnosis and treatment of gout and hyperuricemia.

AUTHOR CONTRIBUTIONS

All authors listed have made a substantial, direct and intellectual contribution to the work, and approved it for publication.

FUNDING

This work was supported by grants from National Natural Science Foundation of China (81960296 and 81871286), Jiangxi Provincial Clinical Research Center for Rheumatic and Immunologic Diseases (20192BCD42005), and Outstanding Innovation Team of Jiangxi Provincial People's Hospital (no. 19-008).

REFERENCES

1. Dalbeth N, Choi HK, Joosten LAB, Khanna PP, Matsuo H, Perez-Ruiz F, et al. Gout. *Nat Rev Dis Primers* (2019) 5:69. doi: 10.1038/s41572-019-0115-y
2. Galozzi P, Bindoli S, Doria A, Oliviero F, Sfriso P. Autoinflammatory Features in Gouty Arthritis. *J Clin Med* (2021) 10(9):1880. doi: 10.3390/jcm10091880
3. Martinon F, Pétrilli V, Mayor A, Tardivel A, Tschopp J. Gout-Associated Uric Acid Crystals Activate the NALP3 Inflammasome. *Nature* (2006) 440:237–41. doi: 10.1038/nature04516
4. Schauer C, Janko C, Munoz LE, Zhao Y, Kienhöfer D, Frey B, et al. Aggregated Neutrophil Extracellular Traps Limit Inflammation by Degrading Cytokines and Chemokines. *Nat Med* (2014) 20:511–7. doi: 10.1038/nm.3547
5. Chen YH, Hsieh SC, Chen WY, Li KJ, Wu CH, Wu PC, et al. Spontaneous Resolution of Acute Gouty Arthritis Is Associated With Rapid Induction of the Anti-Inflammatory Factors Tgfβ1, IL-10 and Soluble TNF Receptors and the Intracellular Cytokine Negative Regulators CIS and SOCS3. *Ann Rheum Dis* (2011) 70:1655–63. doi: 10.1136/ard.2010.145821
6. Li X, Meng X, Timofeeva M, Tzoulaki I, Tsilidis KK, Ioannidis JP, et al. Serum Uric Acid Levels and Multiple Health Outcomes: Umbrella Review of Evidence From Observational Studies, Randomised Controlled Trials, and Mendelian Randomisation Studies. *BMJ* (2017) 357:j2376. doi: 10.1136/bmj.j2376
7. Gicquel T, Le Daré B, Boichot E, Lagente V. Purinergic Receptors: New Targets for the Treatment of Gout and Fibrosis. *Fundam Clin Pharmacol* (2017) 31:136–46. doi: 10.1111/fcp.12256
8. Terkeltaub R. What Makes Gouty Inflammation So Variable? *BMC Med* (2017) 15:158. doi: 10.1186/s12916-017-0922-5
9. Armstrong AW, Read C. Pathophysiology, Clinical Presentation, and Treatment of Psoriasis: A Review. *JAMA* (2020) 323:1945–60. doi: 10.1001/jama.2020.4006
10. Dehlin M, Jacobsson L, Roddy E. Global Epidemiology of Gout: Prevalence, Incidence, Treatment Patterns and Risk Factors. *Nat Rev Rheumatol* (2020) 16:380–90. doi: 10.1038/s41584-020-0441-1
11. Moar P, Tandon R. Galectin-9 as a Biomarker of Disease Severity. *Cell Immunol* (2021) 361:104287. doi: 10.1016/j.cellimm.2021.104287
12. Liu YF, Huang Y, Wen CY, Zhang JJ, Xing GL, Tu SH, et al. The Effects of Modified Simiao Decoction in the Treatment of Gouty Arthritis: A Systematic Review and Meta-Analysis. *Evid Based Complement Alternat Med* (2017) 2017:6037037. doi: 10.1155/2017/6037037

Conflict of Interest: The authors declare that the research was conducted in the absence of any commercial or financial relationships that could be construed as a potential conflict of interest.

frontiers in Immunology

ORIGINAL RESEARCH
published: 15 July 2021
doi: 10.3389/fimmu.2021.703119

Gout Augments the Risk of Cardiovascular Disease in Patients With Psoriasis: A Population-Based Cohort Study

Zhiyong Chen[1], Yiwen Xu[1], Miao Chen[1], Ran Cui[1], Yu-Hsun Wang[2], Sheng-Ming Dai[1] and James Cheng-Chung Wei[3,4,5]**

[1] Department of Rheumatology and Immunology, Shanghai Jiao Tong University Affiliated Sixth People's Hospital, Shanghai, China, [2] Department of Medical Research, Chung Shan Medical University Hospital, Taichung, Taiwan, [3] Institute of Medicine, College of Medicine, Chung Shan Medical University, Taichung, Taiwan, [4] Department of Allergy, Immunology & Rheumatology, Chung Shan Medical University Hospital, Taichung, Taiwan, [5] Graduate Institute of Integrated Medicine, China Medical University, Taichung, Taiwan

OPEN ACCESS

Edited by:
Xiaoxia Zhu,
Fudan University, China

Reviewed by:
José Delgado Alves,
New University of Lisbon, Portugal
Ralf J. Ludwig,
University of Lübeck, Germany

***Correspondence:**
Sheng-Ming Dai
shengmingdai@163.com
James Cheng-Chung Wei
jccwei@gmail.com

Specialty section:
This article was submitted to Autoimmune and Autoinflammatory Disorders, a section of the journal Frontiers in Immunology

Received: *30 April 2021*
Accepted: *28 June 2021*
Published: *15 July 2021*

Citation:
Chen Z, Xu Y, Chen M, Cui R, Wang Y-H, Dai S-M and Wei JC-C (2021) Gout Augments the Risk of Cardiovascular Disease in Patients With Psoriasis: A Population-Based Cohort Study. Front. Immunol. 12:703119. doi: 10.3389/fimmu.2021.703119

Objective: Patients with psoriasis (PsO) have a high frequency of concomitant gout and increased risk of cardiovascular diseases (CVD). We aimed to estimate the synergistic impact of gout on the risk of CVD in patients with PsO.

Methods: A population-based cohort of patients registered in the National Health Insurance Research Database of Taiwan between 2000 and 2013 was stratified according to the presence of PsO and gout. Propensity score analysis was used to match age and gender at a ratio of 1:4. Cox proportional hazard models and subgroup analyses were used to estimate the hazard ratios (HRs) for CVD adjusted for traditional risk factors. The Kaplan–Meier method was used to plot the cumulative incidence curves.

Results: Patients with combined PsO and gout (n = 97), PsO alone (n = 388), gout alone (matched, n = 388) and matched controls (n = 388) were identified. Compared with the patients with PsO alone, the patients with combined PsO and gout had a significantly higher risk of CVD (relative risk 2.39, 95% CI 1.56 to 3.65). After adjustment for traditional risk factors, the risk of CVD was higher in patients with gout alone (HR 2.16, 95% CI 1.54 to 3.04) and in patients with combined PsO and gout (HR 2.72, 95% CI 1.73 to 4.28).

Conclusions: Gout augments the risk of CVD independently of traditional risk factors in patients with PsO.

Keywords: gout, psoriasis, cardiovascular disease, epidemiology, population based cohort study

INTRODUCTION

Psoriasis (PsO) is a common systemic chronic inflammatory disease. It is estimated that approximately 125 million people worldwide have PsO (1). In addition to cutaneous involvement, patients with PsO have an increased prevalence of concomitant psoriatic arthritis (PsA), hyperuricemia, dyslipidemia, hypertension, diabetes, stroke, coronary heart disease, acute

myocardial infarction, obesity and depression (1). A recent study found that the standardized mortality rate of PsO is significantly elevated when compared with the general population, and that circulatory disease is one of the leading causes of death in patients with PsO (2). Gout is one of the most prevalent forms of inflammatory arthritis worldwide. It is generally accepted that gout is caused by hyperuricemia and the deposition of monosodium urate crystals in and around joints (3). Similar to PsO, patients with gout also have high frequencies of hypertension, type 2 diabetes, dyslipidemia, cardiac diseases (including coronary heart disease, heart failure and atrial fibrillation), stroke, chronic kidney disease and obesity (3).

The high prevalence of hyperuricemia and gout in patients with PsO has been documented in several observational studies (4–6) and has been confirmed recently by a large prospective cohort study from the USA, in which Merola et al. found that PsO is associated with an increased risk of subsequent gout, with a multivariate hazard ratio (HR) of 1.71. The risk of gout was substantially increased among those with PsO and concomitant PsA, with an HR of 4.95 when compared with participants without PsO (7). Thus, it is rational to speculate that gout or hyperuricemia may augment the risk of developing cardiovascular diseases (CVD) in patients with PsO. However, to the best of our knowledge, the impact of gout on the incidence of CVD in patients with PsO remains unknown. In particular, it has not been investigated in a large prospective cohort study.

To address this issue, we investigated the association between gout and the incidence of CVD in patients with PsO in a population-based, matched cohort study using the National Health Insurance Research Database (NHIRD) with a population of 1 million and 14 years of follow-up.

PATIENT AND METHODS

Data Sources

This is a population-based prospective cohort study. Data were obtained from NHIRD. The NHIRD enrolls approximately 99% of the 23 million beneficiaries in Taiwan and contains data including diagnoses, drug prescriptions, inpatient care, outpatient visits, emergency hospitalization and diagnoses. The study was approved by the Institutional Review Board of Chung Shan Medical University Hospital.

Study Participants and Matching

As shown in **Figure 1**, the longitudinal health insurance database (LHID) consisting of data from 1 million individuals was compiled from 2000 to 2013. Diagnoses were identified according to the International Classification of Diseases (ICD), Ninth Revision, Clinical Modification (ICD-9-CM) codes. Between January 1, 2000 and December 31, 2002, 2447 patients were diagnosed as having PsO (ICD-9-CM code 696) in the LHID. This code has also been used in previous population-based epidemiologic study of PsO (8). In the general clinical practice in Taiwan, the diagnoses of PsO, gout and CVD were made at least once by the specialist. Among these

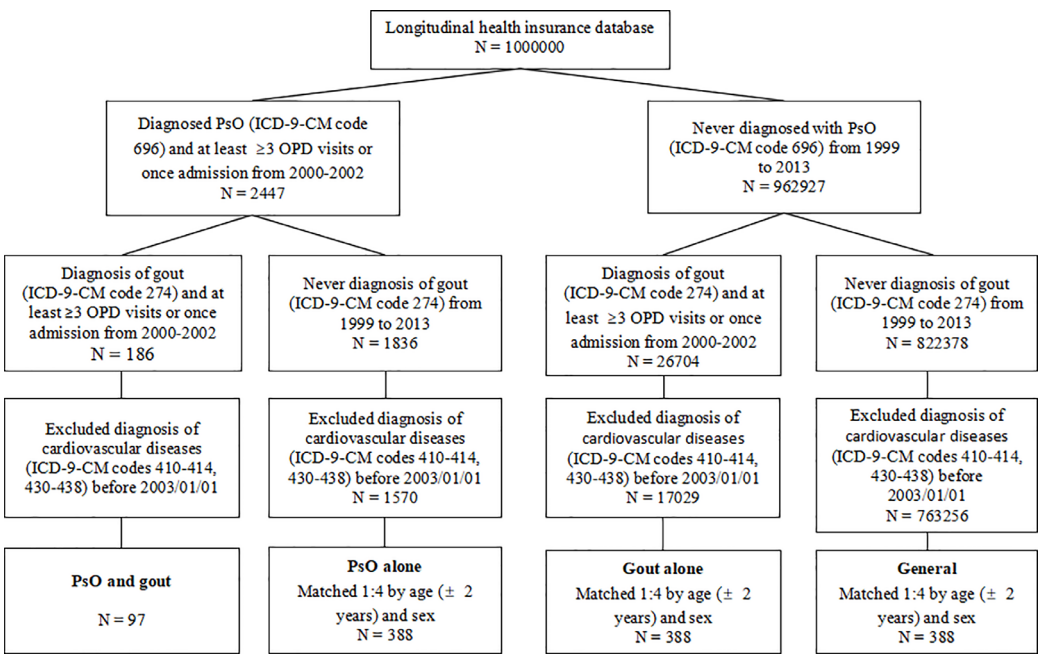

FIGURE 1 | Flow chart of the study design. PsO, psoriasis; OPD, outpatient department; ICD-9-CM, International Classification of Diseases, Ninth Revision, Clinical Modification.

patients, 186 were diagnosed as having gout (ICD-9-CM code 274). Patients receiving at least three outpatient visits or one hospitalization were considered as having PsO and gout. The index date was set as January 1, 2003. Patients diagnosed as having CVD (ICD-9-CM code 410 to 414 for ischemic heart diseases; 430 to 438 for cerebrovascular diseases) before the index date were excluded. Finally, 97 patients were included in the group of patients with combined PsO and gout. Follow-up started on the index date and ended at CVD occurrence, the date of withdrawal from the national insurance system or the end of the study (December 31, 2013). New cases of CVD were identified from the database using the records of ICD-9-CM codes mentioned above, with at least three outpatient visits or one hospitalization.

In each group of patients with PsO alone, patients with gout alone, and the general population (persons without PsO or gout), 388 individuals were matched for sex and age (± 2 years) at the index date to minimize potential confounding effects.

Covariates

The following comorbidities and medications were included in the multivariate analysis to identify the independent risk factors for the incidence of CVD: hypertension (ICD-9-CM codes 401 to 405); hyperlipidemia (ICD-9-CM codes 272.0 to 272.4); chronic liver diseases (ICD-9-CM code 571); chronic kidney diseases (ICD-9-CM code 585); diabetes (ICD-9-CM code 250); chronic obstructive pulmonary diseases (COPD; including ICD9-CM code 491 for chronic bronchitis, ICD-9-CM code 492 for emphysema, ICD-9-CM code 496 for chronic airway obstruction, not elsewhere classified); autoimmune diseases (including ICD-9-CM code 710 for diffuse diseases of connective tissue, ICD-9-CM code 714 for rheumatoid arthritis and other inflammatory polyarthropathies, ICD-9-CM code 720 for ankylosing spondylitis and other inflammatory spondylopathies); arrhythmia (ICD-9-CM codes 426 to 427); and the use of aspirin (defined as at least 30 days of use during the study period). The comorbidities were defined as those receiving a diagnosis within three years before the index date and associated with at least three outpatient visits or one hospitalization.

Statistical Analysis

The chi-square or Fisher exact test for categorical variables and Student's *t*-test for continuous variables were used to compare the demographic data between groups. A Kaplan–Meier analysis was performed to assess the cumulative incidence of CVD and a log-rank test was used to test the significance. A Cox proportional hazard model was used to estimate the HR for CVD between groups. A p-value < 0.05 was considered statistically significant. Analyses were performed using SPSS software (version 18.0; SPSS Inc., Chicago, IL, USA).

RESULTS

Compared with general population, participants with PsO alone, with gout alone, and with combined PsO and gout had higher prevalence of hypertension, hyperlipidemia, chronic liver diseases, chronic kidney diseases, diabetes, COPD, autoimmune diseases, arrhythmia and aspirin use (**Table 1**).

The number of patients who developed CVD during the follow-up period is shown in **Table 2**. The incidence density (ID) was 14.83 (95% confidence interval (CI) 11.41 to 19.27) per 1,000 person–years (PY) in the general population, and the patients with gout alone had a 2-fold increased ID compared with patients with PsO alone (36.3/1,000 PY and 18/1,000 PY, respectively). The patients with combined PsO and gout had the highest ID (42.99/1,000 PY; 95% CI 30.40 to 60.80). Using the general population as a reference, the relative risk (RR) of the development of CVD was 2.44 (95% CI 1.78 to 3.36) in patients with gout alone and 2.90 (95% CI 1.88 to 4.48) in patients with combined PsO and gout. In comparison with patients with PsO alone, the combination of PsO and gout was associated with a 239% increase in the relative risk of CVD.

TABLE 1 | Baseline characteristics of the study population according to the history of psoriasis and gout.

	General (n = 388)	Gout alone (n = 388)	PsO alone (n = 388)	PsO and gout (n = 97)
Age				
<40 years, n (%)	116 (29.9)	91 (23.5)	96 (24.7)	25 (25.8)
40-64 years, n (%)	200 (51.5)	222 (57.2)	216 (55.7)	54 (55.7)
≥65 years, n (%)	72 (18.6)	75 (19.3)	76 (19.6)	18 (18.6)
Mean ± SD	49.2 ± 15.5	50.6 ± 14.9	50.1 ± 15.5	50.3 ± 15.5
Sex				
Female, n (%)	32 (8.2)	32 (8.2)	32 (8.2)	8 (8.2)
Male, n (%)	356 (91.8)	356 (91.8)	356 (91.8)	89 (91.8)
Hypertension, n (%)	28 (7.2)	110 (28.4)	54 (13.9)	31 (32.0)
Hyperlipidemia, n (%)	7 (1.8)	70 (18.0)	19 (4.9)	20 (20.6)
Chronic liver diseases, n (%)	19 (4.9)	69 (17.8)	44 (11.3)	22 (22.7)
Chronic kidney diseases, n (%)	0 (0.0)	11 (2.8)	1 (0.3)	3 (3.1)
Diabetes, n (%)	15 (3.9)	53 (13.7)	29 (7.5)	12 (12.4)
COPD, n (%)	10 (2.6)	27 (7.0)	24 (6.2)	7 (7.2)
Autoimmune diseases, n (%)	1 (0.3)	17 (4.4)	11 (2.8)	11 (11.3)
Arrhythmia, n (%)	2 (0.5)	14 (3.6)	5 (1.3)	0 (0.0)
Aspirin use, n (%)	21 (5.4)	51 (13.1)	25 (6.4)	15 (15.5)

COPD, Chronic obstructive pulmonary diseases; PsO, psoriasis.

TABLE 2 | Incidence density of cardiovascular diseases among different groups.

	Patients	Person-years	Patients with cardiovascular diseases	ID (95% CI)	Relative risk (95% CI)	
General	388	3775	56	14.83 (11.41 to 19.27)	Reference	
Gout alone	388	3254	118	36.26 (30.28 to 43.43)	2.44 (1.78 to 3.36)	
Pso	485	4296	96	22.34 (18.29 to 27.29)	1.51 (1.08 to 2.09)	
PsO alone	388	3552	64	18.02 (14.10 to 23.02)	1.21 (0.85 to 1.74)	Reference
PsO and gout	97	744	32	42.99 (30.40 to 60.80)	2.90 (1.88 to 4.48)	2.39 (1.56 to 3.65)

ID, incidence density (per 1,000 person–years); CI, confidence interval; PsO, psoriasis.

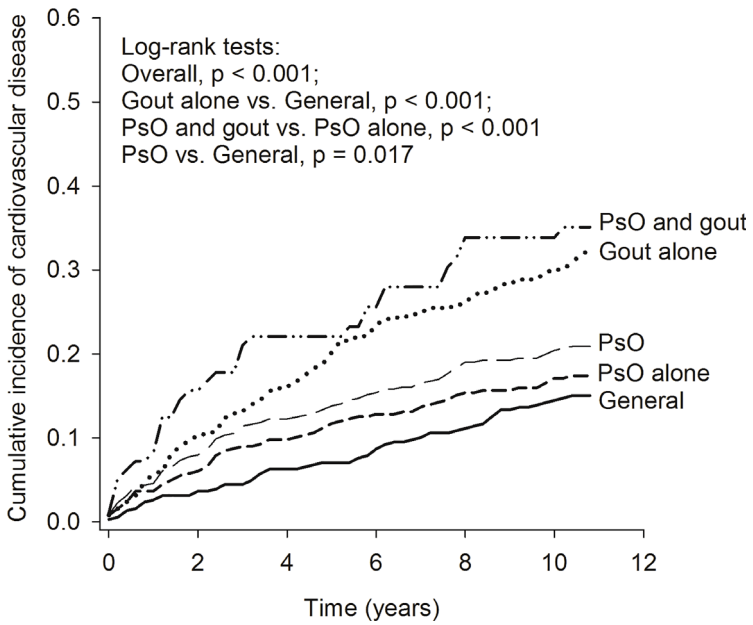

FIGURE 2 | Kaplan–Meier curve of cumulative incidence of cardiovascular diseases in the study groups. PsO, psoriasis.

The Kaplan–Meier curves (**Figure 2**) revealed that the cumulative incidence of CVD increased gradually in the general population, in patients with PsO alone, in patients with PsO (with or without gout), in patients with gout alone, and in patients with combined PsO and gout (log-rank test, overall $p < 0.001$). The risk of CVD in patients with PsO alone tended to be increased but there was no significant difference compared with the general population. The cumulative incidence of CVD was significantly higher in patients with PsO (with or without gout) and in patients with gout alone than in the general population ($p = 0.017$ and $p < 0.001$, respectively). Moreover, the cumulative incidence of CVD in patients with combined PsO and gout was greatly increased when compared with patients with PsO alone ($p < 0.001$).

In the Cox proportional hazard model, the multivariate-adjusted HRs for CVD were increased, ranging from 1.15 (PsO alone) to 2.72 (PsO and gout). The multivariate adjusted HR appeared to be higher among patients aged 40–64 years (HR = 2.80; 95% CI 1.82 to 4.30) and among patients aged ≥ 65 years (HR = 5.68; 95% CI 3.55 to 9.07) than among patients aged 39 years or younger. The presence of hypertension (HR = 1.93; 95% CI 1.45 to 2.58) and COPD (HR = 1.61; 95% CI 1.06 to 2.45) were also associated with increased risk of CVD (**Table 3**).

We further performed a subgroup analysis stratified by age and sex to investigate the impact of the presence of concomitant gout on the incidence of CVD in patients with PsO (**Table 4**). The HRs were adjusted for age, gender, hypertension, hyperlipidemia, chronic liver diseases, chronic kidney diseases, diabetes, COPD, autoimmune diseases, arrhythmia, and aspirin use. In the subgroup of age < 65 years, the patients with gout alone (aHR = 1.99; 95% CI 1.31 to 3.01) and patients with combined PsO and gout (aHR = 2.85; 95% CI 1.66 to 4.88) had a significantly higher risk of CVD than the general population. In the subgroup of age ≥ 65 years, patients with gout alone (aHR = 2.73; 95% CI 1.45 to 5.13) and patients with PsO alone (aHR = 2.00; 95% CI 1.10 to 3.64) had a higher risk of CVD than the general population. Among women, a higher risk of CVD was observed in patients with gout alone (aHR = 6.16; 95% CI 1.56 to 24.39) and in patients with PsO alone (aHR = 3.99; 95% CI 1.16 to 13.69). Among men, we also observed a significantly higher risk of CVD in patients with gout alone (aHR = 2.12; 95% CI 1.49

TABLE 3 | Cox proportional hazard model analysis for risk of cardiovascular diseases.

	Univariate		Multivariate†	
	HR (95% CI)	***p* value**	**HR (95% CI)**	***p* value**
Group				
General	Reference		Reference	
Gout alone	2.40 (1.74 to 3.29)	<0.001	2.16 (1.54 to 3.04)	<0.001
PsO alone	1.21 (0.84 to 1.73)	0.299	1.15 (0.80 to 1.65)	0.462
PsO and gout	2.81 (1.82 to 4.34)	<0.001	2.72 (1.73 to 4.28)	<0.001
Age				
<40	Reference		Reference	
40 to 64	3.17 (2.08 to 4.84)	<0.001	2.80 (1.82 to 4.30)	<0.001
≥65	7.43 (4.77 to 11.56)	<0.001	5.68 (3.55 to 9.07)	<0.001
Sex				
Female	Reference		Reference	
Male	0.89 (0.59 to 1.35)	0.588	0.79 (0.52 to 1.21)	0.280
Hypertension	3.25 (2.52 to 4.18)	<0.001	1.93 (1.45 to 2.58)	<0.001
Hyperlipidemia	1.37 (0.95 to 1.98)	0.095	0.70 (0.47 to 1.04)	0.074
Chronic liver diseases	1.03 (0.72 to -1.48)	0.874	0.88 (0.60 to 1.28)	0.495
Chronic kidney diseases	3.01 (1.34 to 6.76)	0.008	1.31 (0.57 to 3.04)	0.523
Diabetes	2.29 (1.65 to 3.19)	<0.001	1.34 (0.95 to 1.90)	0.096
COPD	2.97 (2.00 to 4.39)	<0.001	1.61 (1.06 to 2.45)	0.026
Autoimmune diseases	1.16 (0.60 to 2.26)	0.659	0.77 (0.39 to 1.51)	0.445
Arrhythmia	2.95 (1.52 to 5.74)	0.001	1.22 (0.60 to 2.48)	0.587
Aspirin use	1.60 (1.13 to 2.28)	0.008	0.78 (0.53 to 1.14)	0.204

HR, hazard ratio; COPD, Chronic obstructive pulmonary diseases; PsO, psoriasis.

†Adjusted for age, sex, hypertension, hyperlipidemia, chronic liver diseases, chronic kidney diseases, diabetes, COPD, autoimmune diseases, arrhythmia and aspirin use.

TABLE 4 | Subgroup analysis of risk for cardiovascular diseases.

	Patients	**Patients with cardiovascular diseases**	**aHR† (95% CI)**	***p* value**
Age < 65				
Group				
General	316	38	Reference	
Gout alone	313	82	1.99 (1.31 to 3.01)	0.001
PsO alone	312	32	0.82 (0.51 to 1.31)	0.400
PsO and gout	79	25	2.85 (1.66 to 4.88)	<0.001
Age ≥ 65				
Group				
General	72	18	Reference	
Gout alone	75	36	2.73 (1.45 to 5.13)	0.002
PsO alone	76	32	2.00 (1.10 to 3.64)	0.023
PsO and gout	18	7	2.23 (0.91 to 5.49)	0.081
Female				
Group				
General	32	4	Reference	
Gout alone	32	11	6.16 (1.56 to 24.39)	0.010
PsO alone	32	10	3.99 (1.16 to 13.69)	0.028
PsO and gout	8	0	NA	NA
Male				
Group				
General	356	52	Reference	
Gout alone	356	107	2.12 (1.49 to 3.03)	<0.001
PsO alone	356	54	1.03 (0.70 to 1.51)	0.894
PsO and gout	89	32	2.96 (1.86 to 4.72)	<0.001

aHR, adjusted hazard ratio; PsO, psoriasis; NA, not applicable.

†Adjusted for age, gender, hypertension, hyperlipidemia, chronic liver diseases, chronic kidney diseases, diabetes, chronic obstructive pulmonary diseases, autoimmune diseases, arrhythmia and aspirin use.

to 3.03) and in patients with combined PsO and gout (aHR = 2.96; 95% CI 1.86 to 4.72) than in the general population. However, the risk of CVD in male patients with PsO alone was comparable with that in the general population.

DISCUSSION

In this prospective, population-based, matched cohort study, we confirmed that the presence of PsO (with or without gout) and

the known risk factors such as age, hypertension and COPD were associated with an increased risk of CVD. The presence of PsO alone increased the risk of CVD in females and individuals aged ≥ 65 years, but not in males or individuals aged < 65. Importantly, we found that the ID for CVD was highest in patients with combined PsO and gout (42.99/1,000 PY). In comparison with patients with PsO alone, the combined presence of PsO and gout was associated with a 239% increase in the relative risk of CVD.

It is well known that PsO is associated with an increased risk of major adverse cardiovascular outcomes such as myocardial infarction (9–12) and stroke (13, 14), and is associated with an increased cardiovascular mortality (15). PsO is also an independent risk factor for coronary artery calcification (16). A high prevalence of metabolic syndrome (MetS) components such as diabetes, hypertension, hyperlipidemia and obesity has been observed in patients with PsO in a previous cross-sectional study (17). These traditional risk factors are generally considered to be the causes of the increased incidence of CVD in patients with PsO. However, the risk of CVD for patients with PsO has not been fully investigated in any large prospective cohort study and has not been analyzed in detail by adjusting for the traditional risk factors in East Asians. In our study, the presence of gout alone was associated with the risk of CVD in all subgroups and in multivariate analyses after adjustment for traditional risk factors. However, the association between the presence of PsO alone and CVD was not statistically significant in multivariate analyses after adjusting for traditional risk factors, and was seen only in females and in individuals aged ≥ 65 years. The discrepancy between the present study and previous studies (9–14) might be explained by the differences in ethnicity, outcomes and confounders included in the analysis. To date, gout or hyperuricemia has not been included in the definition of MetS (18). Our results indicate that there are at least two independent categories of risk factor for CVD in patients with PsO: gout and the components of MetS.

Hyperuricemia is the critical mechanism of the pathogenesis of gout. Various factors can influence serum uric acid (UA) levels, and the serum UA level itself is closely related to conditions such as dyslipidemia, obesity, hypertension, and impaired glucose metabolism, which may contribute to CVD pathophysiology (19). The mechanisms by which hyperuricemia is involved in the pathogenesis of CVD may include but are not limited to the following findings. First, hyperuricemia may induce endothelial dysfunction, which is a key pathophysiological trigger in atherosclerosis. Endothelial cells secrete a number of vasodilators such as nitric oxide, prostaglandin I-2, and endothelium-derived hyperpolarizing factor. It has been found that hyperuricemia can induce human umbilical vein endothelial cell apoptosis and endothelial dysfunction through endothelial nitric oxide synthase (eNOS) phosphorylation and endoplasmic reticulum stress, reducing eNOS activity and nitric oxide production, activating NF-κB, and increasing the levels of inflammatory cytokines (20, 21). It has been suggested that the beneficial effect of allopurinol on CVD may rely more on its ability to reduce oxidative stress than on its impact on urate levels (22). Second, hyperuricemia can increase reactive oxygen species production and inhibit insulin-induced glucose uptake by increasing the phosphorylation of insulin receptor substrate 1 and inhibiting the phosphorylation of Akt. As a result, hyperuricemia can inhibit insulin signaling, induce insulin resistance and accelerate the process of atherosclerosis (23, 24). Third, hyperuricemia may participate in the pathogenesis of CVD by activating the inflammasome pathway. Several studies have shown that UA activates the nod-like receptor protein 3 inflammasome and induces interleukin-1β release in monocytes, macrophages, vascular smooth muscle cells, and endothelial cells (25–28). Other pathogenic roles of UA in CVD may include induction of an imbalance in macrophage M1/M2 polarization (29), HDL dysfunction (30) and increasing the risk of developing high LDL cholesterol and hypertriglyceridemia (31). Several studies have revealed a significant correlation between serum UA levels and increased carotid intima–medial thickness among patients with PsA (32–34).

In the subgroup analyses, we found that the presence of gout alone was associated with increased risk of CVD in all subgroups, with the highest HR (6.16) in females. Although the statistical power may have been insufficient owing to the relatively small number of females, our results suggest a stronger impact of gout/hyperuricemia on the risk of CVD in females than in males. Although the mechanism underlying the impact of gender on the association between UA and CVD remains elusive, our findings are consistent with the previous studies. Fang et al. found that the association between serum uric acid levels and cardiovascular mortality was more robust in women than in men and persisted regardless of traditional cardiovascular risks. They also found that there was no association of serum UA with cardiovascular mortality among men at high traditional cardiovascular risk (35). Hoieggen et al. found also that the association between serum UA and cardiovascular events was stronger in women than in men, with or without adjustment of Framingham risk score (36). An earlier study revealed that an increased serum UA level was an independent predictor of all-cause and heart disease mortality for woman only. Women with a serum UA level of ≥ 416 μmol/L had an almost 5-fold higher risk of ischemic heart disease mortality than those with a level < 238 μmol/L (37).

We found that the presence of COPD was associated with an increased risk of CVD both in univariate analysis (HR = 2.97) and in multivariate analysis (HR = 1.61), which is in line with previous reports. It has been reported that patients with COPD have a 2–3-fold increased risk of CVD compared with age-matched controls after adjustment for tobacco smoking (38). Patients with COPD often have hypoxia during exercise, high resting heart rates, impaired vasodilatory capacity and peripheral, cardiac and neurohumoral sympathetic stress, which may cause CVD. Mechanistically, cytokines involved in the pathogenesis of COPD, such as interferon-γ, interleukin (IL)-1, tumor necrosis factor-α, and IL-6, may contribute to the development of CVD (39). As a well-known risk factor for COPD, smoking is also prevalent in patients with PsO. Our results suggest that the management of COPD and recommendation of smoking cessation may be important for CVD prevention in patients with PsO.

Several guidelines and recommendations for the management of common comorbidities of PsO have been developed (40). However, most of them focus on comorbidities such as MetS, inflammatory bowel disease, psychologic dysfunction and cancer. The management of gout or hyperuricemia is not included in the latest guideline for the care of comorbidities of patients with PsO (41). In addition, a low purine diet was not included in recent dietary recommendations for adults with PsO or PsA (42). A pharmaco-epidemiological study revealed that allopurinol decreased the risk of myocardial infarction by 20% (43). The significant impact of gout on the risk of developing CVD found in the present study strongly suggests that targeted education and therapeutic intervention of gout/hyperuricemia may help to reduce the risk of CVD in patients with PsO, and should be included in the guidelines or recommendations for PsO in the future. Cardiovascular risk is consistently increased in multiple types of arthritis including rheumatoid arthritis, gout, PsA and osteoarthritis (12). Cardiovascular risk algorithms developed for the general population are not accurate in these patients (44, 45). Our study suggests that a PsO specific cardiovascular risk score is needed, in which the presence of gout/hyperuricemia should be included.

The advantages of the present study include that the study involved a population-based prospective design. The large number of participants with a relatively long follow-up period allowed us to perform matching and subgroup analysis to adjust for several possible confounders.

The limitations should also be addressed. First, despite that in the general clinical practice in Taiwan, the diagnoses of PsO, gout and CVD were made at least once by the specialist in LHID, we cannot rule out completely the over- or under-diagnoses of these diseases. Second, owing to the relatively small size of patients with combined PsO and gout, several potential confounding factors such as the use of medications (e.g. allopurinol, statins, anticoagulants and other cardiovascular medications) were not adjusted. Third, laboratory data such as the values of erythrocyte sedimentation rate, C-reactive protein and serum UA were unavailable in the NHIRD. Therefore, the associations between the levels of UA and disease activity of PsO and the risk of CVD could not be investigated in the present study, although it is reported that the association between PsO and metabolic syndrome increases with increasing disease severity of PsO (46). The CVD related life style factors such as smoking, diet preference and body mass index were also not analyzed because of the lack of relevant data.

In summary, our prospective, population-based matched cohort study revealed that concomitant gout is an independent risk factor for CVD in patients with PsO. In addition to control of the traditional CVD risk factors, physicians should consider relevant education and management of gout/hyperuricemia in the care of patients with PsO.

DATA AVAILABILITY STATEMENT

The raw data supporting the conclusions of this article will be made available by the authors, without undue reservation.

ETHICS STATEMENT

The studies involving human participants were reviewed and approved by Chung Shan Medical University Hospital (IRB, CS15134). Written informed consent for participation was not required for this study in accordance with the national legislation and the institutional requirements.

AUTHOR CONTRIBUTIONS

S-MD and JC-CW conceptualized the research. ZC, YX, MC, RC and JC-CW interpreted the data and drafted the manuscript. Y-HW performed data analysis and graph generation and critically revised the manuscript. All authors contributed to the article and approved the submitted version.

REFERENCES

1. Armstrong AW, Read C. Pathophysiology, Clinical Presentation, and Treatment of Psoriasis: A Review. *JAMA* (2020) 323:1945–60. doi: 10.1001/jama.2020.4006
2. Colaco K, Widdifield J, Luo J, Rosen CF, Alhusayen R, Paterson JM, et al. Trends in Mortality and Cause-Specific Mortality Among Patients With Psoriasis and Psoriatic Arthritis in Ontario, Canada. *J Am Acad Dermatol* (2020) S0190-9622:32843–7. doi: 10.1016/j.jaad.2020.10.031
3. Bardin T, Richette P. Impact of Comorbidities on Gout and Hyperuricaemia: An Update on Prevalence and Treatment Options. *BMC Med* (2017) 15:123. doi: 10.1186/s12916-017-0890-9
4. Gisondi P, Targher G, Cagalli A, Girolomoni G. Hyperuricemia in Patients With Chronic Plaque Psoriasis. *J Am Acad Dermatol* (2014) 70:127–30. doi: 10.1016/j.jaad.2013.09.005
5. Kwon HH, Kwon IH, Choi JW, Youn JI. Cross-Sectional Study on the Correlation of Serum Uric Acid With Disease Severity in Korean Patients With Psoriasis. *Clin Exp Dermatol* (2011) 36:473–8. doi: 10.1111/j.1365-2230.2010.03988.x
6. Li X, Miao X, Wang H, Wang Y, Li F, Yang Q, et al. Association of Serum Uric Acid Levels in Psoriasis: A Systematic Review and Meta-Analysis. *Med (Baltimore)* (2016) 95:e3676. doi: 10.1097/MD.0000000000003676
7. Merola JF, Wu S, Han J, Choi HK, Qureshi AA. Psoriasis, Psoriatic Arthritis and Risk of Gout in US Men and Women. *Ann Rheum Dis* (2015) 74:1495–500. doi: 10.1136/annrheumdis-2014-205212
8. Tollefson MM, Crowson CS, McEvoy MT, Maradit Kremers H. Incidence of Psoriasis in Children: A Population-Based Study. *J Am Acad Dermatol* (2010) 62:979–87. doi: 10.1016/j.jaad.2009.07.029
9. Gelfand JM, Neimann AL, Shin DB, Wang X, Margolis DJ, Troxel AB. Risk of Myocardial Infarction in Patients With Psoriasis. *JAMA* (2006) 296:1735–41. doi: 10.1001/jama.296.14.1735
10. Lin HW, Wang KH, Lin HC, Lin HC. Increased Risk of Acute Myocardial Infarction in Patients With Psoriasis: A 5-Year Population-Based Study in Taiwan. *J Am Acad Dermatol* (2011) 64:495–501. doi: 10.1016/j.jaad.2010.01.050
11. Ahlehoff O, Gislason GH, Charlot M, Jørgensen CH, Lindhardsen J, Olesen JB, et al. Psoriasis Is Associated With Clinically Significant Cardiovascular Risk: A Danish Nationwide Cohort Study. *J Intern Med* (2011) 270:147–57. doi: 10.1111/j.1365-2796.2010.02310.x
12. Schieir O, Tosevski C, Glazier RH, Hogg–Johnson S, Badley EM. Incident Myocardial Infarction Associated With Major Types of Arthritis in the General Population: A Systematic Review and Meta-Analysis. *Ann Rheum Dis* (2017) 76:1396–404. doi: 10.1136/annrheumdis-2016-210275

13. Gelfand JM, Dommasch ED, Shin DB, Azfar RS, Kurd SK, Wang X, et al. The Risk of Stroke in Patients With Psoriasis. *J Invest Dermatol* (2009) 129:2411–8. doi: 10.1038/jid.2009.112
14. Ahlehoff O, Gislason GH, Jorgensen CH, Lindhardsen J, Charlot M, Olesen JB, et al. Psoriasis and Risk of Atrial Fibrillation and Ischaemic Stroke: A Danish Nationwide Cohort Study. *Eur Heart J* (2012) 33:2054–64. doi: 10.1093/eurheartj/ehr285
15. Mehta NN, Azfar RS, Shin DB, Neimann AL, Troxel AB, Gelfand JM. Patients With Severe Psoriasis Are at Increased Risk of Cardiovascular Mortality: Cohort Study Using the General Practice Research Database. *Eur Heart J* (2010) 31:1000–6. doi: 10.1093/eurheartj/ehp567
16. Ludwig RJ, Herzog C, Rostock A, Ochsendorf FR, Zollner TM, Thaci D, et al. Psoriasis: A Possible Risk Factor for Development of Coronary Artery Calcification. *Br J Dermatol* (2007) 156:271–6. doi: 10.1111/j.1365-2133.2006.07562.x
17. Neimann AL, Shin DB, Wang X, Margolis DJ, Troxel AB, Gelfand JM. Prevalence of Cardiovascular Risk Factors in Patients With Psoriasis. *J Am Acad Dermatol* (2006) 55:829–35. doi: 10.1016/j.jaad.2006.08.040
18. Kassi E, Pervanidou P, Kaltsas G, Chrousos G. Metabolic Syndrome: Definitions and Controversies. *BMC Med* (2011) 9:48. doi: 10.1186/1741-7015-9-48
19. Wu AH, Gladden JD, Ahmed M, Ahmed A, Filippatos G. Relation of Serum Uric Acid to Cardiovascular Disease. *Int J Cardiol* (2016) 213:4–7. doi: 10.1016/j.ijcard.2015.08.110
20. Cai W, Duan XM, Liu Y, Yu J, Tang YL, Liu ZL, et al. Uric Acid Induces Endothelial Dysfunction by Activating the HMGB1/RAGE Signaling Pathway. *BioMed Res Int* (2017) 2017:4391920. doi: 10.1155/2017/4391920
21. Li P, Zhang L, Zhang M, Zhou C, Lin N. Uric Acid Enhances PKC-Dependent eNOS Phosphorylation and Mediates Cellular ER Stress: A Mechanism for Uric Acid-Induced Endothelial Dysfunction. *Int J Mol Med* (2016) 37:989–97. doi: 10.3892/ijmm.2016.2491
22. Harzand A, Tamariz L, Hare JM. Uric Acid, Heart Failure Survival, and the Impact of Xanthine Oxidase Inhibition. *Congest Heart Fail* (2012) 18:179–82. doi: 10.1111/j.1751-7133.2011.00262.x
23. Zhi L, Yuzhang Z, Tianliang H, Hisatome I, Yamamoto T, Jidong C. High Uric Acid Induces Insulin Resistance in Cardiomyocytes *In Vitro* and *In Vivo*. *PLoS One* (2016) 11:e0147737. doi: 10.1371/journal.pone.0147737
24. Forstermann U, Munzel T. Endothelial Nitric Oxide Synthase in Vascular Disease: From Marvel to Menace. *Circulation* (2006) 113:1708–14. doi: 10.1161/CIRCULATIONAHA.105.602532
25. Martinon F, Petrilli V, Mayor A, Tardivel A, Tschopp J. Gout-Associated Uric Acid Crystals Activate the NALP3 Inflammasome. *Nature* (2006) 440:237–41. doi: 10.1038/nature04516
26. Matias ML, Romao M, Weel IC, Ribeiro VR, Nunes PR, Borges VT, et al. Endogenous and Uric Acid-Induced Activation of NLRP3 Inflammasome in Pregnant Women With Preeclampsia. *PLoS One* (2015) 10:e0129095. doi: 10.1371/journal.pone.0129095
27. Kim SK, Choe JY, Park KY. Anti-Inflammatory Effect of Artemisinin on Uric Acid-Induced NLRP3 Inflammasome Activation Through Blocking Interaction Between NLRP3 and NEK7. *Biochem Biophys Res Commun* (2019) 517:338–45. doi: 10.1016/j.bbrc.2019.07.087
28. Yin W, Zhou QL, OuYang SX, Chen Y, Gong YT, Liang YM. Uric Acid Regulates NLRP3/IL-1beta Signaling Pathway and Further Induces Vascular Endothelial Cells Injury in Early CKD Through ROS Activation and K(+) Efflux. *BMC Nephrol* (2019) 20:319. doi: 10.1186/s12882-019-1506-8
29. Jia G, Habibi J, Bostick BP, Ma L, DeMarco VG, Aroor AR, et al. Uric Acid Promotes Left Ventricular Diastolic Dysfunction in Mice Fed a Western Diet. *Hypertension* (2015) 65:531–9. doi: 10.1161/HYPERTENSIONAHA.114.04737
30. Onat A, Can G, Ornek E, Altay S, Yüksel M, Ademoğlu E. Elevated Serum Uric Acid in Nondiabetic People Mark Pro-Inflammatory State and HDL Dysfunction and Independently Predicts Coronary Disease. *Clin Rheumatol* (2013) 32:1767–75. doi: 10.1007/s10067-013-2339-7
31. Kuwabara M, Borghi C, Cicero AFG, Hisatome I, Niwa K, Ohno M, et al. Elevated Serum Uric Acid Increases Risks for Developing High LDL Cholesterol and Hypertriglyceridemia: A Five-Year Cohort Study in Japan. *Int J Cardiol* (2018) 261:183–88. doi: 10.1016/j.ijcard.2018.03.045
32. Gonzalez-Gay MA, Gonzalez-Juanatey C, Vazquez-Rodriguez TR, Dierssen T, Llorca J. Role of Asymptomatic Hyperuricemia and Serum Uric Acid Levels in the Pathogenesis of Subclinical Atherosclerosis in Psoriatic Arthritis: Comment on the Article by Chen et al. *Arthritis Rheum* (2009) 61:856–7; author reply 57-8. doi: 10.1002/art.24584
33. Lin YC, Dalal D, Churton S, Brennan DM, Korman NJ, Kim ES, et al. Relationship Between Metabolic Syndrome and Carotid Intima-Media Thickness: Cross-Sectional Comparison Between Psoriasis and Psoriatic Arthritis. *Arthritis Care Res (Hoboken)* (2014) 66:97–103. doi: 10.1002/acr.22144
34. Gonzalez-Gay MA, Gonzalez-Juanatey C, Vazquez-Rodriguez TR, Gomez-Acebo I, Miranda-Filloy JA, Paz-Carreira J, et al. Asymptomatic Hyperuricemia and Serum Uric Acid Concentration Correlate With Subclinical Atherosclerosis in Psoriatic Arthritis Patients Without Clinically Evident Cardiovascular Disease. *Semin Arthritis Rheum* (2009) 39:157–62. doi: 10.1016/j.semarthrit.2008.06.001
35. Fang J, Alderman MH. Serum Uric Acid and Cardiovascular Mortality the NHANES I Epidemiologic Follow-Up Study, 1971-1992. National Health and Nutrition Examination Survey. *JAMA* (2000) 283:2404–10. doi: 10.1001/jama.283.18.2404
36. Hoieggen A, Alderman MH, Kjeldsen SE, Julius S, Devereux RB, De Faire U, et al. The Impact of Serum Uric Acid on Cardiovascular Outcomes in the LIFE Study. *Kidney Int* (2004) 65:1041–9. doi: 10.1111/j.1523-1755.2004.00484.x
37. Freedman DS, Williamson DF, Gunter EW, Byers T. Relation of Serum Uric Acid to Mortality and Ischemic Heart Disease. The Nhanes I Epidemiologic Follow-up Study. *Am J Epidemiol* (1995) 141:637–44. doi: 10.1093/oxfordjournals.aje.a117479
38. Chen W, Thomas J, Sadatsafavi M, FitzGerald JM. Risk of Cardiovascular Comorbidity in Patients With Chronic Obstructive Pulmonary Disease: A Systematic Review and Meta-Analysis. *Lancet Respir Med* (2015) 3:631–9. doi: 10.1016/S2213-2600(15)00241-6
39. Brusselle GG, Joos GF, Bracke KR. New Insights Into the Immunology of Chronic Obstructive Pulmonary Disease. *Lancet* (2011) 378:1015–26. doi: 10.1016/S0140-6736(11)60988-4
40. Roubille C, Richer V, Starnino T, McCourt C, McFarlane A, Fleming P, et al. Evidence-Based Recommendations for the Management of Comorbidities in Rheumatoid Arthritis, Psoriasis, and Psoriatic Arthritis: Expert Opinion of the Canadian Dermatology-Rheumatology Comorbidity Initiative. *J Rheumatol* (2015) 42:1767–80. doi: 10.3899/jrheum.141112
41. Elmets CA, Leonardi CL, Davis DMR, Gelfand JM, Lichten J, Mehta NN, et al. Joint AAD-NPF Guidelines of Care for the Management and Treatment of Psoriasis With Awareness and Attention to Comorbidities. *J Am Acad Dermatol* (2019) 80:1073–113. doi: 10.1016/j.jaad.2018.11.058
42. Ford AR, Siegel M, Bagel J, Cordoro KM, Garg A, Gottlieb A, et al. Dietary Recommendations for Adults With Psoriasis or Psoriatic Arthritis From the Medical Board of the National Psoriasis Foundation: A Systematic Review. *JAMA Dermatol* (2018) 154:934–50. doi: 10.1001/jamadermatol.2018.1412
43. Grimaldi-Bensouda L, Alperovitch A, Aubrun E, Danchin N, Rossignol M, Abenhaim L, et al. Impact of Allopurinol on Risk of Myocardial Infarction. *Ann Rheum Dis* (2015) 74:836–42. doi: 10.1136/annrheumdis-2012-202972
44. Hippisley-Cox J, Coupland C, Vinogradova Y, Robson J, Minhas R, Sheikh A, et al. Predicting Cardiovascular Risk in England and Wales: Prospective Derivation and Validation of QRISK2. *BMJ* (2008) 336:1475–82. doi: 10.1136/bmj.39609.449676.25
45. Crowson CS, Gabriel SE, Semb AG, van Riel PLCM, Karpouzas G, Dessein PH, et al. Rheumatoid Arthritis-Specific Cardiovascular Risk Scores Are Not Superior to General Risk Scores: A Validation Analysis of Patients From Seven Countries. *Rheumatol (Oxford)* (2017) 56:1102–10. doi: 10.1093/rheumatology/kex038
46. Langan SM, Seminara NM, Shin DB, Troxel AB, Kimmel SE, Mehta NN, et al. Prevalence of Metabolic Syndrome in Patients With Psoriasis: A Population-Based Study in the United Kingdom. *J Invest Dermatol* (2012) 132(3 Pt 1):556–62. doi: 10.1038/jid.2011.365

Conflict of Interest: The authors declare that the research was conducted in the absence of any commercial or financial relationships that could be construed as a potential conflict of interest.

frontiers in Immunology

REVIEW
published: 17 September 2021
doi: 10.3389/fimmu.2021.752359

Where Epigenetics Meets Food Intake: Their Interaction in the Development/Severity of Gout and Therapeutic Perspectives

Philippe T. Georgel[1*†] *and Philippe Georgel*[2,3*†]

[1] Department of Biological Sciences, Cell Differentiation and Development Center, Joan C. Edwards School of Medicine, Byrd Biotechnology Science Center, Marshall University, Huntington, WV, United States, [2] Laboratoire d'ImmunoRhumatologie Moléculaire, Institut National de la Santé et de la Recherche Médicale (INSERM) UMR_S 1109, Institut thématique interdisciplinaire (ITI) de Médecine de Précision de Strasbourg, Transplantex NG, Faculté de Médecine, Fédération Hospitalo-Universitaire OMICARE, Fédération de Médecine Translationnelle de Strasbourg (FMTS), Université de Strasbourg, Strasbourg, France, [3] Unité de Recherche et d'Expertise Immunity and Inflammation, Institut Pasteur in New Caledonia, Pasteur Network, Nouméa, New Caledonia

OPEN ACCESS

Edited by:
Xiaoxia Zhu,
Fudan University, China

Reviewed by:
Hongbing Guan,
Guangzhou Medical University, China
Ming-Kuei Shih,
National Kaohsiung University of Hospitality and Tourism, Taiwan

***Correspondence:**
Philippe T. Georgel
georgel@marshall.edu
Philippe Georgel
pgeorgel@unistra.fr

[†]These authors have contributed equally to this work

Specialty section:
This article was submitted to Autoimmune and Autoinflammatory Disorders, a section of the journal Frontiers in Immunology

Received: 02 August 2021
Accepted: 31 August 2021
Published: 17 September 2021

Citation:
Georgel PT and Georgel P (2021) Where Epigenetics Meets Food Intake: Their Interaction in the Development/Severity of Gout and Therapeutic Perspectives. Front. Immunol. 12:752359. doi: 10.3389/fimmu.2021.752359

Gout is the most frequent form of inflammatory arthritis in the world. Its prevalence is particularly elevated in specific geographical areas such as in the Oceania/Pacific region and is rising in the US, Europe, and Asia. Gout is a severe and painful disease, in which co-morbidities are responsible for a significant reduction in life expectancy. However, gout patients remain ostracized because the disease is still considered "self-inflicted", as a result of unhealthy lifestyle and excessive food and alcohol intake. While the etiology of gout flares is clearly associated with the presence of monosodium urate (MSU) crystal deposits, several major questions remain unanswered, such as the relationships between diet, hyperuricemia and gout flares or the mechanisms by which urate induces inflammation. Recent advances have identified gene variants associated with gout incidence. Nevertheless, genetic origins of gout combined to diet-related possible uric acid overproduction account for the symptoms in only a minor portion of patients. Hence, additional factors must be at play. Here, we review the impact of epigenetic mechanisms in which nutrients (such as ω-3 polyunsaturated fatty acids) and/or dietary-derived metabolites (like urate) trigger anti/pro-inflammatory responses that may participate in gout pathogenesis and severity. We propose that simple dietary regimens may be beneficial to complement therapeutic management or contribute to the prevention of flares in gout patients.

Keywords: gout, hyperuricemia, food intake, epigenetics, genetic variants, trained immunity 2

INTRODUCTION

Gout is probably the oldest known joint disease, already described by Hippocrates of Kos in the fifth century B.C (1). Gout has been dubbed the "disease of Kings" and indeed, considering only the French royalty, 20 of the 34 kings of France were said to have been afflicted by it (2). Since then, gout has been associated with a decadent and unhealthy lifestyle, caused by excessive calorie-rich food

intake. Unfortunately, such considerations are still prevalent, and gout continues to be considered a self-inflicted disease. Importantly, a recent meta-analysis (3) revealed that, in contrast to this common belief, diet actually only explained some of the variation(s) in serum urate levels, compared to the importance of the genetic contribution. Such data have important psychological consequences, as they should help to relieve the stigmatization of gout patients and encourage them to seek medical help during the first crisis, improve their therapeutic observance, limit the duration of their therapy, and diminish the social and economic burden of the disease. Although this meta-analysis concerned patients of European ancestry and may not be generalized to other ethnic groups (specifically those, like Oceanians (4) in which gout represents a major public healthcare issue), it highlights the importance of genetic variants identified in genome-wide association studies (GWAS), which account for almost one fourth (23.9%) of the variation of serum urate levels compared to 0.3% associated with diet. This study does not however explain what is responsible for the majority of the variation(s) of serum urate levels (approximately 75%). This indicates that, even though hyperuricemia and the subsequent formation of urate crystals have been known for a long time as major determinants of gout etiology, many facets of this disease, which remains the most prevalent form of inflammatory arthritis worldwide, are still unexplained.

Epigenetics describes the mechanisms by which changes in genes expression occur independently from the primary DNA sequence (genome) of an organism. They are divided into three main categories: (i) changes in DNA methylation affecting chromatin compaction, (ii) chromatin alterations through histone post-translational modifications (PTM) and/or incorporation of histone variants and (iii) regulation by non-coding RNAs (ncRNAs), such as microRNAs (miRs) or long non-coding RNAs (lncRNAs) (5). Such modifications are considered as important responses to environmental triggers, enabling adaptive changes of gene expression patterns (6). In the context of gout pathogenesis, epigenetic mechanisms might be of particular interest to account for the remarkable variability seen in patients (7) in terms of crisis intensity or frequency and to assess the relationship [or sometimes the absence of relationship (8)] between uricemia levels and MSU crystals-dependent joint inflammation. In line with these assumptions, it is noteworthy to highlight that genome-wide association studies (GWAS) comparing gout patients to control groups have identified variants in genes encoding important players in epigenetic regulation mechanisms, such as DNA Methyl Transferase 1 (DNMT1) (9) and lncRNAs (10). Furthermore, and as noted above, food intake, despite the recent re-evaluation of its importance in gout development, remains an important environmental source of precursors of uric acid, a molecule that has been shown to affect the physiological and inflammatory properties of monocytes through epigenetic-driven reprogramming (11). This process, coined "trained innate immunity", appears nowadays as a major player in the defense against pathogens and in autoimmunity (12). Finally, besides providing urate precursors, diet is also a source of short-chain fatty acids (which can also originate from the microbiota) that are known to induce epigenetic changes through, most commonly, changes in histone acetylation, and consequently affect pathophysiological responses (13), as shown using a gout mouse model (14).

Up to now, the therapeutic management of gout patients aims, in the short term, at treating the gout flares, and in the long term, at reducing urate levels (15). For these purposes, several molecules are available, among which are colchicine, IL-1β blockers, non-steroidal anti-inflammatory drugs (NSAID), and drugs facilitating urate renal excretion (like Probenecid) or decreasing its production (such as the Xanthine Oxidase inhibitors Allopurinol and Febuxostat). Unfortunately, these treatments can generate serious side effects, including renal and cardiac damages or hepatotoxicity (16). Further, these drugs focus on diminishing the symptoms rather than curing the patient. Of note, novel molecules targeting the aggregation of neutrophil extracellular traps are in development (17). In the long term, though with limited expected benefits, lifestyle modifications are also recommended (15). The possibility that epigenetic mechanisms may contribute to gout pathogenesis offers the potential of a set of completely different therapeutic options and, more importantly, lasting management of patients through epigenetic reprogramming of innate immune cells such as monocytes/macrophages (for instance with the Histone DeAcetylase -HDAC - inhibitor Vorinostat), which are the main producers of Il-1β, a crucial cytokine in gout pathogenesis. This strategy has been already considered for other rheumatic diseases, such as rheumatoid arthritis or systemic lupus erythematosus (18), and implemented in animal models (19). Diet counseling could also be adapted, as indicated by recent findings linking salt (20) or other components (such as hydrogen sulfide) (21) and inflammation as a result of innate immune cells reprogramming (22).

Here, we review the current mechanistic understanding of how several components provided by food intake are capable of modulating inflammation through epigenetic modification/reprogramming of innate cells and how that knowledge could be translated into actionable decisions for the benefit of gout patients.

GOUT AND FOOD INTAKE: NOT ONLY URATE, NOT ONLY INFLAMMASOME-DEPENDENT

Excessive uric acid in the blood circulation (hyperuricemia) and the subsequent formation and deposition of MSU crystals have been known for more than a century [with the work of Sir Alfred Garrod (2)] to be the etiological trigger of gout (23). However, the connections between elevated urate, MSU, and gout flares are more complex than a simple cause and effect relationship. Indeed, only 2-15% of hyperuricemic individuals develop clinical gout and conversely, some patients exhibit urate levels within normal range at the time when they suffer acute gout

flares (23). Nevertheless, the impact of MSU crystals on inflammation and pain is widely recognized. Of note, the loss of URICASE activity in Humans and other Primates explains high urate levels in these species (23). The mutations inactivating the *URICASE* gene that have been selected suggest that urate also carries some beneficial effects, including antioxidant and adjuvant properties, which protect the host against neurodegenerative or infectious diseases (24). As mentioned above, diet has always been associated with gout flares, but this assumption has been recently objectified in a meta-analysis regrouping 16,760 individuals (3). This work demonstrated that the consumption of specific nutrients (beer, liquor, wine, potato, poultry, soft drinks, and meat) increased serum urate levels, while others (eggs, cheese, peanuts) were associated with lower levels. These data are in line with observations linking Mediterranean diet (in which red meat intake is moderate) with reduced gout incidence (25). However, the mechanisms by which nutrition modifies urate production and impacts on gout crises remain elusive. Indeed, urate, the end-product of purine metabolism, can have endogenous or exogenous origins and it is widely accepted that purines originate equally from diet and synthesis under normal circumstances (26). Hyperuricemia can therefore result from two kinds of perturbations: (i) those resulting from excessive purine-rich food, infections, or neoplasms and (ii) those resulting from reduced excretion of urate (**Figure 1**).

With regards to the exogenous origin of hyperuricemia, several nutrients, such as red meat (rich in purines) and fructose-rich beverages appear as clear contributors. Of note, fructose metabolism in the liver, through unregulated phosphorylation of adenosine triphosphate into adenosine monophosphate, increases urate production (27). However, such direct connection is more difficult to validate when one considers that others purine-rich foods of vegetable origin (bean, lentils, peas…) are not known to contribute to any increased risk of hyperuricemia and gout flares (28). Such contradiction indicates that other dietary components, besides those which drive purine-derived uric acid overproduction, are involved in gout pathogenesis.

Indeed, high protein diet-induced gout in chicken has recently been described in a recent report (29). While this regimen also induced serum urate levels, another study in human's suffering hypertension (30) provided contradictory insights by showing lower serum urate levels in patients (mean BMI 30.2) which received a protein-rich diet for 6 weeks. Such contrasting data might reflect differences between chicken and human metabolism, or alternatively between the composition and the origin of the proteins that were enriched in these dietary regimens.

Comparatively to that of proteins and sugar, the impact of lipids on the ignition of gout flares or the severity of the symptoms has seldom been investigated, which is surprising

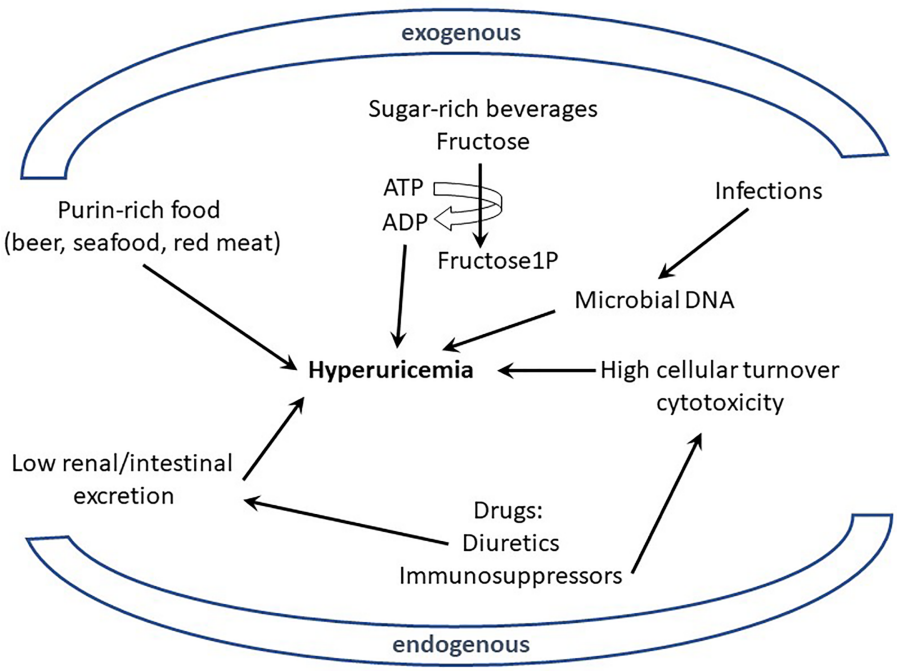

FIGURE 1 | Excessive uric acid in the blood (hyperuricemia) can originate from endogenous or exogenous sources. Various nutrients (purin-rich such as red meat or sugar-rich beverages) have been shown to be environmental (exogenous) factors participating in hyperuricemia; similarly intrinsic (endogenous) determinants from the host, like genetic defects affecting urate excretion, can also participate to hyperuricemia. Metabolism of elevated DNA concentration resulting from infections (exogenous) or cell cytotoxicity (endogenous) is also suspected to generate high levels of urate.

given the strong association between this disease and obesity (31, 32). This issue has been recently explored in a gout mouse model following footpad injections of MSU crystals in animals which were simultaneously fed with a high fat diet (containing 10% yeast extracts, likely to be an ω-6 Fatty acid-rich diet, low in ω-3 Fatty acids) (33). Interestingly, this model reproduced the rise in inflammatory cytokines seen in patients during acute gout flares, as well as the intestinal dysbiosis (commonly associated with high PUFA diet) which is also a hallmark of the disease (34). In another study, the authors analyzed the impact of a fiber-rich food on gout induced by intra-articular injections of MSU crystals in mice (35). Indeed, consumption of fibers, which are abundant in the Mediterranean diet, was shown to limit gout symptoms in humans. Of note, this study reported a faster resolution of the MSU crystal-induced inflammation in high fiber diet-fed animals. Mechanistically, this effect appears to be mediated by short chain fatty acids (SCFA) such as acetate which are produced upon fibers digestion. Of note, an increase of free acetyl Co-A has been shown to contribute to global and local histone hyper-acetylation (to be discussed in sections C and D). Remarkably, providing acetate in the drinking water of mice reduced inflammatory responses, even after MSU crystals injection. Overall, this work suggests that food processing by the intestinal flora can generate lipid compounds, such as acetate, which exhibit a beneficial action (anti-inflammatory) on immune cells. Other lipids, like Omega-3 polyunsaturated fatty acids (ω-3 PUFA), are considered potentially beneficial in gouty arthritis patients. This assumption relies on investigations in gout patients in which questionnaires enabled to observe that the regular consumption of ω-3 PUFA-rich fish was associated to reduced risk of gout flares (36). Of note, taking ω-3 PUFA alone (as a dietary supplement) seemed to have no impact, but the limited number of participants who reported to use such supplements did not enable the authors to be conclusive. Importantly, serum urate levels were not quantified in this study; it is therefore possible to explain the beneficial effect of ω-3 PUFA-rich fish diet by concomitant reduced red meat consumption, anti-inflammatory properties of this compound, or other mechanisms. Indeed, this family of molecules was shown to inhibit the activation of the Nlrp3 (NOD-like receptor family, pyrin domain containing 3) inflammasome (see below) in murine bone marrow-derived macrophages, an effect that could very well account for their anti-inflammatory properties and efficacy against gout, a disease in which the NLRP3 inflammasome has been strongly implicated (37, 38).

Altogether, it appears that the contribution of diet in the development/severity of gout is far more complex than previously anticipated and cannot be simply reduced to a purin rich/poor dichotomic classification. This likely contributes to the poor impact and optimization of dietary education and counseling in the management of gout patients (39, 40).

Finally, in addition to this information showing that diet-derived urate production appears, at best as a contributing factor to gout pathogenesis, it must also be emphasized that the mechanisms linking MSU crystals and severe inflammation remain partially uncovered. While association between the presence of these crystals in the joints and the incidence of gout flares is undisputable (28), several questions are still unanswered. For instance, the mechanisms by which MSU crystals induce an inflammatory response awaits definitive answers. While it has been known for several years that the NLRP3 inflammasome plays a crucial role in this process (37), the model of its activation has been described in cells (mostly macrophages) in which a "priming signal" is delivered by Lipopolysaccharide (LPS) addition, prior to the "activation signal" provided by MSU crystals. *In vivo*, however, MSU crystals alone can induce an inflammatory response manifested by IL-1β secretion and the nature of the priming signal in these conditions remains to be identified. In addition, several groups reported that injection of MSU crystals is able to promote inflammation, even in the absence of the Nlrp3 inflammasome, at least in mouse models (41–43).

All these gaps in knowledge about the relationships between diet, urate production and inflammatory responses prompted us to consider alternative (but not exclusive) explanations to account for their respective involvement in gout pathogenesis. In the next sections, we are attempting to develop an alternative (and under-explored) hypothetical model based on evidences linking epigenetics and trained immunity as critical determinants playing an important role in the modulation of inflammatory responses in the presence of MSU crystals and depending on dietary components.

GENETICS AND EPIGENETICS OF GOUT

Many GWAS performed to identify variants involved in hyperuricemia revealed the importance of genes (such as *SL2A9* or *ABCG2*) regulating the metabolism/transport/excretion of urate. Some of these genes/variants were also associated in gout patients *vs* controls GWAS studies, which, in addition, revealed the importance of genes (like *IL-1β* or *TLR*4) participating in inflammatory pathways [reviewed in (44, 45)]. These observations had important therapeutic ramifications, as they permitted consideration of gout not only as a metabolic, but also as an auto-inflammatory disease. These studies also demonstrated that although monogenic disorders can be associated to gout, its genetic origin is usually complex, involving multiple genomic loci. Importantly, heritability of urate levels (performed in twin studies) was estimated to average 50%, while that of gout appeared variable, from very low (46) to 30% (47). Some of the genes identified by this approach offer opportunities to develop important therapeutic improvement and enable precision medicine, for instance in gout patients carrying a loss-of-function allele of the main urate transporter gene *SLC22A12* (48, 49) and in which uricosuric agents, like probenecid, are inefficient. However, genetic defects still cannot be identified as the main trigger of the disease for many patients, since known sequence variants explain less than 10% of the risk of developing gout (50).

This leaves room for additional mechanisms accounting for gout pathogenesis and eventually ensuing progression from hyperuricemia to gout flares. Interestingly, gout-related polymorphisms were recently identified in genes encoding epigenetic players which are known to modulate immune cell activity (51), opening novel avenues of research and unsuspected mechanistic insights in gout pathogenesis.

Epigenetic-related genes involved in gout pathogenesis encode microRNAs, such as miR-302F, which was identified in GWAS studies (52) or miR-221-5p, which is differentially expressed in the serum of gout patients compared to controls (53). Importantly, this miRNA can modulate *IL-1β* expression, as evidenced by a luciferase assay (53). Long Intergenic Non-Coding RNAs (LINC) were also associated with gout in various studies [reviewed in (10)]. MicroRNAs and long non-coding RNAs are transcripts which are not translated into proteins, but affect the expression of multiples genes through various mechanisms (translational inhibition, enhancement of mRNA degradation). While the identification of the genes that are targeted by non-coding RNAs remains challenging *in vivo*, the stability of these molecules and the possibility to easily quantify them in body fluids makes non-coding RNAs attractive circulating biomarkers (54). Additionally, the role of DNA methylation in gout was demonstrated through the discovery of a variant (rs2228611) in the *DNA MethylTransferase 1* (*DNMT1*) gene whose presence is statistically increased in gout patients compared to controls (9). In line with this information, an innovative multi-OMICs study, in which the cell-specific methylome was compared between gout patients and controls, revealed that many differentially methylated gene regulatory genomic sites were associated with *IL-1β* expression in monocytes (55).

Epigenetic mechanisms can affect gout physiopathology through various ways, like changes in gene expression resulting from modifications of DNA methylation levels or histone post-translational modifications, including acetylation/deacetylations and methylation/demethylation processes. Such genes may encode proteins regulating urate metabolism/excretion. More recently, epigenetic-driven modifications of gene expression were also shown to sustain innate immune memory, a feature of innate immune cells which is also termed "trained immunity" [reviewed in (56)] and that occurs following cell stimulation with Pathogen- or Danger-Associated Molecular Patterns (PAMPs, DAMPs) such as β-glucans (57). While the impact of urate on histone methylation and *IL-1Ra* inhibition was described several years ago (58), the concept of innate immune reprogramming has gained considerable interest and has now major consequences for inflammatory diseases, including gout (11). These different mechanisms are schematized in **Figure 2**.

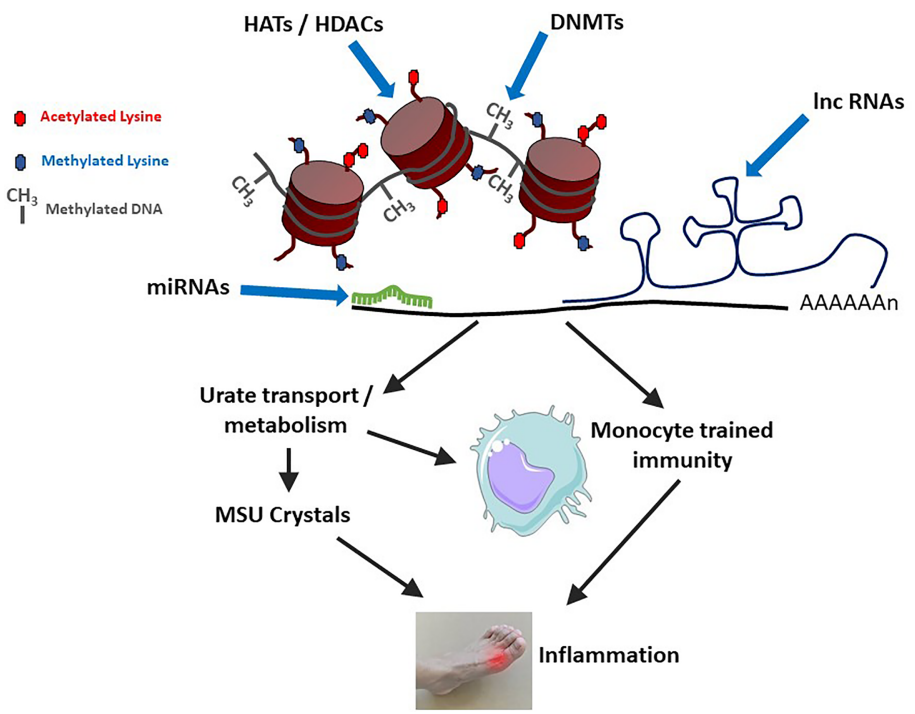

FIGURE 2 | Epigenetic mechanisms modulate gouty inflammation. DNA and histone modifications (by DNA Methyl Transferases – DNMTs or Histone Acetyl Transferases – HATs/Histone Deacetylases - HDACs) affect DNA compaction and subsequent gene transcription. At the mRNA level, gene expression is modulated by microRNAs (miRNAs) and long non-coding RNAs (lnc RNAs). At least two categories of gout-related genes can be affected: (i) those directly regulating urate metabolism/excretion and (ii) those affecting macrophages polarization and activation status. Increased levels of circulating uric acid, in combination with a pro-M1 macrophage polarization (which can also be favorized by high urate conditions) can lead to monosodium urate (MSU) crystals formation and concomitant inflammation.

DIET-DERIVED EPIGENETIC MODIFIERS

Because epigenetics has now been identified as an important player in gouty arthritis, we thought to re-evaluate the impact of diet in light of nutrient-derived epigenetic modifiers. As described in the previous section, a significant number of epigenetic factors potentially affect gout onset and can contribute to further inflammation events worsening the symptoms (9, 55). Among such factors influencing epigenetic changes are multiple compounds (listed in **Table 1**) that are commonly found in one's diet. A recent review by Li and colleagues (90) describes the multiple epigenetic effects engendered by bioactive dietary compounds (summarized in **Figure 3**). DNA methylation (9, 53), as well as changes in histone post-translational modifications (99), and microRNA and long non-coding RNA can be modulated by dietary input and play a role in reducing inflammation (100). A subset of diet-derived epigenetic modifiers has already been identified as modulators of risk of developing gout (65, 91). The meta-analysis performed by Li et al. (90) linked red meat, seafoods, alcohol, sweetened drinks, and dairy products to the list of factors increasing risks of gout and hyperuricemia.

In addition to these factors, specific DNA methylation or demethylation changes can be mediated by DNMT activation or inhibition [DNMT1 in particular, but also DNMT3A and DNMT3B (9)] induced by dietary compounds (**Figure 3**). Two specific dietary compounds have been identified as affecting gout's severity by controlling changes in DNA methylation levels of genes inflammation (65). Deficiencies in folic acids in the diet results in dis-regulation of *IL-1β*, *IL-6* and *TNF-α* genes methylation patterns (101). Similarly, polyphenolic compounds, such as curcumin, genistein, or resveratrol, mediate changes in DNA methylation patterns (65). Curcumin, specifically plays a role in reducing activation of NF-κB, as well as affecting microRNA expression (102).

Methyl donors, in addition to potentially changing DNA methylation patterns are also involved in histone methylation/demethylation processes. For example, the inflammatory response associated with gout can be mediated by tri-methylation of histone H3 Lysine 4 (H3K4me3) (103). Similarly, urate-induced inflammation priming can be reduced by using the histone methyl transferase inhibitor (HMTI) 5'-deoxy-5'-methylthioadenosine (MTA), resulting in limited cytokine production (11, 82). Significant evidence has been gathered to indicate that dietary compounds affecting the DNA methylation level, such as choline (81), vitamin C (95), have also an effect on histone methylation levels and genomic distribution, suggesting a complex interplay between various epigenetic regulatory mechanisms.

The next major epigenetic regulatory component involves histone acetylation. Multiple studies have identified Histone De-Acetylase inhibitors (also referred to as HDACi) as drugs capable of reducing inflammation. Romidepsin, an HDACi for HDAC class1 and class 2, increases Suppressor Of Cytokine Signaling protein 1 (SOCS1) expression leading to a decrease in IL-1β (104). Treatment of peripheral blood mononuclear cells (PBMCs) with sodium butyrate, a less selective HDACi, results in decreased NF-κB expression, and helps suppressing MSU-induced inflammation through a reduction of *IL-6*, *IL-8* and *IL-1β* transcription in PBMCs (105). As was discussed in the preceding section, dietary compounds are also capable of regulating the level of histone acetylation. Vitamin D can reduce inflammation through its action on IL-17A (76). The polyphenolic

TABLE 1 | List of dietary-derived epigenetic modifiers classified according to their mode of action and corresponding references.

Epigenetic regulation	Food Ingredient	Reference
DNMT activation/Inhibition	Selenium	Xiang et al. (59)
		Davis et al. (60)
	Biochanin A	Ito et al. (61)
	Quercetin	Lee et al. (62)
		Fang et al. (63)
	Resveratrol	Kala et al. (64)
		Gao et al. (65)
	Choline	Wolff et al. (66)
	Sulforaphane	Li et al. (67)
	Genistein	Mirza et al. (68)
		Nagaraju et al. (69)
	Curcumin	Mirza et al. (68)
		Zheng et al. (70)
	Luteolin	Kanwal et al. (71)
	Catechin	Lee et al. (62)
		Kanwal et al. (71)
	Apigenin	Fang et al. (63)
	Vitamin D	Tapp et al. (72)
	Vitamin C	Young et al. (73)
HDAC/KAT	Sulforaphane	Gao et al. (65)
	Isothiocynanate	Beklemisheva et al. (74)
	Vitamin D	Fetahu et al. (75)
	Omega-3 FA	Patterson et al. (76)
		Abbas et al. (77)
	Selenium	Xiang et al. (59)
	Caffeic acid	Bora-Tatar et al. (78)
	Resveratrol	Gao et al. (65)
	Kampferol	Berger et al. (79)
HMT/HDM	Folate	Mentch & Locasale (80)
	Vitamin C	Yin et al. (81)
	Omega-3 FA	Abbas et al. (77)
	Choline	Pogribny et al. (82)
	Withaferin	Mirza et al. (68)
	Apigenin	Kanwal et al. (71)
PTM readers (MeCP2)	Genistein	Mirza et al. (68)
	Catechin	Mirza et al. (68)
	Resveratrol	Mirza et al. (68)
	Curcumin	Mizraei et al. (83)
PTM readers (BRCA)	Equol	Bosviel et al. (84)
MicroRNA	Vitamin D	Nunez-Lopez et al. (9)
		Fan et al. (85)
	Anthocyanin	Arola-Arnal & Blade (86)
	Catechin	Arola-Arnal & Blade (86)
	Curcumin	Mizraei et al. (83)
		Xin et al. (87)
	Choline	Pogribny et al. (82)
	Sulforaphane	Gao et al. (65)
	Resveratrol	Xin et al. (87)
		Qin et al. (88)
	Genistein	Zhong et al. (9)
		Hirata et al. (89)
	Folate	Pogribny et al. (82)

DNMT, DNA-Methyl Transferase; HDAC, Histone De-acetylase; KAT, Lysine Acetyl Transferase; HMT, Histone Methyl Transferase; HDM, Histone De-Methylase; PTM, Post-Translational Modification; MeCP2, Methyl CpG Binding Protein 2; BRCA, BRCA1 DNA Repair-Associated protein; miR, microRNA.

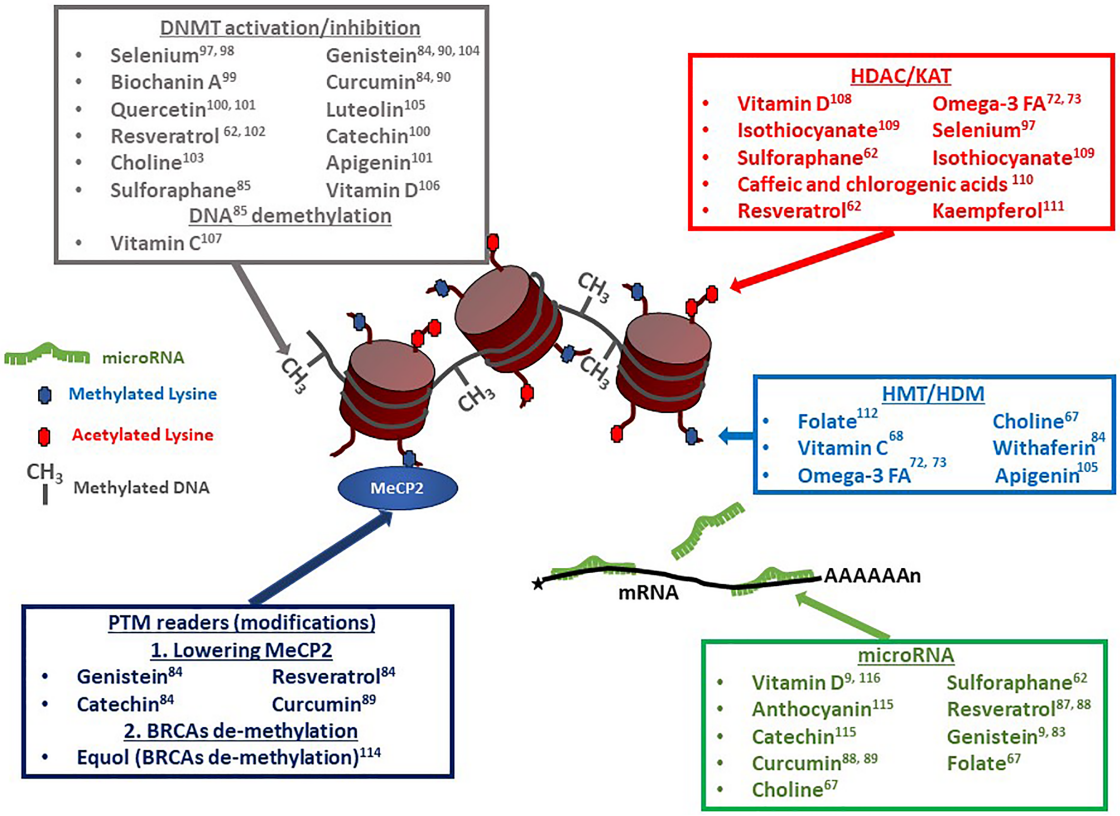

FIGURE 3 | Dietary compounds affecting epigenetic regulatory events. Multiple compounds have pleiotropic effects on chromatin modifiers, transcription factors, and microRNAs (miRs). Vitamin D, Resveratrol and Sulforaphane, for example, can affect DNA methylation levels, as well as histone acetylation and microRNA levels. Resveratrol can additionally affect the transcription factor MeCP2 's expression levels. DNMT, DNA-Methyl Transferase (60–64, 66, 67, 69, 71–73, 75, 91–93); HDAC, Histone De-acetylase (74, 77–80, 88, 91, 92, 94); KAT, Lysine Acetyl Transferase; HMT, Histone Methyl Transferase (67, 72, 77, 81, 84, 95, 96); HDM, Histone De-Methylase; PTM, Post-Translational Modification; MeCP2, Methyl CpG Binding Protein 2 (67); BRCA, BRCA1 DNA Repair-Associated protein (86); miR, microRNA (9, 68, 70, 81, 83, 85, 87, 91, 97, 98).

Epigallocatechin-3 Gallate (EGCG) has been shown to prevent acute gout through its anti-inflammatory activity by suppressing the activation of the NLRP3 inflammasome, acting as a modulator of Lysine Acetyl Transferase (KAT) (50). Short Chains Fatty Acid (SCFA) and ω-3 FAs can also contribute to lowering IL-1β release and NLRP3-mediated caspase 1 activation. Diets using longer poly-unsaturated fatty acids (PUFA), such as docosahexaenoic acid (DHA) and eicosapentaenoic acid (EPA), have been shown to have beneficial effects on cancer cell lines and patients suffering of various types of cancer, through lowering inflammation [for review, see (77)], but perhaps most importantly in the context of this review, through a mechanism leading to a global hyper-acetylation of histone N-termini, as well as at specific loci (94). The high ω-3 FA diet, by inhibiting the enzyme acetyl-CoA carboxylase which function is to convert two acetyl-Co-A into a malonyl-Co-A, leads to an increase in the free pool of acetyl Co-A (which is the acetyl donor for histone acetylation) (106, 107). An unexpected secondary effect of diets rich in ω-3 FA is a modification in the expression level of several microRNAs related to gouty inflammation, specifically miR-146a and miR-155 (100). Note that the mode of action for these observed changes in miR levels is likely to be indirect and mediated by changes in chromatin accessibility through histone hyper-acetylation of the target genes' regulatory elements. miR-155, when over-expressed, has been associated with an increased production of MSU-induced pro-inflammatory cytokines (100).

MicroRNAs expression levels have often been shown to be modulated by various types of dietary polyphenolic compounds. For example, curcumin, which was previously mentioned as affecting DNA methylation pattern (see previous section), is also involved in lowering inflammation (decreased NF-κB expression) through modifying the patterns of expression of miRs (65). Another aspect of the importance of miRs as part of the diet is suggested by the concept of «dietary xenomiRs», miRs coming directly from one's diet (plants (108) or other origins) and used by the consumer's cells (109). It indicates that not only do dietary compounds influence the miR expression in the host cells, but the xenomiRs themselves can provide an additional level of complexity to the effects of diet on gout and inflammation, although this effect is still debated (110). As shown in **Figure 3**, multiple dietary chemicals can act on various aspects of epigenetic regulation in the cells. Resveratrol

can affect DNA methylation, histone methylation, histone acetylation, miRs, and histone PTM readers. Genistein can modify levels of DNA methylation, miRs, and histone PTM readers. Sulforaphane affects DNA methylation, histone acetylation, and miRs. The potential for pleiotropic effects, which could be additive, synergistic, or possibly antagonistic, makes the choice of a specific optimal diet a very complex issue. The meta-analysis by Li and colleagues (90) identified families of food which contain dietary factors associated with gout risk. This list should probably be used as the first screen to determine an optimal diet to minimize the negative effects of high uric acid in the blood, and subsequent formation of MSU crystals, thereby avoiding the risk to develop gout and/or reducing inflammatory crises.

EPIGENETIC MODIFIERS, NOVEL PREVENTIVE/THERAPEUTIC OPTIONS IN GOUT?

As the role of epigenetic events in various aspects of gout onset and worsening symptoms become more evident, it opens the door for the development of novel therapeutic strategies. Early studies have demonstrated that drugs acting as inhibitors of histone modifiers (HDACi, HMT or HDM inhibitors) (104, 105) and drugs modifying the DNA methylation status (65) can prevent or reduce gout symptoms at least in certain cell types. One may consider designing a combination of these epigenetic modifying drugs to be provided to gout patients to reduce MSU crystal accumulation (using HDACi), as well as inflammation (through modifying DNA methylation patterns and use of HDACi). One of the main issues to be addressed, as is the case for many other diseases, remains tissue targeting and cell-specificity. Different cell types may react in opposite ways in response to exposure to drugs such as Sodium Butyrate or Vorinostat. Several HDACi, such as valproic acid (VPA), have been tested in patients suffering neurological disorders or cancer with variable levels of success (111). Issues of toxicity on patients for the HDACi drug Trichostatin A limited its therapeutic use (112). A comparable approach to gout prevention or treatment is likely to result in similar adverse effects. As was done in the context of cancer therapy, modulation of DNA methylation using specific DNMT inhibitors (113) might also provide another option to fight gout onset and symptoms. Similarly to what may reduce the efficiency of HDACi-based treatments, targeting and cell-specificity might be a limiting factor.

If one considers prevention or mitigation of gout symptoms through controlling diet, evidence indicate that specific foods should be avoided (3, 90). Red meat, alcohol, fructose, and certain types of seafood were identified as positively correlated with gout and hyperuricemia, where dairy products and soy foods were deemed beneficial. Dairy products should be a source of short-chain FAs and soy food would provide several of the polyphenolic compounds, such as genistein, known to affect DNA methylation (89), miR expression profile (68), histone methylation (68), and histone PTM readers (67). The other polyphenolic compounds common in human diet and displaying potential beneficial effects in reducing inflammation include sulforaphane [in cruciferous plants (88, 91, 92)] resveratrol [in red wine (83, 87)], and curcumin [in turmeric (67, 70, 93)].

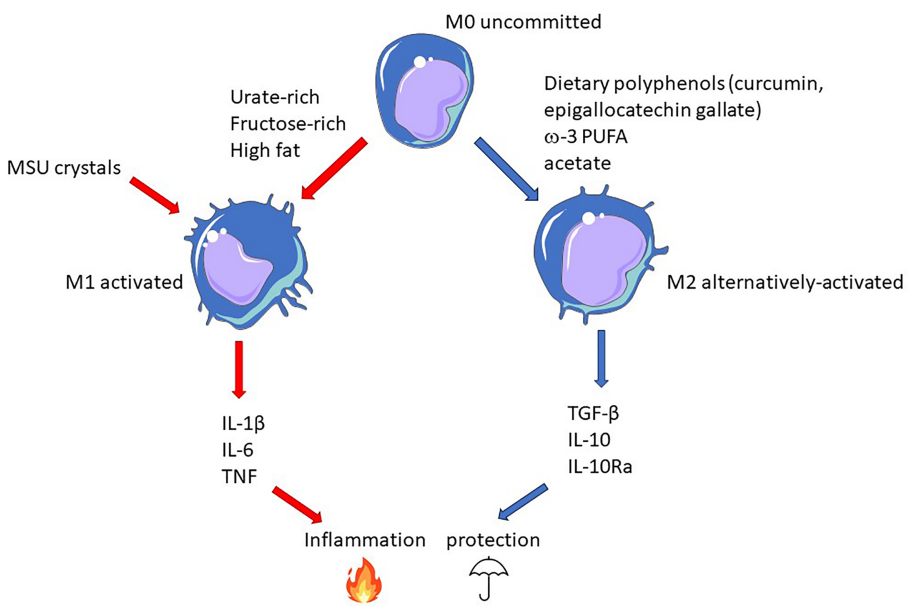

FIGURE 4 | Epigenetic-driven macrophage polarization: an important actionable lever that can be targeted by food-derived inflammatory modifiers. In this model, gout flares result from the conjunction MSU crystals and pro-inflammatory dietary components promoting M1 polarization (red arrows). On the contrary, M2-orienting nutrients favor macrophages that would be more tolerant to crystals and thus confer protection (blue arrows).

Early results from clinical trials on the effect of high ω-3 FA intake on various types of cancers have yielded results showing decreases in symptoms, as well as reduction in inflammation mostly evidenced by lowered NF-κB (114–117). A similar biological response may be expected for gout-suffering patients exposed to a therapeutic regimen of EPA and DHA using a standard dose of 3-9 gram per day (114). A sustained high ω-3 FA daily diet may be considered as a preventive method, but would likely have to be combined with other dietary restrictions.

CONCLUSION

Better knowledge of the interactions between diet-derived epigenetic modifiers will be necessary to elaborate an adapted diet, which, combined to pharmacological epigenetic modifiers, should provide long term benefits to gout patients, complementing present therapies (like uricosuric) that act on the short term. As illustrated in **Figure 4**, macrophage polarization appears as an attractive target on which diet can leverage to promote a protective environment towards the risk of MSU crystals-dependent inflammation that may occur in hyperuricemic individuals.

Many additional factors (previous infections, vaccination, physical activities, stress) which are not considered here also have an impact on trained immunity (118) and the activation status of macrophages. While the difficulty to assess and describe the contribution of these non-heritable, environmental factors on inflammation in general and gout in particular, poses a real challenge, the possibility to change them, as opposed to heritable features, makes their identification an exciting field of research and a promising preventive/therapeutic opportunity. With regards to food intake, variations around the Mediterranean diet, rich in fatty acids from fish, high in polyphenols provided by fruits, vegetables, coffee, tea and red wine, shown to reduce age-related decline of cognitive functions (59), might provide a reasonable basis for a compromise aimed at preventing gout's onset and controlling its progression.

AUTHOR CONTRIBUTIONS

All authors listed have made a substantial, direct, and intellectual contribution to the work and approved it for publication.

FUNDING

Work in PG's lab is supported by the Strasbourg's Interdisciplinary Thematic Instsitute (ITI) for Precision Medicine, TRANSPLANTEX NG, as part of the ITI 2021-2028 program of the University of Strasbourg, CNRS and INSERM, funded by IdEx Unistra (ANR-10-IDEX-0002) and SFRI-STRAT'US (ANR-20-SFRI-0012), the INSERM UMR_S 1109, the University of Strasbourg (IDEX UNISTRA), the European regional development fund (European Union) INTERREG V program (project PERSONALIS) and the MSD-Avenir grant AUTOGEN. Work in PTG's lab is supported in part by the National Science Foundation, Award Number: 1458952 (Proposal Title: RII Track-1: Gravitational Wave Astronomy and the Appalachian Freshwater Initiative), the Marshall University Genomics Core, Bioinformatics Core and the WV-INBRE grant (P20GM103434) NIH/NIGMS.

ACKNOWLEDGMENTS

The authors are thankful to Prof. Jean Sibilia (INSERM U1109 and Strasbourg University Hospital Rheumatology Department), Prof. Thomas Bardin (Hôpital Lariboisière APHP Paris Nord and Université de Paris, INSERM, UMR 1132, Bioscar, F-75010 Paris, France; French Vietnamese Research Center on Gout and Chronic Diseases, Vien Gut Medical Center, Ho Chi Minh City, Vietnam), Dr. Mariko Matsui (Pasteur Institute of New Caledonia, Nouméa) and Prof. Richard Engleton (Marshall University, Huntington, WV, USA) for their critical reading of the manuscript and helpful suggestions.

REFERENCES

1. Tang SCW. Gout: A Disease of Kings. *Contrib Nephrol* (2018) 192:77–81. doi: 10.1159/000484281
2. Bhattacharjee S. A Brief History of Gout. *Int J Rheum Dis* (2009) 12(1):61–3. doi: 10.1111/j.1756-185X.2009.01381.x
3. Major TJ, Topless RK, Dalbeth N, Merriman TR. Evaluation of the Diet Wide Contribution to Serum Urate Levels: Meta-Analysis of Population Based Cohorts. *BMJ* (2018) 363:k3951. doi: 10.1136/bmj.k3951
4. Guillen AG, Te Karu L, Singh JA, Dalbeth N. Gender and Ethnic Inequities in Gout Burden and Management. *Rheum Dis Clin North Am* (2020) 46 (4):693–703. doi: 10.1016/j.rdc.2020.07.008
5. Hamilton JP. Epigenetics: Principles and Practice. *Dig Dis* (2011) 29(2):130–5. doi: 10.1159/000323874
6. Jaenisch R, Bird A. Epigenetic Regulation of Gene Expression: How the Genome Integrates Intrinsic and Environmental Signals. *Nat Genet* (2003) 33 Suppl:245–54. doi: 10.1038/ng1089
7. Terkeltaub R. What Makes Gouty Inflammation So Variable? *BMC Med* (2017) 15(1):158. doi: 10.1186/s12916-017-0922-5
8. Zhang WZ. Why Does Hyperuricemia Not Necessarily Induce Gout? *Biomolecules* (2021) 11(2):280. doi: 10.3390/biom11020280
9. Zhong X, Peng Y, Yao C, Qing Y, Yang Q, Guo X, et al. Association of DNA Methyltransferase Polymorphisms With Susceptibility to Primary Gouty Arthritis. *BioMed Rep* (2016) 5(4):467–72. doi: 10.3892/br.2016.746
10. Punzi L, Scanu A, Galozzi P, Luisetto R, Spinella P, Scirè CA, et al. One Year in Review 2020: Gout. *Clin Exp Rheumatol* (2020) 38(5):807–21.
11. Cabău G, Crisan TO, Klück V, Popp RA, Joosten LAB. Urate-Induced Immune Programming: Consequences for Gouty Arthritis and Hyperuricemia. *Immunol Rev* (2020) 294(1):92–105. doi: 10.1111/imr.12833
12. Bekkering S, Domínguez-Andrés J, Joosten LAB, Riksen NP, Netea MG, et al. Trained Immunity: Reprogramming Innate Immunity in Health and Disease. *Annu Rev Immunol* (2021) 39:667–93. doi: 10.1146/annurev-immunol-102119-073855
13. van der Hee B, Wells JM. Microbial Regulation of Host Physiology by Short-Chain Fatty Acids. *Trends Microbiol* (2021) 29(8):700–12. doi: 10.1016/j.tim.2021.02.001
14. Vieira AT, Galvão I, Macia LM, Sernaglia ÉM, Vinolo MA, Garcia CC, et al. Dietary Fiber and the Short-Chain Fatty Acid Acetate Promote Resolution of

Neutrophilic Inflammation in a Model of Gout in Mice. *J Leukoc Biol* (2017) 101(1):275–84. doi: 10.1189/jlb.3A1015-453RRR
15. Dalbeth N, Choi HK, Joosten LAB, Khanna PP, Matsuo H, Perez-Ruiz F, et al. Gout. *Nat Rev Dis Primers* (2019) 5(1):69. doi: 10.1038/s41572-019-0115-y
16. Guo X, Chen Y, Li Q, Yang X, Zhao G, Peng Y, et al. Studies on Hepatotoxicity and Toxicokinetics of Colchicine. *J Biochem Mol Toxicol* (2019) 33(9):e22366. doi: 10.1002/jbt.22366
17. Oliviero F, Scanu A. How Factors Involved in the Resolution of Crystal-Induced Inflammation Target IL-1β. *Front Pharmacol* (2017) 8:164. doi: 10.3389/fphar.2017.00164
18. Gray SG. Epigenetic-Based Immune Intervention for Rheumatic Diseases. *Epigenomics* (2014) 6(2):253–71. doi: 10.2217/epi.13.87
19. Garcia BA, Busby SA, Shabanowitz J, Hunt DF, Mishra N. Resetting the Epigenetic Histone Code in the MRL-Lpr/Lpr Mouse Model of Lupus by Histone Deacetylase Inhibition. *J Proteome Res* (2005) 4(6):2032–42. doi: 10.1021/pr050188r
20. Willebrand R, Kleinewietfeld M. The Role of Salt for Immune Cell Function and Disease. *Immunology* (2018) 154(3):346–53. doi: 10.1111/imm.12915
21. Mafra D, Borges NA, Lindholm B, Shiels PG, Evenepoel P, Stenvinkel P. Food as Medicine: Targeting the Uraemic Phenotype in Chronic Kidney Disease. *Nat Rev Nephrol* (2021) 17(3):153–71. doi: 10.1038/s41581-020-00345-8
22. Christ A, Lauterbach M, Latz E. Western Diet and the Immune System: An Inflammatory Connection. *Immunity* (2019) 51(5):794–811. doi: 10.1016/j.immuni.2019.09.020
23. Keenan RT. The Biology of Urate. *Semin Arthritis Rheum* (2020) 50(3s):S2–s10. doi: 10.1016/j.semarthrit.2020.04.007
24. Álvarez-Lario B, Macarrón-Vicente J. Uric Acid and Evolution. *Rheumatol (Oxford)* (2010) 49(11):2010–5. doi: 10.1093/rheumatology/keq204
25. Stamostergiou J, Theodoridis X, Ganochoriti V, Bogdanos DP, Sakkas LI. The Role of the Mediterranean Diet in Hyperuricemia and Gout. *Mediterr J Rheumatol* (2018) 29(1):21–5. doi: 10.31138/mjr.29.1.21
26. Benn CL, Dua P, Gurrell R, Loudon P, Pike A, Storer RI, et al. Physiology of Hyperuricemia and Urate-Lowering Treatments. *Front Med (Lausanne)* (2018) 5:160. doi: 10.3389/fmed.2018.00160
27. Ayoub-Charette S, Liu Q, Khan TA, Au-Yeung F, Blanco Mejia S, de Souza RJ, et al. Important Food Sources of Fructose-Containing Sugars and Incident Gout: A Systematic Review and Meta-Analysis of Prospective Cohort Studies. *BMJ Open* (2019) 9(5):e024171. doi: 10.1136/bmjopen-2018-024171
28. Ragab G, Elshahaly M, Bardin T. Gout: An Old Disease in New Perspective - A Review. *J Adv Res* (2017) 8(5):495–511. doi: 10.1016/j.jare.2017.04.008
29. Hong F, Zheng A, Xu P, Wang J, Xue T, Dai S, et al. High-Protein Diet Induces Hyperuricemia in a New Animal Model for Studying Human Gout. *Int J Mol Sci* (2020) 21(6) 21(6):2147. doi: 10.3390/ijms21062147
30. Belanger MJ, Wee CC, Mukamal KJ, Miller ER, Sacks FM, Appel LJ, et al. Effects of Dietary Macronutrients on Serum Urate: Results From the OmniHeart Trial. *Am J Clin Nutr* (2021) 113(6):1593–9. doi: 10.1093/ajcn/nqaa424
31. Roddy E, Choi HK. Epidemiology of Gout. *Rheum Dis Clin North Am* (2014) 40(2):155–75. doi: 10.1016/j.rdc.2014.01.001
32. Bai L, Zhou JB, Zhou T, Newson RB, Cardoso MA. Incident Gout and Weight Change Patterns: A Retrospective Cohort Study of US Adults. *Arthritis Res Ther* (2021) 23(1):69. doi: 10.1186/s13075-021-02461-7
33. Lin X, Shao T, Wen X, Wang M, Wen C, He Z. Combined Effects of MSU Crystals Injection and High Fat-Diet Feeding on the Establishment of a Gout Model in C57BL/6 Mice. *Adv Rheumatol* (2020) 60(1):52. doi: 10.1186/s42358-020-00155-3
34. Guo Z, Zhang J, Wang Z, Ang KY, Huang S, Hou Q, et al. Intestinal Microbiota Distinguish Gout Patients From Healthy Humans. *Sci Rep* (2016) 6:20602. doi: 10.1038/srep20602
35. Vieira AT, Macia L, Galvão I, Martins FS, Canesso MC, Amaral FA, et al. A Role for Gut Microbiota and the Metabolite-Sensing Receptor GPR43 in a Murine Model of Gout. *Arthritis Rheumatol* (2015) 67(6):1646–56. doi: 10.1002/art.39107
36. Zhang M, Zhang Y, Terkeltaub R, Chen C, Neogi T. Effect of Dietary and Supplemental Omega-3 Polyunsaturated Fatty Acids on Risk of Recurrent Gout Flares. *Arthritis Rheumatol* (2019) 71(9):1580–6. doi: 10.1002/art.40896
37. Martinon F, Pétrilli V, Mayor A, Tardivel A, Tschopp J. Gout-Associated Uric Acid Crystals Activate the NALP3 Inflammasome. *Nature* (2006) 440 (7081):237–41. doi: 10.1038/nature04516
38. So AK, Martinon F. Inflammation in Gout: Mechanisms and Therapeutic Targets. *Nat Rev Rheumatol* (2017) 13(11):639–47. doi: 10.1038/nrrheum.2017.155
39. Holland R, McGill NW. Comprehensive Dietary Education in Treated Gout Patients Does Not Further Improve Serum Urate. *Intern Med J* (2015) 45 (2):189–94. doi: 10.1111/imj.12661
40. Topless RKG, Major TJ, Florez JC, Hirschhorn JN, Cadzow M, Dalbeth N, et al. The Comparative Effect of Exposure to Various Risk Factors on the Risk of Hyperuricaemia: Diet Has a Weak Causal Effect. *Arthritis Res Ther* (2021) 23(1):75. doi: 10.1186/s13075-021-02444-8
41. Mariotte A, De Cauwer A, Po C, Abou-Faycal C, Pichot A, Paul N, et al. A Mouse Model of MSU-Induced Acute Inflammation *In Vivo* Suggests Imiquimod-Dependent Targeting of Il-1beta as Relevant Therapy for Gout Patients. *Theranostics* (2020) 10(5):2158–71. doi: 10.7150/thno.40650
42. Joosten LA, Ea HK, Netea MG, Busso N. Interleukin-1beta Activation During Acute Joint Inflammation: A Limited Role for the NLRP3 Inflammasome *In Vivo*. *Joint Bone Spine* (2011) 78(2):107–10. doi: 10.1016/j.jbspin.2010.11.004
43. Joosten LA, Netea MG, Mylona E, Koenders MI, Malireddi RK, Oosting M, et al. Engagement of Fatty Acids With Toll-Like Receptor 2 Drives Interleukin-1beta Production *via* the ASC/caspase 1 Pathway in Monosodium Urate Monohydrate Crystal-Induced Gouty Arthritis. *Arthritis Rheum* (2010) 62(11):3237–48. doi: 10.1002/art.27667
44. Bodofsky S, Merriman TR, Thomas TJ, Schlesinger N. Advances in Our Understanding of Gout as an Auto-Inflammatory Disease. *Semin Arthritis Rheum* (2020) 50(5):1089–100. doi: 10.1016/j.semarthrit.2020.06.015
45. Major TJ, Dalbeth N, Stahl EA, Merriman TR. An Update on the Genetics of Hyperuricaemia and Gout. *Nat Rev Rheumatol* (2018) 14(6):341–53. doi: 10.1038/s41584-018-0004-x
46. Krishnan E, Lessov-Schlaggar CN, Krasnow RE, Swan GE. Nature *Versus* Nurture in Gout: A Twin Study. *Am J Med* (2012) 125(5):499–504. doi: 10.1016/j.amjmed.2011.11.010
47. Cadzow M, Merriman TR, Dalbeth N. Performance of Gout Definitions for Genetic Epidemiological Studies: Analysis of UK Biobank. *Arthritis Res Ther* (2017) 19(1):181. doi: 10.1186/s13075-017-1390-1
48. Dalbeth N, Stamp LK, Merriman TR. The Genetics of Gout: Towards Personalised Medicine? *BMC Med* (2017) 15(1):108. doi: 10.1186/s12916-017-0878-5
49. Ichida K, Hosoyamada M, Hisatome I, Enomoto A, Hikita M, Endou H, et al. Clinical and Molecular Analysis of Patients With Renal Hypouricemia in Japan-Influence of URAT1 Gene on Urinary Urate Excretion. *J Am Soc Nephrol* (2004) 15(1):164–73. doi: 10.1097/01.ASN.0000105320.04395.D0
50. Lee MG, Hsu TC, Chen SC, Lee YC, Kuo PH, Yang JH, et al. Integrative Genome-Wide Association Studies of eQTL and GWAS Data for Gout Disease Susceptibility. *Sci Rep* (2019) 9(1):4981. doi: 10.1038/s41598-019-41434-4
51. Placek K, Schultze JL, Aschenbrenner AC. Epigenetic Reprogramming of Immune Cells in Injury, Repair, and Resolution. *J Clin Invest* (2019) 129 (8):2994–3005. doi: 10.1172/JCI124619
52. Kawamura Y, Nakaoka H, Nakayama A, Okada Y, Yamamoto K, Higashino T, et al. Genome-Wide Association Study Revealed Novel Loci Which Aggravate Asymptomatic Hyperuricaemia Into Gout. *Ann Rheum Dis* (2019) 78(10):1430–7. doi: 10.1136/annrheumdis-2019-215521
53. Li G, Zhang H, Ma H, Qu S, Xing Q, Wang G. MiR-221-5p is Involved in the Regulation of Inflammatory Responses in Acute Gouty Arthritis by Targeting IL-1β. *Int J Rheum Dis* (2021) 24(3):335–40. doi: 10.1111/1756-185X.14028
54. Li X, Pan Y, Li W, Guan P, You C, et al. The Role of Noncoding RNAs in Gout. *Endocrinology* (2020) 161(11) 161(11):bqaa165. doi: 10.1210/endocr/bqaa165
55. Tseng CC, Liao WT, Wong MC, Chen CJ, Lee SC, Yen JH, et al. Cell Lineage-Specific Methylome and Genome Alterations in Gout. *Aging (Albany NY)* (2021) 13(3):3843–65. doi: 10.18632/aging.202353

56. Fanucchi S, Domínguez-Andrés J, Joosten LAB, Netea MG, Mhlanga MM. The Intersection of Epigenetics and Metabolism in Trained Immunity. *Immunity* (2021) 54(1):32–43. doi: 10.1016/j.immuni.2020.10.011
57. Camilli G, Bohm M, Piffer AC, Lavenir R, Williams DL, Neven B, et al. β-Glucan-Induced Reprogramming of Human Macrophages Inhibits NLRP3 Inflammasome Activation in Cryopyrinopathies. *J Clin Invest* (2020) 130 (9):4561–73. doi: 10.1172/JCI134778
58. Crişan TO, Cleophas MC, Oosting M, Lemmers H, Toenhake-Dijkstra H, Netea MG, et al. Soluble Uric Acid Primes TLR-Induced Proinflammatory Cytokine Production by Human Primary Cells *via* Inhibition of IL-1ra. *Ann Rheum Dis* (2016) 75(4):755–62. doi: 10.1136/annrheumdis-2014-206564
59. Román GC, Jackson RE, Gadhia R, Román AN, Reis J. Mediterranean Diet: The Role of Long-Chain Omega-3 Fatty Acids in Fish; Polyphenols in Fruits, Vegetables, Cereals, Coffee, Tea, Cacao and Wine; Probiotics and Vitamins in Prevention of Stroke, Age-Related Cognitive Decline, and Alzheimer Disease. *Rev Neurol (Paris)* (2019) 175(10):724–41. doi: 10.1016/j.neurol.2019.08.005
60. Xiang N, Zhao R, Song G, Zhong W. Selenite Reactivates Silenced Genes by Modifying DNA Methylation and Histones in Prostate Cancer Cells. *Carcinogenesis* (2008) 29(11):2175–81. doi: 10.1093/carcin/bgn179
61. Davis CD, Uthus EO, Finley JW. Dietary Selenium and Arsenic Affect DNA Methylation *In Vitro* in Caco-2 Cells and *In Vivo* in Rat Liver and Colon. *J Nutr* (2000) 130(12):2903–9. doi: 10.1093/jn/130.12.2903
62. Ito K, Lim S, Caramori G, Cosio B, Chung KF, Adcock IM, et al. A Molecular Mechanism of Action of Theophylline: Induction of Histone Deacetylase Activity to Decrease Inflammatory Gene Expression. *Proc Natl Acad Sci U.S.A.* (2002) 99(13):8921–6. doi: 10.1073/pnas.132556899
63. Lee WJ, Shim JY, Zhu BT. Mechanisms for the Inhibition of DNA Methyltransferases by Tea Catechins and Bioflavonoids. *Mol Pharmacol* (2005) 68(4):1018–30. doi: 10.1124/mol.104.008367
64. Fang M, Chen D, Yang CS. Dietary Polyphenols may Affect DNA Methylation. *J Nutr* (2007) 137(1 Suppl):223S–8S. doi: 10.1093/jn/137.1.223S
65. Vanden Berghe W. Epigenetic Impact of Dietary Polyphenols in Cancer Chemoprevention: Lifelong Remodeling of Our Epigenomes. *Pharmacol Res* (2012) 65(6):565–76. doi: 10.1016/j.phrs.2012.03.007
66. Kala R, Tollefsbol TO. A Novel Combinatorial Epigenetic Therapy Using Resveratrol and Pterostilbene for Restoring Estrogen Receptor-Alpha (ERalpha) Expression in ERalpha-Negative Breast Cancer Cells. *PloS One* (2016) 11(5):e0155057. doi: 10.1371/journal.pone.0155057
67. Mirza S, Sharma G, Parshad R, Gupta SD, Pandya P, Ralhan R. Expression of DNA Methyltransferases in Breast Cancer Patients and to Analyze the Effect of Natural Compounds on DNA Methyltransferases and Associated Proteins. *J Breast Cancer* (2013) 16(1):23–31. doi: 10.4048/jbc.2013.16.1.23
68. Hirata H, Hinoda Y, Shahryari V, Deng G, Tanaka Y, Tabatabai ZL, et al. Genistein Downregulates onco-miR-1260b and Upregulates Sfrp1 and Smad4 *via* Demethylation and Histone Modification in Prostate Cancer Cells. *Br J Cancer* (2014) 110(6):1645–54. doi: 10.1038/bjc.2014.48
69. Wolff GL, Kodell RL, Moore SR, Cooney CA. Maternal Epigenetics and Methyl Supplements Affect Agouti Gene Expression in Avy/a Mice. *FASEB J* (1998) 12 (11):949–57. doi: 10.1096/fasebj.12.11.949
70. Mirzaei H, Masoudifar A, Sahebkar A, Zare N, Sadri Nahand J, Rashidi B, et al. MicroRNA: A Novel Target of Curcumin in Cancer Therapy. *J Cell Physiol* (2018) 233(4):3004–15. doi: 10.1002/jcp.26055
71. Nagaraju GP, Zhu S, Wen J, Farris AB, Adsay VN, Diaz R, et al. Novel Synthetic Curcumin Analogues EF31 and UBS109 are Potent DNA Hypomethylating Agents in Pancreatic Cancer. *Cancer Lett* (2013) 341 (2):195–203. doi: 10.1016/j.canlet.2013.08.002
72. Kanwal R, Datt M, Liu X, Gupta S. Dietary Flavones as Dual Inhibitors of DNA Methyltransferases and Histone Methyltransferases. *PloS One* (2016) 11(9):e0162956. doi: 10.1371/journal.pone.0162956
73. Tapp HS, Commane DM, Bradburn DM, Arasaradnam R, Mathers JC, Johnson IT, et al. Nutritional Factors and Gender Influence Age-Related DNA Methylation in the Human Rectal Mucosa. *Aging Cell* (2013) 12 (1):148–55. doi: 10.1111/acel.12030
74. Fetahu IS, Hobaus J, Kallay E. Vitamin D and the Epigenome. *Front Physiol* (2014) 5:164. doi: 10.3389/fphys.2014.00164
75. Young JI, Zuchner S, Wang G. Regulation of the Epigenome by Vitamin C. *Annu Rev Nutr* (2015) 35:545–64. doi: 10.1146/annurev-nutr-071714-034228
76. Joshi S, Pantalena LC, Liu XK, Gaffen SL, Liu H, Rohowsky-Kochan C, et al. 1,25-Dihydroxyvitamin D(3) Ameliorates Th17 Autoimmunity *via* Transcriptional Modulation of Interleukin-17A. *Mol Cell Biol* (2011) 31 (17):3653–69. doi: 10.1128/MCB.05020-11
77. Patterson WL3rd, Georgel PT. Breaking the Cycle: The Role of Omega-3 Polyunsaturated Fatty Acids in Inflammation-Driven Cancers. *Biochem Cell Biol* (2014) 92(5):321–8. doi: 10.1139/bcb-2013-0127
78. Beklemisheva AA, Fang Y, Feng J, Ma X, Dai W, Chiao JW. Epigenetic Mechanism of Growth Inhibition Induced by Phenylhexyl Isothiocyanate in Prostate Cancer Cells. *Anticancer Res* (2006) 26(2A):1225–30.
79. Bora-Tatar G, Dayangaç-Erden D, Demir AS, Dalkara S, Yelekçi K, Erdem-Yurter H. Molecular Modifications on Carboxylic Acid Derivatives as Potent Histone Deacetylase Inhibitors: Activity and Docking Studies. *Bioorg Med Chem* (2009) 17(14):5219–28. doi: 10.1016/j.bmc.2009.05.042
80. Berger A, Venturelli S, Kallnischkies M, Böcker A, Busch C, Weiland T, et al. Kaempferol, a New Nutrition-Derived Pan-Inhibitor of Human Histone Deacetylases. *J Nutr Biochem* (2013) 24(6):977–85. doi: 10.1016/j.jnutbio.2012.07.001
81. Pogribny IP, James SJ, Beland FA. Molecular Alterations in Hepatocarcinogenesis Induced by Dietary Methyl Deficiency. *Mol Nutr Food Res* (2012) 56(1):116–25. doi: 10.1002/mnfr.201100524
82. Joosten LA, Crişan TO, Azam T, Cleophas MC, Koenders MI, van de Veerdonk FL, et al. Alpha-1-Anti-Trypsin-Fc Fusion Protein Ameliorates Gouty Arthritis by Reducing Release and Extracellular Processing of IL-1beta and by the Induction of Endogenous IL-1ra. *Ann Rheum Dis* (2016) 75 (6):1219–27. doi: 10.1136/annrheumdis-2014-206966
83. Xin Y, Zhang H, Jia Z, Ding X, Sun Y, Wang Q, et al. Resveratrol Improves Uric Acid-Induced Pancreatic Beta-Cells Injury and Dysfunction Through Regulation of miR-126. *BioMed Pharmacother* (2018) 102:1120–6. doi: 10.1016/j.biopha.2018.03.172
84. Nunez Lopez YO, Pittas AG, Pratley RE, Seyhan AA. Circulating Levels of miR-7, miR-152 and miR-192 Respond to Vitamin D Supplementation in Adults With Prediabetes and Correlate With Improvements in Glycemic Control. *J Nutr Biochem* (2017) 49:117–22. doi: 10.1016/j.jnutbio.2017.08.007
85. Arola-Arnal A, Blade C. Proanthocyanidins Modulate microRNA Expression in Human HepG2 Cells. *PloS One* (2011) 6(10):e25982. doi: 10.1371/journal.pone.0025982
86. Bosviel R, Durif J, Déchelotte P, Bignon YJ, Bernard-Gallon D. Epigenetic Modulation of BRCA1 and BRCA2 Gene Expression by Equol in Breast Cancer Cell Lines. *Br J Nutr* (2012) 108(7):1187–93. doi: 10.1017/S000711451100657X
87. Qin W, Zhang K, Clarke K, Weiland T, Sauter ER. Methylation and miRNA Effects of Resveratrol on Mammary Tumors *vs*. *Normal Tissue Nutr Cancer* (2014) 66(2):270–7. doi: 10.1080/01635581.2014.868910
88. Royston KJ, Paul B, Nozell S, Rajbhandari R, Tollefsbol TO. Withaferin A and Sulforaphane Regulate Breast Cancer Cell Cycle Progression Through Epigenetic Mechanisms. *Exp Cell Res* (2018) 368(1):67–74. doi: 10.1016/j.yexcr.2018.04.015
89. Sundaram MK, Unni S, Somvanshi P, Bhardwaj T, Mandal RK, Hussain A, et al. Genistein Modulates Signaling Pathways and Targets Several Epigenetic Markers in HeLa Cells. *Genes (Basel)* (2019) 10(12):955. doi: 10.3390/genes10120955
90. Li R, Yu K, Li C. Dietary Factors and Risk of Gout and Hyperuricemia: A Meta-Analysis and Systematic Review. *Asia Pac J Clin Nutr* (2018) 27 (6):1344–56. doi: 10.6133/apjcn.201811_27(6).0022
91. Gao L, Cheng D, Yang J, Wu R, Li W, Kong AN. Sulforaphane Epigenetically Demethylates the CpG Sites of the miR-9-3 Promoter and Reactivates miR-9-3 Expression in Human Lung Cancer A549 Cells. *J Nutr Biochem* (2018) 56:109–15. doi: 10.1016/j.jnutbio.2018.01.015
92. Li Y, Meeran SM, Tollefsbol TO. Combinatorial Bioactive Botanicals Re-Sensitize Tamoxifen Treatment in ER-Negative Breast Cancer *via* Epigenetic Reactivation of ERalpha Expression. *Sci Rep* (2017) 7(1):9345. doi: 10.1038/s41598-017-09764-3

93. Zheng J, Wu C, Lin Z, Guo Y, Shi L, Dong P, et al. Curcumin Up-Regulates Phosphatase and Tensin Homologue Deleted on Chromosome 10 Through microRNA-Mediated Control of DNA Methylation–a Novel Mechanism Suppressing Liver Fibrosis. *FEBS J* (2014) 281(1):88–103. doi: 10.1111/febs.12574
94. Abbas A, Witte T, Patterson WL 3rd, Fahrmann JF, Guo K, Hur J, et al. Epigenetic Reprogramming Mediated by Maternal Diet Rich in Omega-3 Fatty Acids Protects From Breast Cancer Development in F1 Offspring. *Front Cell Dev Biol* (2021) 9(1517) 9:682593. doi: 10.3389/fcell.2021.682593
95. Yin R, Mao SQ, Zhao B, Chong Z, Yang Y, Zhao C, et al. Ascorbic Acid Enhances Tet-Mediated 5-Methylcytosine Oxidation and Promotes DNA Demethylation in Mammals. *J Am Chem Soc* (2013) 135(28):10396–403. doi: 10.1021/ja4028346
96. Mentch SJ, Locasale JW. One-Carbon Metabolism and Epigenetics: Understanding the Specificity. *Ann N Y Acad Sci* (2016) 1363:91–8. doi: 10.1111/nyas.12956
97. Fan P, He L, Hu N, Luo J, Zhang J, Mo LF, et al. Effect of 1,25-(OH)2D3 on Proliferation of Fibroblast-Like Synoviocytes and Expressions of Pro-Inflammatory Cytokines Through Regulating MicroRNA-22 in a Rat Model of Rheumatoid Arthritis. *Cell Physiol Biochem* (2017) 42(1):145–55. doi: 10.1159/000477123
98. Balaraman S, Idrus NM, Miranda RC, Thomas JD. Postnatal Choline Supplementation Selectively Attenuates Hippocampal microRNA Alterations Associated With Developmental Alcohol Exposure. *Alcohol* (2017) 60:159–67. doi: 10.1016/j.alcohol.2016.12.006
99. Claycombe KJ, Brissette CA, Ghribi O. Epigenetics of Inflammation, Maternal Infection, and Nutrition. *J Nutr* (2015) 145(5):1109S–15S. doi: 10.3945/jn.114.194639
100. Jin HM, Kim TJ, Choi JH, Kim MJ, Cho YN, Nam KI, et al. MicroRNA-155 as a Proinflammatory Regulator *via* SHIP-1 Down-Regulation in Acute Gouty Arthritis. *Arthritis Res Ther* (2014) 16(2):R88. doi: 10.1186/ar4531
101. Kolb AF, Petrie L. Folate Deficiency Enhances the Inflammatory Response of Macrophages. *Mol Immunol* (2013) 54(2):164–72. doi: 10.1016/j.molimm.2012.11.012
102. Lim B, Ju H, Kim M, Kang C. Increased Genetic Susceptibility to Intestinal-Type Gastric Cancer Is Associated With Increased Activity of the RUNX3 Distal Promoter. *Cancer* (2011) 117(22):5161–71. doi: 10.1002/cncr.26161
103. Kleinnijenhuis J, Quintin J, Preijers F, Joosten LA, Ifrim DC, Saeed S, et al. Bacille Calmette-Guerin Induces NOD2-Dependent Nonspecific Protection From Reinfection *via* Epigenetic Reprogramming of Monocytes. *Proc Natl Acad Sci U.S.A.* (2012) 109(43):17537–42. doi: 10.1073/pnas.1202870109
104. Cleophas MCP, Crişan TO, Klück V, Hoogerbrugge N, Netea-Maier RT, Dinarello CA, et al. Romidepsin Suppresses Monosodium Urate Crystal-Induced Cytokine Production Through Upregulation of Suppressor of Cytokine Signaling 1 Expression. *Arthritis Res Ther* (2019) 21(1):50. doi: 10.1186/s13075-019-1834-x
105. Cleophas MC, Crişan TO, Lemmers H, Toenhake-Dijkstra H, Fossati G, Jansen TL, et al. Suppression of Monosodium Urate Crystal-Induced Cytokine Production by Butyrate is Mediated by the Inhibition of Class I Histone Deacetylases. *Ann Rheum Dis* (2016) 75(3):593–600. doi: 10.1136/annrheumdis-2014-206258
106. Galdieri L, Vancura A. Acetyl-CoA Carboxylase Regulates Global Histone Acetylation. *J Biol Chem* (2012) 287(28):23865–76. doi: 10.1074/jbc.M112.380519
107. Carrer A, Parris JLD, Trefely S, Henry RA, Montgomery DC, Torres A, et al. Impact of a High-Fat Diet on Tissue Acyl-CoA and Histone Acetylation Levels. *J Biol Chem* (2017) 292(8):3312–22. doi: 10.1074/jbc.M116.750620
108. Zhao Q, Liu Y, Zhang N, Hu M, Zhang H, Joshi T, et al. Evidence for Plant-Derived xenomiRs Based on a Large-Scale Analysis of Public Small RNA Sequencing Data From Human Samples. *PloS One* (2018) 13(6):e0187519. doi: 10.1371/journal.pone.0187519
109. Tosar JP, Rovira C, Naya H, Cayota A. Mining of Public Sequencing Databases Supports a non-Dietary Origin for Putative Foreign miRNAs: Underestimated Effects of Contamination in NGS. *Rna* (2014) 20(6):754–7. doi: 10.1261/rna.044263.114
110. Mar-Aguilar F, Arreola-Triana A, Mata-Cardona D, Gonzalez-Villasana V, Rodríguez-Padilla C, Reséndez-Pérez D. Evidence of Transfer of miRNAs From the Diet to the Blood Still Inconclusive. *PeerJ* (2020) 8:e9567. doi: 10.7717/peerj.9567
111. Hassell KN. Histone Deacetylases and Their Inhibitors in Cancer Epigenetics. *Diseases* (2019) 7(4):57. doi: 10.3390/diseases7040057
112. Licciardi PV, Ververis K, Karagiannis TC. Histone Deacetylase Inhibition and Dietary Short-Chain Fatty Acids. *ISRN Allergy* (2011) 2011:869647. doi: 10.5402/2011/869647
113. Myasoedova VA, Sukhorukov V, Grechko AV, Zhang D, Romanenko E, Orekhov V, et al. Inhibitors of DNA Methylation and Histone Deacetylation as Epigenetically Active Drugs for Anticancer Therapy. *Curr Pharm Des* (2019) 25(6):635–41. doi: 10.2174/1381612825666190405144026
114. Fahrmann JF, Ballester OF, Ballester G, Witte TR, Salazar AJ, Kordusky B, et al. Inhibition of Nuclear Factor Kappa B Activation in Early-Stage Chronic Lymphocytic Leukemia by Omega-3 Fatty Acids. *Cancer Invest* (2013) 31(1):24–38. doi: 10.3109/07357907.2012.743553
115. Hardman WE, Ion G. Suppression of Implanted MDA-MB 231 Human Breast Cancer Growth in Nude Mice by Dietary Walnut. *Nutr Cancer* (2008) 60(5):666–74. doi: 10.1080/01635580802065302
116. Fahrmann JF, Hardman WE. Omega 3 Fatty Acids Increase the Chemo-Sensitivity of B-CLL-Derived Cell Lines EHEB and MEC-2 and of B-PLL-Derived Cell Line JVM-2 to Anti-Cancer Drugs Doxorubicin, Vincristine and Fludarabine. *Lipids Health Dis* (2013) 12:36. doi: 10.1186/1476-511X-12-36
117. D'Angelo S, Motti ML, Meccariello R. Omega-3 and Omega-6 Polyunsaturated Fatty Acids, Obesity and Cancer. *Nutrients* (2020) 12(9):2751. doi: 10.3390/nu12092751
118. Bajpai G, Nahrendorf M. Infectious and Lifestyle Modifiers of Immunity and Host Resilience. *Immunity* (2021) 54(6):1110–22. doi: 10.1016/j.immuni.2021.05.011

Conflict of Interest: The authors declare that the research was conducted in the absence of any commercial or financial relationships that could be construed as a potential conflict of interest.

frontiers in Immunology

ORIGINAL RESEARCH
published: 28 October 2021
doi: 10.3389/fimmu.2021.762016

Galectin-9 Regulates Monosodium Urate Crystal-Induced Gouty Inflammation Through the Modulation of Treg/Th17 Ratio

Adel Abo Mansour[1,2†], *Federica Raucci*[3†], *Anella Saviano*[3], *Samantha Tull*[1], *Francesco Maione*[3*] *and Asif Jilani Iqbal*[1,3*]

[1] Institute of Cardiovascular Sciences (ICVS), College of Medical and Dental Sciences, University of Birmingham, Birmingham, United Kingdom, [2] Department of Clinical Laboratory Sciences, College of Applied Medical Sciences, King Khalid University, Abha, Saudi Arabia, [3] ImmunoPharmaLab, Department of Pharmacy, School of Medicine and Surgery, University of Naples Federico II, Naples, Italy

OPEN ACCESS

Edited by:
Xiaoxia Zhu,
Fudan University, China

Reviewed by:
Ursula Norman,
Monash University, Australia
Lorenzo Di Cesare Mannelli,
University of Florence, Italy

***Correspondence:**
Asif Jilani Iqbal
A.J.Iqbal@bham.ac.uk
Francesco Maione
francesco.maione@unina.it

[†]These authors share first authorship

Specialty section:
This article was submitted to Autoimmune and Autoinflammatory Disorders, a section of the journal Frontiers in Immunology

Received: 20 August 2021
Accepted: 14 October 2021
Published: 28 October 2021

Citation:
Mansour AA, Raucci F, Saviano A, Tull S, Maione F and Iqbal AJ (2021) Galectin-9 Regulates Monosodium Urate Crystal-Induced Gouty Inflammation Through the Modulation of Treg/Th17 Ratio. Front. Immunol. 12:762016. doi: 10.3389/fimmu.2021.762016

Gout is caused by depositing monosodium urate (MSU) crystals within the articular area. The infiltration of neutrophils and monocytes drives the initial inflammatory response followed by lymphocytes. Interestingly, emerging evidence supports the view that *in situ* imbalance of T helper 17 cells (Th17)/regulatory T cells (Treg) impacts the subsequent damage to target tissues. Galectin-9 (Gal-9) is a modulator of innate and adaptive immunity with both pro- and anti-inflammatory functions, dependent upon its expression and cellular location. However, the specific cellular and molecular mechanisms by which Gal-9 modulates the inflammatory response in the onset and progression of gouty arthritis has yet to be elucidated. In this study, we sought to comprehensively characterise the functional role of exogenous Gal-9 in an *in vivo* model of MSU crystal-induced gouty inflammation by monitoring *in situ* neutrophils, monocytes and Th17/Treg recruited phenotypes and related cyto-chemokines profile. Treatment with Gal-9 revealed a dose-dependent reduction in joint inflammation scores, knee joint oedema and expression of different pro-inflammatory cyto-chemokines. Furthermore, flow cytometry analysis highlighted a significant modulation of infiltrating inflammatory monocytes ($CD11b^+/CD115^+/LY6\text{-}C^{hi}$) and Th17 ($CD4^+/IL\text{-}17^+$)/Treg ($CD4^+/CD25^+/FOXP\text{-}3^+$) cells following Gal-9 treatment. Collectively the results presented in this study indicate that the administration of Gal-9 could provide a new therapeutic strategy for preventing tissue damage in gouty arthritic inflammation and, possibly, in other inflammatory-based diseases.

Keywords: galectin-9 (Gal-9), gout, MSU crystals, inflammation, cyto-chemokines

Abbreviations: APCs, antigen-presenting cells; BLC, B lymphocyte chemoattractant; c5/c5a, component 5a; CRDs, carbohydrate recognition domains; CTRL, Control; DMSO, dimethyl sulfoxide; G-CSF, granulocyte colony-stimulating factor; Gal-, Galectin-; FBS, fetal bovine serum; i.a., intra-articular; IL-, interleukin-; JE, junctional epithelium; KC, keratinocyte chemoattractant; MCP-5, monocytes chemoattractant protein-5; M-CSF, macrophage colony-stimulating factor; MAPK, mitogen-activated protein kinase; MIG, monokine induced by interferon-γ MIP, macrophage inflammatory protein; MSU, monosodium urate; NETs, neutrophil extracellular traps; PDIs, protein disulfide isomerase; RA, rheumatoid arthritis; SDF-1, IL-1β stromal cell-derived factor-1; sICAM-1, intercellular adhesion molecular-1; TGF-β, transforming growth factor-β; Th17, T helper 17 cells; TIM-3, T cell immunoglobulin mucin-3; TIMP-1, metallopeptidase inhibitor-1; TNF-α, tumor necrosis factor-α; Treg, regulatory T-cells; TREM-1, triggering receptor expressed on myeloid cells-1.

INTRODUCTION

Inflammation is broadly defined as a host response to homeostatic imbalance triggered by conditions such as infection, tissue injury and noxious stimuli, including exposure to chemicals or radiation (1). One of the preliminary steps in the onset of inflammation is the recruitment of leukocytes to the site of injury or infection (2). Leukocyte recruitment is a highly intricate process comprising of several well-defined steps which include capture, rolling, adhesion/activation, intraluminal crawling and paracellular or transcellular transmigration (3). The infiltration of innate immune cells drives the initial inflammatory response followed by lymphocytes (3, 4). Emerging evidence supports the view that, in different inflammatory-based responses such as gouty arthritis, systemic imbalance of Th17/Treg induces their infiltration *in situ* and related damage to target tissues (5, 6). Tregs represent a small subset of T cells that control both innate and adaptive immune responses and are critical in maintaining self-tolerance and homeostasis (7). Treg have been shown to inhibit osteoclastogenesis by secreting immunosuppressive cytokines interleukin (IL)-10, transforming growth factor-β (TGF-β), and reducing gout bone damage (8, 9). Moreover, an increase in Treg levels has been shown to prevent an excessive immune response, while their loss is associated with major autoimmune diseases (10, 11). In contrast, Th17 cells are a subset of $CD4^+$ T cells, characterised by IL-17 cytokine production that plays a powerful pro-inflammatory role in the immune system amplifying, rather than dampening, the progression of the inflammatory cascade (12). Indeed, the Th17/Treg balance provides a basis for understanding the immunological mechanisms that induce and regulate autoimmune and some inflammatory-based diseases (13).

Galectins are a family of carbohydrate-binding proteins that have a range of physiological functions, including regulation of cellular migration, cell cycle, proliferation, apoptosis and signal transduction (14). Galectins are found in the cytoplasm as well as the nucleus and are structurally characterised by the presence of one or two conserved ~130 amino-acid long carbohydrate recognition domains (CRDs) (15). To date, 15 genes encoding galectins have been identified in mammals, among which 12 have been identified in humans. The galectins can be broadly categorised into three subtypes: (a) prototype single CRD-galectins with the ability to form non-covalent homodimers (Gal-1, -2, -7, -10, -13, -14) in solution *via* non-covalent interaction, (b) chimeric-type comprising of a single CRD at the c-terminal and an n-terminal domain with an intrinsically disordered sequence (Gly-Pro-Tyr rich) which aids in oligomerisation (Gal-3) (16) and (c) tandem repeat-type which contain two unique CRD motifs at their n- and c-termini that are connected by a flexible linker of variable length (Gal-4, -8, -9, -12).

Here we focus on Gal-9 which was first identified as a novel eosinophil chemoattractant secreted by T cells (17). Among its major roles, in the context of inflammation, Gal-9 has been shown to have a range of pro- and anti-inflammatory functions dependent upon its expression and cellular localisation (18). It was shown that Gal-9 modulates the adaptive immune response by stimulating the maturation of antigen-presenting cells (APCs), specifically dendritic cells (19). This interaction elicits a selective production of IL-12 by dendritic cells which promotes the secretion of Th1 cytokines by $CD4^+$ T cells (19). A study from Hafler et al., showed that this inflammatory activity observed in dendritic cells was dependent upon interaction with the T cell immunoglobulin mucin-3 (TIM-3) receptor (20). It has been further suggested that Gal-9 may have a beneficial role in the treatment of several inflammatory and autoimmune diseases (21, 22). Therapeutic application with recombinant Gal-9 was shown to inhibit the development of pathogenic Th17 cells and promote the expansion of Treg in a preclinical model of autoimmune arthritis (23).

In the context of gouty inflammation, MSU crystals promote the expansion of Th17 cells and their cognate cytokines. This inflammatory response can be inhibited by targeting IL-17 with neutralising antibodies, thereby reducing leukocyte infiltration into the inflamed tissue (5). As Gal-9 has previously been shown to both suppress the generation of Th17 (23, 24) and promote the induction of anti-inflammatory Treg cells (5, 23), we sought to investigate the action of exogenous Gal-9 in MSU-gouty inflammation in this current study. To address this, we assessed changes in both the innate and adaptive compartments (i.e. the numbers and types of cells infiltrating the joint and the severity of the disease) and local mediator production at the site of inflammation in a mouse model of gouty arthritis.

MATERIALS AND METHODS

Reagents

Collagenase (Type VIII), dimethyl sulfoxide (DMSO), E-Toxate™ reagent from Limulus Polyphemus, fetal bovine serum (FBS), hyaluronidase, monosodium urate crystals (MSU), and RPMI-1640 cell medium were purchased from Sigma-Aldrich Co. (Milan, Italy). Flow cytometry fixation and permeabilization buffer kit I, proteome profiler mouse cytokine array kit and recombinant mouse Gal-9 were purchased from R&D System (Milan, Italy). FACS buffer and conjugated antibodies from BioLegend (London, UK). Ficoll-Paque Plus (endotoxin tested, ≤ 0.12 EU/ml) was obtained from GE Healthcare Bio-Sciences AB (Uppsala, Sweden). Unless otherwise stated, all the other reagents were from BioCell (Milan, Italy).

Animals

Mice care and experimental procedures were performed in accordance with international and national laws and policies. Mice experiments were designed in accordance with ARRIVE guidelines and the recommendations of the European Directive 2010/63/EU for animal experiments and the Basel Declaration, including the 3R concept (25, 26). Male mice CD-1 (age 10-14 weeks and weight 25-30 g) were obtained from Charles River (Milan, Italy) and preserved in a temperature- and humidity-controlled animal care facility, with a 12-h light/dark cycle, with *ad libitum* access to water and standard laboratory diet. All procedures were performed to reduce the number of animals used (n = 6 per group).

Preparation of MSU Crystals

MSU crystals were prepared as previously described (27). Briefly, 800mg of MSU was dissolved in 155ml of boiling milli-Q water containing 5ml of NaOH, and the pH was adjusted to 7.2.

The solution was cooled gradually by stirring at RT and crystals collected after centrifugation at 3000rpm for 5 mins at 4°C. The crystals were washed twice with 100% ethanol, dried, autoclaved (180°C for 2h), and weighed under sterile conditions. Crystals were resuspended in PBS by sonication and stored in a sterile environment until use. MSU crystals were confirmed as endotoxin-free by a commercial test kit of limulus polyphemus lysate assay (<0.01 EU/10 mg).

MSU-Induced Acute Gouty Arthritis Model and Drug Administration

Acute gouty arthritis was induced by intra-articular (i.a.) administration of MSU crystals (200μg/20μl) into the right tibio-tarsal joint (ankle) of mice under isoflurane anaesthesia (28). Control (CTRL) group mice received an i.a. injection of sterile PBS (20μl). The successful establishment of the gouty arthritis model was judged by obvious swelling 2-3h after MSU injection (29). Animals from the groups treated with MSU received 1, 3 and 9μg (i.a.; in 20μl) of Gal-9 (single dose), 30 mins after MSU crystal administration. At the peak of inflammation (18h), tissues (knee joints) were collected, processed, and stored (-80°C) for further *ex vivo* analysis.

Evaluation of Joint Scoring and Oedema

A first set of experiments were carried out to validate the dose-responsive effect of Gal-9. Mouse Joints were evaluated macroscopically using a scale ranging from 0 to 3, where 0 = no inflammation, 1 = mild inflammation, 2 = moderate inflammation and 3 = severe inflammation, in 0.25 increments. A score of 0.25 was given when the first signs of swelling and redness were present. Simultaneously, knee joint oedema was measured with a calliper before and after i.a. injection of MSU crystals or MSU crystals plus Gal-9 at the indicated times (4, 18, 24 and 48h). Knee joint oedema was determined by subtracting (for each mouse) the basal paw value from the value measured at each time point and expressed as Δ mm.

Isolation and Characterisation of Joint-Infiltrating Cells

At the experimental end-point (18h) mice ankle joints were digested with hyaluronidase (2.4mg/ml) and collagenase (1mg/ml) in RPMI 1640 plus 10% FBS for 1h at 37°C, as previously described (30). Cells collected after digestion were filtered through a 70-μm nylon mesh filter (Becton Dickinson, Franklin Lakes, NJ, USA) and washed with RPMI 1640 plus 10% FBS. Subsequently, cells were washed in PBS for total cell counting prior to flow cytometry analysis.

Cytokines and Chemokines Protein Array

Ankle joints were homogenised in ice-cooled Tris-HCl buffer (20mM, pH 7.4) containing 1mM EDTA, 1mM EGTA, 1mM PMSF, 1mM sodium orthovanadate, and one protease inhibitor tablet per 50ml of buffer. Protein concentration was determined by the BioRad protein assay kit (BioRad, Italy). According to the manufacturer's instructions, equal volumes (1.5ml) of the pooled knee joint homogenates for all experimental conditions were then incubated with the pre-coated proteome profiler array membranes. Proteins were detected using the enhanced chemiluminescence detection kit and GE Healthcare Image Quant 400 software (GE Healthcare, Italy) and subsequently quantified using the GS 800 imaging densitometer software (Bio-Rad, Italy).

In Vitro Treg Differentiation

Blood was collected from healthy donors with written and verbal informed consent and approval from the University of Birmingham Local Ethical Review Committee (ERN_18-0382). Human peripheral blood mononuclear cells (PBMCs) were isolated as previously described (31) and naive $CD4^+$ T cells were isolated by negative selection using a commercial kit (Miltenyi, Biotec, Germany). Briefly, PBMCs were incubated with a biotin antibody cocktail for 5 mins at 4°C to bind with unwanted non-T cells, followed by incubation with anti-$CD4^+$ microbeads for 10 mins at 4°C. Cells were added to MACS LS separation columns, and flow through containing the enriched $CD4^+$ T cell fraction was collected.

On day one, $CD4^+$ T cells were resuspended in 36ml of RPMI containing penicillin (50U/ml), streptomycin (50μg/m), L-glutamine (2mM) (Sigma), 5% FBS, and split into 6-well plates (6ml/well) and rested overnight in 5% CO_2 at 37°C. 48-well plate was coated with anti-CD3 antibodies (1μg/ml, clone OKT3, BioLegend, UK) and incubated overnight at 4°C). On day two, $CD4^+$ T cells were transferred into a 50 ml falcon tube and centrifuged at 250g for 10 mins at RT. The supernatant was discarded, and cell pellet was resuspended at a concentration of $8x10^5$ cells/ml in ImmunoCult™-XF T cell expansion medium (StemCell Technologies, Oxford, UK). Anti-CD3 antibody coated plates were washed with 150μl PBS without Ca^{2+} and Mg^{2+}.

Separate plates were prepared by firstly adding either 50μl of blank T cell expansion medium or 50μl of a 4x concentration of a T cell polarization cocktail (final concentration: anti-CD28 1μg/ml (clone CD28.2, BioLegend), TGF-β 1ng/ml (R&D), IL-2 20U/ml (Roche). 50μl of blank T cell expansion medium or 50μl of Gal-9 was then added, followed by the addition of T cells ($8x10^4$ cells/well). Cell suspensions were then mixed, transferred to the CD3-coated plate and incubated for 5 days at 37°C in 5% CO_2. Treg expansion and purity was quantified by flow cytometry. Briefly, cells were washed in FACS buffer (PBS containing 1% BSA and 0.02% NaN_2) and directly stained with the following conjugated antibodies (all from BioLegend, London, UK): CD3 (1:100, clone UCHT-1), CD4, (1:100, clone SK3), CD25 (1:50; clone AF-700) for 20 mins at 4°C. After washing, cells were fixated, permeabilized, and stained intracellularly with FOXP-3 antibody (1:50: clone 206D). At least 1×10^4 cells were analysed per sample, and determination of positive and negative populations was performed based on the staining obtained with related IgG isotypes. After staining, samples were resuspended in PBS without Ca^{2+} and Mg^{2+} and analysed using the CyAn flow cytometer (Beckmann Coulter, USA). The flow cytometry data was analysed using Flowjo.

Gal-9 Binding Human $CD4^+$ T Cells

$CD4^+$ T cells were incubated with or without recombinant Gal-9 (10nM) for 20 mins at RT. Cells were washed twice and incubated with anti-human Gal-9 antibody goat IgG (1:200,

R&D Systems) and stained with the following conjugated antibodies (BioLegend, London, UK): CD4 (1:50, clone RPAT4), donkey anti-goat IgG (1:200, polyclonal) for 20 mins at 4°C. After washing, cells were fixated fixed in 1% PFA for storage before analysis with CyAn flow cytometer (Beckmann Coulter, USA).

Human IL-10 ELISA

IL-10 Duo Set (R&D Systems, Abingdon, UK) was used to measure IL-10 levels in cell culture supernatants following manufacturer guidelines. Briefly, 96 well plates were coated with a human IL-10 capture antibody and incubated at RT overnight. Plates were washed 3 times with washing buffer to remove unbound antibodies and blocked for 1h at RT. 100µl of samples or standards (diluted with assay diluent) were added to the plate and incubated for 2h at RT. Plates were washed three times before the addition of 100µl of human IL-10 detection antibody for 1h at RT. Plates were washed three times before the addition of streptavidin-HRP for 20 mins at RT. Plates were washed three times before the addition of 100µl of substrate and left for 20 mins protected from light. Lastly, 50µl of stop (2M H_2SO_4) solution was added. A microplate reader was used to measure absorbance at 450nm.

Flow Cytometry

Cells from digested joints were washed in FACS buffer (PBS containing 1% BSA and 0.02% NaN_2) and directly stained with the following conjugated antibodies (all from BioLegend, London, UK): CD3 (1:200, clone 17A2), CD4 (1:200; clone GK1.5), CD25 (1:200; clone 3C7) for 60 mins at 4°C. After washing, cells were fixated, permeabilized, and stained intracellularly with IL-17A (1:200; clone TC11-18H10.1) and FOXP-3 antibody (1:200: clone MF-14). Moreover, for the characterization of joint-infiltration, cells were stained for CD45 (1:100; clone 30-F11), Ly6-C (1:100; clone HK1.4), Ly6-G (1:100; clone 1A8), CD11b (1:100; clone M1/70), CD115 (1:100; clone AFS98), prior to analysis. Th17, Treg, neutrophils, and patrolling/inflammatory monocytes were defined according to the flow cytometry procedure previously described (32). At least 1×10^4 cells were analysed per sample, and determination of positive and negative populations was performed based on the staining obtained with related IgG isotypes (data not shown). Flow cytometry was performed on BriCyte E6 flow cytometer (Mindray Bio-Medical Electronics, Nanshan, China) using MRFlow and FlowJo software operation (28). Absolute numbers of positive cells for neutrophils ($CD45^+$/Ly6-G^{hi}/Ly6-C^{hi}), monocytes (inflammatory: $CD11b^+$/$CD115^+$/Ly6-C^{hi}; patrolling: $CD11b^+$/$CD115^+$/Ly6-C^{lo}), Th17 ($CD4^+$/$IL\text{-}17^+$) and Treg (gated for $CD4^+$ and then for $CD25^+$/$FOXP3^+$) were calculated converting the % of positive cells (for the mentioned staining) on the total number of leukocytes and $CD4^+$ positive cells.

Data and Statistical Analysis

All data are presented as means ± SEM and were analysed using students T-test or a one- or two-way ANOVA followed by Bonferroni's or Tukey's test for multiple comparisons. GraphPad Prism 8.0 software (San Diego, CA, USA) was used for analysis. Differences between means were considered statistically significant when $P \leq 0.05$ was achieved. Sample size was chosen to ensure alpha 0.05 and power 0.8. Animal weight was used for randomisation and group allocation to reduce unwanted sources of variations by data normalisation. No animals and related *ex vivo* samples were excluded from the analysis. *In vivo* study was carried out to generate groups of equal size (n = 6 of independent values), using randomisation and blind analysis.

RESULTS

Gal-9 Attenuates the Severity of MSU-Induced Gouty Inflammation

To investigate the potential anti-inflammatory effect of Gal-9, we used a mouse model in which MSU crystals were injected into knee joints, to mimic the etiologic cause of human gouty inflammation (33). MSU crystals injection (200µg/20µl) evoked an intense and robust joint inflammatory score (peak at 18h) that was dose-dependently attenuated by Gal-9 (1-9µg/20µl) administration (**Supplementary Figure 1A**), with maximum inhibition observed at a dose of 9µg/20µl (**Figure 1A**). In addition to joint inflammation scores, we evaluated ankle swelling and found Gal-9 treatment (9µg/20µl) significantly reduced ankle swelling between 18 and 24 h (**Figure 1B**), indicating an enhanced resolution profile in the presence of Gal-9. A significant reduction was also observed at 18 h at a concentration of 3µg/20µl, however at a lower concentration of 1µg/20µl no appreciable effects were observed on joint scores or swelling (**Supplementary Figure 1**). Based on the results obtained, we selected the most effective dose of Gal-9 (9µg/20µl) for all subsequent experiments.

Gal-9 Modulates, *In Situ*, the Recruitment of Leukocytes

During the onset and resolution phases of gouty arthritis, a major hallmark of disease pathogenesis is the infiltration of immune cells, with mainly neutrophils and inflammatory monocytes in the early phases (34, 35) followed by $CD4^+$ T cells in the latter (9, 36). We, therefore, characterised the phenotype of recruited cells following MSU injection and Gal-9 administration. Flow cytometry was employed to determine neutrophil, monocytes, Th17 and Treg populations in single cell suspensions following digestion of knee joint tissues harvested from the 18h time-point. To identify leukocyte subpopulations, total cells followed by single-cells were gated, and CD45 (pan leukocyte/immune cell marker) in combination with CD11b (myeloid marker) and CD4 (accessory protein for MHC class-II antigen/T-cell receptor interaction) were used to identify neutrophils, monocytes and T cells. Neutrophils were further characterised as $CD45^+$/Ly6-G^{hi}/Ly6-C^{hi} (**Figure 2A**) and monocytes were delineated based upon Ly6-C and CD115 expression to distinguish $CD11b^+$/$CD115^+$/Ly6-C^{lo} patrolling monocytes from $CD11b^+$/$CD115^+$/Ly6-C^{hi} inflammatory monocytes (**Figure 2B**). In agreement with our previous studies (5), injection of MSU crystals resulted in a significant increase in the total number of leukocytes recruited to joints when compared to CTRL (**Figure 2C**). A significant reduction in total leukocytes was

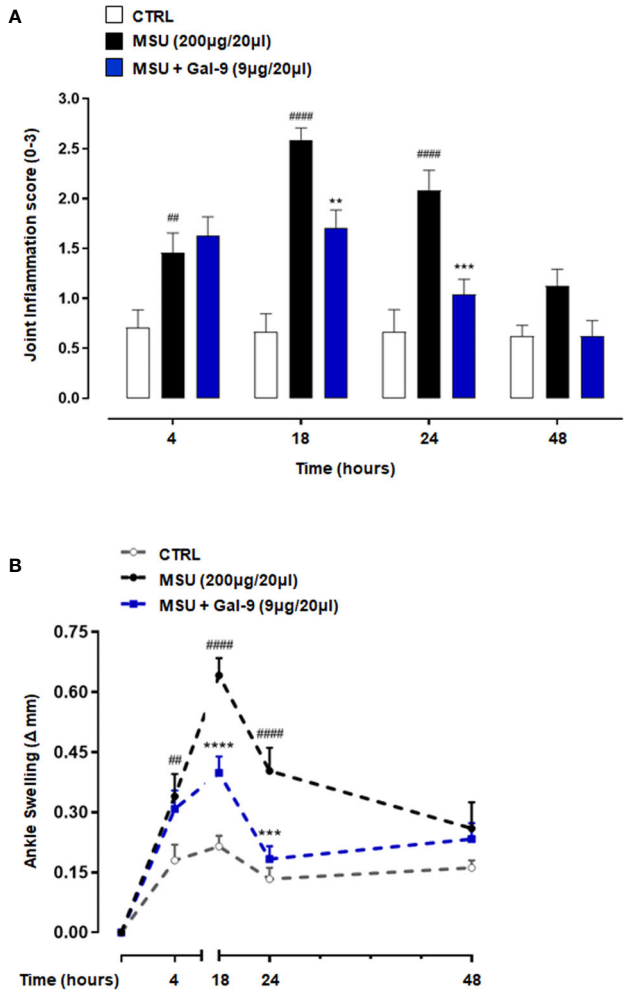

FIGURE 1 | Gal-9 attenuates MSU crystals-induced gouty inflammation in mouse knee joints. Mice were treated with intra-articular (i.a.) dose of Gal-9 (9µg/20µl) or vehicle (PBS, 20µl) 30 mins after i.a. stimulation with MSU crystals (200µg/20µl) in the right knee joints. **(A)** Joint inflammation score (0-3 in increments of 0.25) and **(B)** joint inflammation oedema was evaluated at 4, 18, 24 and 48h after the stimulus with MSU. Data (expressed as joint inflammation score and Δ increase of knee joints mm respectively) are presented as means ± SEM of n = 6 mice per group. Statistical analysis was conducted by one- or two-way ANOVA followed by Bonferroni's for multiple comparisons. $^{##}P \leq 0.01$, $^{####}P \leq 0.0001$ *vs* Ctrl group; $^{**}P \leq 0.01$, $^{***}P \leq 0.001$, $^{****}P \leq 0.0001$ *vs* MSU group.

observed in mice administered with Gal-9 when compared to MSU alone (**Figures 2C**). Moreover, mice injected with MSU crystals alone compared to CTRL showed significant recruitment of neutrophils (**Figure 2D**) and inflammatory monocytes (**Figure 2E**). In line with total leukocyte counts, treatment with Gal-9 significantly reduced neutrophil and inflammatory monocytes levels when compared to MSU-injected mice alone, in terms of cell percentages as well as absolute numbers (**Figures 2A, B, D, E**). In all experimental conditions, no significant differences were found in the proportion of patrolling monocytes (data not shown).

To clarify if potential differences in inflammatory/resolution profiles *in situ* were a result of alterations in T cell subset ratios, we stained knee joint homogenates for CD3/CD4 (**Figures 3A, B**) and CD4 to identify Th17 and Treg populations defined as $CD4^+$/IL-17^+ and $CD4^+$/$CD25^+$/FOXP-3^+ respectively (**Figures 3A, C–E**). MSU-injected mice displayed a significant increase in total $CD4^+$ T cells compared to control mice (**Figure 3F**). This increase was associated with elevated Th17 cells and reduced Treg levels when compared to CTRL (**Figures 3G, H**). In stark contrast mice treated with Gal-9 displayed a significant reduction in Th17 cells and sustained levels of Tregs (**Figures 3G, H**). We also analysed the circulating Th17/Tregs profile but did not see differences between groups after Gal-9 injection (data not shown).

Gal-9 Treatment Reduces Local Production of Pro-Inflammatory Cyto-Chemokines

Considering the importance of pro-inflammatory mediators in driving recruitment and local immune cell activation in disease onset and progression (37), we next sought to determine the effect of Gal-9 treatment on local cytokine and chemokine production. As shown in **Figure 4**, knee joint homogenates (collected at 18h time-point) obtained from MSU-administered mice showed a large increase of pro-inflammatory cyto-chemokines compared to CTRL group (**Figures 4A, B**). Interestingly, after Gal-9 treatment, there was a significant decrease in a range of mediators (**Figure 4C**). According to cellular profile previously characterised by FACS, densitometric analysis, presented as a heatmap (**Figure 4D**), revealed that the Gal-9 treated group had a significant ($P \leq 0.0001$) modulation in the following factors: B lymphocyte chemoattractant (BLC), component 5a (c5/c5a), soluble intercellular adhesion molecule-1 (sICAM-1), IL-1α, IL-1β, IL-1ra, IL-16, keratinocyte chemoattractant (KC), macrophage colony-stimulating factor (M-CSF), monokine induced by interferon-γ (MIG), macrophage inflammatory protein (MIP)-1α, MIP-1β, MIP-2, IL-1β stromal cell-derived factor-1 (SDF-1), TNF-α and triggering receptor expressed on myeloid cells-1 (TREM-1). To a lesser extent, we also observed a modulation ($P \leq 0.01$) of granulocyte colony-stimulating factor (G-CSF), IL-17 and junctional epithelium (JE) compared to MSU group. A minor inhibitory profile ($P \leq 0.05$) was found for IL-7, IL-10, monocytes chemoattractant protein-5 (MCP-5), and metallopeptidase inhibitor-1 (TIMP-1) (**Figure 4D**). Major cytokines and chemokines involved in driving disease (IL-10, IL-17, KC, JE, MIP-1α and TNF-α) have been extrapolated from the heatmap and represented graphically (**Figure 4E**).

Gal-9 Promotes the Differentiation of Naïve CD4 T Cell Towards Treg Phenotype

Previous reports and data in this study support the view that therapeutic application of Gal-9 *in vivo* promotes Treg induction which dampens inflammation and promotes resolution. We, therefore, carried out *in vitro* assays with purified human naive $CD4^+$ T cells to test the capacity of Gal-9 to induce Treg differentiation. Initially, we confirmed with flow cytometry that exogenously added Gal-9 binds to $CD4^+$ T cells (**Figures 5A, B**).

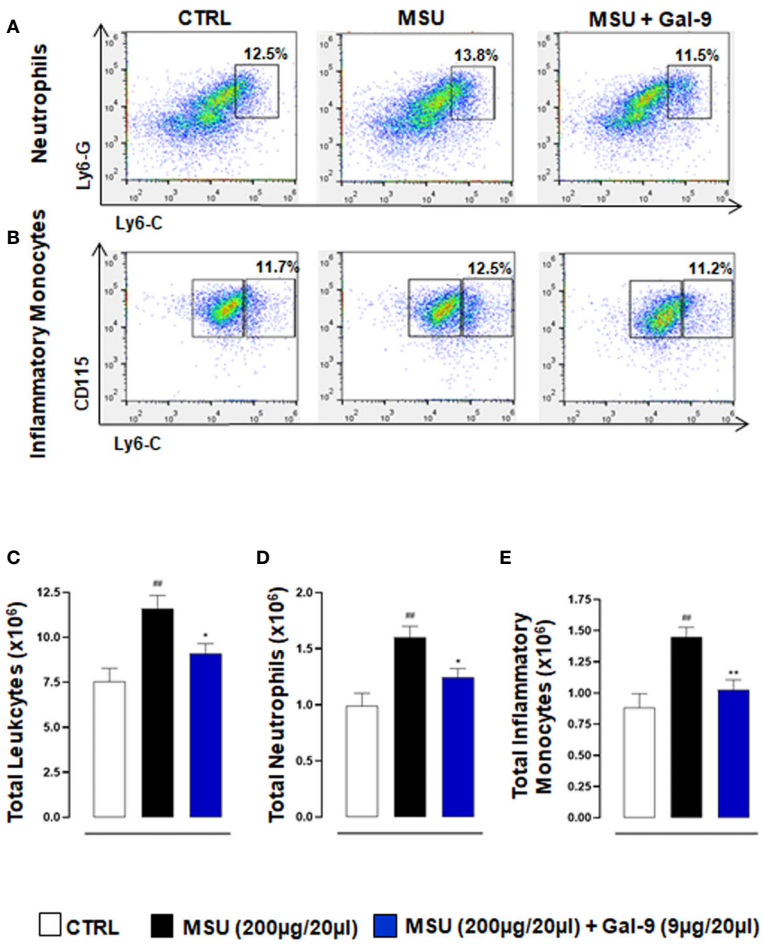

FIGURE 2 | Gal-9 modulates the recruitment of innate immune cells. Flow cytometry analysis was employed to determine *in situ* neutrophil and monocyte subsets. At the peak of inflammatory reaction (18h), ankle joints were digested, and single cell suspensions were obtained. Flow cytometry strategy applied to identify neutrophils **(A)**, and monocytes **(B)**, after Gal-9 treatment are shown. Cells were washed and stained with: CD45, LY6-C, LY6-G, CD11b, and CD115/CD45$^+$ cells were plotted for LY6-C and LY6-G expression to identify CD45$^+$/LY6-C^{hi}/LY6-G^{hi} as neutrophils **(A)**. CD11b$^+$ cells were plotted for LY6-C and CD115 expression to distinguish CD11b$^+$/CD115$^+$/LY6-C^{lo} patrolling monocytes from CD11b$^+$/CD115$^+$/LY6-C^{hi} inflammatory monocytes **(B)**. **(C)** Total infiltrated leukocytes, **(D)** neutrophil and **(E)** inflammatory monocytes were quantified in the different experimental conditions. Representative FACS plots of three independent experiments with similar results are shown. Values are presented as means ± SEM of n = 6 mice per group. Statistical analysis was conducted by one-way ANOVA followed by Bonferroni's for multiple comparisons. $^{\#\#}P \leq 0.01$ *vs* Ctrl group; $^*P \leq 0.05$, $^{**}P \leq 0.01$ *vs* MSU group.

Moreover, we found that Gal-9 alone did indeed promote Treg differentiation, defined as CD4$^+$/FoxP3$^+$, and that this effect was concentration-dependent, with 10nM far more efficient (similar degree to the activation cocktail) compared to 2nM Gal-9 (**Figures 5C, D**). We also measured IL-10 release into cell culture supernatants, a functional readout of Tregs, and found a similar significant increase in cells treated with 10nM Gal-9 compared to control (**Figure 5E**).

DISCUSSION

In the presence of sodium, uric acid from purine metabolism precipitates as MSU needles and can contribute to the development of gouty arthritis, characterised by redness, heat, and swollen joints (37). Analyses of synovial fluids and tissue sections of patients suffering from gout has revealed the presence of granuloma and neutrophil extracellular traps (NETs) formation which, after prolonged exposure, carries the risk for the development of chronic inflammation (38). The pathogenesis of chronic gouty arthritis is intricate, and its progression involves a variety of immunological factors. T-cell dysfunction (in particular the imbalance between Treg/Th17) plays an essential role in the occurrence and development of disease. Indeed, restoring the protective levels of Treg (36) or reducing the self-perpetuating inflammatory Th17 subset (5) represents one of the key immunological features in gouty arthritis.

Findings from several studies have shown that expression profile of Gal-9 is highly elevated in many inflammatory autoimmune diseases, such as systemic lupus erythematosus

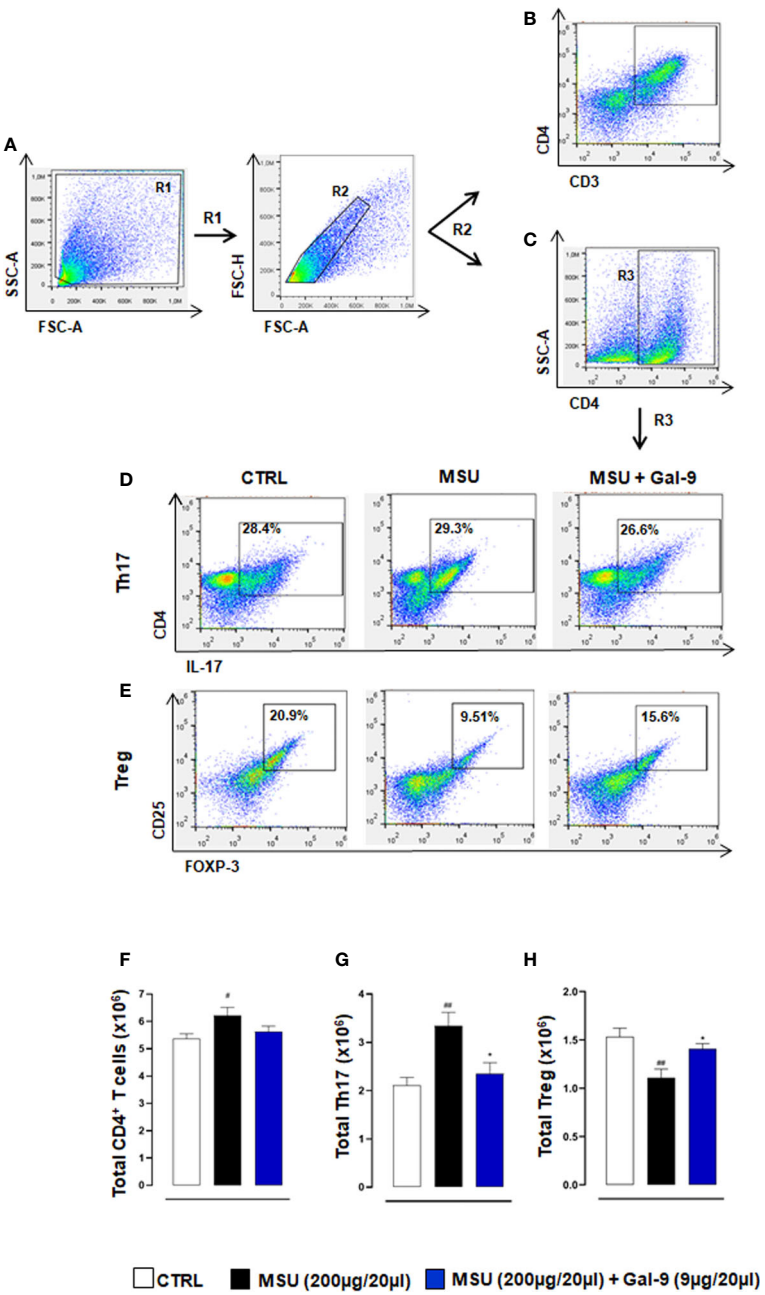

FIGURE 3 | Gal-9 sustains local Treg levels. Flow cytometry analysis was employed to determine *in situ* levels of $CD4^+$ T cells, Th17 and Tregs subsets. At the peak of the inflammatory reaction (18h), ankle joints were digested, and single cell suspensions were obtained. Flow cytometry strategy applied to identify the modulation of CD3/CD4 **(A, B)**, $CD4^+$ T cells **(A, C)**, Th17 **(A, C, D)** and Tregs **(A, C, E)** after Gal-9 treatment are shown. Cells were washed and stained with: CD3, CD4, CD25, and intracellular antibodies IL-17A and FOXP-3. Th17 and Treg populations were defined as $CD4^+$/IL-17^+ **(A, C, D)** and $CD4^+$/$CD25^+$/FOXP-3^+ **(A, C, E)** respectively. **(F)** Total $CD4^+$ T cells, **(G)** Th17 and **(H)** Tregs were quantified in the different experimental conditions. Representative FACS plots of three independent experiments with similar results are shown. Values are presented as means ± SEM of n = 6 mice per group. Statistical analysis was conducted by one-way ANOVA followed by Bonferroni's test for multiple comparisons. $^{\#}P \leq 0.05$, $^{\#\#}P \leq 0.01$ *vs* Ctrl group; $^{*}P \leq 0.05$ *vs* MSU group.

(39), rheumatoid arthritis (RA) (40, 41), and systemic sclerosis (42). Gene polymorphisms in LGALS2, LGALS3 and LGALS9 have been linked with predisposition to RA (43). Studies have also proposed the participation of Gal-9 in the immunopathogenesis of systemic inflammatory processes (44) and as a pro-active serum checkpoint molecule in RA (45).

The current study used an MSU-driven model of acute gouty arthritis and, in that context, our results showed that injection of

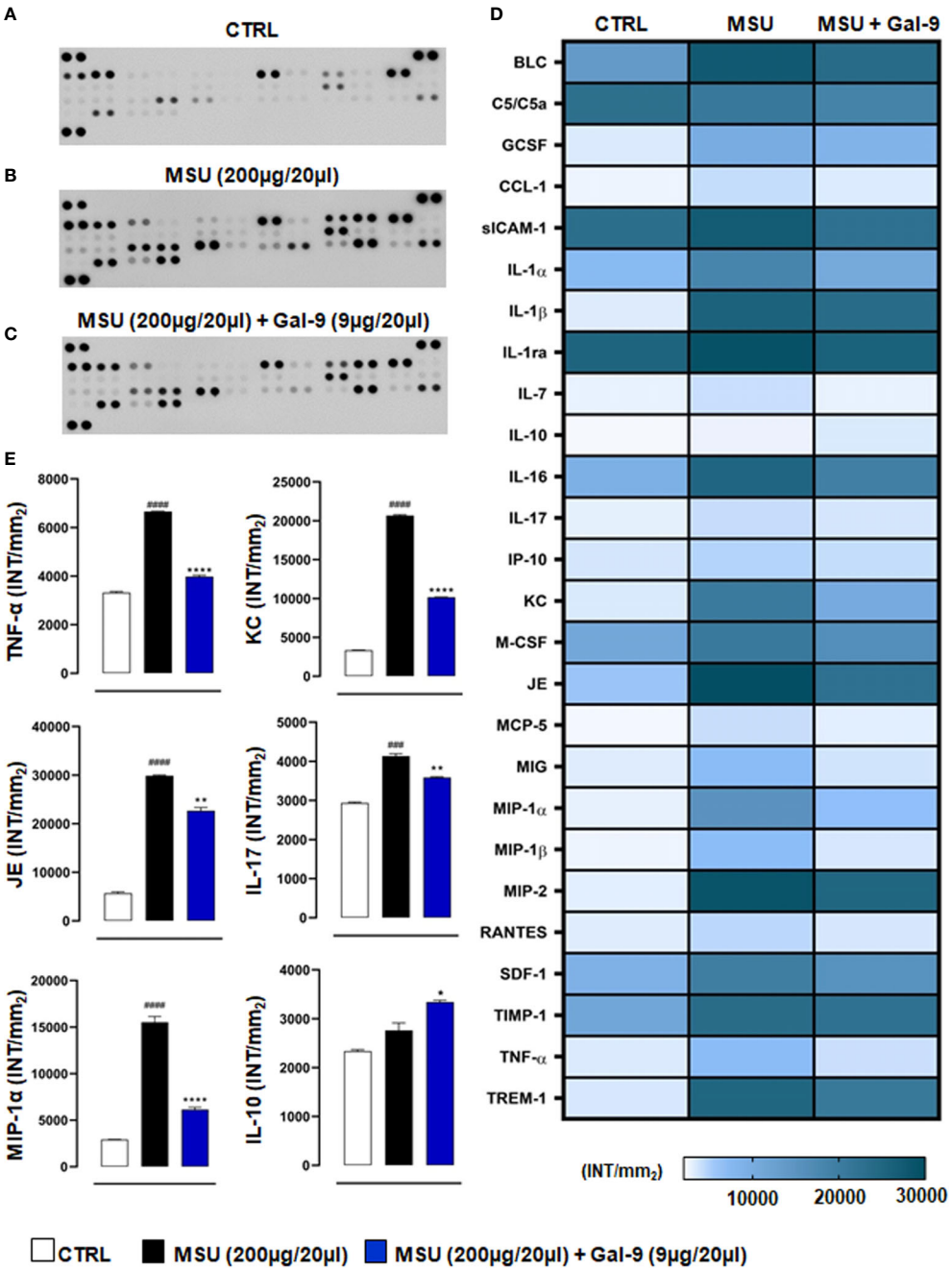

FIGURE 4 | Gal-9 decreases the release of cyto-chemokines in knee joints. Inflammatory fluids obtained from knee joint homogenates at 18h time-point, were assayed using a proteome profiler cytokine array for **(A)** CTRL, **(B)** MSU and **(C)** MSU + Gal-9 group. Densitometric analysis is presented as heatmap **(D)**. Thereafter, IL-10, IL-17, KC, JE, MIP-1α and TNF-α were extrapolated from heatmap and represented graphically **(E)**. Data (expressed as INT/mm^2) are presented as means ± SEM. of positive spots of three separate independent experiments run each with n = 6 mice per group pooled. Statistical analysis was performed by using two-way ANOVA followed by Bonferroni's test for multiple comparisons. $^{###}P \leq 0.001$, $^{####}P \leq 0.0001$ *vs* Ctrl group; $^{*}P \leq 0.05$, $^{**}P \leq 0.01$, $^{****}P \leq 0.0001$ *vs* MSU group.

MSU crystals (200µg/20µl) induced ankle swelling (with a peak at 18h) and inflammation. Therapeutic application of Gal-9 (9µg/20µl) significantly reduced ankle swelling observed at 18h and 24h after MSU crystal administration. Moreover, our results showed that Gal-9 administration reduced inflammatory cell infiltration and levels of pro-inflammatory mediators produced by neutrophils/inflammatory monocytes (e.g. IL-1α/β, TNF-α, JE, KC) and by Th17/Treg cell subtypes (e.g. IL-10, IL-17, G-CSF) at the local site of inflammation, which suggests an anti-inflammatory mode of action for Gal-9 in this model.

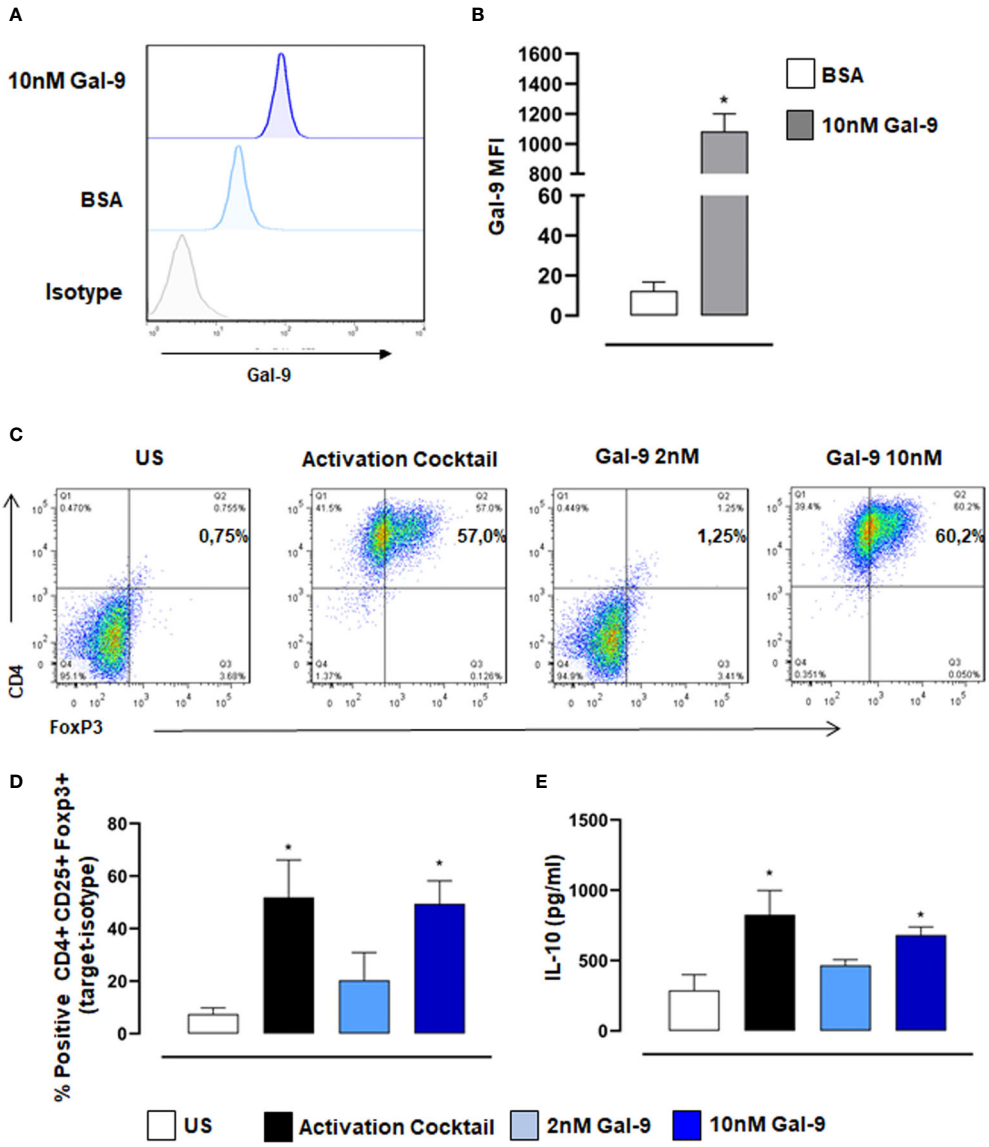

FIGURE 5 | Gal-9 induces Treg differentiation of naïve human CD4$^+$ T cells. CD4$^+$ T cells were isolated from PBMCs and incubated with 10nM Gal-9 before staining with anti-Gal-9. **(A)** Representative histogram showing exogenous Gal-9 binding in CD4$^+$ cells compared to isotype control levels. **(B)** Quantification of Gal-9 protein levels using median fluorescence intensity (MFI) of Gal-9. Data are expressed as mean ± SEM (n=4). Statistical analysis was performed with Students T-test; *P < 0.05 vs BSA. Naïve CD4$^+$ T cells were differentiated with activation cocktail (CD3/CD28, IL2, TGFβ) or Gal-9 alone for 5 days. **(C, D)** Flow cytometry was used to measure % positive expression of CD4$^+$,CD25$^+$ and Foxp3$^+$. **(E)** Cell culture supernatants were collected, and IL-10 levels were measured by ELISA. Data are expressed as mean ± SEM (n=3). Statistical analysis was performed with one-way ANOVA with Tukey multiple comparisons; *P < 0.05.

To investigate which types of immune cells were preferentially recruited in response to MSU crystals and those to MSU in combination with Gal-9 treatment, we employed flow cytometry. Cytometric data showed that neutrophils and inflammatory monocytes were the main hallmarks of the MSU group compared to CTRL, with a significant increase in Th17 infiltration. In contrast, Gal-9 treatment maintained the total CD4$^+$ and Treg numbers at CTRL levels, whilst abolishing any MSU-induced increase in Th17 numbers, thereby maintaining a Th17/Treg balance. Furthermore, treatment with Gal-9 clearly suppressed the initial innate immune response, with a significant reduction observed in neutrophil and inflammatory monocyte recruitment. This coupled with the reduction in local inflammatory mediators could have a major impact on the secondary wave of T cell recruitment and subsequent amplification of the inflammatory response. Raucci and colleagues recently demonstrated the importance of T cells in driving pathogenesis in this model of gouty arthritis (5). They highlighted that suppressing Th17 cells using a neutralizing antibody against IL-17, resulted in elevated circulating Treg

levels, which in turn accelerated inflammation resolution, thus indicating a potential modulatory role for Tregs in MSU gouty inflammation. In another experimental model of autoimmune induced arthritis, therapeutic application of Gal-9 was shown to inhibit the development of Th17 cells and promote the expansion of Tregs cells (23). The authors showed that Gal-9 suppressed arthritis in a dose-dependent fashion by inhibiting the expression of pro-inflammatory cytokines, mainly IL-17, IL-12, and IFN-γ in the joints. Previous studies have shown that Gal-9 selectively induces apoptosis in Th1 and Th17 cells through its interaction with TIM-3 (46, 47). This could also be a potential mode of action in this current study and warrants further investigation.

In human settings, Gal-9 expression and role in autoimmune arthritis has been previously demonstrated, with elevated expression of this protein in the synovial fluid of RA patients compared to those with osteoarthritis (21). More recently a study from Sun et al., demonstrated that Gal-9 expression in T cells positively correlated with disease activity and could be potentially used as a novel biomarker for evaluating RA activity and therapeutic effect (40). Gal-9 modulation of RA *via* the regulation of synovial fibroblast activity/viability has been shown to be complex, with endogenous Gal-9 protecting synovial fibroblasts against apoptosis (48), while exogenous Gal-9 has been shown to induce apoptosis in fibroblast-like synoviocytes in RA patients (21). Here, we selectively isolated human naive $CD4^+$ T cells and treated them with Gal-9, to assess the ability of Gal-9 to drive human T cell differentiation. In line with previous studies (49, 50), we found that Gal-9 alone was effective at inducing Treg differentiation in a dose-dependent manner. Moreover, there was also a dose-dependent increase in IL-10 levels in supernatants from Gal-9 treated T cell cultures, suggesting a specific role for Gal-9 in inducing Treg functions (i.e., IL-10 production).

In conclusion, our findings suggest that Gal-9 has a crucial role in regulating the acute inflammation and resolution associated with gouty arthritis through sustaining anti-inflammatory Treg populations locally at the site of inflammation, while simultaneously reducing Th17 levels. Administration of Gal-9 could provide a new therapeutic strategy for preventing tissue damage associated with gouty arthritis.

DATA AVAILABILITY STATEMENT

The raw data supporting the conclusions of this article will be made available by the authors, without undue reservation.

ETHICS STATEMENT

Blood was collected from healthy donors with written and verbal informed consent and approval from the University of Birmingham Local Ethical Review Committee (ERN_18-0382). The patients/participants provided their written informed consent to participate in this study. All animal care and experimental procedures were carried out in compliance with the international and national law and policies and approved by the Italian Ministry of Health. Animal studies were reported in compliance with the ARRIVE guidelines and with the recommendations made by EU Directive 2010/63/EU for animal experiments.

AUTHOR CONTRIBUTIONS

AM, FR, AS, ST, and FM performed experiments. AM, FR, FM, and AI analysed results and made the figures. AI and FM designed the research. AM, FR, FM, and AI wrote the paper. All authors contributed to the article and approved the submitted version.

FUNDING

AM is supported by a KSA government-funded scholarship. FR is supported by a University of Naples Federico II PhD scholarship in Pharmaceutical Sciences. AS is supported by a Dompé Farmaceutici S.p.A fellowship for PhD programme in "Nutraceuticals, functional foods and human health" (University of Naples Federico II). AI is supported by a Birmingham Fellowship.

SUPPLEMENTARY MATERIAL

The Supplementary Material for this article can be found online at: https://www.frontiersin.org/articles/10.3389/fimmu.2021.762016/full#supplementary-material

Supplementary Figure 1 | Mice were treated with Gal-9 (1-9μg/20μl) or vehicle (PBS, 20μl) 30 mins after i.a. stimulation with MSU crystals (200μg/20μl) in the right knee joints. **(A)** Joint inflammation score (0-3 in increments of 0.25) and **(B)** joint inflammation oedema was evaluated at 4, 18, 24 and 48h after MSU. Data (expressed as joint inflammation score and Δ increase of knee joints mm respectively) are presented as means ± SEM of n = 6 mice per group. Statistical analysis was conducted by one- or two-way ANOVA followed by Bonferroni's for multiple comparisons. $^{\#}P \leq 0.05$, $^{\#\#}P \leq 0.01$, $^{\#\#\#\#}P \leq 0.0001$ *vs* Ctrl group; $^{*}P \leq 0.05$, $^{**}P \leq 0.01$, $^{***}P \leq 0.001$, $^{****}P \leq 0.0001$ *vs* MSU group.

REFERENCES

1. Medzhitov R. Origin and Physiological Roles of Inflammation. *Nature* (2008) 454(7203):428–35. doi: 10.1038/nature07201
2. Hannoodee S, Nasuruddin DN. Acute Inflammatory Response. In: *StatPearls*. Treasure Island (FL: StatPearls Publishing LLC (2021). StatPearls Publishing Copyright © 2021.
3. Ley K, Laudanna C, Cybulsky MI, Nourshargh S. Getting to the Site of Inflammation: The Leukocyte Adhesion Cascade Updated. *Nat Rev Immunol* (2007) 7(9):678–89. doi: 10.1038/nri2156
4. Rajakariar R, Lawrence T, Bystrom J, Hilliard M, Colville-Nash P, Bellingan G, et al. Novel Biphasic Role for Lymphocytes Revealed During Resolving Inflammation. *Blood* (2008) 111(8):4184–92. doi: 10.1182/blood-2007-08-108936
5. Raucci F, Iqbal AJ, Saviano A, Minosi P, Piccolo M, Irace C, et al. IL-17A Neutralizing Antibody Regulates Monosodium Urate Crystal-Induced Gouty Inflammation. *Pharmacol Res* (2019) 147:104351. doi: 10.1016/j.phrs.2019.104351
6. Kadiyoran C, Zengin O, Cizmecioglu HA, Tufan A, Kucuksahin O, Cure MC, et al. Monocyte to Lymphocyte Ratio, Neutrophil to Lymphocyte Ratio, and Red Cell Distribution Width are the Associates With Gouty Arthritis. *Acta Med (Hradec Kralove)* (2019) 62(3):99–104. doi: 10.14712/18059694.2019.132

7. Shevyrev D, Tereshchenko V. Treg Heterogeneity, Function, and Homeostasis. *Front Immunol* (2019) 10:3100. doi: 10.3389/fimmu.2019.03100
8. Luo CY, Wang L, Sun C, Li DJ. Estrogen Enhances the Functions of CD4(+) CD25(+)Foxp3(+) Regulatory T Cells That Suppress Osteoclast Differentiation and Bone Resorption In Vitro. *Cell Mol Immunol* (2011) 8 (1):50–8. doi: 10.1038/cmi.2010.54
9. Wu M, Tian Y, Wang Q, Guo C. Gout: A Disease Involved With Complicated Immunoinflammatory Responses: A Narrative Review. *Clin Rheumatol* (2020) 39(10):2849–59. doi: 10.1007/s10067-020-05090-8
10. Sakaguchi S, Miyara M, Costantino CM, Hafler DA. FOXP3+ Regulatory T Cells in the Human Immune System. *Nat Rev Immunol* (2010) 10(7):490–500. doi: 10.1038/nri2785
11. Arellano B, Graber DJ, Sentman CL. Regulatory T Cell-Based Therapies for Autoimmunity. *Discov Med* (2016) 22(119):73–80.
12. Maione F, Paschalidis N, Mascolo N, Dufton N, Perretti M, D'Acquisto F. Interleukin 17 Sustains Rather Than Induces Inflammation. *Biochem Pharmacol* (2009) 77(5):878–87. doi: 10.1016/j.bcp.2008.11.011
13. Zhou L, Lopes JE, Chong MM, Ivanov II, Min R, Victora GD, et al. TGF-Beta-Induced Foxp3 Inhibits T(H)17 Cell Differentiation by Antagonizing RORgammat Function. *Nature* (2008) 453(7192):236–40. doi: 10.1038/nature06878
14. Seetharaman J, Kanigsberg A, Slaaby R, Leffler H, Barondes SH, Rini JM. X-Ray Crystal Structure of the Human Galectin-3 Carbohydrate Recognition Domain at 2.1-A Resolution. *J Biol Chem* (1998) 273(21):13047–52. doi: 10.1074/jbc.273.21.13047
15. Hirabayashi J, Hashidate T, Arata Y, Nishi N, Nakamura T, Hirashima M, et al. Oligosaccharide Specificity of Galectins: A Search by Frontal Affinity Chromatography. *Biochim Biophys Acta* (2002) 1572(2-3):232–54. doi: 10.1016/S0304-4165(02)00311-2
16. Cooper DN. Galectinomics: Finding Themes in Complexity. *Biochim Biophys Acta* (2002) 1572(2-3):209–31. doi: 10.1016/S0304-4165(02)00310-0
17. Sato M, Nishi N, Shoji H, Seki M, Hashidate T, Hirabayashi J, et al. Functional Analysis of the Carbohydrate Recognition Domains and a Linker Peptide of Galectin-9 as to Eosinophil Chemoattractant Activity. *Glycobiology* (2002) 12 (3):191–7. doi: 10.1093/glycob/12.3.191
18. Tsuchiyama Y, Wada J, Zhang H, Morita Y, Hiragushi K, Hida K, et al. Efficacy of Galectins in the Amelioration of Nephrotoxic Serum Nephritis in Wistar Kyoto Rats. *Kidney Int* (2000) 58(5):1941–52. doi: 10.1111/j.1523-1755.2000.00366.x
19. Yamauchi A, Dai SY, Nakagawa R, Kashio Y, Abe H, Katoh S, et al. Galectin-9 Induces Maturation of Human Monocyte-Derived Dendritic Cells. *Nihon Rinsho Men'eki Gakkai kaishi = Japanese J Clin Immunol* (2005) 28(6):381–8. doi: 10.2177/jsci.28.381
20. Anderson AC, Anderson DE, Bregoli L, Hastings WD, Kassam N, Lei C, et al. Promotion of Tissue Inflammation by the Immune Receptor Tim-3 Expressed on Innate Immune Cells. *Science* (2007) 318(5853):1141–3. doi: 10.1126/science.1148536
21. Seki M, Sakata KM, Oomizu S, Arikawa T, Sakata A, Ueno M, et al. Beneficial Effect of Galectin 9 on Rheumatoid Arthritis by Induction of Apoptosis of Synovial Fibroblasts. *Arthritis Rheum* (2007) 56(12):3968–76. doi: 10.1002/art.23076
22. Chen HY, Wu YF, Chou FC, Wu YH, Yeh LT, Lin KI, et al. Intracellular Galectin-9 Enhances Proximal TCR Signaling and Potentiates Autoimmune Diseases. *J Immunol* (2020) 204(5):1158–72. doi: 10.4049/jimmunol.1901114
23. Seki M, Oomizu S, Sakata KM, Sakata A, Arikawa T, Watanabe K, et al. Galectin-9 Suppresses the Generation of Th17, Promotes the Induction of Regulatory T Cells, and Regulates Experimental Autoimmune Arthritis. *Clin Immunol* (2008) 127(1):78–88. doi: 10.1016/j.clim.2008.01.006
24. Oomizu S, Arikawa T, Niki T, Kadowaki T, Ueno M, Nishi N, et al. Galectin-9 Suppresses Th17 Cell Development in an IL-2-Dependent But Tim-3-Independent Manner. *Clin Immunol* (2012) 143(1):51–8. doi: 10.1016/j.clim.2012.01.004
25. Kilkenny C, Browne WJ, Cuthill IC, Emerson M, Altman DG. Improving Bioscience Research Reporting: The ARRIVE Guidelines for Reporting Animal Research. *J Pharmacol Pharmacotherapeutics* (2010) 1(2):94–9. doi: 10.4103/0976-500X.72351
26. McGrath JC, Lilley E. Implementing Guidelines on Reporting Research Using Animals (ARRIVE etc.): New Requirements for Publication in BJP. *Br J Pharmacol* (2015) 172(13):3189–93. doi: 10.1111/bph.12955
27. Ruiz-Miyazawa KW, Staurengo-Ferrari L, Mizokami SS, Domiciano TP, Vicentini F, Camilios-Neto D, et al. Quercetin Inhibits Gout Arthritis in Mice: Induction of an Opioid-Dependent Regulation of Inflammasome. *Inflammopharmacology* (2017). doi: 10.1007/s10787-017-0356-x
28. Raucci F, Iqbal AJ, Saviano A, Casillo GM, Russo M, Lezama D, et al. In-Depth Immunophenotyping Data Relating to IL-17Ab Modulation of Circulating Treg/Th17 Cells and of *in Situ* Infiltrated Inflammatory Monocytes in the Onset of Gouty Inflammation. *Data Brief* (2019) 25:104381. doi: 10.1016/j.dib.2019.104381
29. Trevisan G, Hoffmeister C, Rossato MF, Oliveira SM, Silva MA, Silva CR, et al. TRPA1 Receptor Stimulation by Hydrogen Peroxide is Critical to Trigger Hyperalgesia and Inflammation in a Model of Acute Gout. *Free Radic Biol Med* (2014) 72:200–9. doi: 10.1016/j.freeradbiomed.2014.04.021
30. Akitsu A, Ishigame H, Kakuta S, Chung SH, Ikeda S, Shimizu K, et al. IL-1 Receptor Antagonist-Deficient Mice Develop Autoimmune Arthritis Due to Intrinsic Activation of IL-17-Producing CCR2(+)Vγ6(+)γδ T Cells. *Nat Commun* (2015) 6:7464. doi: 10.1038/ncomms8464
31. Riedhammer C, Halbritter D, Weissert R. Peripheral Blood Mononuclear Cells: Isolation, Freezing, Thawing, and Culture. *Methods Mol Biol* (2016) 1304:53–61. doi: 10.1007/7651_2014_99
32. Kapellos TS, Taylor L, Feuerborn A, Valaris S, Hussain MT, Rainger GE, et al. Cannabinoid Receptor 2 Deficiency Exacerbates Inflammation and Neutrophil Recruitment. *FASEB J* (2019) 33(5):6154–67. doi: 10.1096/fj.201802524R
33. Ragab G, Elshahaly M, Bardin T. Gout: An Old Disease in New Perspective - A Review. *J advanced Res* (2017) 8(5):495–511. doi: 10.1016/j.jare.2017.04.008
34. Busso N, So A. Mechanisms of Inflammation in Gout. *Arthritis Res Ther* (2010) 12(2):206. doi: 10.1186/ar2952
35. Caution K, Young N, Robledo-Avila F, Krause K, Abu Khweek A, Hamilton K, et al. Caspase-11 Mediates Neutrophil Chemotaxis and Extracellular Trap Formation During Acute Gouty Arthritis Through Alteration of Cofilin Phosphorylation. *Front Immunol* (2019) 10:2519. doi: 10.3389/fimmu.2019.02519
36. Dai XJ, Tao JH, Fang X, Xia Y, Li XM, Wang YP, et al. Changes of Treg/Th17 Ratio in Spleen of Acute Gouty Arthritis Rat Induced by MSU Crystals. *Inflammation* (2018) 41(5):1955–64. doi: 10.1007/s10753-018-0839-y
37. So AK, Martinon F. Inflammation in Gout: Mechanisms and Therapeutic Targets. *Nat Rev Rheumatol* (2017) 13(11):639–47. doi: 10.1038/nrrheum.2017.155
38. Schorn C, Janko C, Krenn V, Zhao Y, Munoz LE, Schett G, et al. Bonding the Foe - NETting Neutrophils Immobilize the Pro-Inflammatory Monosodium Urate Crystals. *Front Immunol* (2012) 3:376. doi: 10.3389/fimmu.2012.00376
39. Matsuoka N, Fujita Y, Temmoku J, Furuya MY, Asano T, Sato S, et al. Galectin-9 as a Biomarker for Disease Activity in Systemic Lupus Erythematosus. *PloS One* (2020) 15(1):e0227069. doi: 10.1371/journal.pone.0227069
40. Sun J, Sui Y, Wang Y, Song L, Li D, Li G, et al. Galectin-9 Expression Correlates With Therapeutic Effect in Rheumatoid Arthritis. *Sci Rep* (2021) 11 (1):5562. doi: 10.1038/s41598-021-85152-2
41. Fujita Y, Asano T, Matsuoka N, Temmoku J, Sato S, Matsumoto H, et al. Differential Regulation and Correlation Between Galectin-9 and Anti-CCP Antibody (ACPA) in Rheumatoid Arthritis Patients. *Arthritis Res Ther* (2020) 22(1):80. doi: 10.1186/s13075-020-02158-3
42. Chihara M, Kurita M, Yoshihara Y, Asahina A, Yanaba K. Clinical Significance of Serum Galectin-9 and Soluble CD155 Levels in Patients With Systemic Sclerosis. *J Immunol Res* (2018) 2018:9473243. doi: 10.1155/2018/9473243
43. Xu WD, Wu Q, He YW, Huang AF, Lan YY, Fu L, et al. Gene Polymorphisms of LGALS2, LGALS3 and LGALS9 in Patients With Rheumatoid Arthritis. *Cell Immunol* (2021) 368:104419. doi: 10.1016/j.cellimm.2021.104419
44. Gualberto Cavalcanti N, Melo Vilar K, Branco Pinto Duarte AL, Barreto de Melo Rêgo MJ, Pereira MC, da Rocha Pitta I, et al. Increased Serum Levels of Galectin-9 in Patients With Chikungunya Fever. *Virus Res* (2020) 286:198062. doi: 10.1016/j.virusres.2020.198062

45. Matsumoto H, Fujita Y, Matsuoka N, Temmoku J, Yashiro-Furuya M, Asano T, et al. Serum Checkpoint Molecules in Patients With IgG4-Related Disease (IgG4-Rd). *Arthritis Res Ther* (2021) 23(1):148. doi: 10.1186/s13075-021-02527-6
46. Zhu C, Anderson AC, Schubart A, Xiong H, Imitola J, Khoury SJ, et al. The Tim-3 Ligand Galectin-9 Negatively Regulates T Helper Type 1 Immunity. *Nat Immunol* (2005) 6(12):1245–52. doi: 10.1038/ni1271
47. van de Weyer PS, Muehlfeit M, Klose C, Bonventre JV, Walz G, Kuehn EW. A Highly Conserved Tyrosine of Tim-3 is Phosphorylated Upon Stimulation by its Ligand Galectin-9. *Biochem Biophys Res Commun* (2006) 351(2):571–6. doi: 10.1016/j.bbrc.2006.10.079
48. Pearson MJ, Bik MA, Ospelt C, Naylor AJ, Wehmeyer C, Jones SW, et al. Endogenous Galectin-9 Suppresses Apoptosis in Human Rheumatoid Arthritis Synovial Fibroblasts. *Sci Rep* (2018) 8(1):12887. doi: 10.1038/s41598-018-31173-3
49. Pang N, Alimu X, Chen R, Muhashi M, Ma J, Chen G, et al. Activated Galectin-9/Tim3 Promotes Treg and Suppresses Th1 Effector Function in Chronic Lymphocytic Leukemia. *FASEB J* (2021) 35(7):e21556. doi: 10.1096/fj.202100013R
50. Ju Y, Shang X, Liu Z, Zhang J, Li Y, Shen Y, et al. The Tim-3/Galectin-9 Pathway Involves in the Homeostasis of Hepatic Tregs in a Mouse Model of Concanavalin A-Induced Hepatitis. *Mol Immunol* (2014) 58(1):85–91. doi: 10.1016/j.molimm.2013.11.001

Conflict of Interest: The authors declare that the research was conducted in the absence of any commercial or financial relationships that could be construed as a potential conflict of interest.

Publisher's Note: All claims expressed in this article are solely those of the authors and do not necessarily represent those of their affiliated organizations, or those of the publisher, the editors and the reviewers. Any product that may be evaluated in this article, or claim that may be made by its manufacturer, is not guaranteed or endorsed by the publisher.

frontiers in Immunology

REVIEW
published: 01 December 2021
doi: 10.3389/fimmu.2021.785425

Purinergic Signaling in the Regulation of Gout Flare and Resolution

Xiaoling Li[†], *Jie Gao*[†] *and Jinhui Tao*[*]

Department of Rheumatology and Immunology, The First Affiliated Hospital of University of Science and Technology of China (USTC), Division of Life Sciences and Medicine, University of Science and Technology of China, Hefei, China

Gout flares require monosodium urate (MSU) to activate the NLRP3 inflammasome and secrete sufficient IL-1β. However, MSU alone is not sufficient to cause a flare. This is supported by the evidence that most patients with hyperuricemia do not develop gout throughout their lives. Recent studies have shown that, besides MSU, various purine metabolites, including adenosine triphosphate, adenosine diphosphate, and adenosine bind to different purine receptors for regulating IL-1β secretion implicated in the pathogenesis of gout flares. Purine metabolites such as adenosine triphosphate mainly activate the NLRP3 inflammasome through P2X ion channel receptors, which stimulates IL-1β secretion and induces gout flares, while some purine metabolites such as adenosine diphosphate and adenosine mainly act on the G protein-coupled receptors exerting pro-inflammatory or anti-inflammatory effects to regulate the onset and resolution of a gout flare. Given that the purine signaling pathway exerts different regulatory effects on inflammation and that, during the inflammatory process of a gout flare, an altered expression of purine metabolites and their receptors was observed in response to the changes in the internal environment. Thus, the purine signaling pathway is involved in regulating gout flare and resolution. This study was conducted to review and elucidate the role of various purine metabolites and purinergic receptors during the process.

Keywords: purinergic signaling, gout flare, ATP, Adenosine, $P2X_7R$, IL-1β

OPEN ACCESS

Edited by:
Xiaoxia Zhu,
Fudan University, China

Reviewed by:
Haibing Chen,
Tongji University, China
Gang Chen,
University of Kentucky, United States

***Correspondence:**
Jinhui Tao
taojinhui@ustc.edu.cn

[†]*These authors have contributed equally to this work and share first authorship*

Specialty section:
This article was submitted to Autoimmune and Autoinflammatory Disorders, a section of the journal Frontiers in Immunology

Received: *29 September 2021*
Accepted: *15 November 2021*
Published: *01 December 2021*

Citation:
Li X, Gao J and Tao J (2021) Purinergic Signaling in the Regulation of Gout Flare and Resolution. Front. Immunol. 12:785425. doi: 10.3389/fimmu.2021.785425

INTRODUCTION

Gout is an inflammatory disease that manifests clinically as redness, swelling, and pain in the joints. Research involving multiple ethnicities has reported that the prevalence of gout in adults ranges between 0.68% and 3.90% (1). With the development of the economy, the incidence of gout is increasing every year, while the social danger of the disease is becoming a growing concern among scholars. Hyperuricemia underlies the pathogenesis of gout, with supersaturated uric acid being deposited in the joint cavity to form monosodium urate (MSU). The MSU stimulates abnormal IL-1β secretion to cause gout flares, which is achieved through recognition by Toll-like receptors

(TLRs) or NOD-like receptors (NLRs) to activate the innate immune system (1). The activation of NLRP3 inflammasome releases large amounts of IL-1β is a central process of MSU-mediated gout flares (2). However, clinical studies have shown that most patients with hyperuricemia do not experience gout flares (3). Additionally, the presence of triggering factors, including alcohol abuse, overeating, and exertion, is often required for a gout flare, which suggests that MSU alone is not sufficient to induce gout flares, and there is a need for other causative signals to act *in vivo* for gout flares.

The activation of NLRP3 inflammasome and subsequent induction of the release of IL-1β exerts a central role in the initiation of gout flares. Besides MSU, extracellular DAMPs and PAMPs, including bacteria, viruses, and adenosine triphosphate (ATP), are known to be responsible for the activation of the NLRP3 inflammasome. Among them, ATP-mediated activation of the $P2X_7R$-NLRP3 signaling pathway has gradually been recognized in the pathogenesis of gout (4, 5). Following tissue necrosis caused by MSU deposition, local ATP arising from the cellular release is increased, which can activate the $P2X_7$ receptor leading to intra-and extracellular ion flow, activation of the NLRP3 inflammasome, and secretion of IL-1β, ultimately triggering a gout flare. Furthermore, gene polymorphisms in the $P2X_7$ receptor have been shown to regulate IL-1β secretion *in vivo*. Several studies have demonstrated that a gain-in-function of the $P2X_7$ receptor is associated with an elevated rate of gout flares (6–8). Moreover, colchicine, a classical drug for treating acute gout flares, was found to inhibit the activation of ATP-induced $P2X_7$ receptor (9), which could be the mechanism of action against gout. This indirectly confirmed the role of ATP and $P2X_7$ receptor in gout resolution. Therefore, as an important messenger of the purinergic pathway, ATP is considered a second pathogenic signal for gout.

Besides ATP, other purinergic metabolites, such as adenosine diphosphate (ADP) and adenosine, can bind to the corresponding purinergic receptors affecting IL-1β secretion in gout. However, the purine signaling pathway exerts different regulatory effects on inflammation. For example, in contrast to ATP and ADP, adenosine exerts an inhibitory effect on inflammation *in vivo* (10). In addition, the expression of purine metabolites and their receptors varies in response to changes in the inflammatory internal environment during a gout flare. MSU was found to regulate the expression of the $P2X_7$ receptor (11). Thus, the interaction between purinergic metabolites and purinergic receptors mediates the intracellular signaling communication, which jointly regulates the onset and resolution of gout flares. In this article, we have reviewed the possible regulatory role of the purinergic signaling pathway in gout flares to understand and combat gout in a more precise manner.

CLASSIFICATION AND FUNCTION OF PURINERGIC RECEPTORS

The existence of purinergic receptors in the body was first proposed by Burnstock (12) in 1972. Since then, an increasing number of purinergic receptors have been identified, and researchers have gradually noticed the role of purinergic signaling pathways in the biological effects of diseases. The purinergic receptors, also known as P receptors, are classified as P1 and P2 receptors based on their ligands; the former binds to adenosine while the latter binds to ATP, ADP, uridine triphosphate (UTP), and uridine diphosphate (UDP). The P1 receptors are G protein-coupled receptors, which can be classified into four subtypes (A_1, A_{2A}, A_{2B}, and A_3) depending on the structure of the G proteins and intracellular conductance. The A_{2A} and A_{2B} receptors preferentially couple to G_s and exert their effects *via* the AC-cAMP-PKA pathway while the A_1 and A_3 subtypes couple to G_i and inhibit the AC activity (13). The P2 receptors, on the other hand, are divided into two major groups, P2X and P2Y receptors, depending on the signal transduction pathway. The P2X receptors are ligand-gated ion channel receptors that recognize ATP. Upon activation, the pore channels open and allow the flow of extracellular Na^+, Ca^{2+}, K^+, and the entry of macromolecules. Seven P2X receptors have been identified so far ($P2X_{1-7}$ receptors). The P2Y receptors are G protein-coupled receptors that primarily recognize ATP, UTP, and its metabolites. They can be further classified into $P2Y_1$-like receptors (coupled to G_q, including $P2Y_1$, $P2Y_2$, $P2Y_4$, $P2Y_6$, and $P2Y_{11}$ receptors) and $P2Y_{12}$-like receptors (coupled to G_i, including $P2Y_{12}$, $P2Y_{13}$, and $P2Y_{14}$ receptors) based on the intracellular signaling proteins coupled to the G proteins (14). The former receptors exert their effect *via* the PLC-IP3/DAG-PKC pathway while the latter inhibits the activity of AC, thus, producing different biological effects (**Supplementary Table 1**).

The purinergic receptors are distributed in almost all cell types, and upon recognition of the corresponding ligands, they mediate a variety of biological effects and enable the development of many diseases, including cardiovascular (15, 16), metabolic (17, 18), neurological diseases (19), and cancer (20, 21). In inflammatory diseases, purinergic receptors play an important regulatory role and participate in immune- (22), infectious- (23), and neurotransmission (24)-mediated inflammatory responses to maintain homeostasis in the organism. In the regulation of inflammation, the role of different purine signals varies. For example, the activation of $P2X_7$ receptors promotes the inflammatory response, whereas the activation of P1 receptors inhibits it. Therefore, the P receptors can coordinate the initiation, persistence, and resolution of the inflammatory response (25). Gout is an inflammatory disease caused by abnormal purine metabolism. The purine metabolites exert complex regulatory effects on the inflammatory response, influencing the onset and resolution of gout to varying degrees.

EFFECT OF PURINERGIC SIGNALING PATHWAY ON GOUT FLARES

Gout flares are a result of a complex acute inflammatory response, where the macrophages recognize MSU deposited on the joint surface, leading to the secretion of IL-1β. This is thought to be the central process in the initiation of gout flares (26).

Immediately after the release of IL-1β, the inflammatory cascade response induces neutrophil accumulation in the joints, thus, exacerbating gout flare (27). Therefore, overproduction of IL-1β is a central link in the MSU-induced gouty joint inflammation. It is essential to explore the mechanism of activation of IL-1β for investigating the pathogenesis of gout flares, and it is found that the purinergic signaling pathway is involved in the regulation of IL-1β secretion in gout.

Activation of the P2X Receptor Signaling Pathway Leads to the Promotion of Gout Flares

The P2X receptors are ATP-gated ion channel receptors, and of these P2X receptors, the $P2X_7$ receptor, initially defined as the P2Z receptor, possesses a unique sequence and rich function despite being the latest identified (28). Activation of the $P2X_7$ receptor by ATP opens ion channels causing Ca^{2+} influx and K^+ outflux to activate the NLRP3 inflammasome in the innate immune system, where Ca^{2+} may represent the second messenger of inflammasome activation (29). Also, the $P2X_7$ receptor has a unique structure and function, which does not only form ion channels but also forms the pore channels, allowing the passage of up to 900 Da molecules upon continuous activation by high concentrations of ATP. The formation of such pores appears to be required to activate the NLRP3 inflammasome (30, 31). Upon activation, the NLRP3 proteins interact with apoptosis-associated speck-like protein containing a CARD (ASC), which then recruits the pro-caspase-1 forming the NLRP3 inflammasome, which subsequently undergoes cleavage to form active caspase-1. This is further processed, leading to the secretion of mature IL-1β and IL-18 that exert inflammatory effects (32). Following pharmacological inhibition of the $P2X_7$ receptor, the level of ATP-induced IL-1β release is reduced in inflammatory cells (33). A similar reduction was observed in the levels of the $P2X_7$ receptor, ASC, or NLRP3-deficient mouse macrophages. These findings suggested that the activation of the ATP-mediated $P2X_7$ receptor plays a crucial role in promoting IL-1β secretion in inflammatory cells (34). Currently, it is recognized that the $P2X_7$ receptor, among the family of P2XRs, is the most relevant in the inflammatory response.

Gout is an acute inflammatory disease based on hyperuricemia. Predisposing factors, including alcohol abuse, overeating, cold, and late nights, are required to initiate a gout flare. We evaluated the pathogenic signals embedded in these factors associated with gout flares and found that under these conditions, ATP fluctuations were observed *in vivo*. This, for example, included mechanical stimulation during strenuous exercise promotes ATP release (35), and the adaptive febrile response of the body during cold increases ATP (36). Dramatic changes in ATP levels can activate the $P2X_7$R-NLRP3 signaling pathway and promote the IL-1β secretion associated with gout flares. Thus, ATP is considered to be involved in gout flares. A study by Tao et al. observed no difference in the IL-1β concentrations in peripheral blood leukocyte cultures from gout and hyperuricemia patients when stimulated with MSU alone, but upon stimulation with MSU and ATP together, IL-1β concentrations were found to be significantly higher in gout patients than that of the hyperuricemia patients (6). Thus, it is suggested that ATP is the second pathogenic signal for gout besides MSU. Importantly, the ability of the $P2X_7$ receptor to promote IL-1β secretion upon activation may be a major determinant of gout flares, which is influenced by the gene polymorphisms of the $P2X_7$ receptor. Studies have confirmed that gout patients possess single nucleotide polymorphism in functionally enhanced $P2X_7$ receptor compared to hyperuricemia patients (37), thus establishing an essential role of $P2X_7$ receptor in gout flares.

In hyperuricemic patients, synergistic action between MSU and ATP is required to fully activate the NLRP3 inflammasome, which causes sufficient secretion of IL-1β, leading to the onset of gout flares. Thus, it can be argued that as a receptor for ATP, the $P2X_7$ receptor is an important regulator in determining gout flares, explaining why most hyperuricemic patients do not develop gouty arthritis throughout their lives.

Besides the $P2X_7$ receptor, the $P2X_4$ receptor can also be activated by ATP, causing an inflammatory response, which is functionally similar to the $P2X_7$ receptor. Upon activation, it forms large-conductance pores in the cell membrane facilitating the ion flow, which subsequently activates the NLRP3 inflammasome. This further enhances the body's inflammatory response through its synergy with the $P2X_7$ receptor (38).

Different Roles of Activated P2Y Receptor Signaling Pathway in Gout Flares

P2Y receptors belong to the G protein-coupled receptor family and are further divided into $P2Y_1$-like receptors (coupled to G_q) and $P2Y_{12}$-like receptors (coupled to G_i), which exert regulatory effects on inflammation by affecting the activity of PLC and AC, respectively (39). Upon recognizing the corresponding nucleotide, $P2Y_1$-like receptors coupled to G_q activate the PLC-IP3/DAG-PKC pathway, promoting Ca^{2+} mobilization and inflammatory response. Also, the $P2Y_1$-like receptors can activate AC; for example, the $P2Y_{11}$ receptor promotes the activation of the AC-cAMP-PKA pathway to initiate the inflammatory response (40). The $P2Y_{12}$-like receptors coupled to G_i can exert an inhibitory effect on AC, further reducing the conversion of dephosphorylation of ATP to cAMP, thus, inhibiting the cAMP-PKA pathway-mediated inflammatory response.

The $P2Y_1$-like receptors, including the $P2Y_1$, $P2Y_2$, $P2Y_4$, $P2Y_6$, and $P2Y_{11}$ receptors, can promote inflammation either through the PLC-IP3/DAG-PKC pathway or through the activation of AC. Among these $P2Y_1$-like receptors, the $P2Y_2$ receptor may be closely associated with gout flares. Besides its inflammatory function, the $P2Y_2$ receptor can activate the NLRP3 inflammasome by stimulating the action of ATP release to further activate the $P2X_7$ receptor (41).

The $P2Y_2$ receptors are expressed on various cells, including macrophages, lymphocytes, neutrophils, and eosinophils, and

are activated by multiple nucleotides such as ATP and UTP to participate in immune regulation and inflammatory responses. The activated $P2Y_2$ receptors exhibit upregulated expression of inflammatory cytokines and chemokines, while the release of inflammatory factors is blocked by the treatment used to inhibit the $P2Y_2$ receptors (42, 43). Furthermore, the activated $P2Y_2$ receptors open pannexin-1 channels by inducing PLC activation and Ca^{2+} mobilization, which leads to further release of ATP promoting IL-1β maturation and secretion through the $P2X_7R$-NLRP3 pathway (41). Thus, the binding of the $P2Y_2$ receptors to ligands promoted the release of inflammatory factors and initiated the inflammatory response in multiple ways. The absence of the $P2Y_2$ receptor is observed to reverse the increase of the nucleotide-induced IL-1β release (44).

The current study suggested that the $P2Y_6$ receptor activated by UDP and UTP is involved in the pathogenesis of gout. Uratsuji et al. found that the $P2Y_6$ receptors were involved in the MSU-induced inflammatory responses. The activation of the $P2Y_6$ receptors in a variety of cells was observed to contribute to the production of inflammatory cytokines; particularly, the inhibition of the $P2Y_6$ receptor in THP-1 cells could reduce MSU-induced IL-1β production (45). Additionally, the $P2Y_6$ receptor affected the MSU-induced neutrophil function associated closely with gout. Sil et al. found that the inhibition of the $P2Y_6$ receptors reduced neutrophil migration and IL-8 production, which is responsible for recruiting neutrophils to the joint cavity during a gout flare, thereby amplifying the effects of gout (46). In addition, treatment with the $P2Y_6$ receptor antagonist MRS2578 inhibited the formation of MSU-induced neutrophil extracellular traps (NETs) in gout (46). Therefore, activation of the $P2Y_6$ receptor may contribute to the persistence of gout flares.

The $P2Y_{12}$-like receptors coupled to G_i, including $P2Y_{12}$, $P2Y_{13}$, and $P2Y_{14}$ receptors, inhibit the cAMP-PKA pathway-mediated inflammatory response and theoretically inhibit gout pathogenesis. However, due to the complexity of the mechanisms of action in different internal environments, the regulation of inflammation by $P2Y_{12}$-like receptors is also diverse. For example, cAMP has long been considered an inducer of inflammation. Activation of the cAMP-PKA-ERK signaling pathway promotes IL-1β secretion (47). Additionally, the AC/cAMP/PKA upregulates IL-1β-induced IL-6 production by enhancing the JAK2/STAT3 pathway (48). However, cAMP has also been recently pointed out as an important factor in regulating inflammation relief (49). The cAMP inhibits NF-κB transcription by activating downstream PKA to reduce the production of pro-inflammatory factors. Also, it promotes the phosphorylation of CENP to increase the production of anti-inflammatory factors and stimulate macrophage polarization. Moreover, cAMP has been found to inhibit the assembly of the NLRP3 inflammasome by directly binding to NLRP3 proteins, and promotes their ubiquitination and degradation (50, 51), thus acting as a negative regulator of the NLRP3 inflammasome reducing the secretion of IL-1β. Therefore, the $P2Y_{12}$-like receptors can not only exert inhibitory inflammatory effects but can also often exhibit pro-inflammatory effects through the regulation of cAMP. In microglia, extracellular ADP was observed to act on $P2Y_{12}$ receptors that activated NF-κB and NLRP3 inflammasomes while the inhibition of the $P2Y_{12}$ receptors reduced the IL-1β levels (52). Similarly, the $P2Y_{14}$ receptors promoted the secretion of inflammatory factors IL-1α, IL-8, and IL-6 in response to MSU stimulation (53).

Complex regulatory effects of inflammation are manifested in the $P2Y_{14}$ receptor. In a gout study, Li et al. found that the $P2Y_{14}$ receptors on macrophages negatively regulated cAMP, which enhanced the MSU-induced activation of the NLRP3 signaling pathway. The knockdown of the $P2Y_{14}$ receptor then limited the activation of the NLRP3 inflammasome, which in turn attenuated the MSU-induced inflammatory infiltration of synovial tissue (54). Thus, in acute gouty arthritis, the activation of the $P2Y_{14}$ receptor can exert a pro-inflammatory effect through the cAMP/NLRP3 signaling pathway.

The P2Y receptors in gout often play conflicting roles both in promoting remission of inflammation and maintaining the persistence of inflammation. As mentioned earlier, the $P2Y_{12}$-like receptor signaling pathway that inhibits inflammation can have pro-inflammatory effects through activation of NLRP3 inflammasome. Similarly, the $P2Y_1$-like receptor signaling pathway that promotes inflammation may exhibit an inhibitory effect on inflammation. For example, in a gout mouse model, the activation of the $P2Y_6$ receptors reduces 1-palmitoyl-2-linoleyl-3-acetyl-rac-glycerol-induced neutrophil infiltration, alleviating joint symptoms (55). Thus, the P2Y receptors play a complex role in inflammatory diseases, either as a friend or foe. Besides modulating the pro-inflammatory factors in the regulation of inflammatory responses, P2Y receptors can also influence the expression of anti-inflammatory cytokines. TGF-β and IL-10 are the major cytokines responsible for gout resolution (56). The $P2Y_1$ receptors were found to enhance the effects of TGF-β1 and IL-10 (57, 58), while the $P2Y_{11}$ receptor, although reported to inhibit TGF-β1 production through activation of cAMP, was found to upregulate the IL-10 expression (57, 58). Overall, the data suggested that the P2Y receptor signaling pathway was involved in the pathogenesis of gout in different ways.

Activation of the P1 Receptor Signaling Pathway Inhibits Inflammation in Gout Flares

The P1 receptors belong to the family of G protein-coupled receptors and include A_1, A_{2A}, A_{2B}, and A_3 receptors. These are widely expressed on immune cells and exhibit anti-inflammatory effects. The ligand of the P1 receptor, adenosine, is the main product of sequential hydrolysis of extracellular ATP, which is catalyzed by CD39 and CD73. Under physiological conditions, the adenosine concentration is maintained at low levels, but under certain conditions such as inflammation, hypoxia, and cellular injury, the concentration of adenosine is increased by degrading extracellular ATP and ADP. Adenosine is then rapidly metabolized to AMP and inosine by the action of adenosine kinase or adenosine deaminase. The contribution of adenosine in alleviating inflammation and maintaining homeostasis in the organism has been recognized widely (10).

The P1 receptor signaling exerts anti-inflammatory effects through a variety of pathways. The adenosine-activated P1 receptors (A_1, A_3) increase the inhibition of neutrophil adhesion, reducing the production of superoxide and secretion of inflammatory cytokines (59–61). Furthermore, the interaction of adenosine with A_1, A_{2A}, and A_3 receptors inhibits the release of IL-1β from activated human peripheral blood mononuclear lymphocytes (62). Also, the interaction of adenosine with A_3 receptors was found to reduce TNF-α production in the macrophage cell lines (63), while the interaction of adenosine with A_1 receptors was found to reduce parasite-stimulated production of reactive oxygen species (ROS) and IL-8 from neutrophils (64). Besides its inhibitory effect on the secretion of inflammatory factors, the activation of the P1 receptor signaling pathway also promotes the secretion of anti-inflammatory cytokines, including TGF-β1 and IL-10, by the immune cells (57, 60).

The targeting of adenosine receptors has been efficient in the treatment of several inflammatory diseases. The activation of adenosine-mediated A_{2A} receptor contributed to block the activity of NLRP3 inflammasome, thereby reducing the production of pro-inflammatory cytokines while increasing the production of anti-inflammatory cytokines (65, 66). In post-traumatic brain injury events, agonizing the A_3 adenosine receptor could improve the neurocognitive function by inhibiting the activation of the NLRP3 inflammasome (67). Similarly, in arthritic mice, activating the A_3 adenosine receptors could reduce the production of TNF-α and alleviate arthritic symptoms (68). Thus, increased adenosine levels following an inflammatory episode could activate the P1 receptors, exerting anti-inflammatory effects through modulation of the NLRP3 inflammasome, thus, contributing to the resolution of gout flares.

Currently, only limited evidence is available to directly demonstrate the involvement of P1 receptors in suppressing gout inflammation or promoting gout resolution. However, based on the anti-inflammatory effect of the P1 receptor signaling pathway, we can see an inevitable impact on the pathogenesis of gout through changes in adenosine concentrations during the different stages of gout flares.

ALTERATIONS IN PURINE SIGNALING PATHWAY DURING GOUT FLARES

As previously mentioned, the purine signaling pathway plays a different role in the inflammatory regulation of gout, with ATP playing a central role in its initiation. The type and concentration of purinergic metabolites during a gout flare are altered by various mediators in the inflammatory environment, which can influence the onset and resolution of gout.

Conversion of Purinergic Metabolites During Gout Flares

MSU alone is not sufficient for initiating a gout flare; the synergistic effect of high levels of extracellular ATP is also required. After the initiation of gout, an increased expression of nucleoside triphosphate dihydrolase 1 (CD39) and 5'-nucleotidase (CD73) can be seen in an inflammatory environment. CD39 dephosphorylates extracellular ATP to ADP and adenosine monophosphate (AMP), which is further converted to adenosine by CD73 (69, 70). Thus, the changes in the expression of CD39 and CD73 during a gout flare can determine the level of nucleotides and the state of inflammation that affects the course of gout disease.

The CD39 and CD73 are extracellular nucleotidases expressed on monocytes, macrophages, B cells, T cells, natural killer cells, dendritic cells, and neutrophils. They mainly maintain a balance between the extracellular ATP and the concentration of adenosine. This homeostasis is important for the persistence and extent of the inflammatory state (71). Changes in the levels of nucleotide enzymes can occur during gout flares. Inflammatory cytokines, oxidative stress, and a hypoxic environment may increase the activity of CD39 and CD73 (72), thereby reducing ATP levels and increasing adenosine concentration. Further, tissue hypoxia can also reduce the expression of nucleoside transporters, increasing the adenosine levels. CD39 is the main enzyme that metabolizes ATP. *In vitro* studies in macrophages have found that activated $P2X_7$ receptor could upregulate the expression of cytosolic CD39 by triggering a lipid raft-dependent mechanism (73). In contrast, the elevated CD39 could limit the $P2X_7$R-mediated pro-inflammatory response. The knockdown of CD39 results in excessive IL-1β release (74, 75). This implies that in addition to catabolizing ATP and promoting adenosine production, the interaction between CD39 and the $P2X_7$ receptor can modulate the upregulated inflammatory state of the organism in time to restore cellular homeostasis.

Macrophages are the primary sites of signaling events that regulate the onset and remission of gout. During the disease progression, macrophages show a shift from a pro-inflammatory M1 phenotype to an anti-inflammatory M2 phenotype. Zanin et al. found (76) that M1 macrophages showed a decrease in the expression of CD39 and CD73 along with a reduction in ATP and AMP hydrolysis, whereas the M2 macrophages displayed higher CD39 and CD73 expression, as well as increased ATP and AMP hydrolysis. Also, the addition of adenosine led to an increase in the expression of the M2 macrophage gene, which in turn promoted the conversion of M1 phenotype to M2 phenotype (77). Moreover, after the initiation of inflammation, adenosine was found to decrease the production of pro-inflammatory cytokines and increase the secretion of anti-inflammatory cytokines by macrophages (78). These data suggested that purinergic signaling may be involved in gout resolution by regulating the conversion of macrophages from the M1 to M2 phenotype.

Changes of Purinergic Receptors During Gout Flares

Besides changes in the purine metabolites, the expression of purinergic receptors seems to be altered in response to the internal environment during the inflammatory process of gout

flares. Among them, the changes in the expression of the $P2X_7$ receptor have the most important impact. In addition to directly activating the NLRP3 inflammasome, MSU was found to stimulate the expression of $P2X_7$ receptors and $P2X_4$ receptors, secreting IL-1β and causing gout flares (11). Besides, an interesting experiment found that ethanol can upregulate the expression of $P2X_7$ receptors to induce NLRP3 inflammasome activation (79), which partly explains why alcohol consumption predisposes to gout flares.

The expression of the P2Y receptor is also altered during a gout flare. The MSU stimulation of human keratinocytes resulted in an increased expression of $P2Y_6$ receptors and $P2Y_{14}$ receptors (45, 53). The $P2Y_6$ receptor belongs to the $P2Y_1$-like receptor family, which promotes the inflammatory responses and the upregulation by MSU facilitates the initiation and persistence of gout. In contrast, the $P2Y_{14}$ receptor belonging to the $P2Y_{12}$-like receptors inhibits cAMP and exhibits an inflammatory suppressive effect. The upregulation of $P2Y_{14}$ by MSU appears to be detrimental to the development of gout. However, its upregulation can also promote gout pathogenesis through the negative effect of cAMP on the NLRP3 inflammasome (54).

The transition of macrophages from the phenotypes M1 to M2 promotes remission of gout inflammation. Upon macrophage activation, an increase was observed in the expression of P1 receptors (A_1 and A_3), which was accompanied by a decrease in the production of pro-inflammatory cytokines IL-6 and TNF-α and an increase in the production of anti-inflammatory factor IL-10. This promoted macrophage polarization and contributed to the suppression of inflammation (80, 81).

Modulation of Purinergic Signaling in Different Stages of Gout Flares

The previous section showed *in vivo* conversions of purine metabolites at different stages of a gout flare. Early in the flare, large amounts of ATP were released extracellularly by the necrotic, apoptotic, and inflammatory cells through pannexins or connexin channels (82). First, ATP was bound to the $P2X_7$ receptors in the cytosol. Then, in concert with MSU, it stimulated the activation of the NLRP3 inflammasome, thus, prompting IL-1β secretion. Next, the expressions of CD39 and CD73 were increased in the inflammatory hypoxic environment following gout initiation, which promoted the dephosphorylation of ATP to adenosine. This inhibited the inflammatory response and promotes the self-resolution of gout flares by activating the P1 receptor signaling pathway. During the process, changes in the expression of purinergic receptor induced by the internal environment contributed to the ordered changes in purine signaling that regulated both gout flare and resolution (**Figure 1**). The main reasons for this seemingly contradictory mechanism are the ordered changes in the expression of purine metabolites and their receptors in the inflammatory environment, as well as the different purine signaling pathways they mediate in response to inflammation. Also, the accumulation of acidic metabolites in the inflammatory environment inhibits the cAMP/PKA signaling pathway reducing the IL-1β production (83), which indirectly counteracts the purinergic signaling-mediated cAMP/PKA pathway activity, favoring gout resolution.

Gout is a self-limiting disease with numerous causes contributing to its self-resolution. It is widely recognized that after initiating the inflammatory response in gout, neutrophils phagocytose MSU to form NETs. The aggregated NETs act by reducing the expression of pro-inflammatory cytokines (IL-1β, IL-6, IL-8), which promote the production of anti-inflammatory cytokines (TGF-β1, IL-1Ra, IL-10, IL-37), attenuating the inflammatory response (1, 84). Additionally, CD14 plays a role in the self-relief of gout. The knockdown of CD14 can reduce the activation of MSU-induced NLRP3 and release IL-1β (85). Studies have observed that a reduction of CD14 expression in gout patients may contribute to gout resolution (86). Besides neutrophils and CD14, purinergic signaling pathways play a synergistic role in gout resolution through the regulation of inflammatory responses.

CONCLUSION AND OUTLOOK

In summary, purinergic signaling pathways are involved in regulating the entire process of gout flare and resolution. After the initiation of the inflammatory response in gout, inflammation-induced microenvironmental changes lead to an orderly alteration in the type of purinergic metabolites in the body, gradually converting a large amount of ATP released from necrotic cells into ADP and adenosine. These purinergic metabolites stimulate the corresponding purinergic receptors and exert different regulatory effects on the inflammatory response. With the conversion of ATP to adenosine, the pro-inflammatory response mediated by the P2X and P2Y receptor signaling pathway shifts to an anti-inflammatory effect mediated mainly by the P1Y receptor signaling pathway, which then balances and restores the body's homeostasis. These changes may therefore be an important mechanism of action for self-resolution of gout flares.

The purinergic signaling pathways can be potential targets for future interventions in gout pathogenesis. Currently, attempts are made to use targeted purinergic receptor therapy in gout. In a recent study, researchers designed and synthesized a novel $P2Y_{14}$ receptor antagonist, which reduced the MSU-induced joint swelling and inflammatory infiltration in an acute gouty arthritis mouse model (87, 88), thus, improving the clinical value of targeted purinergic signaling in gout. However, the regulation of inflammation by purinergic signaling is much more complex than expected. It is not only manifested by the complexity of purinergic receptor-mediated signaling mechanisms, for example, the same receptor exhibiting opposite effects on inflammation in different settings, but it is also manifested by the diversity of their ligands. Besides activation by purinergic metabolites, receptors can be activated

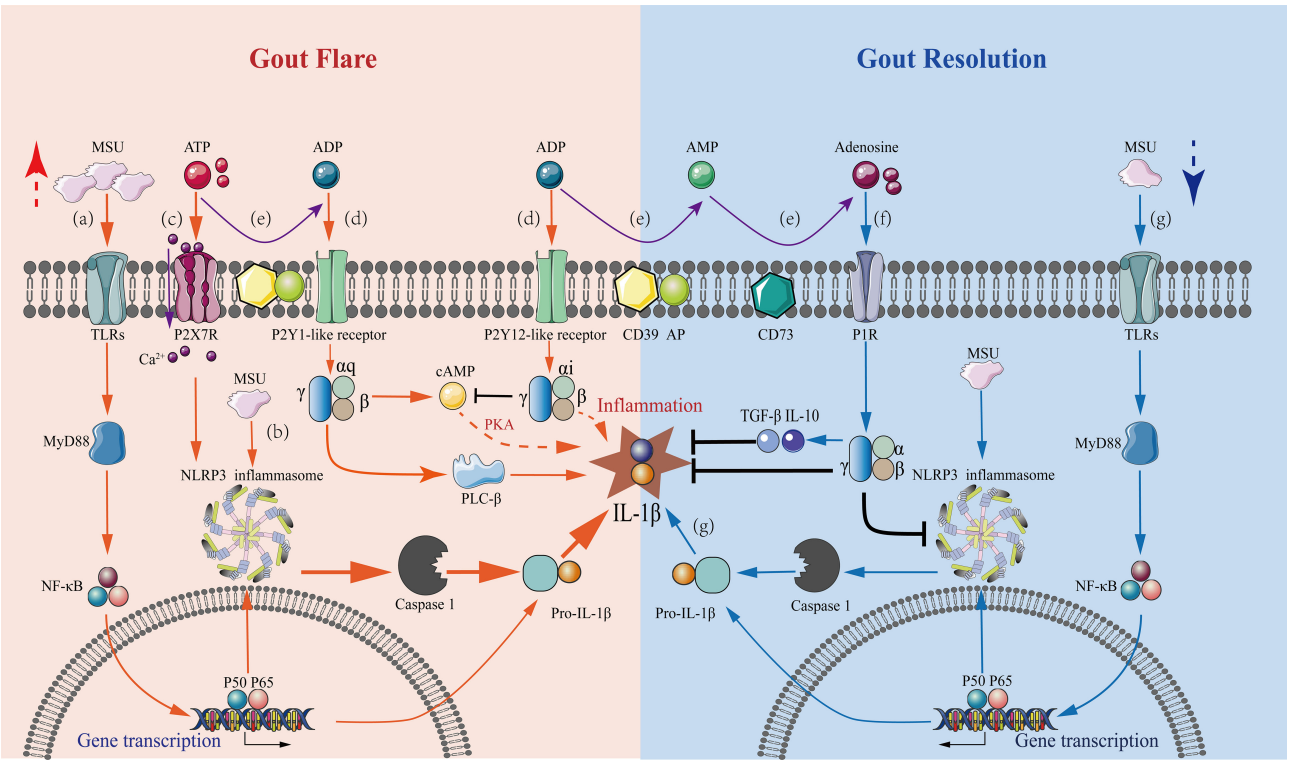

FIGURE 1 | Mechanisms underlying purinergic signaling pathways in the regulation of gout flares and resolution. A series of purinergic receptor-mediated intracellular signaling events in macrophages are involved in gout flare and resolution, with the regulation of IL-1β levels being a central event. Gout flare: **(A)** The binding of extracellular MSU to TLR induces intracellular transcription and accumulation of the pro-IL-1β gene through activation of MyD88-NFκB signaling. **(B)** The uptake of MSU then activates the NLRP3 inflammasome, releasing active caspase-1, which cleaves pro-IL-1β to mature IL-1β. **(C)** Increased extracellular ATP binds to $P2X_7$ receptors causing Ca^{2+} influx, which stimulates the NLRP3 inflammasome activation in concert with MSU, leading to massive IL-1β secretion. **(D)** Extracellular ATP and ADP stimulate the $P2Y_1$-like receptors coupled to Gq, activating the PLC-IP3/DAG-PKC signaling pathway and cAMP-PKA pathway, which promotes the release of IL-1β. The stimulation of $P2Y_{12}$-like receptors coupled to G_i exerts an inhibitory effect on the AC-cAMP-PKA pathway reducing the IL-1β production. However, inhibition of IL-1β production *via* other pathways also exists. Gout resolution: **(E)** In an inflammatory hypoxic environment, the activation of CD39 and CD73 during gout flares results in the progressive degradation of ATP and ADP to adenosine. **(F)** The resultant adenosine activates P1 receptors, decreasing the secretion of pro-inflammatory cytokine IL-1β, thus, promoting the production of anti-inflammatory cytokines TGF-β1 and IL-10. **(G)** Under the inflammatory conditions of gout, ATP is degraded, which affects the sustained stimulation of the $P2X_7$R-NLRP3 signaling pathway. This results in a marked reduction of IL-1β secretion by MSU stimulation alone, which is not sufficient to sustain gout, and the condition then tends toward inflammatory remission.

by additional endogenous ligands. A complex regulation network is formed between the endogenous ligands and P2Y receptors, finely tuning the nucleotide receptor signaling pathway (89). Therefore, the internal environment also has an important influence on purinergic signaling. An in-depth study of the regulatory mechanisms underlying different purinergic signals and the integration of various upstream and downstream influencing factors can accurately determine the role of purinergic signaling in gout flares, providing effective strategies for clinical intervention.

AUTHOR CONTRIBUTIONS

XL wrote the manuscript. JG drafted the figures. JT contributed to provide the general idea and edited the manuscript. All authors contributed to the article and approved the submitted version.

FUNDING

This work was supported by the National Natural Science Foundation of China (81771774) and Anhui Provincial Key research and development plan (201904a07020103).

SUPPLEMENTARY MATERIAL

The Supplementary Material for this article can be found online at: https://www.frontiersin.org/articles/10.3389/fimmu.2021.785425/full#supplementary-material

REFERENCES

1. Dalbeth N, Gosling AL, Gaffo A, Abhishek A. Gout. *Lancet* (2021) 397:1843–55. doi: 10.1016/S0140-6736(21)00569-9
2. Martinon F, Pétrilli V, Mayor A, Tardivel A, Tschopp J. Gout-Associated Uric Acid Crystals Activate the NALP3 Inflammasome. *Nature* (2006) 440:237–41. doi: 10.1038/nature04516
3. Bardin T, Richette P. Definition of Hyperuricemia and Gouty Conditions. *Curr Opin Rheumatol* (2014) 26:186–91. doi: 10.1097/BOR.0000000000000028
4. Gicquel T, Le Daré B, Boichot E, Lagente V. Purinergic Receptors: New Targets for the Treatment of Gout and Fibrosis. *Fundam Clin Pharmacol* (2017) 31:136–46. doi: 10.1111/fcp.12256
5. Tao JH, Zhang Y, Li XP. P2X7R: A Potential Key Regulator of Acute Gouty Arthritis. *Semin Arthritis Rheumatol* (2013) 43:376–80. doi: 10.1016/j.semarthrit.2013.04.007
6. Tao JH, Cheng M, Tang JP, Dai XJ, Zhang Y, Li XP, et al. Single Nucleotide Polymorphisms Associated With P2X7R Function Regulate the Onset of Gouty Arthritis. *PloS One* (2017) 12:e0181685. doi: 10.1371/journal
7. Ying Y, Chen Y, Li Z, Huang H, Gong Q. Investigation Into the Association Between P2RX7 Gene Polymorphisms and Susceptibility to Primary Gout and Hyperuricemia in a Chinese Han Male Population. *Rheumatol Int* (2017) 37:571–78. doi: 10.1007/s00296-017-3669-6
8. Gong QY, Chen Y. Correlation Between P2X7 Receptor Gene Polymorphisms and Gout. *Rheumatol Int* (2015) 35:1307–10. doi: 10.1007/s00296-015-3258-5
9. Marques-da-Silva C, Chaves MM, Castro NG, Coutinho-Silva R, Guimaraes MZ. Colchicine Inhibits Cationic Dye Uptake Induced by ATP in P2X2 and P2X7 Receptor-Expressing Cells: Implications for its Therapeutic Action. *Br J Pharmacol* (2011) 163:912–26. doi: 10.1111/j.1476-5381.2011.01254.x
10. Linden J, Cekic C. Regulation of Lymphocyte Function by Adenosine. *Arterioscler Thromb Vasc Biol* (2012) 32:2097–103. doi: 10.1161/ATVBAHA.111.226837
11. Gicquel T, Robert S, Loyer P, Victoni T, Bodin A, Ribault C, et al. IL-1β Production is Dependent on the Activation of Purinergic Receptors and NLRP3 Pathway in Human Macrophages. *FASEB J* (2015) 29:4162–73. doi: 10.1096/fj.14-267393
12. Burnstock G. Purinergic Nerves. *Pharmacol Rev* (1972) 24:509–81.
13. Pasquini S, Contri C, Borea PA, Vincenzi F, Varani K. Adenosine and Inflammation: Here, There and Everywhere. *Int J Mol Sci* (2021) 22:7685. doi: 10.3390/ijms22147685
14. Klaver D, Thurnher M. Control of Macrophage Inflammation by P2Y Purinergic Receptors. *Cells* (2021) 10:1098. doi: 10.3390/cells10051098
15. Godoy-Marín H, Duroux R, Jacobson KA, Soler C, Colino-Lage H, Jiménez-Sábado V, et al. Adenosine A2A Receptors Are Upregulated in Peripheral Blood Mononuclear Cells From Atrial Fibrillation Patients. *Int J Mol Sci* (2021) 22:3467. doi: 10.3390/ijms22073467
16. Tian G, Zhou J, Quan Y, Kong Q, Wu W, Liu X. P2Y1 Receptor Agonist Attenuates Cardiac Fibroblasts Activation Triggered by TGF-β1. *Front Pharmacol* (2021) 12:627773. doi: 10.3389/fphar.2021.627773
17. Jain S, Jacobson KA. Purinergic Signaling in Diabetes and Metabolism. *Biochem Pharmacol* (2021) 187:114393. doi: 10.1016/j.bcp.2020.114393
18. Jain S, Pydi SP, Toti KS, Robaye B, Idzko M, Gavrilova O, et al. Lack of Adipocyte Purinergic P2Y6 Receptor Greatly Improves Whole Body Glucose Homeostasis. *Proc Natl Acad Sci USA* (2020) 117:30763–74. doi: 10.1073/pnas.2006578117
19. D'Angelo V, Giorgi M, Paldino E, Cardarelli S, Fusco FR, Saverioni I, et al. A2A Receptor Dysregulation in Dystonia DYT1 Knock-Out Mice. *Int J Mol Sci* (2021) 22:2691. doi: 10.3390/ijms22052691
20. Cao Y, Wang X, Li Y, Evers M, Zhang H, Chen X. Extracellular and Macropinocytosis Internalised ATP Work Together to Induce Epithelial-Mesenchymal Transition and Other Early Metastatic Activities in Lung Cancer. *Cancer Cell Int* (2019) 19:254. doi: 10.1186/s12935-019-0973-0
21. Zhang Y, Ding J, Wang L. The Role of P2X7 Receptor in Prognosis and Metastasis of Colorectal Cancer. *Adv Med Sci* (2019) 64:388–94. doi: 10.1016/j.advms.2019.05.002
22. Shakya AK, Naik RR, Almasri IM, Kaur A. Role and Function of Adenosine and its Receptors in Inflammation, Neuroinflammation, IBS, Autoimmune Inflammatory Disorders, Rheumatoid Arthritis and Psoriasis. *Curr Pharm Des* (2019) 25:2875–91. doi: 10.2174/1381612825666190716145206
23. Di Virgilio F, Dal Ben D, Sarti AC, Giuliani AL, Falzoni S. The P2X7 Receptor in Infection and Inflammation. *Immunity* (2017) 47:15–31. doi: 10.1016/j.immuni.2017.06.020
24. Illes P, Rubini P, Ulrich H, Zhao Y, Tang Y. Regulation of Microglial Functions by Purinergic Mechanisms in the Healthy and Diseased CNS. *Cells* (2020) 9:1108. doi: 10.3390/cells9051108
25. Di Virgilio F, Sarti AC, Coutinho-Silva R. Purinergic Signaling, DAMPs, and Inflammation. *Am J Physiol Cell Physiol* (2020) 318:C832–35. doi: 10.1152/ajpcell.00053.2020
26. Schett G, Dayer JM, Manger B. Interleukin-1 Function and Role in Rheumatic Disease. *Nat Rev Rheumatol* (2016) 12:14–24. doi: 10.1038/nrrheum.2016.166
27. Mitroulis I, Kambas K, Ritis K. Neutrophils. IL-1beta, and Gout:is There a Link? *Semin Immunopathol* (2013) 35:501–12. doi: 10.1007/s00281-013-0361-0
28. North RA. Molecular Physiology of P2X Receptors. *Physiol Rev* (2002) 82:1013–67. doi: 10.1152/physrev.00015.2002
29. Latz E, Xiao TS, Stutz A. Activation and Regulation of the Inflammasomes. *Nat Rev Immunol* (2013) 13:397–411. doi: 10.1038/nri3452
30. Monif M, Reid CA, Powell KL, Smart ML, Williams DA. The P2X7 Receptor Drives Microglial Activation and Proliferation: A Trophic Role for P2X7R Pore. *J Neurosci* (2009) 29:3781–91. doi: 10.1523/JNEUROSCI.5512-08.2009
31. Burnstock G. P2X Ion Channel Receptors and Inflammation. *Purinergic Signal* (2016) 12:59–67. doi: 10.1007/s11302-015-9493-0
32. Zahid A, Li B, Kombe AJK, Jin T, Tao J. Pharmacological Inhibitors of the NLRP3 Inflammasome. *Front Immunol* (2019) 10:2538. doi: 10.3389/fimmu.2019.02538
33. Faria RX, Oliveira FH, Salles JP, Oliveira AS, von Ranke NL, Bello ML, et al. 1,4-Naphthoquinones Potently Inhibiting P2X7 Receptor Activity. *Eur J Med Chem* (2018) 143:1361–72. doi: 10.1016/j.ejmech.2017.10.033
34. Liu YH, Chang YC, Chen LK, Su PA, Ko WC, Tsai YS, et al. The ATP-P2X7 Signaling Axis Is an Essential Sentinel for Intracellular Clostridium Difficile Pathogen-Induced Inflammasome Activation. *Front Cell Infect Microbiol* (2018) 8:84. doi: 10.3389/fcimb.2018.00084
35. Sauer H, Hescheler J, Wartenberg M. Mechanical Strain-Induced Ca(2+) Waves are Propagated *via* ATP Release and Purinergic Receptor Activation. *Am J Physiol Cell Physiol* (2000) 279:C295–307. doi: 10.1152/ajpcell.2000.279.2.C295
36. Lowell BB, Spiegelman BM. Towards a Molecular Understanding of Adaptive Thermogenesis. *Nature* (2000) 404:652–60. doi: 10.1038/35007527
37. Tao JH, Tang JP, Chen M, Li XP, Liu Q, Wang YL. Study on the Association Between P2X7R Gene Rs1621388 Polymorphism and Gout Susceptibility. *Chin J Dis Control Prev* (2017) 21:698–701. doi: 10.16462/j.cnki.zhjbkz.2017.07.012
38. Kanellopoulos JM, Almeida-da-Silva CLC, Rüütel Boudinot S, Ojcius DM. Structural and Functional Features of the P2X4 Receptor: An Immunological Perspective. *Front Immunol* (2021) 12. doi: 10.3389/fimmu
39. Cattaneo M. P2Y12 Receptors: Structure and Function. *J Thromb Haemost* (2015) Suppl 1:S10–6. doi: 10.1111/jth.12952
40. Franke H, Krügel U, Illes P. P2 Receptors and Neuronal Injury. *Pflugers Arch* (2006) 452:622–44. doi: 10.1007/s00424-006-0071-8
41. Thorstenberg ML, Rangel Ferreira MV, Amorim N, Canetti C, Morrone FB, Alves Filho JC, et al. Purinergic Cooperation Between P2Y2 and P2X7 Receptors Promote Cutaneous Leishmaniasis Control: Involvement of Pannexin-1 and Leukotrienes. *Front Immunol* (2018) 9:1531. doi: 10.3389/fimmu.2018.01531
42. Kobayashi T, Kouzaki H, Kita H. Human Eosinophils Recognise Endogenous Danger Signal Crystalline Uric Acid and Produce Pro-Inflammatory Cytokines Mediated by Autocrine ATP. *J Immunol* (2010) 184:6350–8. doi: 10.4049/jimmunol.0902673
43. Kobayashi T, Soma T, Noguchi T, Nakagome K, Nakamoto H, Kita H, et al. ATP Drives Eosinophil Effector Responses Through P2 Purinergic Receptors. *Allergol Int* (2015) 64 Suppl(0):S30–6. doi: 10.1016/j.alit.2015.04.009
44. de la Rosa G, Gómez AI, Baños MC, Pelegrín P. Signaling Through Purinergic Receptor P2Y2 Enhances Macrophage IL-1β Production. *Int J Mol Sci* (2020) 21:4686. doi: 10.3390/ijms21134686

45. Uratsuji H, Tada Y, Kawashima T, Kamata M, Hau CS, Asano Y, et al. P2Y6 Receptor Signaling Pathway Mediates Inflammatory Responses Induced by Monosodium Urate Crystals. *J Immunol* (2012) 188:436–44. doi: 10.4049/jimmunol.1003746
46. Sil P, Hayes CP, Reaves BJ, Breen P, Quinn S, Sokolove J, et al. P2Y6 Receptor Antagonist MRS2578 Inhibits Neutrophil Activation and Aggregated Neutrophil Extracellular Trap Formation Induced by Gout-Associated Monosodium Urate Crystals. *J Immunol* (2017) 198:428–42. doi: 10.4049/jimmunol.1600766
47. Permpoonputtana K, Porter JE, Govitrapong P. Calcitonin Gene-Related Peptide Mediates an Inflammatory Response in Schwann Cells Via cAMP-Dependent ERK Signaling Cascade. *Life Sci* (2016) 144:19–25. doi: 10.1016/j.lfs.2015.11.015
48. Tanabe K, Kozawa O, Iida H. cAMP/PKA Enhances Interleukin-1β-Induced Interleukin-6 Synthesis Through STAT3 in Glial Cells. *Cell Signal* (2016) 28:19–24. doi: 10.1016/j.cellsig.2015.10.009
49. Tavares LP, Negreiros-Lima GL, Lima KM, E Silva PMR, Pinho V, Teixeira MM, et al. Blame the Signaling: Role of cAMP for the Resolution of Inflammation. *Pharmacol Res* (2020) 159:105030. doi: 10.1016/j.phrs.2020.105030
50. Lee GS, Subramanian N, Kim AI, Aksentijevich I, Goldbach-Mansky R, Sacks DB, et al. The Calcium-Sensing Receptor Regulates the NLRP3 Inflammasome Through Ca2+ and cAMP. *Nature* (2012) 492:123–7. doi: 10.1038/nature11588
51. Sokolowska M, Chen LY, Liu Y, Martinez-Anton A, Qi HY, Logun C, et al. Prostaglandin E2 Inhibits NLRP3 Inflammasome Activation Through EP4 Receptor and Intracellular Cyclic AMP in Human Macrophages. *J Immunol* (2015) 194:5472–87. doi: 10.4049/jimmunol.1401343
52. Suzuki T, Kohyama K, Moriyama K, Ozaki M, Hasegawa S, Ueno T, et al. Extracellular ADP Augments Microglial Inflammasome and NF-κb Activation *via* the P2Y12 Receptor. *Eur J Immunol* (2020) 50:205–19. doi: 10.1002/eji.201848013
53. Uratsuji H, Tada Y, Hau CS, Shibata S, Kamata M, Kawashima T, et al. Monosodium Urate Crystals Induce Functional Expression of P2Y14 Receptor in Human Keratinocytes. *J Invest Dermatol* (2016) 136:1293–6. doi: 10.1016/j.jid.2016.01.026
54. Li H, Jiang W, Ye S, Zhou M, Liu C, Yang X, et al. P2Y14 Receptor has a Critical Role in Acute Gouty Arthritis by Regulating Pyroptosis of Macrophages. *Cell Death Dis* (2020) 11:394. doi: 10.1038/s41419-020-2609-7
55. Shin SH, Jeong J, Kim JH, Sohn KY, Yoon SY, Kim JW. 1-Palmitoyl-2-Linoleoyl-3-Acetyl-Rac-Glycerol (PLAG) Mitigates Monosodium Urate (MSU)-Induced Acute Gouty Inflammation in BALB/c Mice. *Front Immunol* (2020) 11:710. doi: 10.3389/fimmu.2020.00710
56. Scanu A, Oliviero F, Ramonda R, Frallonardo P, Dayer JM, Punzi L. Cytokine Levels in Human Synovial Fluid During the Different Stages of Acute Gout: Role of Transforming Growth Factor β1 in the Resolution Phase. *Ann Rheum Dis* (2012) 71:621–4. doi: 10.1136/annrheumdis-2011-200711
57. Zuccarini M, Giuliani P, Buccella S, Di Liberto V, Mudò G, Belluardo N, et al. Modulation of the TGF-β1-Induced Epithelial to Mesenchymal Transition (EMT) Mediated by P1and P2 Purine Receptors in MDCK Cells. *Purinergic Signal* (2017) 13:429–42. doi: 10.1007/s11302-017-9571-6
58. Seo DR, Kim SY, Kim KY, Lee HG, Moon JH, Lee JS, et al. Cross Talk Between P2 Purinergic Receptors Modulates Extracellular ATP-Mediated Interleukin-10 Production in Rat Microglial Cells. *Exp Mol Med* (2008) 40:19–26. doi: 10.3858/emm.2008.40.1.19
59. Barletta KE, Ley K, Mehrad B. Regulation of Neutrophil Function by Adenosine. *Arterioscler Thromb Vasc Biol* (2012) 32:856–64. doi: 10.1161/ATVBAHA.111.226845
60. Koscso B, Csoka B, Selmeczy Z, Himer L, Pacher P, Virag L, et al. Adenosine Augments IL-10 Production by Microglial Cells Through an A2B Adenosine Receptor-Mediated Process. *J Immunol* (2012) 188:445e453. doi: 10.4049/jimmunol.1101224
61. Haskó G, Pacher P. Regulation of Macrophage Function by Adenosine. *Arterioscler Thromb Vasc Biol* (2012) 32:865–9. doi: 10.1161/ATVBAHA.111.226852
62. Sipka S, Kovács I, Szántó S, Szegedi G, Brugós L, Bruckner G, et al. Adenosine Inhibits the Release of Interleukin-1beta in Activated Human Peripheral Mononuclear Cells. *Cytokine* (2005) 31:258–63. doi: 10.1016/j.cyto.2005.05.002
63. Sajjadi FG, Takabayashi K, Foster AC, Domingo RC, Firestein GS. Inhibition of TNF-Alpha Expression by Adenosine: Role of A3 Adenosine Receptors. *J Immunol* (1996) 156:3435–42.
64. Frasson AP, Menezes CB, Goelzer GK, Gnoatto SCB, Garcia SC, Tasca T. Adenosine Reduces Reactive Oxygen Species and Interleukin-8 Production by Trichomonas Vaginalis-Stimulated Neutrophils. *Purinergic Signal* (2017) 13:569–77. doi: 10.1007/s11302-017-9584-1
65. Zhou Y, Zeng X, Li G, Yang Q, Xu J, Zhang M, et al. Inactivation of Endothelial Adenosine A_{2A} Receptors Protects Mice From Cerebral Ischaemia-Induced Brain Injury. *Br J Pharmacol* (2019) 176:2250–63. doi: 10.1111/bph.14673
66. Ohta A, Sitkovsky M. Role of G-Protein-Coupled Adenosine Receptors in Downregulation of Inflammation and Protection From Tissue Damage. *Nature* (2001) 414:916–20. doi: 10.1038/414916a
67. Farr SA, Cuzzocrea S, Esposito E, Campolo M, Niehoff ML, Doyle TM, et al. Adenosine A_3 Receptor as a Novel Therapeutic Target to Reduce Secondary Events and Improve Neurocognitive Functions Following Traumatic Brain Injury. *J Neuroinflammation* (2020) 17:339. doi: 10.1186/s12974-020-02009-7
68. Baharav E, Bar-Yehuda S, Madi L, Silberman D, Rath-Wolfson L, Halpren M, et al. Anti-Inflammatory Effect of A3 Adenosine Receptor Agonists in Murine Autoimmune Arthritis Models. *J Rheumatol* (2005) 32:469–76.
69. Yegutkin GG. Nucleotide- and Nucleoside-Converting Ectoenzymes: Important Modulators of Purinergic Signaling Cascade. *Biochim Biophys Acta* (2008) 1783:673–94. doi: 10.1016/j.bbamcr.2008.01.024
70. Liu X, Ma L, Zhang S, Ren Y, Dirksen RT. CD73 Controls Extracellular Adenosine Generation in the Trigeminal Nociceptive Nerves. *J Dent Res* (2017) 96:671–77. doi: 10.1177/0022034517692953
71. Murphy PS, Wang J, Bhagwat SP, Munger JC, Janssen WJ, Wright TW, et al. CD73 Regulates Anti-Inflammatory Signaling Between Apoptotic Cells and Endotoxin-Conditioned Tissue Macrophages. *Cell Death Differ* (2017) 24:559–70. doi: 10.1038/cdd.2016.159
72. Synnestvedt K, Furuta GT, Comerford KM, Louis N, Karhausen J, Eltzschig HK, et al. Ecto-5'-Nucleotidase (CD73) Regulation by Hypoxia-Inducible Factor-1 Mediates Permeability Changes in Intestinal Epithelia. *J Clin Invest* (2002) 110:993–1002. doi: 10.1172/JCI15337
73. Savio LEB, de Andrade Mello P, Santos SACS, de Sousa JC, Oliveira SDS, Minshall RD, et al. P2X7 Receptor Activation Increases Expression of Caveolin-1 and Formation of Macrophage Lipid Rafts, Thereby Boosting CD39 Activity. *J Cell Sci* (2020) 133:jcs237560. doi: 10.1242/jcs.237560
74. Savio LEB, de Andrade Mello P, Figliuolo VR, de Avelar Almeida TF, Santana PT, Oliveira SDS, et al. CD39 Limits P2X7 Receptor Inflammatory Signaling and Attenuates Sepsis-Induced Liver Injury. *J Hepatol* (2017) 67:716–26. doi: 10.1016/j.jhep.2017.05.021
75. Lévesque SA, Kukulski F, Enjyoji K, Robson SC, Sévigny J. NTPDase1 Governs P2X7-Dependent Functions in Murine Macrophages. *Eur J Immunol* (2010) 40:1473–85. doi: 10.1002/eji.200939741
76. Zanin RF, Braganhol E, Bergamin LS, Campesato LF, Filho AZ, Moreira JC, et al. Differential Macrophage Activation Alters the Expression Profile of NTPDase and Ecto-5'-Nucleotidase. *PloS One* (2012) 7:e31205. doi: 10.1371/journal.pone.0031205
77. Barberà-Cremades M, Baroja-Mazo A, Pelegrín P. Purinergic Signaling During Macrophage Differentiation Results in M2 Alternative Activated Macrophages. *J Leukoc Biol* (2016) 99:289–99. doi: 10.1189/jlb.1A0514-267RR
78. Haskó G, Cronstein BN. Adenosine: An Endogenous Regulator of Innate Immunity. *Trends Immunol* (2004) 25:33–9. doi: 10.1016/j.it.2003.11.003
79. Le Daré B, Victoni T, Bodin A, Vlach M, Vene E, Loyer P, et al. Ethanol Upregulates the P2X7 Purinergic Receptor in Human Macrophages. *Fundam Clin Pharmacol* (2019) 33:63–74. doi: 10.1111/fcp.12433
80. Antonioli L, Csóka B, Fornai M, Colucci R, Kókai E, Blandizzi C, et al. Adenosine and Inflammation: What's New on the Horizon? *Drug Discov Today* (2014) 19:1051–68. doi: 10.1016/j.drudis.2014.02.010
81. Haskó G, Szabó C, Németh ZH, Kvetan V, Pastores SM, Vizi ES. Adenosine Receptor Agonists Differentially Regulate IL-10, TNF-Alpha, and Nitric Oxide Production in RAW 264.7 Macrophages and in Endotoxemic Mice. *J Immunol* (1996) 157:4634–40.
82. Eltzschig HK, Eckle T, Mager A, Küper N, Karcher C, Weissmüller T, et al. ATP Release From Activated Neutrophils Occurs *via* Connexin 43 and

Modulates Adenosine-Dependent Endothelial Cell Function. *Circ Res* (2006) 99:1100–8. doi: 10.1161/01.RES.0000250174.31269.70
83. Jin Y, Sato K, Tobo A, Mogi C, Tobo M, Murata N, et al. Inhibition of Interleukin-1β Production by Extracellular Acidification Through the TDAG8/cAMP Pathway in Mouse Microglia. *J Neurochem* (2014) 129:683–95. doi: 10.1111/jnc.12661
84. Schauer C, Janko C, Munoz LE, Zhao Y, Kienhöfer D, Frey B, et al. Aggregated Neutrophil Extracellular Traps Limit Inflammation by Degrading Cytokines and Chemokines. *Nat Med* (2014) 20:511–7. doi: 10.1038/nm.3547
85. Scott P, Ma H, Viriyakosol S, Terkeltaub R, Liu-Bryan R. Engagement of CD14 Mediates the Inflammatory Potential of Monosodium Urate Crystals. *J Immunol* (2006) 177:6370–8. doi: 10.4049/jimmunol.177.9.6370
86. Duan L, Luo J, Fu Q, Shang K, Wei Y, Wang Y, et al. Decreased Expression of CD14 in MSU-Mediated Inflammation May Be Associated With Spontaneous Remission of Acute Gout. *J Immunol Res* (2019) 2019:7143241. doi: 10.1155/2019/7143241
87. Lu R, Wang Y, Liu C, Zhang Z, Li B, Meng Z, et al. Design, Synthesis and Evaluation of 3-Amide-5-Aryl Benzoic Acid Derivatives as Novel P2Y14R Antagonists With Potential High Efficiency Against Acute Gouty Arthritis. *Eur J Med Chem* (2021) 216:113313. doi: 10.1016/j.ejmech.2021.113313
88. Wang W, Liu C, Li H, Tian S, Liu Y, Wang N, et al. Discovery of Novel and Potent P2Y14R Antagonists *via* Structure-Based Virtual Screening for the Treatment of Acute Gouty Arthritis. *J Adv Res* (2020) 23:133–42. doi: 10.1016/j.jare.2020.02.007
89. Volonté C, Amadio S, D'Ambrosi N, Colpi M, Burnstock G. P2 Receptor Web: Complexity and Fine-Tuning. *Pharmacol Ther* (2006) 112:264–80. doi: 10.1016/j.pharmthera.2005.04.012

Conflict of Interest: The authors declare that the research was conducted in the absence of any commercial or financial relationships that could be construed as a potential conflict of interest.

Publisher's Note: All claims expressed in this article are solely those of the authors and do not necessarily represent those of their affiliated organizations, or those of the publisher, the editors and the reviewers. Any product that may be evaluated in this article, or claim that may be made by its manufacturer, is not guaranteed or endorsed by the publisher.

frontiers in Immunology

ORIGINAL RESEARCH
published: 21 December 2021
doi: 10.3389/fimmu.2021.771677

Recombinant Human Proteoglycan 4 Regulates Phagocytic Activation of Monocytes and Reduces IL-1β Secretion by Urate Crystal Stimulated Gout PBMCs

*Sandy ElSayed[1], Gregory D. Jay[2], Ralph Cabezas[2], Marwa Qadri[3], Tannin A. Schmidt[4] and Khaled A. Elsaid[1]**

[1] Department of Biomedical and Pharmaceutical Sciences, Chapman University, Irvine, CA, United States, [2] Department of Emergency Medicine, Rhode Island Hospital, Providence, RI, United States, [3] Department of Pharmacology, School of Pharmacy, Jazan University, Jazan, Saudi Arabia, [4] Biomedical Engineering Department, University of Connecticut Health Center, Farmington, CT, United States

OPEN ACCESS

Edited by:
Lihua Duan,
Jiangxi Provincial People's Hospital, China

Reviewed by:
Laure Campillo-Gimenez, University of California, San Diego, United States
Ya-Fei Liu, First Affiliated Hospital of Zhengzhou University, China

***Correspondence:**
Khaled A. Elsaid
elsaid@chapman.edu

Specialty section:
This article was submitted to Autoimmune and Autoinflammatory Disorders, a section of the journal Frontiers in Immunology

Received: 06 September 2021
Accepted: 30 November 2021
Published: 21 December 2021

Citation:
ElSayed S, Jay GD, Cabezas R, Qadri M, Schmidt TA and Elsaid KA (2021) Recombinant Human Proteoglycan 4 Regulates Phagocytic Activation of Monocytes and Reduces IL-1β Secretion by Urate Crystal Stimulated Gout PBMCs. Front. Immunol. 12:771677. doi: 10.3389/fimmu.2021.771677

Objectives: To compare phagocytic activities of monocytes in peripheral blood mononuclear cells (PBMCs) from acute gout patients and normal subjects, examine monosodium urate monohydrate (MSU) crystal-induced IL-1β secretion ± recombinant human proteoglycan 4 (rhPRG4) or interleukin-1 receptor antagonist (IL-1RA), and study the anti-inflammatory mechanism of rhPRG4 in MSU stimulated monocytes.

Methods: Acute gout PBMCs were collected from patients in the Emergency Department and normal PBMCs were obtained from a commercial source. Monocytes in PBMCs were identified by flow cytometry. PBMCs were primed with Pam3CSK4 (1μg/mL) for 24h and phagocytic activation of monocytes was determined using fluorescently labeled latex beads. MSU (200μg/mL) stimulated IL-1β secretion was determined by ELISA. Reactive oxygen species (ROS) generation in monocytes was determined fluorometrically. PBMCs were incubated with IL-1RA (250ng/mL) or rhPRG4 (200μg/mL) and bead phagocytosis by monocytes was determined. THP-1 monocytes were treated with MSU crystals ± rhPRG4 and cellular levels of NLRP3 protein, pro-IL-1β, secreted IL-1β, and activities of caspase-1 and protein phosphatase-2A (PP2A) were quantified. The peritoneal influx of inflammatory and anti-inflammatory monocytes and neutrophils in Prg4 deficient mice was studied and the impact of rhPRG4 on immune cell trafficking was assessed.

Results: Enhanced phagocytic activation of gout monocytes under basal conditions ($p<0.001$) was associated with ROS generation and MSU stimulated IL-1β secretion ($p<0.05$). rhPRG4 reduced bead phagocytosis by normal and gout monocytes compared to IL-1RA and both treatments were efficacious in reducing IL-1β secretion ($p<0.05$). rhPRG4 reduced pro-IL-1β content, caspase-1 activity, conversion of pro-IL-1β to mature IL-1β and restored PP2A activity in monocytes ($p<0.05$). PP2A inhibition reversed rhPRG4's effects on pro-IL-1β and mature IL-1β in MSU stimulated monocytes.

Neutrophils accumulated in peritoneal cavities of Prg4 deficient mice ($p<0.01$) and rhPRG4 treatment reduced neutrophil accumulation and enhanced anti-inflammatory monocyte influx ($p<0.05$).

Conclusions: MSU phagocytosis was higher in gout monocytes resulting in higher ROS and IL-1β secretion. rhPRG4 reduced monocyte phagocytic activation to a greater extent than IL-1RA and reduced IL-1β secretion. The anti-inflammatory activity of rhPRG4 in monocytes is partially mediated by PP2A, and *in vivo*, PRG4 plays a role in regulating the trafficking of immune cells into the site of a gout flare.

Keywords: acute gout flare, PRG4, monocytes, interleukin-1 receptor antagonist (IL-1 ra), urate crystals

INTRODUCTION

Gout is the most common form of crystal induced arthritis with an estimated 2012 global prevalence of 0.6% (1). The country-specific prevalence estimates vary significantly with a reported prevalence in the U.S. of 3.9%, compared to 1% or lower in China and Northern Europe (2–5). The incidence of newly diagnosed gout has more than doubled over the past decade, with greater incidences observed in males and in the later decades of life (1, 6). Hyperuricemia is the most significant risk factor for gout development where gout-associated inflammation is triggered by the deposition of poorly soluble monosodium urate monohydrate (MSU) crystals in peripheral joints and tissues (7). The most affected joints include the first metatarsophalangeal joint, and the knee, where gout often presents as an acute flare of pain and inflammation that usually resolves within one week (7, 8). Interspersed between acute gout flares are asymptomatic periods of low-grade chronic inflammation and progressive joint damage (7). Acute gout flares are treated with anti-inflammatory agents e.g., colchicine, non-steroidal anti-inflammatory drugs (NSAIDs) and corticosteroids, either alone or in combination (9, 10). None of these pharmacological agents have demonstrated superiority in controlling acute gout inflammation and their use is complicated by considerable side effects, toxicities, and relative contraindications (7, 11, 12). For patients with comorbid diabetes, renal or cardiovascular diseases, the use of interleukin-1 receptor antagonist (IL-1RA) was shown to be efficacious in the management of acute gout (13, 14). However, suboptimal clinical treatment outcomes are prevalent, with significant economic and humanistic burdens and therefore the development of novel and safer therapeutics remains an unmet clinical need.

The pathophysiology of acute gout involves the recognition of urate crystals by monocytes/macrophages in joint tissues and their subsequent phagocytosis (15, 16). Urate crystals initiate NOD-, LRR- and pyrin domain containing protein 3 (NLRP3) inflammasome activation in a mechanism that involves the generation of reactive oxygen species (ROS), resulting in recruitment of pro-caspase-1 and its conversion to active caspase-1 (16, 17). Active caspase-1 catalyzes the conversion of pro-interleukin-1 beta (pro-IL-1β) to mature IL-1β, which is the primary effector *pro*-inflammatory cytokine in gout (15, 16). Damage-associated molecular patterns (DAMPs) can also activate the NLRP3 inflammasome in gout and increase IL-1β gene expression *via* activation of toll-like receptors 2 and 4 (TLR2 and TLR4) (7, 18, 19). During an acute gout flare, circulating monocytes are recruited to the affected joint, where they contribute to inflammation *via* phagocytosis of urate crystals and differentiation into M1-like inflammatory macrophages (15, 16, 20). In response to TLR2 ligands and crystals, monocytes in peripheral blood mononuclear cells (PBMCs) from gout patients were shown to secrete higher IL-1β and other *pro*-inflammatory cytokines and chemokines compared to PBMCs from normal subjects, and the extent of IL-1β secretion was positively correlated to the annual number of acute gout attacks (21). The enhanced production of mature IL-1β by gout PBMCs was shown to likely be due to enhanced caspase-1 mediated conversion of pro-IL-1β (21). A possible explanation for the enhanced generation of mature IL-1β by gout PBMCs is chronic hyperuricemia where uric acid priming enhances IL-1β secretion by human PBMCs, *via* activating the AKT-PRAS40 autophagy pathway (22).

In our laboratory, we have previously shown that proteoglycan 4 (PRG4) and its receptor CD44, and one of several CD44 transducers, protein phosphatase-2A (PP2A) signaling axis plays a biologically significant role in regulating urate crystal inflammation. Recombinant human PRG4 (rhPRG4) inhibited urate crystal phagocytosis by murine and human macrophages, NLRP3 inflammasome activation and conversion of pro-IL-1β to mature IL-1β (23). rhPRG4 also attenuated pain and inflammation in a rat model of acute gout in the knee (23). The efficacy of rhPRG4 was likely due to its binding CD44 receptor, as CD44 was shown to mediate phagocytic uptake of urate crystals by murine and human macrophages (24, 25). The significance of the PRG4/CD44/PP2A axis was further highlighted by our recent observations that uptake of urate crystals by human monocytes was associated with a reduction in PP2A activity and that a small molecule PP2A activator reduced IL-1β secretion in human monocytes *via* attenuating pro-IL-1β production (26). While available *in vitro* and *in vivo* data suggest that rhPRG4 may be of considerable utility as a novel therapeutic in acute gout, the efficacy of rhPRG4 in gout monocytes remains unclear.

In this investigation, we aimed to quantify the *pro*-inflammatory response of normal and gout PBMCs towards

combined TLR2 ligand and urate crystal stimulation with a particular focus on monocytes' phagocytic activation and downstream IL-1β secretion. We compared the anti-inflammatory efficacy of IL-1RA and rhPRG4 and investigated how rhPRG4 regulates the activation of gout PBMCs. We also studied urate crystal stimulated THP-1 monocytes and evaluated whether rhPRG4's effect was mediated by PP2A activity enhancement. We supplemented our *in vitro* assays with an *in vivo* peritoneal model of acute gout flare where we studied the impact of *Prg4* expression on the peritoneal influx of inflammatory classical monocytes (CMs), anti-inflammatory non-classical monocytes (NCMs) and neutrophils as well as IL-1β and CXCL1 levels (24, 27). We hypothesized that gout PBMCs display enhanced IL-1β secretion due to increased phagocytosis of urate crystals by monocytes which can be suppressed by rhPRG4, and rhPRG4's anti-inflammatory effect is PP2A-dependent.

METHODS

Patient Characteristics and Study Overview

Blood samples were collected from patients presenting to the Emergency Departments at Rhode Island and The Mariam Hospitals (located in Providence, RI, USA and are members of the Lifespan network) with a chief complaint of an acute gout flare. The acute gout cohort included 36 patients (28 males and 8 females) whose median age was 68 years with a range between 42 and 91 years. A total of 22 patients were on a urate-lowering therapy at the time of admission and 5 patients were using oral colchicine. PBMCs were isolated from blood samples using the Ficoll-Paque density gradient centrifugation method (28), and cells were stored in liquid nitrogen until the time of experimentation. Our study was approved by the Institutional Review Board (IRB) at Lifespan. PBMCs from twelve normal subjects were obtained from a commercial source (ATCC, USA). Monocytes in normal and gout PBMCs were identified by flow cytometry using CD14 and CD45 surface markers (29) and their phagocytic activity was determined using FITC-labeled rabbit IgG coated latex beads. Urate crystal phagocytosis by monocytes was determined by estimating the percentage of monocytes with elevated side-scatter values above a pre-determined threshold (23). Generation of reactive oxygen species (ROS) in monocytes from normal and gout PBMCs and THP-1 monocytes, following urate crystal exposure, was determined fluorometrically, and the contribution of ROS generation to IL-1β secretion by PBMCs was investigated by treating PBMCs with urate crystals ± the antioxidant N-acetylcysteine. The anti-inflammatory dose-response efficacies of IL-1RA and rhPRG4 were investigated in normal PBMCs and doses that produced maximal IL-1β attenuation by both biologics were used in follow-up experiments utilizing urate crystal stimulated gout PBMCs. The modulation of monocytes' phagocytic activity by IL-RA and rhPRG4 was also studied in normal and gout PBMCs. To further investigate the anti-inflammatory mechanism of rhPRG4, we studied urate crystal stimulated THP-1 monocytes and assessed the impact of rhPRG4 treatment on NLRP3 protein levels, caspase-1 activation, and conversion of pro-IL-1β to mature IL-1β. Since PRG4 is a ligand of the CD44 receptor and building on our previous report that a CD44 antibody treatment activated PP2A in murine and human macrophages (24), we aimed to study the impact of rhPRG4 on PP2A activity in THP-1 monocytes. To further characterize the contribution of PP2A to rhPRG4's mechanism of action, we evaluated the effect of co-incubating rhPRG4 with okadaic acid, a potent PP2A inhibitor (30). Normal and gout PBMCs and THP-1 monocytes were primed with a TLR2 ligand, Pam3CSK4, for 24h prior to adding urate crystals, as PBMCs and monocytes fail to secrete significant IL-1β in response to crystals alone (22, 26). Across all experiments, assays were performed with two technical replicates per experimental group, with 3-4 independent experiments for THP-1 monocytes. Our *in vivo* experiments were approved by the IACUC committee at Chapman University. We utilized the peritoneal model of acute gout flare after intraperitoneal administration of urate crystals (24). We studied the peritoneal influx of CMs (identified as CD11b+ Ly6C^{hi} CCR2+), NCMs (identified as CD11b+ Ly6C^{lo} CD43^{hi} CX3CR1+), and neutrophils (Ly6G+ Ly6B.2+) at 6h and 24h in *Prg4* gene-trap (*Prg4*^{GT}) mice. We also determined IL-1β and CXCL1 levels in peritoneal lavages. The *Prg4*^{GT} mouse (stock no. 025740, JAX, USA) is born lacking *Prg4* expression which can be restored *via* CRE-mediated recombination (31). We compared the peritoneal influx of immune cells in the *Prg4*$^{GT/GT}$ animals to that in *Prg4*$^{+/+}$ animals (stock # 101045, JAX; B6/129S background).

Immunophenotyping of Monocytes and Determinations of Phagocytic Activity and ROS Generation

Normal and gout PBMCs were washed, centrifuged at 300x*g* for 10 min and seeded in RPMI 1640 media (ATCC) supplemented with 2% heat-inactivated fetal bovine serum (FBS) and 1% penicillin-Streptomycin (Sigma Aldrich, USA) at a density of 1.0 x 10^6 cells per well. Culture media was supplemented with 50 IU benzonase (Sigma Aldrich) to avoid cell clumping. Human THP-1 leukemic monocytic cells (ATCC) were seeded as described above. Immunophenotyping of monocytes in PBMCs was performed by flow cytometry using APC/Cyanine7 anti-human CD14 antibody (monocyte marker; 1:20 dilution) (BioLegend, USA) and PE-anti human CD45 antibody (pan-leukocyte marker; 1:25 dilution) (BioLegend). Following treatments, PBMCs were collected and centrifuged at 3,000 rpm for 5 min. Cells were then incubated with Zombie Violet viability dye in FACS blocking buffer (0.5% BSA, 2% FBS in PBS) for 10 min on ice. Subsequently, cells were stained with anti-CD14 and anti-CD45 antibodies in FACS staining/washing buffer (0.5% BSA, 0.05% sodium azide in PBS) for 20 min. Cells were then washed twice with FACS washing buffer followed by flow cytometric analysis (BD FACSAria). Flow cytometry plots and analyses were generated using Flow Jo® software (BD Biosciences, USA), and positive staining thresholds were determined using fluorescence minus one (FMO) control.

Phagocytic activity of monocytes was performed using FITC-labeled rabbit IgG-coated latex beads (Cayman Chemicals, USA). PBMCs or THP-1 monocytes were incubated with Pam3CSK4 (1μg/mL) (Invivogen, USA) for 24h. Subsequently, fluorescently labeled beads were co-incubated with cells for 4h and the fluorescence intensity (FI) geometric means of bead-positive cells were calculated. Bead-positive cells were determined using an FMO control.

ROS generation in monocytes of normal and gout PBMCs and THP-1 monocytes was determined using the DCFDA/H2DCFDA cellular ROS Assay Kit (Abcam, USA). The principle of the assay is based on the oxidation of a non-fluorescent probe by cellular hydroxyl, peroxyl and other ROS species into a fluorescent product. PBMCs were incubated with DCFDA/H2DCFDA for 30 min at 37°C followed by incubation with MSU crystals (200μg/mL) (Invivogen) for 2h. Subsequently, PBMCs were collected and stained with anti-CD14 and anti-CD45 antibodies as described above to identify monocytes. Quantitation of ROS generation in monocytes was performed by initially gating for AlexFluor-488 positive monocytes and then calculating the FI geometric means of this population. Supernatant mature IL-1β levels were also measured at 2h using an ELISA kit (R&D Systems, USA).

Dose Response and Anti-Inflammatory Efficacies of IL-1RA and rhPRG4 in Urate Crystal Treated Normal and Gout PBMCs

Normal PBMCs were stimulated with Pam3CSK4 (1μg/mL) ± recombinant human IL-1RA (GenScript, USA; MW ~ 25 kDa) (100, 250, 500 ng/mL, 1 and 2μg/mL) or rhPRG4 (Lubris, USA; apparent MW ~ 460 kDa and ~ 1M Da as disulfide bonded dimer) (10, 50, 100 and 200μg/mL) (32) for 24h followed by MSU crystals (200μg/mL) for 6h and secreted IL-1β levels were determined by ELISA (R&D Systems). Gout PBMCs were stimulated with Pam3CSK4 (1μg/mL) ± IL-1RA (250ng/mL) or rhPRG4 (200μg/mL) for 24h followed by adding urate crystals and measurement of secreted IL-1β levels as described above. The efficacy of IL-1RA (250ng/mL) or rhPRG4 (200μg/mL) in modulating the extent of bead phagocytosis by normal and gout monocytes was determined as described above following Pam3CSK4 (1μg/mL) priming ± IL-1RA or rhPRG4 for 24h.

Impact of N-Acetylcysteine (NAC) Treatment on ROS Generation in Normal PBMCs and Related IL-1β Secretion

Normal PBMCs were primed with Pam3CSK4 (1μg/mL) for 24h followed by treatment with MSU crystals (200μg/mL) ± N-acetylcysteine (20 mM) (Sigma Aldrich) and ROS generation and secreted IL-1β levels were determined as described above at 2h and 6h, *respectively*. In these ROS experiment, we used 20μM DCFDA while in the gout and normal monocyte ROS experiments, we used 10μM DCFDA. THP-1 monocyte ROS experiments were performed as described above using 20μM DCFDA.

Impact of IL-1RA or rhPRG4 Treatments on IL-1β Gene Expression, Intracellular Pro-IL-1β and Secreted IL-1β in Urate Crystal Stimulated THP-1 Monocytes

THP-1 monocytes were treated with Pam3CSK4 (1μg/mL) for 24h followed by MSU crystals (200μg/mL) ± IL-1RA (250ng/mL) or rhPRG4 (200μg/mL) for 6h. IL-1β gene expression was performed as previously described (26), using commercially available primers and probes for IL-1β (Hs01555410_m1) and β-actin (Hs00194899_m1) (ThermoFisher Scientific, USA), and the cycle threshold (Ct) value of IL-1β was normalized to the Ct value of β-actin in the same sample, and the relative expression in the different experimental groups compared to untreated controls was computed using the $2^{-\Delta\Delta Ct}$ method (26). In another set of experiments, cells were treated and subsequently collected and lysed using RIPA buffer + 1% protease inhibitor (ThermoFisher Scientific), and cell lysate total protein was determined using the micro-BCA assay kit (Sigma Aldrich). Pro-IL-1β levels in cell lysates (MyBioSource, USA) and supernatant mature IL-1β levels were determined by ELISA and analyte concentrations in cell lysates were normalized to total protein.

Role of PP2A in Mediating rhPRG4's Anti-Inflammatory Efficacy in Urate Crystal Stimulated Human THP-1 Monocytes

PP2A was immunoprecipitated from THP-1 monocyte cell lysates following Pam3CSK4 priming for 24h and MSU crystals (200μg/mL) ± IL-1RA (250ng/mL) or rhPRG4 (200μg/mL) for 6h. PP2A activity was determined as previously described (26), and normalized to cell lysate total protein. To further investigate the role of PP2A in mediating rhPRG4's effect, THP-1 monocytes were stimulated with Pam3CSK4 for 24h followed by MSU crystals (200μg/mL) ± rhPRG4 (200μg/mL) ± okadaic acid (5nM) (Cayman Chemicals) for 6h. Intracellular pro-IL-1β, NLRP3 protein (MyBioSource) and secreted IL-1β levels were determined as described above. To determine caspase-1 activity in THP-1 monocytes, 500,000 cells were seeded in black 96-well plate with clear bottoms (Sigma Aldrich) and stimulated as described above. Caspase-1 activity was determined using the cell based active capase-1 staining kit (Abcam).

In Vivo Peritoneal Model of Acute Gout Flare in *Prg4*$^{GT/GT}$ and *Prg4*$^{+/+}$ Mice and Impact of rhPRG4 Treatment on Peritoneal Influx of Monocytes and Neutrophils and Peritoneal Lavage IL-1β and CXCL1 Levels

We have utilized the murine peritoneal model of acute gout as previously described (24), and compared the influx of pro-inflammatory CMs, anti-inflammatory NCMs and neutrophils at 6h and 24h following intra-peritoneal administration of MSU crystals (2mg in 200μL) in *Prg4*$^{GT/GT}$ and *Prg4*$^{+/+}$ mice. Animals were 2-3 months old and included equal numbers of males and females (n=4 in each group at each time point). Lavaging was performed by injecting 3 mL of cold PBS into the peritoneal

cavity followed by shaking for 30–60 seconds and lavage aspiration. Lavage fluids were centrifuged at 450 g for 10 min and cell pellets were resuspended in 1 mL PBS and subjected to immunophenotyping, as described above, while supernatants were used for ELISAs. The following fluorochrome-conjugated antibodies were used at manufacturer's recommended dilutions: APC-Cy7-anti-CD11b, Alexa-488-anti-Ly6C, PE-anti-CCR2, APC-anti-CD43, PerCP-Cy5.5-anti-CX3CR1, APC-Cy7-anti-Ly6G (BioLegend) and Alexa-488-anti-Ly6B.2 (Fisher Scientific). Immunophenotyping for CMs and NCMs was performed independently of neutrophil immunophenotyping, and the number of cells in populations of interest were estimated using Precision Counting Beads (BioLegend). In another set of experiments, rhPRG4 (50μL; 1 mg/mL) or PBS (50μL) were administered at 6h following urate crystal administration and peritoneal lavaging and immunophenotyping were performed at 24h. IL-1β and CXCL1 levels were determined by ELISA (R&D Systems).

Statistical Analyses

Continuous variables were initially evaluated to determine if they satisfy the requirements of parametric statistical tests. Statistical comparisons between two groups were performed using Student's *t*-test or the non-parametric Mann-Whitney U test. Statistical comparisons of multiple groups were performed using one-way and two-way analysis of variance (ANOVA) followed by Tukey's *post*-hoc test for parametric data or the equivalent ANOVA on the ranks for non-parametric data. A p value of < 0.05 was considered statistically significant. Data are graphically represented as scatter plot bar graphs with mean ± standard deviation indicated.

RESULTS

Monocytes From Gout Patients Demonstrated Enhanced Basal Bead Uptake and Elevated IL-1β Secretion in Response to TLR2 Ligand Priming and Urate Crystal Exposure

The flow cytometry gating strategy to identify monocytes in PBMCs and quantitation of FITC-labeled beads' uptake by monocytes are shown in **Figure 1A**. We initially identified monocytes using a combination of side scatter area (SSC-A) and forward scatter area (FSC-A) values (29). Singlet cells were subsequently identified based on FSC-A and FSC-height (FSC-H) and monocytes were confirmed by dual positive staining for CD14 and CD45 markers. Monocytes' phagocytic activity was determined by estimating the percentage of monocytes positive for FITC-labeled beads. Representative flow cytometry plots showing enhanced bead uptake in gout monocytes are shown in **Figure 1B**. We observed that uptake of FITC-labeled beads by gout monocytes under basal condition was higher than their uptake by normal monocytes ($p<0.001$; **Figure 1C**). Under TLR2 stimulated condition, bead phagocytosis by normal monocytes increased ($p<0.05$) while gout monocytes showed no significant change in their bead uptake ($p>0.05$). In stimulated samples, bead phagocytosis was not different between normal and gout monocytes ($p>0.05$). The enhanced basal phagocytic activity of gout monocytes indicates that these cells may have already been primed towards urate crystal uptake, potentially due to the systemic inflammatory environment in acute gout. In contrast, normal subjects' monocytes had to be primed with a TLR2 ligand to increase their phagocytic activity, to a level comparable to that of gout monocytes at baseline. A combination of TLR2 ligand and urate crystals resulted in greater IL-1β secretion from gout PBMCs compared to normal PBMCs ($p<0.05$; **Figure 1D**).

IL-1RA and rhPRG4 Displayed Dose-Dependent Reductions in IL-1β Secretion From Normal PBMCs and the Anti-Inflammatory Effect of Both Treatments Was Related to Reducing Phagocytic Activation of Normal Monocytes

IL-1RA treatment reduced IL-1β secretion by MSU stimulated normal PBMCs with efficacy observed at 250 ng/mL and higher ($p<0.0001$; **Figure 2A**), whereby the anti-inflammatory efficacy of IL-1RA did not change above the 250 ng/mL level. Meanwhile, rhPRG4 reduced IL-1β secretion in the same model at 100 and 200 μg/mL ($p<0.01$; $p<0.001$; **Figure 2B**), with the 200 μg/mL concentration appearing to produce marginally better reduction in IL-1β secretion compared to the 100 μg/mL concentration. The magnitudes of IL-1β secretion from positive control groups were different between the IL-1RA and rhPRG4 experiments, with approximately 30% less IL-1β secretion in the rhPRG4 dose-response experiment. This might be attributed to the different normal PBMCs specimens used between the two experiments. Nonetheless, IL-1RA and rhPRG4 produced robust maximal reductions in IL-1β secretions. At dose levels that maximally reduced IL-1β secretion, IL-1RA (250 ng/mL) and rhPRG4 (200 μg/mL) reduced normal monocytes' phagocytic activity following TLR2 ligand treatment ($p<0.01$; $p<0.0001$; **Figure 2C**) but rhPRG4 displayed a greater reduction in FITC-labeled beads' uptake by normal monocytes compared to IL-1RA ($p<0.05$).

rhPRG4 But Not IL-1RA Reduced Basal and TLR2 Ligand Stimulated Bead Uptake by Gout Monocytes and the Anti-Inflammatory Effects of Both IL-1RA and rhPRG4 Were Dependent on the Magnitude of IL-1β Secretion by Gout PBMCs

rhPRG4 (200 μg/mL) reduced basal and TLR2 stimulated bead uptake by gout monocytes compared to IL-1RA (250 ng/mL) treatment ($p<0.0001$ for both comparisons; **Figure 2D**). We observed high variability in the anti-inflammatory effects of IL-1RA and rhPRG4 in urate crystal stimulated gout PBMCs (**Figure 2E**). The mean reduction in IL-1β (95% CI) in the gout cohort was 27.3% (15.2%-39.4%) with IL-1RA and 30.9% (21.1%-40.6%) with rhPRG4. PBMCs from patients on oral colchicine had blunted IL-1β secretion, as 4 out of 5 specimens

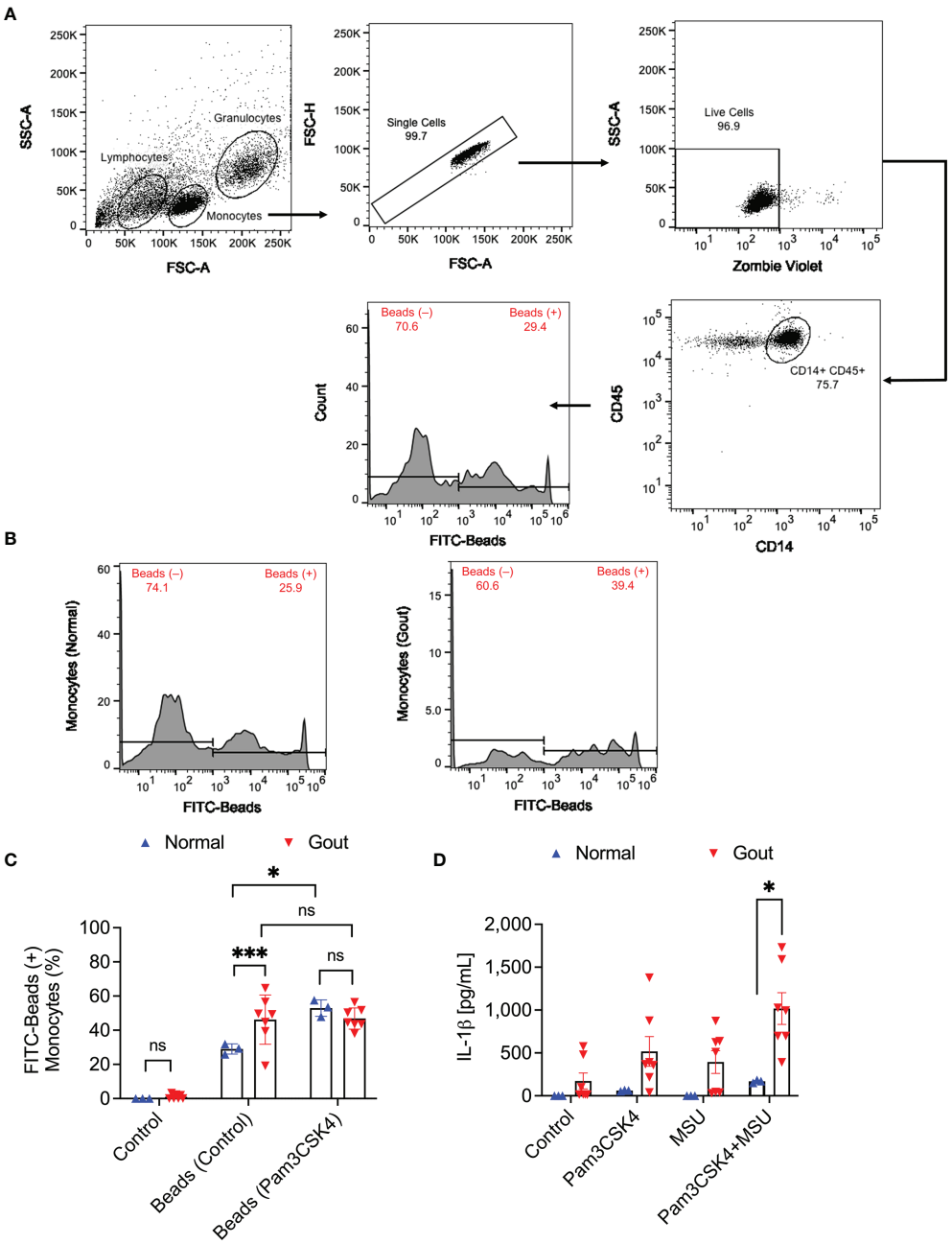

FIGURE 1 | Analysis of the phagocytic activity of monocytes in peripheral blood mononuclear cells (PBMCs) of normal subjects (n=3) and gout patients (n=7) and its relationship to interleukin-1 beta (IL-1β) release in response to priming with Pam3CSK4, a toll-like receptor 2 ligand, and treatment with monosodium urate monohydrate (MSU) crystals. To assess phagocytic activation, PBMCs were treated with Pam3CSK4 (1μg/mL) for 24h followed by co-incubation with FITC-labeled rabbit IgG-coated latex beads and determination of percent bead-positive monocytes. Alternatively, PBMCs were incubated with MSU crystals (200μg/mL) and secreted IL-1β levels were determined by ELISA at 6h. Analysis of FITC-bead positive monocytes was performed using 2-way ANOVA followed by Tukey's *post*-hoc test, and analysis of IL-1β levels was performed by multiple *t*-tests followed by a *post*-hoc false discovery rate analysis using two stage step-up approach. ns, non-significant; $*p < 0.05$; $***p < 0.001$. **(A)** Flow cytometry gating strategy for monocytes in PBMCs. Identification of monocytes was conducted using the expected forward and side scatter (FSC-A and SSC-A) ranges and single cells were gated using FSC-A and FSC-H. Viable cells were identified using Zombie Violet viability dye and monocytes were confirmed using CD14 and CD45 surface markers. Subsequently, bead positive monocytes were gated based on thresholds established using fluorescence minus one control. **(B)** Representative flow cytometry histograms depicting a higher percentage of bead-positive monocytes in a gout patient compared to a normal subject. **(C)** Monocytes of gout patients had higher basal phagocytic activities compared to normal subjects. TLR2 ligand priming increased phagocytic activities of normal subjects' monocytes but not gout patients and phagocytic activities in primed samples were not different between normal and gout subjects. **(D)** A combination of TLR2 ligand priming and MSU crystal challenge resulted in higher secreted IL-1β levels from gout patients' PBMCs.

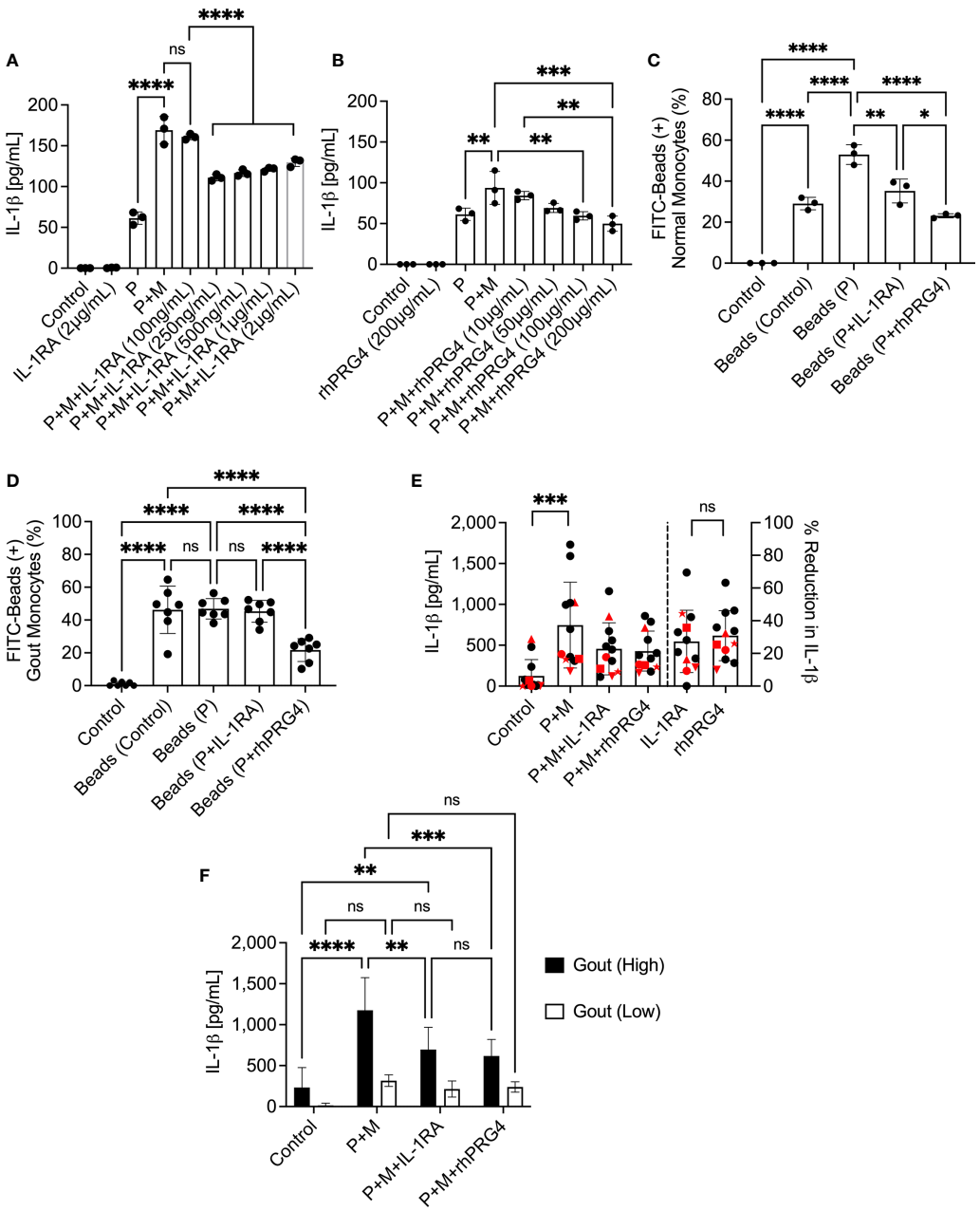

FIGURE 2 | Dose-response of interleukin-1 receptor antagonist (IL-1RA) and recombinant human proteoglycan 4 (rhPRG4) in Pam3CSK4 (P), a toll-like receptor 2 ligand, and monosodium urate monohydrate (M) crystal-stimulated peripheral blood mononuclear cells (PBMCs) of normal subjects and efficacy of IL-1RA and rhPRG4 in modulating phagocytic activation of monocytes of normal subjects (n=3) and gout patients (n=7 to 12) and secretion of mature interleukin-1 beta (IL-1β) by urate crystal-stimulated gout PBMCs. To assess phagocytic activation, PBMCs were treated with Pam3CSK4 (1μg/mL) for 24h followed by co-incubation with FITC-labeled rabbit IgG-coated latex beads and determination of percent bead-positive monocytes, using the gating strategy shown in **Figure 1A**. Alternatively, PBMCs were incubated with urate crystals (200μg/mL) and secreted IL-1β levels were determined by ELISA. Gout PBMCs were categorized, based on urate crystal-induced IL-1β secretion, as either high IL-1β secreting (IL-1β concentrations > 500pg/mL) (n=6) or low IL-1β secreting (IL-1β concentrations < 500pg/mL) (n=6) and the differential efficacies of IL-1RA and rhPRG4 on both populations was investigated. Statistical analyses included one and two-way ANOVAs followed by Tukey's *post*-hoc test. ns, non-significant; *$p < 0.05$; **$p < 0.01$; ***$p < 0.001$; ****$p < 0.0001$. **(A)** IL-1RA (250ng/mL and higher) reduced IL-1β secretion by PBMCs of normal subjects. **(B)** rhPRG4 (100&200μg/mL) reduced IL-1β secretion by PBMCs of normal subjects. **(C)** IL-1RA (250ng/mL) and rhPRG4 (200μg/mL) reduced phagocytic activation of monocytes in PBMCs of normal subjects. rhPRG4 treatment reduced bead phagocytosis by normal monocytes compared to IL-1RA. **(D)** rhPRG4 (200μg/mL) reduced bead phagocytosis by gout monocytes, while IL-1RA (250ng/mL) did not alter fluorescent bead uptake by the same monocytes. **(E)** IL-1RA (250ng/mL) and rhPRG4 (200μg/mL) reduced IL-1β secretion by gout PBMCs by similar magnitudes. PBMCs from patients receiving colchicine (n=5) are highlighted in red. 4 out of 5 samples are classified as low-IL-1β secreting gout PBMCs. **(F)** IL-1RA (250ng/mL) and rhPRG4 (200μg/mL) reduced IL-1β secretion from high-IL-1β secreting gout PBMCs but not from low-IL-1β secreting PBMCs.

(all 5 specimens are highlighted in red) were in the low IL-1β secreting group (**Figure 2E**, left panel). In addition, percentage reductions in IL-1β secretion by IL-1RA or rhPRG4 in the majority of these specimens were lower than the average for the entire cohort (**Figure 2E**, right panel). IL-1RA and rhPRG4 treatments reduced IL-1β secretion by gout PBMC specimens that exhibited high urate crystal stimulated IL-1β release (>500 pg/mL) ($p<0.01$; $p<0.001$; **Figure 2F**). In gout PBMCs with IL-1β secretion < 500 pg/mL, IL-1RA and rhPRG4 treatments showed no significant reductions in IL-1β release ($p>0.05$). These findings argue that rhPRG4 exerts its anti-inflammatory effect by virtue of reducing monocytes' phagocytic activation and thus their ability to internalize urate crystals and that the greater the stimulation of monocytes by urate crystals, the more significant is the anti-inflammatory effect of rhPRG4.

Enhanced Urate Crystal Uptake by Gout Monocytes Elicited Higher ROS Levels and NAC Treatment Reduced IL-1β Secretion in Urate Crystal Stimulated Normal PBMCs

We identified monocytes with urate crystal uptake according to changes in SSC-A values as shown in representative flow cytometry histograms in **Figure 3A**. In gout monocytes, we detected higher crystal positive fractions compared to normal monocytes ($p<0.05$; **Figure 3B**). The enhanced urate crystal phagocytosis by gout monocytes was associated with a significant increase in secreted IL-1β levels, at 2h, by gout PBMCs compared to normal PBMCs ($p<0.05$; **Figure 3C**). The gating strategy to quantify ROS generation in normal and gout monocytes is shown in **Figure 3D**. Monocytes were gated according to the strategy presented in **Figure 1A** and the percentage of monocytes positive for ROS was quantified. The positivity threshold was determined using control untreated samples, and the FI geometric means in ROS-positive monocytes were determined and compared across treatment groups. Urate crystals did not appreciably increase ROS levels in normal monocytes ($p>0.05$; **Figure 3E**), which might be due to the quantity of urate crystals vis-à-vis the number of monocytes in the PBMC specimen, as well as the concentration of the DCFDA reagent used. In contrast, ROS levels in urate crystal stimulated gout monocytes were higher than corresponding levels in normal monocytes ($p<0.05$). Collectively, our findings argue that the higher secreted IL-1β levels in gout PBMCs were associated with increased ROS levels in monocytes, potentially due to increased urate crystal uptake. To further evaluate the significance of ROS generation in urate crystal stimulated monocytes in the context of IL-1β secretion, we neutralized ROS using NAC. Representative flow cytometry histograms showing attenuated ROS signal in TLR2 ligand primed and urate crystal stimulated normal monocytes with NAC are presented in **Figure 3F**. We optimized the staining protocol for normal PBMCs to detect a positive ROS signal with TLR2 ligand priming and MSU crystals at 2h. Gating of monocytes was performed as shown in **Figures 1A**, **3A**. NAC treatment reduced basal and urate crystal stimulated ROS levels ($p<0.05$; $p<0.0001$; **Figure 3G**). The reduction in ROS levels resulted in a reduction in secreted IL-1β levels ($p<0.05$; **Figure 3H**). This indicates that ROS generation plays a causal role in IL-1β secretion by urate crystal stimulated monocytes.

rhPRG4 Reduced TLR2 Ligand Stimulated Bead Uptake, ROS Generation, Intracellular Pro-IL-1β and Secreted Mature IL-1β Levels and Enhanced PP2A Activity in Human THP-1 Monocytes

Representative flow cytometry histograms depicting uptake of FITC-labeled beads by TLR2 ligand primed THP-1 monocytes ± IL-1RA (250 ng/mL) or rhPRG4 (200 μg/mL) are presented in **Figure 4A**. rhPRG4 treatment reduced uptake of FITC-labeled beads by THP-1 monocytes ($p<0.0001$; **Figure 4B**). In contrast, IL-1RA treatment did not alter bead uptake by THP-1 monocytes ($p>0.05$). Representative flow cytometry histograms showing qualitatively blunted ROS generation in rhPRG4-treated THP-1 monocytes are shown in **Figure 4C**. Quantitatively, FI geometric means of rhPRG4-treated monocytes were reduced ($p<0.01$; **Figure 4D**), supporting a significant reduction in urate crystal associated ROS generation with rhPRG4 treatment. rhPRG4 reduced IL-1β gene expression ($p<0.05$; **Figure 4E**). In addition, rhPRG4 reduced intracellular pro-IL-1β ($p<0.05$; **Figure 4F**) and secreted IL-1β ($p<0.001$; **Figure 4G**) levels in urate crystal stimulated THP-1 monocytes. Urate crystals reduced PP2A activity in THP-1 monocytes ($p<0.05$; **Figure 4H**), and rhPRG4 treatment restored PP2A activity to basal levels ($p<0.05$; **Figure 4H**). In summary, the reduction in monocytic phagocytic activity by rhPRG4 was associated with a reduction in ROS generation, IL-1β expression, pro-IL-1β production and ultimately secretion of mature IL-1β. The phagocytosis of urate crystals was associated with a reduction in PP2A activity which was reversed with rhPRG4. Since ROS generation plays a causal role in IL-1β secretion by urate crystal stimulated monocytes, rhPRG4's anti-inflammatory mechanism appears to be mediated by reducing ROS generation, subsequent to reducing monocyte phagocytic activation.

The Anti-Inflammatory Effect of rhPRG4 in Urate Crystal Stimulated THP-1 Monocytes Is Partially Mediated by PP2A

Okadaic acid and rhPRG4 co-treatment increased intracellular pro-IL-1β levels compared to rhPRG4 treatment alone ($p<0.01$; **Figure 5A**). Similarly, okadaic acid co-treatment increased secreted IL-1β levels ($p<0.001$; **Figure 5B**) in urate crystal stimulated THP-1 monocytes. NLRP3 protein levels in THP-1 monocytes did not change with urate crystals ± rhPRG4 ± okadaic acid treatments ($p>0.05$ for all comparisons; **Figure 5C**). Casepase-1 activity in THP-1 monocytes increased following urate crystal exposure, which was reversed with rhPRG4 treatment ($p<0.0001$; **Figure 5D**). PP2A activity enhancement appeared to contribute to rhPRG4's inhibition of capsase-1 activity as okadaic acid co-treatment partially reversed rhPRG4's effect ($p<0.05$). These results support the conclusion

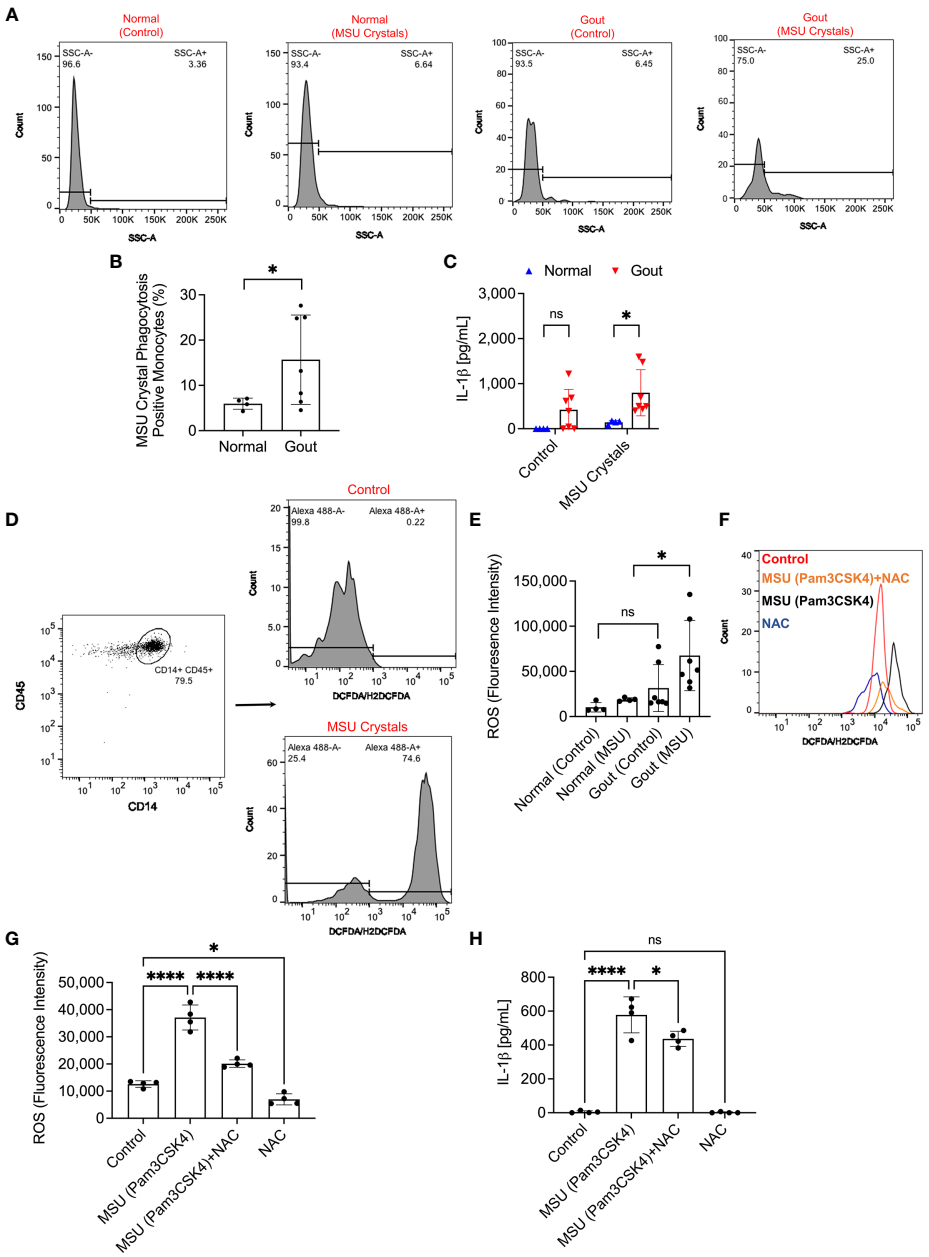

FIGURE 3 | Analysis of monosodium urate monohydrate (MSU) crystal phagocytosis and its relationship to reactive oxygen species (ROS) generation in monocytes of peripheral blood mononuclear cells (PBMCs) of normal subjects (n=3) and gout patients (n=7) and secretion of interleukin-1 beta (IL-1β). PBMCs were primed with Pam3CSK4 (1μg/mL) for 24h followed by MSU crystals (200μg/mL) and MSU crystal phagocytosis was determined by assessing the change in monocytes' side scatter (SSC-A) profile and mature IL-1β levels were determined by ELISA at 2h. ROS generation in monocytes was determined using DCFDA/H2DCFDA probe, and geometric means of fluorescence intensities (FI) of Alexa Fluor 488-positive monocytes were calculated and compared across groups. To further delineate the role of ROS in IL-1β secretion, PBMCs of normal subjects (n=4) were primed with Pam3CSK4 (1μg/mL) for 24h followed by MSU crystals (200μg/mL) ± N-acetylcysteine (NAC) (20 mM). Statistical analyses included Student's *t*-test and one-way ANOVA followed by Tukey's *post*-hoc test. ns, non-significant; $*p < 0.05$; $****p < 0.0001$. **(A)** Representative flow cytometry histograms showing increased monocytes with SSC-A values above a pre-determined threshold indicative of MSU crystal phagocytosis. **(B)** Phagocytosis of MSU crystals by gout monocytes was higher than normal monocytes. **(C)** IL-1β secretion from MSU-challenged gout PBMCs was higher than normal PBMCs. **(D)** Representative flow cytometry histograms of DCFDA/H2DCFDA stained normal monocytes at baseline and following MSU crystal incubation. Monocytes with Alexa Fluor 488 FI values above 1.0 x 10^3 were considered positive and the FI geometric mean of this population was determined. Gating of monocytes was performed as shown in **Figure 1A**. **(E)** ROS generation was higher in gout monocytes compared to normal monocytes. **(F)** Representative flow cytometry histogram showing an increase in ROS generation in monocytes as a result of MSU crystal exposure compared to control, which was attenuated with NAC treatment. **(G)** NAC treatment reduced ROS generation in monocytes of MSU crystal challenged PBMCs. **(H)** NAC treatment reduced IL-1β release by MSU challenged PBMCs.

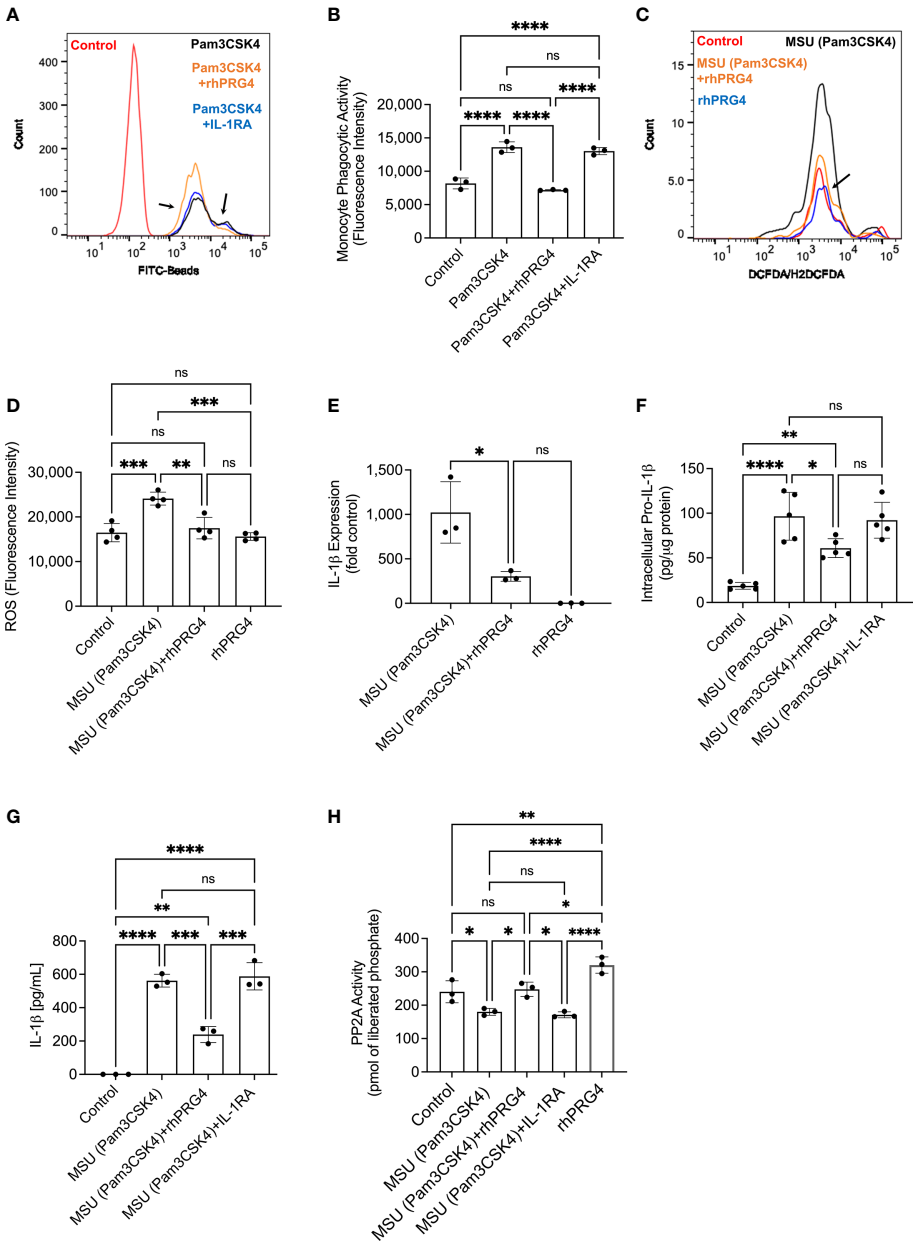

FIGURE 4 | Impact of recombinant human proteoglycan-4 (rhPRG4) or interleukin-1 receptor antagonist (IL-1RA) treatments on phagocytic activation of human THP-1 monocytes, intracellular pro interleukin-1 beta (pro-IL-1β), secreted mature IL-1β and activation of NLRP3 in response to monosodium urate monohydrate (MSU) crystal challenge and role of protein phosphatase-2A (PP2A) in mediating rhPRG4's effect. Reactive oxygen species (ROS) generation in THP-1 monocytes ± rhPRG4 was determined using the DCFDA/H2DCFDA probe, and geometric means of fluorescence intensities (FI) of Alexa Fluor 488-positive cells were calculated and compared across groups at 2h post treatments. THP-1 monocytes were primed with Pam3CSK4 (1μg/mL) for 24h ± rhPRG4 (200μg/mL) or IL-1RA (250ng/mL) followed by co-incubation with FITC-beads for 2h and THP-1 phagocytic activation was determined as shown in **Figure 1A**. Alternatively, THP-1 monocytes were challenged with MSU crystals (200μg/mL) for 6h ± rhPRG4 (200μg/mL) or IL-1RA (250ng/mL) followed by analysis of IL-1β gene expression, intracellular pro-IL-1β and secreted mature IL-1β by ELISA and PP2A activity following PP2A immunoprecipitation. Intracellular pro-IL-1β and PP2A activity were normalized to total isolated protein. Statistical analysis was performed using one-way ANOVA followed by Tukey's *post*-hoc test. ns, non-significant; $*p < 0.05$; $**p < 0.01$; $***p < 0.001$; $****p < 0.0001$. **(A)** Representative flow cytometry histograms showing enhanced phagocytosis of FITC labeled beads by TLR2 ligand primed THP-1 monocytes and rhPRG4 treatment appeared to reduce phagocytosis of FITC-labeled beads (shown by arrows). **(B)** rhPRG4 treatment reduced FITC-labeled beads' phagocytosis by THP-1 monocytes. **(C)** Representative flow cytometry histograms showing reduced ROS fluorescence intensity with rhPRG4 treatment (shown by an arrow). **(D)** rhPRG4 treatment reduced ROS generation in THP-1 monocytes. **(E)** rhPRG4 reduced IL-1β gene expression in THP-1 monocytes. **(F)** rhPRG4 reduced pro-IL-1β levels in THP-1 monocytes. **(G)** rhPRG4 reduced mature IL-1β secreted by THP-1 monocytes. **(H)** rhPRG4 treatment increased PP2A activity in MSU challenged THP-1 monocytes.

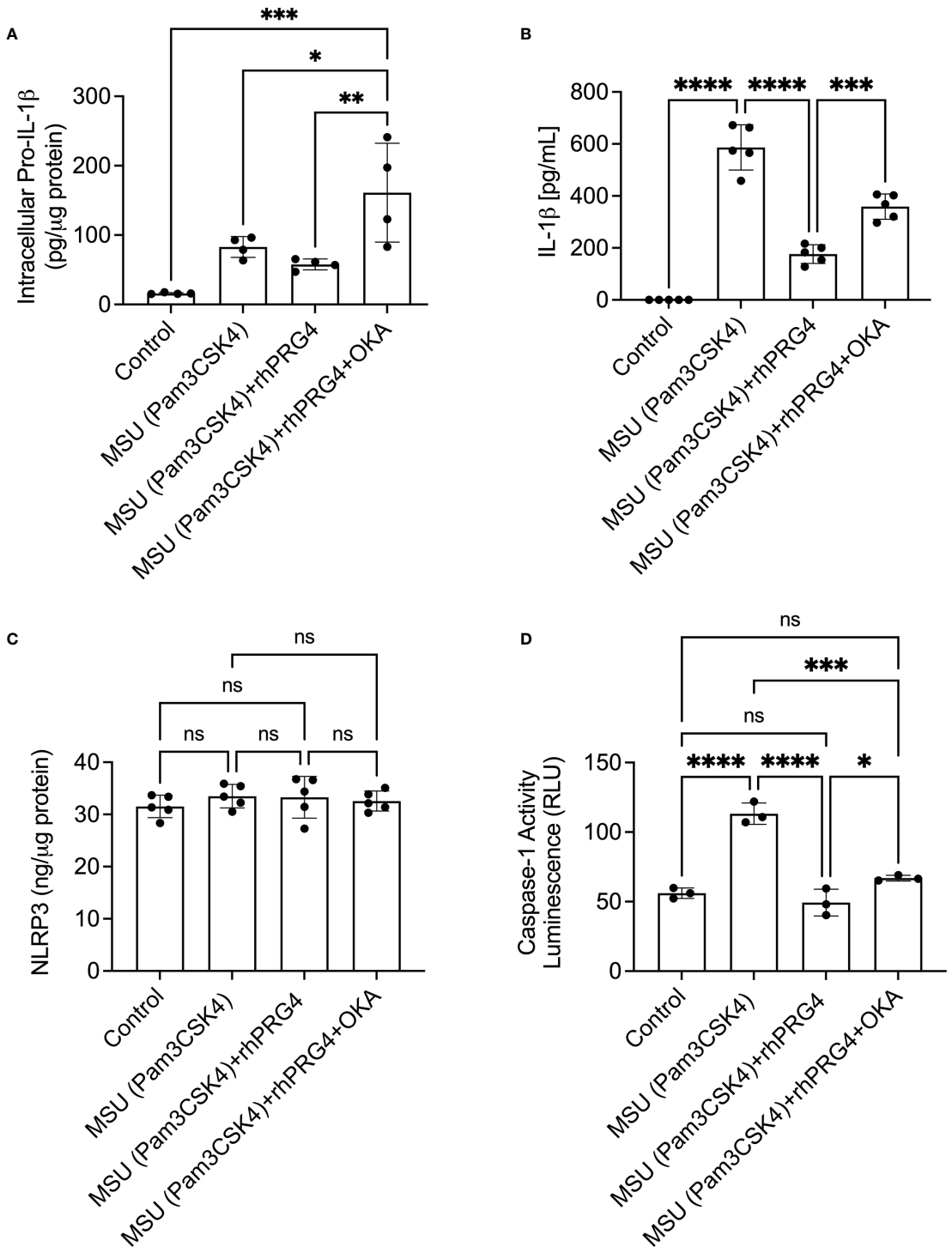

FIGURE 5 | Role of protein phosphatase-2A (PP2A) in mediating rhPRG4's anti-inflammatory effect in monosodium urate monohydrate (MSU) crystals challenged THP-1 human monocytes. THP-1 monocytes were primed with Pam3CSK4 (1μg/mL) for 24h followed by MSU (200μg/mL) crystals ± rhPRG4 (200μg/mL) ± okadaic acid (OKA) (5nM) for 6h and intracellular pro-interleukin-1 beta (pro-IL-1β), secreted mature IL-1β, NLRP3 protein, and caspase-1 activity were quantified. Intracellular pro-IL-1β, NLRP3 and caspase-1 activity were normalized to total isolated protein. Statistical analysis was performed using one-way ANOVA followed by Tukey's *post*-hoc test. ns, non-significant; *$p < 0.05$; **$p < 0.01$; ***$p < 0.001$; ****$p < 0.0001$. **(A)** OKA co-treatment increased pro-IL-1β content in rhPRG4-treated THP-1 monocytes. **(B)** OKA co-treatment increased secreted IL-1β levels in rhPRG4-treated THP-1 monocytes. **(C)** NLRP3 protein content did not change as a result of rhPRG4 ± OKA treatments. **(D)** OKA co-treatment increased caspase-1 activity in rhPRG4-treated THP-1 monocytes.

that rhPRG4's biological effects in urate crystal stimulated THP-1 monocytes were partially mediated by PP2A, where PP2A activation was seen with rhPRG4 addition and inhibition of PP2A activity significantly reduced rhPRG4's anti-inflammatory effect.

Lack of Effective Resolution of Gout Inflammation Was Observed in *Prg4*$^{GT/GT}$ Animals, and rhPRG4 Treatment Increased Anti-Inflammatory NCMs Influx and Reduced Neutrophil Accumulation in the Peritoneal Acute Gout Flare Model

The gating strategies to identify CMs and NCMs are illustrated in **Figure 6A**. Singlets were identified followed by gating for viable cells using Zombie Violet dye as shown in **Figure 1A**. CMs were identified as CD11b+ Ly6C^{hi} CCR2+ while NCMs were identified as CD11b+ Ly6C^{lo} CD43^{hi} CX3CR1+. Neutrophils were identified in lavages using dual positivity for Ly6G and Ly6B.2 (**Figure 6B**). We observed that in *Prg4*$^{GT/GT}$ and *Prg4*$^{+/+}$ animals, CMs were higher at 6h compared to 24h ($p<0.05$) with no difference between the two genotypes ($p>0.05$) (**Figure 6C**). This was expected since peak inflammation in this model is typically seen at 4h to 6h, and rhPRG4 treatment at 6h did not affect CMs at 24h ($p>0.05$). NCMs were higher at 24h compared to 6h ($p<0.05$) with no difference observed between the two genotypes ($p>0.05$) (**Figure 6D**). rhPRG4 treatment increased NCMs in *Prg4*$^{GT/GT}$ peritoneal lavages ($p<0.05$) (**Figure 6D**). At 24h, we also observed more neutrophils in *Prg4*$^{GT/GT}$ indicative of unresolved inflammation ($p<0.01$) (**Figure 6E**) and rhPRG4 treatment appeared to reduce neutrophil accumulation at 24h compared to PBS ($p<0.05$) (**Figure 6E**). IL-1β lavage levels were not different between the two genotypes at 6h but higher IL-1β levels were detected at 24h in *Prg4*$^{GT/GT}$ animals ($p<0.05$) (**Figure 6F**). While rhPRG4 treatment showed a trend towards a reduction in PL IL-1β at 24h in *Prg4*$^{GT/GT}$ animals, this trend was not statistically significant ($p>0.05$), due to a high degree of variability in calculated IL-1β concentrations in specimens from the same experimental group. CXCL1 levels in *Prg4*$^{GT/GT}$ PLs decreased with rhPRG4 treatment ($p<0.05$) (**Figure 6G**). Our *in vivo* data support that in the absence of *Prg4* expression, the tissue microenvironment is shifted towards lack of resolution of acute gout inflammation, as indicated by higher neutrophil tissue accumulation and IL-1β levels, and that rhPRG4 promotes effective resolution by increasing the influx of anti-inflammatory NCMs and decreasing CXCL1 and neutrophil tissue accumulation.

DISCUSSION

In this study, we have documented biologically relevant differences between monocytes from normal and gout patients that advance our understanding of the pathophysiology of acute gout flares. Gout monocytes were phagocytically active under basal conditions, while normal monocytes required a TLR2 stimulatory signal for their phagocytic activation. The phagocytic activation of gout monocytes is potentially related to the systemic inflammatory nature of acute gout which sets it apart from normal monocytes that are not typically exposed to *pro*-inflammatory signals, and thus require priming to be phagocytically active. Gout monocytes showed a greater propensity to uptake antibody-coated beads and urate crystals and the phagocytosis of the latter resulted in enhanced ROS generation and downstream IL-1β production. Phagocytosis is an important cellular process to maintain tissue homeostasis and is a salient component of innate immune defenses against invading microorganisms and foreign particles (33). In phagocytes, internalization of apoptotic cells, microorganisms or insoluble particles is carried out by different receptors, depending on the nature of the ingested particles (33). Antibody-driven phagocytosis of latex beads typically occurs *via* the FCγ receptor (33), while urate crystals are internalized by a receptor-mediated mechanism with CD44, TLR2 and TLR4 being the most prominent mediating receptors (23, 24, 34). IL-1RA and rhPRG4 exhibited interesting differences in modulating normal and gout monocytes under basal and TLR2-stimulated conditions. rhPRG4 has consistently shown superiority in arresting the phagocytic activation of normal and gout monocytes irrespective of their priming status, while the anti-phagocytic effect of IL-1RA was only manifested in normal monocytes following TLR2 ligand priming. Such difference is likely attributed to rhPRG4's ability to bind multiple cell surface receptors in addition to CD44 *e.g.*, TLR2, TLR4 and other integrins where PRG4 shields monocytes from recognizing extracellular innate immune danger signals (35–37). In contrast, IL-1RA has a specific mechanism of action where it functions through the IL-1 receptor (IL-1R) to inhibit IL-1β mediated signaling. IL-1R and TLR2 belong to the same receptor superfamily and activate similar signaling pathways (38). Furthermore, there is evidence of a crosstalk between TLR2 and IL-1R (39), raising the possibility that IL-1RA inhibits phagocytic activation of normal monocytes by interfering with this crosstalk circuit and thus attenuating the priming effect of TLR2 ligands on monocytes. This conclusion is further supported by IL-1RA's inability to modulate the phagocytic activity of gout monocytes, where such activity was not dependent on TLR2 ligand priming.

We have also observed that both IL-1RA and rhPRG4 demonstrated dose-dependent reductions in IL-1β release from normal PBMCs with IL-1RA exhibiting higher potency compared to rhPRG4, with an estimated 20-fold potency difference between the two biologics. However, the maximal efficacy of rhPRG4 against normal PBMCs was higher than that of IL-1RA, where rhPRG4 reduced IL-1β release by ~50% compared to 35% with IL-1RA. While gout PBMCs had variable responses to IL-1RA and rhPRG4, both treatments showed biologically meaningful anti-inflammatory effects against gout PBMCs with substantial IL-1β release. In our experiments, both IL-1RA and rhPRG4 were introduced at the TLR2 priming step, and as such most of their anti-inflammatory effect is potentially related to attenuating TLR2 priming of monocytes. In our THP-1 monocyte experiments, rhPRG4 and IL-1RA were introduced at the time monocytes were challenged with urate crystals, allowing

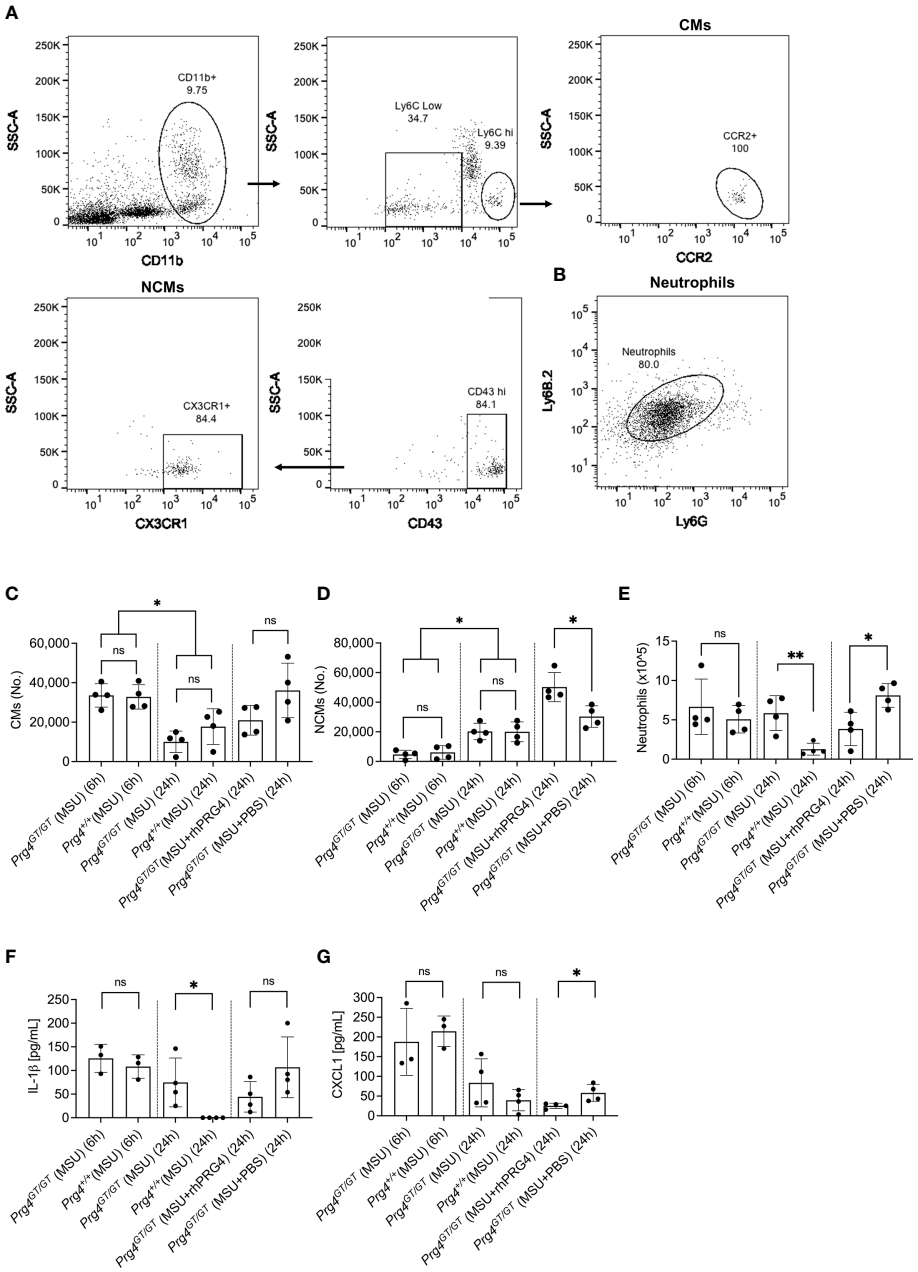

FIGURE 6 | Recruitment of inflammatory classical monocytes (CMs), anti-inflammatory nonclassical monocytes (NCMs) and neutrophils in monosodium urate (MSU) crystal induced peritoneal inflammation model in proteoglycan 4 (Prg4) gene-trap (*Prg4*$^{GT/GT}$) and Prg4 competent (*Prg4*$^{+/+}$) mice. Peritoneal lavages (PLs) were collected at 6h and 24h. CMs were identified as CD11b+ Ly6C^{hi} CCR2+ and NCMs were identified as CD11b+ Ly6C^{lo} CD43^{hi} CX3CR1+. Neutrophils were identified using Ly6G and Ly6B.2 surface markers. PL cell populations of interest were determined using Precision Counting Beads. PL IL-1β and CXCL1 levels were determined by ELISAs. Recombinant human PRG4 (rhPRG4) (50μL; 1 mg/mL) or PBS (50μL) were administered intra-peritoneally at 6h following MSU crystal injection in the *Prg4*$^{GT/GT}$ mice with PLs collected at 24h. We utilized 4 animals in each group at each time point balanced between males and females with an age range of 2-3 months. Statistical analyses included Student's *t*-test and two-way ANOVA followed by Tukey's *post*-hoc test. ns, non-significant; *$p < 0.05$; **$p < 0.01$. **(A)** Flow cytometry gating strategy to identify inflammatory CMs and anti-inflammatory NCMs. Singlets were initially identified followed by gating for viable cells using Zombie Violet dye as shown in **Figure 1A**. CMs were identified as CD11b+ Ly6C^{hi} CCR2+ and NCMs were identified as CD11b+ Ly6C^{lo} CD43^{hi} CX3CR1+. **(B)** Flow cytometry gating strategy to identify neutrophils. Singlets were initially identified followed by gating for viable cells using Zombie Violet dye as shown in **Figure 1A**. Neutrophils were identified as Ly6G+ Ly6B.2+. **(C)** CMs in *Prg4*$^{GT/GT}$ and *Prg4*$^{+/+}$ PLs were higher at 6h. rhPRG4 treatment did not alter CMs in *Prg4*$^{GT/GT}$ PLs at 24h. **(D)** NCMs in *Prg4*$^{GT/GT}$ and *Prg4*$^{+/+}$ PLs were higher at 24h. rhPRG4 treatment increased NCMs in *Prg4*$^{GT/GT}$ PLs. **(E)** Neutrophils in *Prg4*$^{GT/GT}$ PLs were higher at 24h. rhPRG4 treatment reduced neutrophils in *Prg4*$^{GT/GT}$ PLs. **(F)** PL IL-1β levels in *Prg4*$^{GT/GT}$ animals at 24h were higher than *Prg4*$^{+/+}$ animals and rhPRG4 did not significantly modify IL-1β levels in *Prg4*$^{GT/GT}$ animals. **(G)** PL CXCL1 levels in *Prg4*$^{GT/GT}$ animals were not different from *Prg4*$^{+/+}$ animals at 6h and 24h. rhPRG4 treatment reduced CXCL1 levels in *Prg4*$^{GT/GT}$ animals at 24h.

for the full TLR2 priming effect to occur. Under these conditions, rhPRG4 suppressed IL-1β to a greater extent, and this suppression was a direct downstream effect of attenuating monocyte phagocytic activation, and ROS generation. Taken together, our data suggests that IL-1RA's efficacy was dependent on interfering with monocyte priming through the TLR2 pathway while rhPRG4 exerted its biological effect independent of the priming status of monocytes.

The classical NLRP3 inflammasome activation pathway is described as a two-signal pathway with signal one, the priming step mediated by IL-1β or TLR agonists (40). As a result of TLR or IL-1R activation, cellular levels of pro-IL-1β and the inflammasome components increase. The second signal is triggered by DAMPs *e.g.*, urate crystals which results in ROS generation, K+ efflux, activation of the inflammasome and generation of mature IL-1β (40). In monocytes, NLRP3 inflammasome activation is non-classical in nature and several studies have described an alternative inflammasome activation pathway where the priming step is dispensable and the inflammasome activation is gradual in nature with no pyroptotic cell death (41–43). Interestingly, expression of the NLRP3 inflammasome components was not affected by TLR2 priming or urate crystal activation in gout monocytes (44). In our cohort, we have detected higher ROS levels with priming and urate crystal activation in gout monocytes. Gout monocytes displayed increased crystal uptake associated with enhanced ROS generation and IL-1β release, which raises the prospect of a putative mechanism by which higher urate crystal phagocytosis triggers increased ROS burden, which in turn activates the inflammasome. To further examine whether ROS played a causal role in IL-1β release, we treated PBMCs with NAC, which caused a significant reduction in ROS levels in monocytes and a parallel reduction in IL-1β release. This finding lends support to the significant role of urate crystal-generated ROS in IL-1β secretion and provides a rationale for the enhanced IL-1β secretion from gout PBMCs. Our THP-1 monocyte experiments further support that rhPRG4's anti-inflammatory effect is linked to its ability to reduce ROS generation in monocytes. NLRP3 protein levels remained unchanged in THP-1 monocytes following priming and urate crystal activation, consistent with our previous observation (26). In our experiments, transcriptional priming of pro-IL-1β was observed along with an increase in caspase-1 activity, which combined explain IL-1β release by THP-1 monocytes. rhPRG4's anti-inflammatory effect was mediated by attenuation of pro-IL-1β transcriptional priming and normalization of caspase-1 activity and therefore, its effect is a combination of inflammasome activation dependent and independent effects. The blunted priming step with rhPRG4 treatment is likely due to the latter's ability to attenuate nuclear factor kappa B (NFκB) signaling axis downstream of TLR2 activation (23, 35). We observed that PP2A activity in monocytes was impaired with TLR2 priming and urate crystals. While the underlying mechanism remains unknown, one potential explanation is the inactivation of PP2A by ROS, generated following urate crystal uptake by monocytes (45). PP2A is a cytosolic serine/threonine phosphatase that is expressed in multiple organs and in the immune system (46). In monocytes and macrophages, PP2A functions to regulate the innate immune response by TLR ligands including urate crystals. Conditional knockout of the PP2A catalytic subunit enhanced tumor necrosis factor alpha (TNF-a) expression in lipopolysaccharide (LPS)-stimulated murine macrophages (47). Using THP-1 monocytes, we have also shown that PP2A catalytic subunit knockdown exacerbated IL-1β secretion in response to urate crystals (26). CD44 receptor engagement can activate various signaling pathways dependent on the nature of the ligand and the specific cell type (48). In our study, rhPRG4 activated PP2A, potentially due to its binding CD44, which in turn contributed to its anti-inflammatory efficacy. Using okadaic acid, we showed that PP2A inhibition reverses rhPRG4's effect, magnifies pro-IL-1β production and increases caspase-1 activity in monocytes without altering NLRP3 levels. While okadaic acid was shown to also inhibit protein phosphatase-1 (PP-1), okadaic acid's potency against PP2A is more than 50 times higher than that of PP-1 (30). Considering the concentration of okadaic acid in our experiments, it is reasonable to expect that its effect was solely due to PP2A inhibition. Our data indicate that the biological effect of rhPRG4 in urate crystal stimulated monocytes was partially mediated by PP2A activation resulting in attenuating pro-IL-1β production and caspase-1 activity and thus suppressing mature IL-1β secretion.

In acute gout flares, tissue influx of immune cells e.g., monocytes and neutrophils is temporally regulated, where these cells play important roles in orchestrating the onset, progression and resolution of inflammation (7). CMs are *pro*-inflammatory and are characterized by high expression levels of Ly6C and predominantly express the pro-recruitment receptor CCR2 (27, 49). CMs extravasate into inflamed tissues where they differentiate into inflammatory M1 macrophages (49). In contrast, NCMs aid in wound healing, clearance of debris and preferentially differentiate into the alternatively activated wound-healing macrophages (50). In the peritoneal model of acute gout, an initial surge of CMs and neutrophils was observed at 6h, coinciding with peak inflammation, followed by delayed tissue influx of NCMs coinciding with resolution of inflammation. We did not detect meaningful differences in the numbers of recruited CMs or neutrophils between *Prg4* null and competent animals, which indicates that the inflammatory response in this model is not dependent on *Prg4* expression. However, the absence of Prg4's biological function was associated with accumulation of viable neutrophils and hence inadequate resolution of inflammation. This assumption is buttressed by detectable IL-1β at 24h in Prg4 deficient mice but not Prg4 competent counterparts. This is especially true since the introduction of exogenous PRG4 had a resolving effect, demonstrated by enhanced NCM tissue influx and proper clearance of neutrophils. Our CXCL1 data are also in line with less neutrophils recovered from rhPRG4-treated animals, since CXCL1 is a neutrophil chemoattractant, where its reduced levels may have contributed to resolution of inflammation (7). Our *in vivo* observations should be rationalized in the context of our recent discoveries regarding PRG4's role in tissue macrophage homeostasis and function. We have recently shown that in $Prg4^{GT/GT}$ mice, the synovial microenvironment skews the balance of resident macrophages towards a pro-inflammatory M1 phenotype with age-dependent progressive decline in the numbers

of anti-inflammatory wound-healing macrophages (51). Furthermore, macrophages from *Prg4*$^{GT/GT}$ animals had reduced anti-inflammatory interleukin-10 (IL-10) expression at baseline and in response to TLR2 ligand stimulation (51). Extending these findings to our peritoneal model, it is plausible to expect that the impaired expression of IL-10 in *Prg4*$^{GT/GT}$ mice contributed to the lack of adequate resolution of inflammation (27). Furthermore, the re-introduction of PRG4 may have blunted the overall pro-inflammatory tissue microenvironment in *Prg4*$^{GT/GT}$ animals (51), therefore allowing for more NCM influx and clearance of neutrophils.

PRG4 is a mucinous glycoprotein with the highest expression seen in the synovial joint, bone and liver (52). PRG4's protein core is 1,404 amino acid long with *N* and C termini globular domains, and a central mucin domain that is heavily glycosylated *via O*-linked β (1-3) Gal-GalNac oligosaccharides (53). In the articular joint, PRG4 fulfills a multifaceted role as a cartilage boundary lubricant and a homeostatic regulator of the synovium (54–56). PRG4 has anti-inflammatory activity, mediated by its CD44 interaction, resulting in attenuating NFκB nuclear translocation (55, 57). This activity may explain rhPRG4's disease-modifying activity seen in pre-clinical osteoarthritis models (58, 59). The anti-inflammatory activity of rhPRG4 was also demonstrated in an *in vitro* sepsis model, where rhPRG4 at 50 or 100μg/mL reduced interleukin-6 (IL-6) secretion from murine and human endothelial cells (60). rhPRG4 was also shown to reduce cytokine and chemokine secretions from immortalized corneal epithelial cells at 300μg/mL *in vitro* and inflammation in an experimental dry eye disease model (61). rhPRG4 reduced neuroinflammation and influx of monocytes in a rat model of traumatic brain injury, mediated by its regulation of the ERK1/2 pathway, downstream of CD44 and TLR2/4 engagements (62). Our current study extends the anti-inflammatory activity of rhPRG4 to controlling IL-1β secretion by PBMCs from patients with acute gout flares, where the efficacious rhPRG4 concentration was in the range of what was reported as efficacious in *in vitro* models of human synoviocytes, macrophages, endothelial and corneal epithelial cells. Our study was limited by the sparse clinical characteristics data collected on our acute gout patient cohort, *e.g.*, comorbidities and medication history. The use of oral colchicine probably reduced the amounts of IL-1β secreted from gout PBMCs. In addition, the conclusions of our study are limited by the small size of the cohort, as we plan to investigate the efficacy of rhPRG4 using monocytes from a large gout cohort.

In summary, our study is the first to show experimental evidence supporting the anti-inflammatory activity of rhPRG4 using PBMCs from patients with acute gout flares. rhPRG4 reduced phagocytic activation of gout monocytes both under basal and primed conditions and this reduction resulted in a downstream attenuation of IL-1β secretion, and rhPRG4's efficacy was equivalent to a clinically approved biologic, IL-1RA. The anti-inflammatory activity of rhPRG4 was mediated by its ability to reduce ROS generation, IL-1β expression and caspase-1 activity, and hence conversion of pro-IL-1β to mature IL-1β, in human monocytes following TLR2 ligand priming and urate crystal activation. rhPRG4's effect was a combined result of inhibiting phagocytic activation of monocytes and cytosolic PP2A activity enhancement. PRG4 may also play a significant role in mediating the resolution of acute gout inflammation. We conclude that rhPRG4 is a potential new therapeutic for treatment of acute gout flares.

DATA AVAILABILITY STATEMENT

The raw data supporting the conclusions of this article will be made available by the authors, without undue reservation.

ETHICS STATEMENT

The studies involving human participants were reviewed and approved by Institutional Review Board (IRB) at The Rhode Island and Mariam Hospitals. The patients/participants provided their written informed consent to participate in this study. The animal study was reviewed and approved by IACUC Committee, Chapman University.

AUTHOR CONTRIBUTIONS

Authors SE, GJ, and KE conceived the study. Authors RC and GJ enrolled patients, collected blood and isolated PBMCs, and participated in data analysis and interpretation of results. Authors SE, MQ, and KE carried out experiments and participated in analysis of data. Author TS provided reagents and critical interpretation of results. All authors have participated in drafting and critical evaluation of the manuscript. All authors have read and approved the final version of the manuscript.

FUNDING

This work is supported by R01AR067748 to KE and GJ.

REFERENCES

1. Dehlin M, Jacobsson L, Roddy E. Global Epidemiology of Gout: Prevalence, Incidence, Treatment Patterns and Risk Factors. *Nat Rev Rheumatol* (2020) 16:380–90. doi: 10.1038/s41584-020-0441-1
2. Chen-Xu M, Yokose C, Rai SK, Pillinger MH, Choi HK. Contemporary Prevalence of Gout and Hyperuricemia in the United States and Decadal Trends: The National Health and Nutrition Examination Survey, 2007-2016. *Arthritis Rheumatol* (2019) 71:991–9. doi: 10.1002/art.40807
3. Chen Y, Tang Z, Huang Z, Zhou W, Li Z, Li X, et al. The Prevalence of Gout in Mainland China From 2000 to 2016: A Systematic Review and Meta-Analysis. *J Public Health* (2017) 25:521–9. doi: 10.1007/s10389-017-0812-5

4. Wandell P, Carlsson AC, Ljunggren G. Gout and Its Comorbidities in the Total Population of Stockholm. *Prev Med* (2015) 81:387–91. doi: 10.1016/j.ypmed.2015.10.003
5. Kinge JM, Knudsen AK, Skirbekk V, Vollset SE. Musculoskeletal Disorders in Norway: Prevalence of Chronicity and Use of Primary and Specialist Health Care Services. *BMC Musculoskelet Disord* (2015) 16:75. doi: 10.1186/s12891-015-0536-z
6. Elfishawi M, Zleik N, Kvergic Z, Michet CJ, Crowson CS, Matteson EL, et al. The Rising Incidence of Gout and the Increasing Burden of Comorbidities: A Population-Based Study Over 20 Years. *J Rheumatol* (2018) 45:574–9. doi: 10.3899/jrheum.170806
7. Dalbeth N, Choi HK, Joosten LA, Khanna PP, Matsuo H, Perez-Ruiz F, et al. Gout. *Nat Rev Dis Primers* (2019) 5:69. doi: 10.1038/s41572-019-0115-y
8. Taylor WJ, Fransen J, Jansen TL, Dalbeth N, Schumacher HR, Brown M, et al. Study for Updated Gout Classification Criteria (SUGAR): Identification of Features to Classify Gout. *Arthritis Care Res (Hoboken)* (2015) 67:1304–15. doi: 10.1002/acr.22585
9. Khanna D, Khanna PP, Fitzgerald JD, Singh MK, Bae S, Neogi T, et al. 2012 American College of Rheumatology Guidelines for Management of Gout Part II: Therapy and Anti-Inflammatory Prophylaxis of Acute Gouty Arthritis. *Arthritis Care Res (Hoboken)* (2012) 64:1447–61. doi: 10.1002/acr.21773
10. Richette P, Doherty M, Pascual E, Barskova V, Becce F, Castaneda-Sanabria J, et al. 2016 Updated EULAR Evidence-Based Recommendations for the Management of Gout. *Ann Rheum Dis* (2017) 76:29–42. doi: 10.1136/annrheumdis-2016-209707
11. Janssens HJ, Lucassen PL, Van de Laar FA, Janssen M, Van de Lisdonk EH. Systemic Corticosteroids for Acute Gout. *Cochrane Database Syst Rev* (2008) 2:CD005521. doi: 10.1002/14651858.CD005521.pub2
12. Van Echted I, Wechalekar MD, Schlesinger N, Buchbinder R, Aletaha D. Colchicine for Acute Gout. *Cochrane Database Syst Rev* (2014) 8:CD006190. doi: 10.1002/14651858.CD006190.pub2
13. So A, Dumusc A, Nasi S. The Role of IL-1 in Gout: From Bench to Bedside. *Rheumatology* (2018) 57:i12–9. doi: 10.1093/rheumatology/kex449
14. Schlesinger N. Anti-Interleukin-1 Therapy in the Management of Gout. *Curr Rheumatol Rep* (2014) 16:398. doi: 10.1007/s11926-013-0398-z
15. Martin WJ, Walton M, Harper J. Resident Macrophages Initiating and Driving Inflammation in a Monosodium Urate Monohydrate Crystal-Induced Murine Peritoneal Model of Acute Gout. *Arthritis Rheum* (2009) 60:281–9. doi: 10.1002/art.24185
16. Busso N, So A. Mechanisms of Inflammation in Gout. *Arthritis Res Ther* (2010) 12:206. doi: 10.1186/ar2952
17. Yang G, Yeon SH, Lee HE, Kang HC, Cho YY, Lee HS, et al. Suppression of NLRP3 Inflammasome by Oral Treatment With Sulforaphane Alleviates Acute Gouty Inflammation. *Rheumatology* (2018) 57:727–36. doi: 10.1093/rheumatology/kex499
18. Giamarellos-Bourboulis EJ, Mouktaroudi M, Boder E, van der Ven J, Kullberg B-J, Netea MG, et al. Crystals of Monosodium Urate Monohydrate Enhance Lipopolysaccharide-Induced Release of Interleukin-1 Beta by Mononuclear Cells Through a Caspase-1 Mediated Process. *Ann Rheum Dis* (2009) 68:273–8. doi: 10.1136/ard.2007.082222
19. Joosten LA, Netea MG, Mylona E, Koenders MI, Malireddi RKS, Oosting M, et al. Engagement of Fatty Acids With Toll-Like Receptor 2 Drives Interleukin-1b Production *via* the ASC/caspase 1 Pathway in Monosodium Urate Monohydrate Crystal-Induced Gouty Arthritis. *Arthritis Rheum* (2010) 62:3237–48. doi: 10.1002/art.27667
20. Martin WJ, Shaw O, Liu X, Steiger S, Harper JL. Monosodium Urate Monohydrate Crystal-Recruited Noninflammatory Monocytes Differentiate Into M1-Like Proinflammatory Macrophages in a Peritoneal Murine Model of Gout. *Arthritis Rheum* (2011) 63:1322–32. doi: 10.1002/art.30249
21. Mylona EE, Mouktaroudi M, Crisan TO, Makri S, Pistiki A, Georgitsi M, et al. Enhanced Interleukin-1β Production of PBMCs From Patients With Gout After Stimulation With Toll-Like Receptor-2 Ligands and Urate Crystals. *Arthritis Res Ther* (2012) 14:R158. doi: 10.1186/ar3898
22. Crisan TO, Cleophas MCP, Novakovic B, Erler K, van de Veerdonk FL, Stunnenberg HG, et al. Uric Acid Priming in Human Monocytes Is Driven by the AKT-PRAS40 Autophagy Pathway. *Proc Natl Acad Sci USA* (2017) 114:5485–90. doi: 10.1073/pnas.1620910114
23. Qadri M, Jay GD, Zhang LX, Wong W, Reginato AM, Sun C, et al. Recombinant Human Proteoglycan-4 Reduces Phagocytosis of Urate Crystals and Downstream Nuclear Factor Kappa B and Inflammasome Activation and Production of Cytokines and Chemokines in Human and Murine Macrophages. *Arthritis Res Ther* (2018) 20:192. doi: 10.1186/s13075-018-1693-x
24. Bousoik E, Qadri M, Elsaid KA. CD44 Receptor Mediates Crystal Phagocytosis by Macrophages and Regulates Inflammation in a Murine Peritoneal Model of Acute Gout. *Sci Rep* (2020) 10:5748. doi: 10.1038/s41598-020-62727-z
25. Zoghbi K, Bousoik E, Parang K, Elsaid KA. Design and Biological Evaluation of Colchicine-CD44-Targeted Peptide Conjugate in an *In Vitro* Model of Crystal Induced Inflammation. *Molecules* (2020) 25:45. doi: 10.3390/molecules25010046
26. Qadri M, Elsayed S, Elsaid KA. Fingolimod Phosphate (FTY720-P) Activates Protein Phosphatase 2A in Human Monocytes and Inhibits Monosodium Urate Crystal-Induced IL-1β Production. *J Pharmacol Exp Ther* (2021) 376:222–30. doi: 10.1124/jpet.120.000321
27. Narasimhan PB, Marcovecchio P, Hamers AA, Hedrick CC. Nonclassical Monocytes in Health and Disease. *Ann Rev Immunol* (2019) 37:439–56. doi: 10.1146/annurev-immunol-042617-053119
28. Grievink HW, Luisman T, Kluft C, Moerland M, Malone K. Comparison of Three Isolation Techniques for Human Peripheral Blood Mononuclear Cells: Cell Recovery and Viability, Population Composition, and Cell Functionality. *Biopreserv Biobank* (2016) 14:410–5. doi: 10.1089/bio.2015.0104
29. Flynn CM, Garbers Y, Lokau J, Wesch D, Schulte DM, Laudes M, et al. Activation of Toll-Like Receptor 2 (TLR2) Induces Interleukin-6 Trans-Signaling. *Sci Rep* (2019) 9:7306. doi: 10.1038/s41598-019-43617-5
30. Valdiglesias V, Prego-Faraldo MV, Pasaro E, Mendez J, Laffon B. Okadaic Acid: More Than a Diarrheic Toxin. *Mar Drugs* (2013) 11:4328–49. doi: 10.3390/md11114328
31. Hill A, Waller KA, Cui Y, Allen JM, Smits P, Zhang LX, et al. Lubricin Restoration in a Mouse Model of Congenital Deficiency. *Arthritis Rheumatol* (2015) 67(11):3070–81. doi: 10.1002/art.39276
32. Samson ML, Morrison S, Masala N, Sullivan BD, Sullivan DA, Sheardown H, et al. Characterization of Full-Length Recombinant Human Proteoglycan 4 as an Ocular Surface Boundary Lubricant. *Exp Eye Res* (2014) 127:14–9. doi: 10.1016/j.exer.2014.06.015
33. Uribe-Querol E, Rosales C. Phagocytosis: Our Current Understanding of a Universal Biological Process. *Front Immunol* (2020) 11:1066. doi: 10.3389/fimmu.2020.01066
34. Liu-Bryan R, Scott P, Sydlaske A, Rose DM, Terkeltaub R. Innate Immunity Conferred by Toll-Like Receptors 2 and 4 and Myeloid Differentiation Factor 88 Expression Is Pivotal to Monosodium Urate Monohydrate Crystal-Induced Inflammation. *Arthritis Rheum* (2005) 52:2936–46. doi: 10.1002/art.21238
35. Alquraini A, Garguilo S, D'Souza G, Zhang LX, Schmidt TA, Jay GD, et al. The Interaction of Lubricin/Proteoglycan 4 (PRG4) With Toll-Like Receptors 2 and 4: An Anti-Inflammatory Role of PRG4 in Synovial Fluid. *Arthritis Res Ther* (2015) 17:353. doi: 10.1186/s13075-015-0877-x
36. Iqbal SM, Leonard C, Regmi SC, De Rantere D, Tailor P, Ren G, et al. Lubricin/proteoglycan 4 Binds to and Regulates the Activity of Toll-Like Receptors. *vitro Sci Rep* (2016) 6:18910. doi: 10.1038/srep18910
37. Jin C, Ekwell AK, Bylund J, Bjorkman L, Estrella RP, Whitelock JM, et al. Human Synovial Lubricin Expresses Sialyl Lewis X Determinant and has L-Selectin Ligand Activity. *J Biol Chem* (2012) 287:35922–33. doi: 10.1074/jbc.M112.363119
38. O'Neil LA. The Interleukin-1 Receptor/Toll-Like Receptor Superfamily: 10 Years of Progress. *Immunol Rev* (2008) 226:10–8. doi: 10.1111/j.1600-065X.2008.00701.x
39. Kawai T, Akira S. Toll-Like Receptors and Their Crosstalk With Other Innate Receptors in Infection and Immunity. *Immunity* (2011) 34:637–50. doi: 10.1016/j.immuni.2011.05.006
40. Yang Y, Wang H, Koudair M, Song H, Shi F. Recent Advances in the Mechanisms of NLRP3 Inflammasome Activation and Its Inhibitors. *Cell Death Dis* (2019) 10:128. doi: 10.1038/s41419-019-1413-8
41. Crisan TO, Cleophas MC, Oosting M, Lemmers H, Dijkstra HT, Netea MG, et al. Soluble Uric Acid Primes TLR-Induced Proinflammatory Cytokine

Production by Human Primary Cells *via* Inhibition of IL-1ra. *Ann Rheum Dis* (2016) 75:755–62. doi: 10.1136/annrheumdis-2014-206564
42. Gaidt M, Ebert TS, Chauhan D, Schmidt T, Schmid-Burgk JL, Rapino F, et al. Human Monocytes Engage an Alternative Inflammasome Pathway. *Immunity* (2016) 44:833–46. doi: 10.1016/j.immuni.2016.01.012
43. Gritsenko A, Yu S, Martin-Sanchez F, Diaz-del-Olmo I, Nichols EM, Davis DM, et al. Priming Is Dispensable for NLRP3 Inflammasome Activation in Human Monocytes *In Vitro*. *Front Immunol* (2020) 11:565924. doi: 10.3389/fimmu.2020.565924
44. Alberts BM, Bruce C, Basnayake K, Ghezzi P, Davies KA, Mullen M. Secretion of IL-1β From Monocytes in Gout Is Redox Independent. *Front Immunol* (2019) 10:70. doi: 10.3389/fimmu.2019.00070
45. Raman D, Pervaiz S. Redox Inhibition of Protein Phosphatase Pp2A: Potential Implications in Oncogenesis and Its Progression. *Redox Biol* (2019) 27:101105. doi: 10.1016/j.redox.2019.101105
46. Reynhaut S, Janssens V. Physiologic Functions of PP2A: Lessons From Genetically Modified Mice. *Biochem Biophys Acta Mol Cell Res* (2019) 1866:31–50. doi: 10.1016/j.bbamcr.2018.07.010
47. Sun L, Pham TT, Cornell TT, McDonough KL, McHugh WM, Blatt NB, et al. Myeloid-Specific Gene Deletion of Protein Phosphatase 2A Magnifies MyD88- and TRIF-Dependent Inflammation Following Endotoxin Challenge. *J Immunol* (2017) 198:404–16. doi: 10.4049/jimmunol.1600221
48. Jordan AR, Racine RR, Henning MJ, Lokeshwar VB. The Role of CD44 in Disease Pathophysiology and Targeted Treatment. *Front Immunol* (2015) 6:182. doi: 10.3389/fimmu.2015.00182
49. Cormican S, Griffin M. Human Monocyte Subset Distinctions and Function: Insights From Gene Expression Analysis. *Front Immunol* (2020) 11:1070. doi: 10.3389/fimmu.2020.01070
50. Olingy CE, San Emeterio CL, Ogle ME, Krieger JR, Bruce AC, Pfau DD, et al. Non-Classical Monocytes Are Biased Progenitors of Wound Healing Macrophages During Soft Tissue Injury. *Sci Rep* (2017) 7:447. doi: 10.1038/s41598-017-00477-1
51. Qadri M, Zhang LX, Jay GD, Schmidt TA, Totonchy J, Elsaid KA. Proteoglycan-4 Is an Essential Regulator of Synovial Macrophage Polarization and Inflammatory Macrophage Joint Infiltration. *Arthritis Res Ther* (2021) 23:241. doi: 10.1186/s13075-021-02621-9
52. Novince CM, Koh AJ, Michalski MN, Marchesan JT, Wang J, Jung Y, et al. Proteoglycan 4, a Novel Immunomodulatory Factor, Regulates Parathyroid Hormone Actions on Hematopoietic Cells. *Am J Pathol* (2011) 179:2431–42. doi: 10.1016/j.ajpath.2011.07.032
53. Jay GD, Tantravahi U, Britt DE, Barrach HJ, Cha CJ. Homology of Lubricin and Superficial Zone Protein (SZP): Products of Megakaryocyte Stimulating Factor (MSF) Gene Expression by Human Synovial Fibroblasts and Articular Chondrocytes Localized to Chromosome 1q25. *J Orthop Res* (2001) 194:677–87. doi: 10.1016/S0736-0266(00)00040-1
54. Jay GD, Waller KA. The Biology of Lubricin: Near Frictionless Joint Motion. *Matrix Biol* (2014) 39:17–24. doi: 10.1016/j.matbio.2014.08.008
55. Alquraini A, Jamal M, Zhang L, Schmidt TA, Jay GD, Elsaid KA. The Autocrine Role of Proteoglycan-4 (PRG4) in Modulating Osteoarthritic Synoviocyte Proliferation and Expression of Matrix Degrading Enzymes. *Arthritis Res Ther* (2017) 19:89. doi: 10.1186/s13075-017-1301-5
56. Qadri M, Jay GD, Zhang LX, Richendrfer H, Schmidt TA, Elsaid KA. Proteoglycan-4 Regulates Fibroblast to Myofibroblast Transition and Expression of Fibrotic Genes in the Synovium. *Arthritis Res Ther* (2020) 22:113. doi: 10.1186/s13075-020-02207-x
57. Al-Sharif A, Jamal M, Zhang LX, Larson K, Schmidt TA, Jay GD, et al. Lubricin/Proteoglycan 4 Binding to CD44 Receptor: A Mechanism of the Suppression of Proinflammatory Cytokine-Induced Synoviocyte Proliferation by Lubricin. *Arthritis Rheumatol* (2015) 67:1503–13. doi: 10.1002/art.39087
58. Jay GD, Fleming BC, Watkins BA, McHugh KA, Anderson SC, Zhang LX, et al. Prevention of Cartilage Degeneration and Restoration of Chondroprotection by Lubricin Tribosupplementation in the Rat Following Anterior Cruciate Ligament Transection. *Arthritis Rheum* (2010) 62:2382–91. doi: 10.1002/art.27550
59. Waller KA, Chin KE, Jay GD, Zhang LX, Teeple E, McAllister S, et al. Intra-Articular Recombinant Human Proteoglycan-4 Mitigates Cartilage Damage After Destabilization of the Medial Meniscus in the Yucatan Minipig. *Am J Sports Med* (2017) 45:1512–21. doi: 10.1177/0363546516686965
60. Richendrfer HA, Levy M, Elsaid KA, Schmidt TA, Zhang L, Cabezas R, et al. Recombinant Human Proteoglycan-4 Mediates Interleukin-6 Response in Both Human and Mouse Endothelial Cells Induced Into a Sepsis Phenotype. *Crit Care Explor* (2020) 2:e0126. doi: 10.1097/CCE.0000000000000126
61. Menon NG, Goyal R, Lema C, Woods PS, Tanguay AP, Morin AA, et al. Proteoglycan 4 (PRG4) Expression and Function in Dry Eye Associated Inflammation. *Exp Eye Res* (2021) 208:108628. doi: 10.1016/j.exer.2021.108628
62. Bennett M, Chin A, Lee HJ, Cestero EM, Strazielle N, Ghersi-Egea JF, et al. Proteoglycan 4 Reduces Neuroinflammation and Protects the Blood-Brain Barrier After Traumatic Brain Injury. *J Neurotrauma* (2021) 38:385–98. doi: 10.1089/neu.2020.7229

Conflict of Interest: Author GJ authored patents on rhPRG4 and holds equity in Lubris LLC, MA, USA. Author TS authored patents on rhPRG4, is a paid consultant for Lubris LLC, MA, USA and holds equity in Lubris LLC, MA, USA. Author KE authored patents on rhPRG4.

The remaining authors declare that the research was conducted in the absence of any commercial or financial relationships that could be construed as a potential conflict of interest.

Publisher's Note: All claims expressed in this article are solely those of the authors and do not necessarily represent those of their affiliated organizations, or those of the publisher, the editors and the reviewers. Any product that may be evaluated in this article, or claim that may be made by its manufacturer, is not guaranteed or endorsed by the publisher.

frontiers in Immunology

ORIGINAL RESEARCH
published: 05 January 2022
doi: 10.3389/fimmu.2021.777522

The Anti-Inflammatory and Uric Acid Lowering Effects of Si-Miao-San on Gout

Ling Cao[1,2†], Tianyi Zhao[1,2†], Yu Xue[1,2], Luan Xue[3], Yueying Chen[3], Feng Quan[3], Yu Xiao[4], Weiguo Wan[1,2], Man Han[5], Quan Jiang[5], Liwei Lu[6], Hejian Zou[1,2] and Xiaoxia Zhu[1,2*]*

[1] Division of Rheumatology, Huashan Hospital, Fudan University, Shanghai, China, [2] Institute of Rheumatology, Immunology and Allergy, Fudan University, Shanghai, China, [3] Department of Rheumatology, Yueyang Hospital of Integrated Traditional Chinese and Western Medicine, Shanghai University of Traditional Chinese Medicine, Shanghai, China, [4] Institute of Spacecraft Equipment, Shanghai, China, [5] Guang'anmen Hospital, China Academy of Chinese Medical Sciences, Beijing, China, [6] Department of Pathology and Shenzhen Institute of Research and Innovation, The University of Hong Kong, Hong Kong, Hong Kong SAR, China

Background: Si-Miao-San (SMS) is a well-known traditional Chinese medicine. This study aims to evaluate the anti-inflammatory effects of SMS on gouty arthritis and its potential mechanism of action.

Methods: The effects and mechanism of SMS were evaluated in monosodium urate (MSU)-treated mice or macrophages. The expression of cytokines and PI3K/Akt was analyzed using real-time PCR and Western blotting analyses. Macrophage polarization was assessed with immunofluorescence assays, real-time PCR, and Western blotting. Mass spectrometry was used to screen the active ingredients of SMS.

Results: Pretreatment with SMS ameliorated MSU-induced acute gouty arthritis in mice with increased PI3K/Akt activation and M2 macrophage polarization in the joint tissues. *In vitro*, SMS treatment significantly inhibited MSU-triggered inflammatory response, increased p-Akt and Arg-1 expression in macrophages, and promoted M2 macrophage polarization. These effects of SMS were inhibited when PI3K/Akt activation was blocked by LY294002 in the macrophages. Moreover, SMS significantly reduced serum uric acid levels in the hyperuricemia mice. Using mass spectrometry, the plant hormones ecdysone and estrone were detected as the potentially effective ingredients of SMS.

Conclusion: SMS ameliorated MSU-induced gouty arthritis and inhibited hyperuricemia. The anti-inflammatory mechanism of SMS may exert anti-inflammatory effects by promoting M2 polarization *via* PI3K/Akt signaling. Ecdysone and estrone might be the potentially effective ingredients of SMS. This research may provide evidence for the application of SMS in the treatment of gout.

Keywords: gout, hyperuricemia, Si-Miao-San, inflammation, uric acid

OPEN ACCESS

Edited by:
Philipp Starkl,
Medical University of Vienna, Austria

Reviewed by:
Zhu Chen,
University of Science and Technology of China, China
James Cheng-Chung Wei,
Chung Shan Medical University Hospital, Taiwan
Yan Yang,
University of Texas MD Anderson Cancer Center, United States

***Correspondence:**
Xiaoxia Zhu
xxzhu@unirheuma.org
Hejian Zou
hjzou@fudan.edu.cn

†These authors have contributed equally to this work

Specialty section:
This article was submitted to Autoimmune and Autoinflammatory Disorders, a section of the journal Frontiers in Immunology

Received: *15 September 2021*
Accepted: *13 December 2021*
Published: *05 January 2022*

Citation:
Cao L, Zhao T, Xue Y, Xue L, Chen Y, Quan F, Xiao Y, Wan W, Han M, Jiang Q, Lu L, Zou H and Zhu X (2022) The Anti-Inflammatory and Uric Acid Lowering Effects of Si-Miao-San on Gout. Front. Immunol. 12:777522. doi: 10.3389/fimmu.2021.777522

INTRODUCTION

Gouty arthritis is a common inflammatory arthropathy induced by monosodium urate (MSU) crystals deposited in joints and soft tissues (1–3). Hyperuricemia is the key pathophysiological condition for the development of symptomatic gout (4, 5). The prevalence of hyperuricemia was about 2.6%-36.0% (6), the prevalence of gout was about 0.03%-15.3% (7). Clinical remission can be achieved in most patients through anti-inflammatory treatment and urate-lowering therapy (ULT) (8–10). However, some patients experience recurrent flares during ULT. Currently, the anti-inflammatory treatments, such as colchicine, glucocorticoid, and non-steroidal anti-inflammatory drugs are restricted in the patients with digestive diseases (e.g., peptic ulcer, gastrointestinal bleeding) or renal insufficiency (11). Therefore, it is imperative to explore new approaches for the treatment of gouty arthritis, especially with complementary and alternative medicine.

Si-Miao-San (SMS), a well-known traditional Chinese medicine, was first described in the monograph "Dan Xi Xin Fa" (Chinese comprehensive medicinal book) in the Yuan Dynasty in China (12). SMS has been widely used in the treatment of gout and gouty arthritis for approximately 700 years, showing clinically confirmed efficacy as effective therapy in patients with gout (13–15). SMS comprises four individual herbs, namely *Phellodendron chinese* SCHNEID (Rutaceae), *Atractylodes lancea* (Thunb.) DC. (Asteraceae), *Achyranthes bidentata* BL. (Amaranthaceae), and *Coix lacryma-jobi* L. (Poaceae), each of which was reported to be safe in clinical application in Chinese medicine theory (16). Previous studies have reported that SMS can significantly relieve the symptoms of gouty arthritis through its anti-inflammatory effects (17–19).

Clinically, SMS has been safely used in gouty patients with concomitant complications such as chronic renal insufficiency, heart problems, gastrointestinal bleeding, or ulcers (20). However, further studies are needed to investigate the mechanism of action for SMS in the treatment of gout. We have recently shown that resident macrophages trigger the inflammation in gouty arthritis (21) while depletion of tissue resident macrophages or blocking M1 macrophages polarization significantly decreased IL-1β expression and neutrophil infiltration (22). In this study, we aim to examine anti-inflmmatory effects of SMS in gouty arthritis and further investigate the potential mechanism of SMS on macrophages polarization.

MATERIAL AND METHODS

SMS Preparation

Simiao San were purchased from Jiling Zixin Pharmaceutical Industrial Company, LTD. (Jiling,China) and authenticated by Guang'anmen Hospital, China Academy of Chinese Medical Sciences (Beijing, China). SMS comprises a mixture of 66.7 g of *Phellodendron chinese* SCHNEID, 33.3 g of *Atractylodes lancea*, 33.3 g of *Coix lacryma-jobi* L., and 66.7 g of *Achyranthes bidentata* BL. SMS medicinal juice was prepared using a well established protocol (18). The four herbs were mixed with distilled water for 2 h, added to a volatile oil extractor, refluxed, and extracted twice for 1.5 h each. A 7-fold excess of distilled water was added for the first extraction, whereas a 6-fold excess of distilled water was added for the second extraction. The mixture was then filtered, sealed for storage, concentrated, and mixed with the volatile oil. Finally, we dispensed the mixture into a 1 g/mL medicinal juice and sterilized it for packaging.

Mass Spectrometry

Mass spectrometry as performed using an Agilent 1290 UHPLC and 6530 QTOF-MS/MS LC-MS system (Agilent Technologies, Santa Clara, CA, USA), and an Agilent Eclipse Plus C18 column (2.1 × 100 mm, 1.8 μm) column (Agilent Technologies) was used for the acquisition of metabolic data. Gradient elution was performed using 0.1% formic acid and methanol.

For sample preparation, 1 mL of SMS concentrate was added to 4 mL of methanol solution, and the mixture was sonicated for 30 min, centrifuged, and filtered through a 0.1-μm microporous filter.

Liquid chromatography–mass spectrometry was performed on an Agilent 1290 UHPLC and 6530 QTOF-MS/MS system with a 2.1 m × 100 mm × 1.8 μm Agilent Eclipse Plus C18 column. The atomizing temperature was 350°C, the nebulizer flow rate was 10 L/min, the atomization gas pressure was 30 psi, the capillary voltage was 3500 V, the Skimmer voltage was 65 V, the octopole RF voltage was 750 V, and the papillary outlet voltage was 150 V. The data matrix comprised the retention times, m/z 50–1500 values, and the corresponding peak areas for subsequent statistical analysis.

MSU Crystal Preparation

MSU crystals were prepared as we previously reported (23) and then assessed using compensated polarized light microscopy. Endotoxin was present at <0.015 EU/mL in the MSU crystal preparations, as determined using the Limulus amebocyte lysate assay (Sigma-Aldrich, St Louis, MO, USA). Before each experiment, the MSU crystals were milled and then sterilized for 2 h.

Cell Culture

THP-1 cells were purchased from the Cell Bank of the Chinese Academy of Sciences (Shanghai, China) and cultured in complete medium comprising RPMI supplemented with 2 mM L-glutamine, 100 units/mL penicillin, 100 μg/mL streptomycin, and 10% fetal bovine serum (FBS) (Gibco BRL, Grand Island, NY, USA). THP-1 cells were used after treatment with 100 ng/μL PMA for 48 h. Cells were seeded in 24-well culture plates (2×10^5 cells/mL/well), pretreated with 1 or 2 μg/mL SMS for 12 h, and then incubated with 100 μg/mL MSU for 48 h. To block the PI3K/Akt pathway, cells were pretreated with 50 μM LY294002 (Selleckchem) for 1 h before MSU treatment. SMS was added for 30min after LY294002 treatment.

Animals

Specific pathogen-free male C57BL/6 mice (6-8 weeks old) were purchased from the Shanghai Laboratory Animal Center (Chinese Academy of Sciences, China) and maintained at the Animal Center of Shanghai Medical School of Fudan University. This study was approved by the Ethics Committee of the

Department of Laboratory Animal Science, Fudan University (No. 20160981A302).

To establish mice with gout, 50 μL of an MSU suspension (1 mg/50 μL Normal saline) was intra-articularly injected in the right footpad of each animal, whereas the left footpad was injected with 50 μL of Normal saline (N.S). The joint index evaluation was performed as we previously reported (23–27). In the SMS treatment group, mice were intra-gastrically injected with a low dose (1 mg/kg·day) or high dose (10 mg/kg·day) of SMS for 14 days before MSU administration, samples were collected at 8h after MSU injection. The foot joint tissues were immediately isolated, snap-frozen in liquid nitrogen, and stored at -80°C.

Hyperuricemic mice were established *via* treatment with yeast polysaccharide (YP) and potassium oxonate (OP) for 3 weeks as previously described (28). Mice were orally feed containing 1/4 yeast polysaccharide (Sigma, USA) or intraperitoneally injected with potassium oxonate (250 mg/kg; OP, Sigma, USA) at 8:00 a.m. every day. In the SMS treatment group, different concentrations (1 or 10 mg/kg·day) of SMS were intra-gastrically administered to mice simultaneously with OP for 3 weeks. Samples were collected after the last drug administration. Blood samples were obtained from the eye socket vein of each mouse and centrifuged at 2500rpm for 10 min at 4°C. The kidney tissues were immediately isolated, snap-frozen in liquid nitrogen, and stored at -80°C.

Histological Studies and Immunostaining

After the joint index evaluation, mice were sacrificed, and joint tissue and kidneys sections were prepared for hematoxylin and eosin (H&E) staining and immunostaining. The paraffin-embedded sections were cut at a thickness of 4 μm and placed on positively charged slides for staining. In H&E staining, inflammatory cells were counted using ImageJ software (version 1.51p, National Institutes of Health, Bethesda, MD, USA).

For immunofluorescence, slides were placed in target retrieval solution, and staining was performed manually at room temperature with anti–Arg-1 antibody (Clone #CI:A3-1, 1:500 dilution, Abcam, Cambridge, MA, USA) or anti-F4/80 antibody (Clone #SP156, 1:400 dilution, Abcam, Cambridge, MA, USA). Arg-1 expression was visualized using Alexa Fluor 647 secondary antibody (ab150115, 1:400 dilution, Abcam, Cambridge, MA, USA). F4/80 expression was visualized using Alexa Fluor 488 secondary antibody (ab150077, 1:400 dilution, Abcam, Cambridge, MA, USA). Slides were counterstained with Vectashield hard-set mounting medium with DAPI (Vector Laboratories, Burlingame, CA, USA) and kept in the dark at 4°C until visualization using fluorescence microscopy. Images were obtained *via* optical sectioning using a Nikon epifluorescence microscope for analysis. $F4/80^+/Arg\text{-}1^+$ cells (M2 macrophage) analysis was performed using ImageJ software from randomly chosen fields [the average of 5 to 10 fields (× 200) in the section]. $F4/80^+/Arg\text{-}1^+$ cells were determined by using a standardized custom histogram-based colored thresholding technique and then subjected to "particle analysis" using ImageJ.

For immunohistochemistry, slides were placed in target retrieval solution, and staining was performed manually at 4°C for 18 hours with Akt (Clone #11E7, 1:1000 dilution, Cell Signaling Technology, Boston, USA). Then goat anti-Rabbit IgG H&L (HRP) (ab6721, 1:500 dilution, Abcam, Cambridge, MA, USA) was added and incubation continued for 20 minutes. Staining was visualized using DAB and the sections were then observed. Finally, sections were further dyed and sealed with hematoxylin. Images were obtained *via* optical sectioning using a Nikon epifluorescence microscope for analysis. To display the results more intuitively, the average optical density of positive areas (40×,100X) was calculated using ImageJ software.

Determination of Serum Uric Acid (SUA) and Creatinine Levels

SUA concentrations and creatinine levels were separately determined using colorimetric method (#MAK077, #MAK080, Sigma, USA).

Real-Time Quantitative PCR (qPCR) Detection System

Total RNA was extracted from joint tissue or cells with Trizol (Invitrogen, Carlsbad, CA, USA) according to the manufacturer's instructions, and reverse translation was conducted using an iScript™ cDNA Synthesis Kit (Bio-Rad, Hercules, CA, USA). The PCR primers (BioTNT, Shanghai, China) used for qPCR were as shows in **Supplementary Table 1**.

The RNA expression in samples was normalized to that of control housekeeping genes (murine Gapdh), and the relative mRNA levels of target genes were calculated using the $2^{-\Delta\Delta Ct}$ method.

Western Blot Analysis

The joint samples were homogenized by tissue tearor, and added with 10 equivalent volumes of RIPA lysis buffer supplemented with 1 mM PMSF (protease inhibitor) in an ice bath for 30 min and then centrifuged (12,000*g*, 10 min) to extract total proteins. The protein concentration was determined using a BCA protein assay kit (Beyotime Biotechnology, Shanghai, China). Mouse joint tissues or cell lysates from different groups were prepared, and equal aliquots of protein extract were electrophoresed *via* SDS-PAGE. Protein levels were expressed as a ratio of the protein level to that of β-actin.

The following antibodies were obtained from commercial sources as indicated: NLRP3(Clone #Ala306, 1:1000 dilution, Cell Signaling Technology, Boston, USA), p-Akt (Ser473) (Clone #587F11, 1:1000 dilution, Cell Signaling Technology, Boston, USA), Akt (Clone #11E7, 1:1000 dilution, Cell Signaling Technology, Boston, USA), β-actin(Clone #8H10D10, 1:1000 dilution, Cell Signaling Technology, Boston, USA), anti-rabbit IgG HRP-conjugated antibody(#7074, 1:5000 dilution, Cell Signaling Technology, Boston, USA), anti-moude IgG HRP-conjugated antibody(#7076, 1:5000 dilution, Cell Signaling Technology, Boston, USA). The immunoblots were visualized *via* ECL (Pierce, Rockford, IL, USA). The results were normalized to β-actin. Gel quantification was performed using the ImageJ software.

Statistical Analysis

Data were analyzed using GraphPad Prism 6.0 (GraphPad Software, La Jolla, CA, USA) and presented as the mean ± SEM or median

(range). Repeated-measures analysis of variance followed by the Student-Newman-Keuls test was used for *post hoc* analyses of differences among groups. $P < 0.05$ indicated statistical significance.

RESULTS

SMS Ameliorate MSU-Induced Acute Gouty Arthritis in Mice

Mice were pretreated with different doses of SMS (1 or 10 mg/kg.day) for 2 weeks, and then acute gouty arthritis was induced by MSU. Eight hours after MSU injection, joint thickness and the mRNA expression of *Nlrp3*, *IL-6*, *IL-1β*, *IL-4*, *Tgf-β* in the joints were significantly elevated. The joint swelling was significantly reduced in the mice treated with SMS compared with that in the MSU mice (**Figure 1A**). Moreover, the over-expression of *Nlrp3*, *IL-6*, and *IL-1β* mRNA in MSU-injured joints was inhibited by SMS, especially the high-dose SMS (10mg/kg.day). Notably, the anti-inflammatory factors, IL-4 and Tgf-β, were further increased by SMS treatment (**Figure 1B**). H&E pathological staining further revealed that inflammatory cell infiltration in gouty joints was notably inhibited by SMS pretreatment, especially in the SMS high-dose group (**Figure 1C**).

SMS Ameliorate Gouty Arthritis *via* the PI3K/Akt Pathway

Nlrp3 protein expression was significantly increased in the injured joints of MSU mice, whereas p-Akt (S473) expression was decreased. SMS treatment suppressed the upregulation of Nlrp3, but further increased the expression of p-Akt (S473), especially in the SMS high-dose group (10mg/kg) (**Figure 2Aa**). No significant difference of the total Akt expression was detected in mice joint of all the groups.

In vitro, inflammatory factors NLRP3, IL-6, and IL-1β were also reduced by SMS treatment in the MSU stimulated THP-1 cells, while p-AKT (S473) was upregulated (**Figures 2Ab**, **2Ba**). However, the inhibitory effects of SMS on NLRP3 were notably

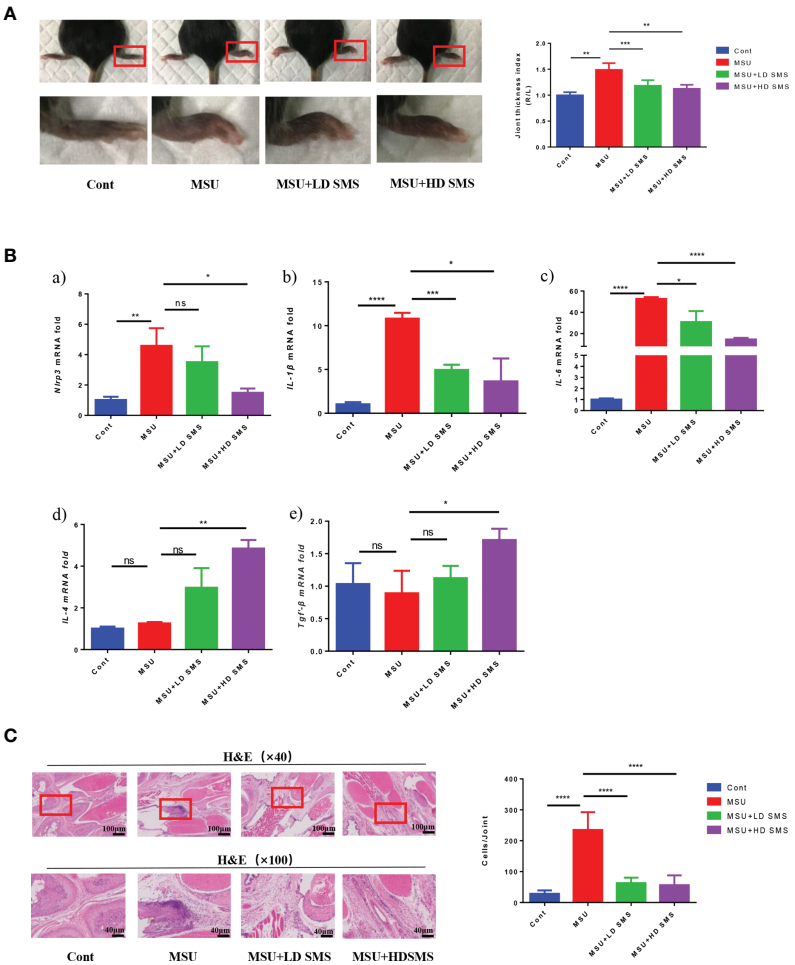

FIGURE 1 | SMS ameliorate MSU induced acute gouty arthritis in mice. Joint swelling and the joint thickness index at 8 hours after MSU injection in the mice **(A)**. The mRNA expression of *Nlrp3*, *IL-1β*, *IL-6*, *IL-4*, *Tgf-β* in the injured joints of the mice **(B)**. H&E staining, and inflammatory cells infiltration in the joints **(C)**. (mean ± SEM. ns $p > 0.05$, *$p < 0.05$, **$p < 0.01$, ***$p < 0.001$, ****$p < 0.0001$; n = 6/group; LD SMS: 1mg/kg.day low dose SMS; HD SMS:10mg/kg.day high dose SMS).

suppressed by pre-treatment with the PI3K/Akt inhibitor LY294002 (**Figure 2Bb**).

SMS Promote M2 Macrophage Polarization

To identify the macrophage polarization, joint tissue from mice was subjected to double immunofluorescence staining for the marker F4/80 and Arg-1. F4/80^{+}/Arg-1^{+} cells were ubiquitously observed in mouse joints (**Figure 3Aa**), and were significantly increased by SMS treatment (**Figure 3Ab**). In MSU-treated THP-1 cells, iNOS expression was induced, whereas ARG-1 remained stable. Upon SMS administration, iNOS expression was inhibited but ARG-1 was elevated. After blocking Akt activation with LY294002, Arg-1 upregulation and the anti-inflammatory effects of SMS were simultaneously suppressed in macrophages (**Figure 3B**).

SMS Inhibit Hyperuricemia in Mice

In this study, we further evaluated the effects of SMS on SUA levels. As presented in **Figure 4A**, hyperuricemia was induced in

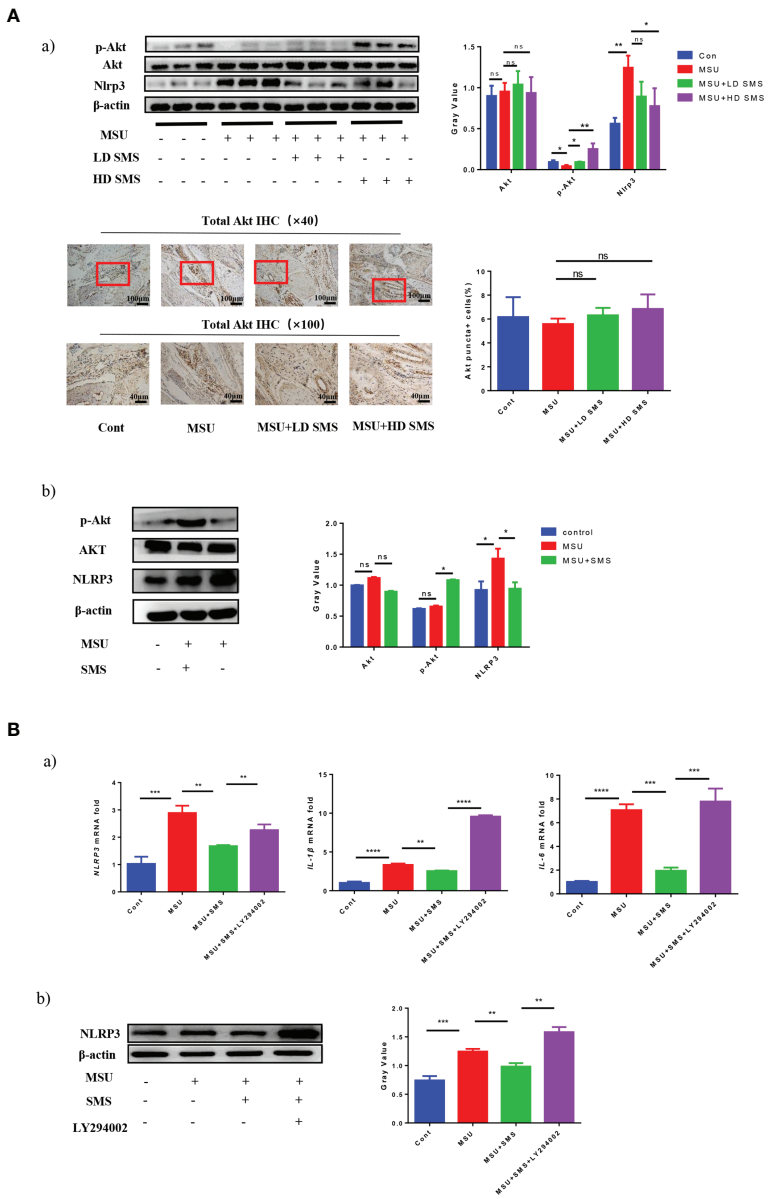

FIGURE 2 | SMS ameliorate gouty arthritis by PI3K/Akt pathway. The expression of Akt, p-Akt (Ser473) and Nlrp3 protein was detected by Western blot analysis in the MSU injured joints of the mice, and total Akt expression was detected by IHC staining **(Aa)**. *In vitro*, p-AKT (Ser473), AKT and NLRP3 protein was detected by Western blot analysis in the THP-1 cells treated by MSU with/without SMS **(Ab)**. Akt activation was inhibited by LY294002, the expression of NLRP3, IL-6 and IL-1β were detected by RT-PCR **(Ba)** or Western blot analysis **(Bb)**. (mean ± SEM. ns $p > 0.05$, *$p < 0.05$, **$p < 0.01$, ***$p < 0.001$, ****$p < 0.0001$; n = 6/group; LD SMS: 1mg/kg.day low dose SMS; HD SMS:10mg/kg.day high dose SMS).

mice treated with PO and YP for 3 weeks. However, hyperuricemia was inhibited when the mice were simultaneously treated with SMS. Compared with the control group, the hyperuricemia and the SMS-treated mice did not show histological changes in the kidney (**Figure 4B**).

Ecdysone and Estrone Detected in SMS *via* Mass Spectrometry

Because of the anti-inflammatory and uric acid lowering effects of SMS, mass spectrometry was used to screen the ingredients responsible for the observed benefits. Total Ion Chromatography of SMS was presented in **Figure 5A** with mass spectrometry. SMS did not exhibit any ion currents of the common ingredients of steroid (the spectra of the ingredients screened were listed in the **Supplement Table 2**) or non-steroidal anti-inflammatory drugs (the spectra of the ingredients screened were listed in the **Supplement Table 3**). Then phytohormones, estrogen and its analogs, and other potential hormones in plants were further examined by mass spectrometry (**Figure 5B**), ecdysone and estrone were finally detected in SMS (**Figure 5C**).

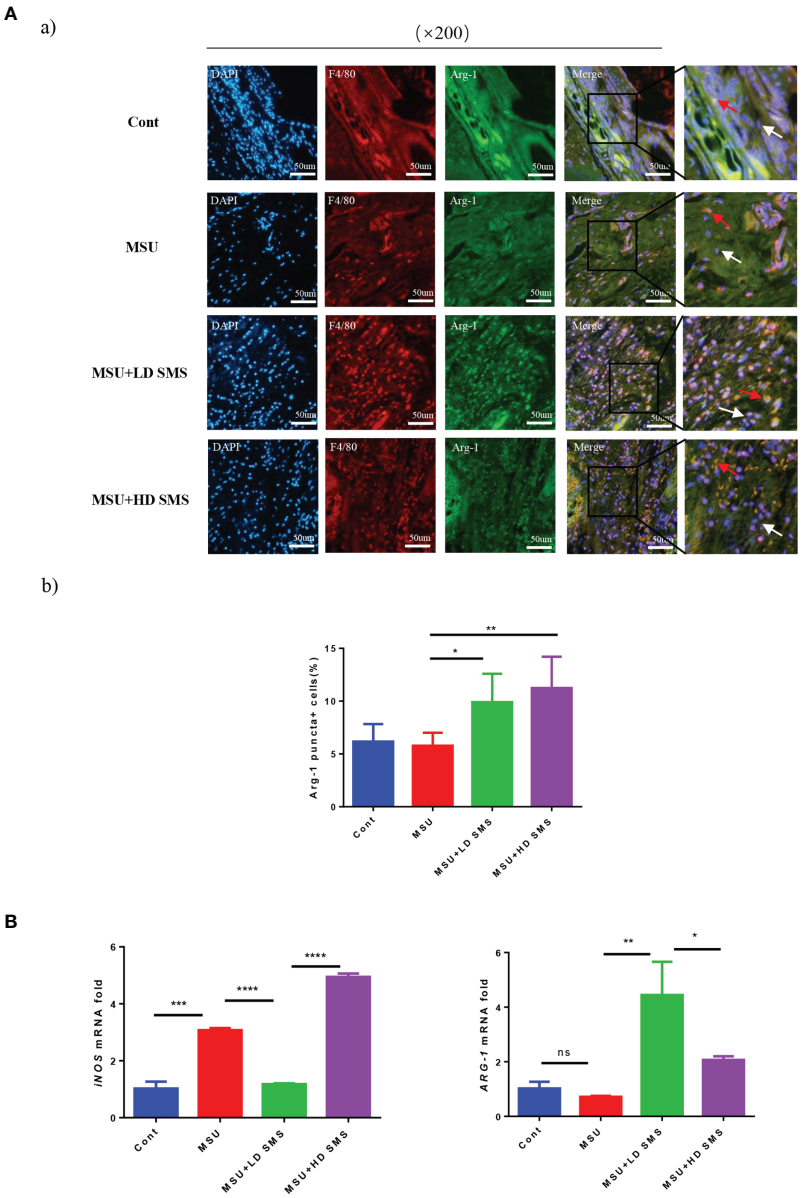

FIGURE 3 | SMS promote M2 macrophage polarization. IF co-localization staining of F4/80, Arg-1, DAPI in joint sections of mice were performed to estimate macrophage polarization **(Aa)**, the red arrows represent F4/80$^+$/Arg-1$^+$ cells, white arrows represent F4/80$^+$/Arg-1$^-$ cells. The F4/80$^+$/Arg-1$^+$ cells were counted **(Ab)**. The mRNA expression of ARG-1 and iNOS were detected by RT-PCR **(B)**. (mean ± SEM. ns $p > 0.05$, *$p < 0.05$, **$p < 0.01$, ***$p < 0.001$, ****$p < 0.0001$; n = 6/group; LD SMS: 1mg/kg.day low dose SMS; HD SMS:10mg/kg.day high dose SMS).

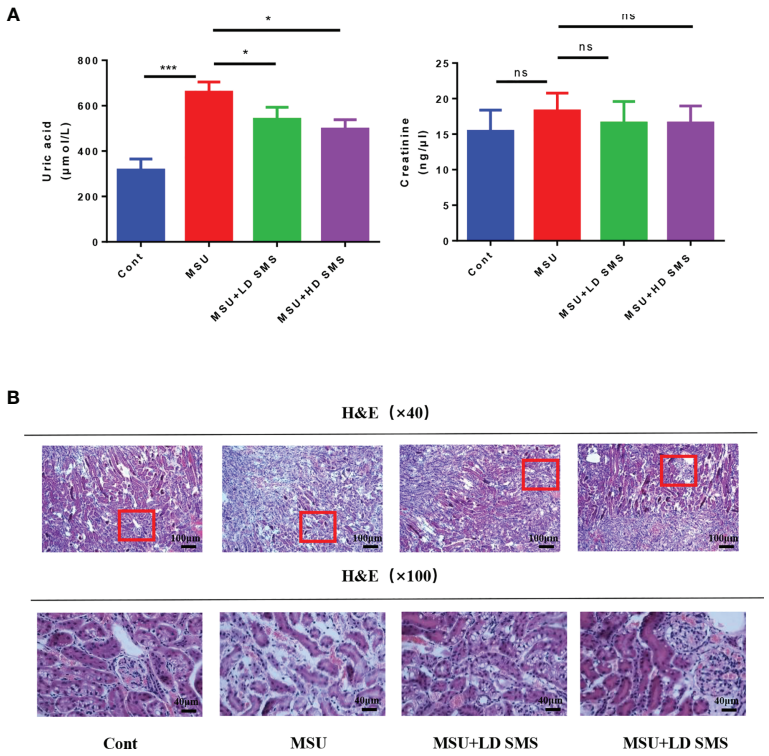

FIGURE 4 | SMS inhibit hyperuricemia in mice. Serum uric acid and serum creatinine were detected in the different groups of mice **(A)**. H&E staining of kidney in the different groups of mice **(B)**. (mean ± SEM. ns $p > 0.05$, *$p < 0.05$, ***$p < 0.001$; n = 6/group; LD SMS: 1mg/kg.day low dose SMS; HD SMS:10mg/kg.day high dose SMS).

DISCUSSION

Gout was first recorded in "Gezhiyulun" by DanXi Zhu in 1347 (Yuan Dynasty), and some effective traditional Chinese medicines against gout were described in ancient medical records. Colchicine, NSAIDs, or glucocorticoids were suggested as appropriate first-line therapy for gout flares in the recent recommendations for gout management (8). But the use of these drugs are often limited in gouty patients with concomitant complications such as chronic renal insufficiency, heart problems, gastrointestinal bleeding, or ulcer (29–31). Among the various Chinese medicines against gout, SMS was clinically confirmed to be effective and safe as an anti-inflammatory therapy for gout, and remains in use to the present day (18). In this study, we further researched its effects on gouty mice and examined the potential mechanism of SMS.

Gout is an inflammatory disease caused by serum uric acid oversaturation and MSU crystal irritation (3). Inflammatory cells infiltrated the joints release inflammatory mediators such as cytokines and chemokines, which result in acute gouty inflammation (32–36). Therefore, anti-inflammatory therapy is the primary approach for preventing gouty arthritis. In this study, SMS was found to ameliorate joint swelling and local inflammatory cell infiltration. Expression of the specific inflammatory factors Nlrp3 and IL-1β in gouty joints was notably inhibited by SMS treatment. These results confirmed that SMS is effective against MSU-induced gouty arthritis. Based on its characteristics, SMS may be an effective treatment of gout.

According to our previous research, Akt phosphorylation was increased in the MSU-induced inflammatory environment (21). Studies suggested that activation of the PI3K/Akt pathway inhibits inflammation, and these effects are mainly attributed to its inhibitory effects on nuclear factor-κB activity (37). The results suggested that PI3K/Akt pathway activation may be a beneficial response to inflammation or injury. In our study, Akt phosphorylation at Ser473 was significantly increased after SMS treatment in the injured joints of gouty mice. When PI3K/Akt activation was blocked by the specific inhibitor LY294002 in macrophages, the inhibitory action of SMS on inflammation was consequently suppressed. The results suggested that SMS can prevent gouty inflammation through activating the PI3K/Akt pathway.

Recent studies have shown the involvement of the neutrophils, macrophages and other immune cells in the inflammation progress and alleviation of gout (3). Macrophages usually exhibit distinct phenotypes in different tissue microenvironments (22, 38–40). In previous research, we found that the activation status of macrophages determines their function in gouty inflammation progression or restoration (21). Generally, there are two major phenotypes of activated macrophages depending on the inflammatory microenvironment, classically activated (M1) and alternatively activated (M2) macrophages (41). M1 macrophages

A

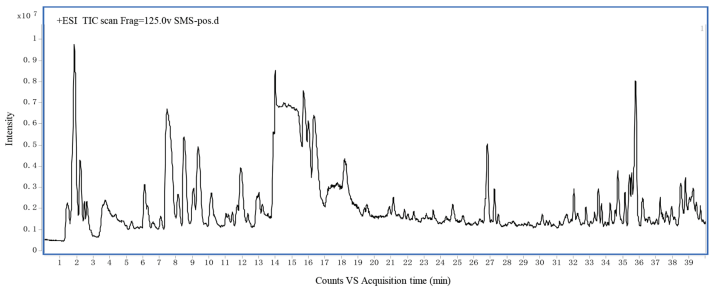

B

	Molecular formula	Molecular weight
Phytohormone		
Auxin	C10H9NO2	175.19
Gibberellin	C19H22O6	346.37
Cytokinin	C10H9N5OClH	251.67
Abscisic acid	C15H20O4	264.32
Ethylene	C2H4	28.06
Brassinosteroid	C28H46O6	480.68
Estrogen and analogues		
Epicatechin	C15H14O6	290.26806
Puerarin	C21H20O9	416.38
Huang Censu	C15H10O5	270.24
Myricin	C15H10O8	318.24
Kaempferol-3-O-galactoside	C21H20O11	448.38
Astragalin	C21H20O11	448.38
Quercetin	C15H10O7	302.23
Foxglove	C15H10O6	286.23
Kaempferol	C15H10O6	286.24
Apigenin	C15H10O5	270.24
Isorhamnetin	C16H12O7	316.27
Astaxanthin	C15H10O4	358.39
Estrone	C18H22O2	270.37
Puerarin	C20H22O6	358.39
Oxysqualene	C30H50	410.7
Potential insect hormones in plants		
Juvenile hormone	C16H26O3	266.37584
Ecdysone	C27H44O7	480.63406

C

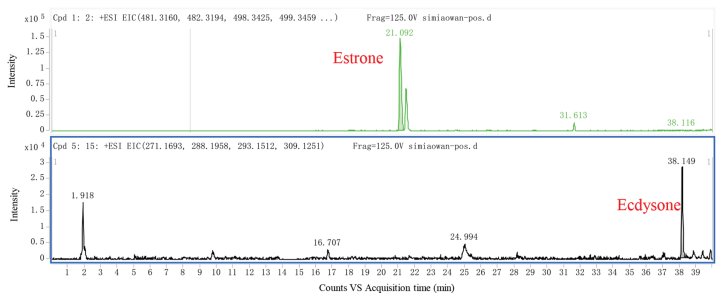

FIGURE 5 | Ecdysone and estrone detected in SMS *via* mass spectrometry. Total Ion Chromatography of SMS was detected by mass spectrometry **(A)**. Common phytohormone, estrogen and its analogs, and other potential hormones in plants to be screened in our study are listed **(B)**. Ecdysone and estrone were detected in SMS **(C)**.

exhibit high iNOS expression and mainly play pro-inflammatory roles, whereas M2 macrophages exhibit high Arg-1 expression and play anti-inflammatory roles (42–44). In our research, macrophages exhibited abundant iNOS expression upon MSU stimulation. After SMS administration, MSU-induced iNOS overexpression was suppressed, while Arg-1 was upregulated. It showed that SMS induced macrophage polarization toward M2 phenotype. In macrophages treated with LY294002 to block the

PI3K/Akt pathway, Arg-1 expression was consequently inhibited. It suggested that SMS induces M2 macrophage polarization by activating the PI3K/Akt pathway, which might be the mechanism of its anti-inflammatory effects on gout.

From the aforementioned results, SMS was confirmed to inhibit gouty inflammation, which prompted us to examine its potential anti-inflammatory ingredients. However, no such compound was detected in SMS by screening for the common ingredients of steroid and non-steroidal anti-inflammatory drugs *via* mass spectrometry. Then, the spectra of phytohormones, estrogen and its analogs, and potential insect hormones in plants were further screened. Interestingly, ecdysone and estrone were finally detected in SMS.

Ecdysone (20-hydroxyecdysone) is a phytoecdysteroid with biological activity that has not been thoroughly investigated to date. It has been reported to regulate the immune response and inhibit bacterial infection in Drosophila embryos (45, 46). Ecdysone inhibited the inflammatory cascade and oxidative stress process in rats with collagen-induced rheumatoid arthritis (47). Based on its effect, ecdysone might be the ingredient responsible for the anti-inflammatory effects of SMS against gout.

In this study, estrone was another plant hormone detected in SMS. It is a relatively abundant hormone that is widely distributed in tissues of animal and plant origin (48). As the predominant estrogen, estrone was reported to regulate metabolism (49) and increase uric acid excretion (50). Women of productive age are well known to seldom experience hyperuricemia or gout because of the regulatory effects of estrogen on SUA content (51). SMS might prevent hyperuricemia because of being rich in estrone. In this study, we found that SMS treatment in hyperuricemia mice resulted in significantly decreases in SUA levels. This result was consistent with previous studies in which SMS ameliorated high fructose-induced insulin resistance, dyslipidemia, high uric acid levels, and kidney injury in rats (52). However, further research is needed to verify the specific role of ecdysone and estrone in gout and hyperuricemia.

CONCLUSION

This study demonstrated that SMS ameliorate MSU-induced gouty arthritis and inhibit hyperuricemia. The anti-inflammatory mechanism of SMS might involve M2 macrophages polarization *via* activation of the PI3K/Akt pathway. These findings provided insight for developing therapeutic approaches to treat gout. The plant hormones ecdysone and estrone were detected in SMS. However, further research is needed to clarify their anti-inflammatory function and mechanism of action for uric acid lowering effects.

DATA AVAILABILITY STATEMENT

The datasets presented in this study can be found in online repositories. The names of the repository/repositories and accession number(s) can be found in the article/**Supplementary Material**.

ETHICS STATEMENT

The animal study was reviewed and approved by The Ethics Committee of the Department of Laboratory Animal Science, Fudan University (No. 20160981A302).

AUTHOR CONTRIBUTIONS

LC and TZ performed mouse experiments and *in vitro* experiments. YXu, LX, YC, and FQ contributed to the experimental design. YXi performed mass spectrometry. WW conducted the statistical analysis and computational data analysis. MH and QJ contributed to the data interpretation. LL contributed to the revise the manuscript with significant input. XZ and HZ contributed to manuscript drafting and conceived the study. All authors reviewed the manuscript. All authors read and approved the final manuscript.

FUNDING

This work was supported by the National Natural Science Foundation of China (82071830) and Research Funding from the Shanghai Hospital Development Center (SHDC12016227) and Shanghai Municipal Health Commission (20204Y0428) and Young Elite Scientists Sponsorship Program by CACM(CACM-2020-QNRC2-05).

SUPPLEMENTARY MATERIAL

The Supplementary Material for this article can be found online at: https://www.frontiersin.org/articles/10.3389/fimmu.2021.777522/full#supplementary-material

REFERENCES

1. Ragab G, Elshahaly M, Bardin T. Gout: An Old Disease in New Perspective–A Review. *J Adv Res* (2017) 8:495–511. doi: 10.1016/j.jare.2017.04.008
2. Dalbeth N, Choi HK, Joosten LAB, Khanna PP, Matsuo H, Perez-Ruiz F, et al. Gout. *Nat Rev Dis Primers* (2019) 5:69. doi: 10.1038/s41572-019-0115-y
3. Nicola Dalbeth HKCL, Stamp FPRA. Gout. *Nat Rev* (2019) 5:69. doi: 10.1038/s41572-019-0115-y
4. Borghi C, Agabiti-Rosei E, Johnson RJ, Kielstein JT, Lurbe E, Mancia G, et al. Hyperuricaemia and Gout in Cardiovascular, Metabolic and Kidney Disease. *Eur J Intern Med* (2020) 80:1–11. doi: 10.1016/j.ejim.2020.07.006
5. Joosten L, Crişan TO, Bjornstad P, Johnson RJ. Asymptomatic Hyperuricaemia: A Silent Activator of the Innate Immune System. *Nat Rev Rheumatol* (2020) 16:75–86. doi: 10.1038/s41584-019-0334-3
6. Xia Y, Wu Q, Wang H, Zhang S, Jiang Y, Gong T, et al. Global, Regional and National Burden of Gout, 1990-2017: A Systematic Analysis of The Global

Burden of Disease Study. *Rheumatol (Oxf)* (2020) 59:1529–38. doi: 10.1093/rheumatology/kez476
7. Mikuls TR, Saag KG. New Insights Into Gout Epidemiology. *Curr Opin Rheumatol* (2006) 18:199–203. doi: 10.1097/01.bor.0000209435.89720.7c
8. FitzGerald JD, Dalbeth N, Mikuls T, Brignardello-Petersen R, Guyatt G, Abeles AM, et al. 2020 American College of Rheumatology Guideline for the Management of Gout. *Arthritis Care Res (Hoboken)* (2020) 72:744–60. doi: 10.1002/acr.24180
9. Richette P, Doherty M, Pascual E, Barskova V, Becce F, Castaneda J, et al. 2018 Updated European League Against Rheumatism Evidence-Based Recommendations for the Diagnosis of Gout. *Ann Rheum Dis* (2019) 79:31–8. doi: 10.1136/annrheumdis-2019-215315
10. Max Hamburger HSBB, Lewis Bass BCPP, Hamburger RHJA, Didier A, Mandelbrot BPME, Mount RSPK B, et al. 2011 Recommendations for the Diagnosis and Management of Gout and Hyperuricemia. *Postgrad Med* (2011) 39:98–123. doi: 10.3810/psm.2011.11.1946
11. Khanna D, Khanna PP, FitzGerald JD, Singh MK, Bae S, Neogi T, et al. 2012 American College of Rheumatology Guidelines for Management of Gout Part II: Therapy and Anti-Inflammatory Prophylaxis of Acute Gouty Arthritis. *Arthrit Care Res* (2012) 64:1447–61. doi: 10.1002/acr.21773
12. Shi XD, Li GC, Qian ZX, Jin ZQ, Song Y. Randomized and Controlled Clinical Study of Modified Prescriptions of Simiao Pill in The Treatment of Acute Gouty Arthritis. *Chin J Integr Med* (2008) 14:17–22. doi: 10.1007/s11655-007-9001-7
13. Ma CH, Kang LL, Ren HM, Zhang DM, Kong LD. Simiao Pill Ameliorates Renal Glomerular Injury *via* Increasing Sirt1 Expression and Suppressing NF-κb/NLRP3 Inflammasome Activation in High Fructose-Fed Rats. *J Ethnopharmacol* (2015) 172:108–17. doi: 10.1016/j.jep.2015.06.015
14. Zhao F, Guochun L, Yang Y, Shi L, Xu L, Yin L. A Network Pharmacology Approach to Determine Active Ingredients and Rationality of Herb Combinations of Modified-Simiaowan for Treatment of Gout. *J Ethnopharmacol* (2015) 168:1–16. doi: 10.1016/j.jep.2015.03.035
15. Liu Y, Huang Y, Wen C, Zhang J, Xing G, Tu S, et al. The Effects of Modified Simiao Decoction in the Treatment of Gouty Arthritis: A Systematic Review and Meta-Analysis. *Evid-Based Compl Alt* (2017) 2017:1–12. doi: 10.1155/2017/6037037
16. Qiu R, Shen R, Lin D, Chen Y, Ye H. Treatment of 60 Cases of Gouty Arthritis With Modified Simiao Tang. *J Tradit Chin Med* (2008) 28:94–7. doi: 10.1016/S0254-6272(08)60023-0
17. Zhu F, Yin L, Ji L, Yang F, Zhang G, Shi L, et al. Suppressive Effect of Sanmiao Formula on Experimental Gouty Arthritis by Inhibiting Cartilage Matrix Degradation: An *In Vivo* and *In Vitro* Study. *Int Immunopharmacol* (2016) 30:36–42. doi: 10.1016/j.intimp.2015.11.010
18. Lin X, Shao T, Huang L, Wen X, Wang M, Wen C, et al. Simiao Decoction Alleviates Gouty Arthritis by Modulating Proinflammatory Cytokines and the Gut Ecosystem. *Front Pharmacol* (2020) 11:955. doi: 10.3389/fphar.2020.00955
19. Shi L, Yuan Z, Liu J, Cai R, Hasnat M, Yu H, et al. Modified Simiaowan Prevents Articular Cartilage Injury in Experimental Gouty Arthritis by Negative Regulation of STAT3 Pathway. *J Ethnopharmacol* (2021) 270:113825. doi: 10.1016/j.jep.2021.113825
20. Wang H, Huang Y, Shen P, Wang Y, Qin K, Huang Y, et al. Modified Si-Miao Pill for Rheumatoid Arthritis: A Systematic Review and Meta-Analysis. *Evid Based Complement Alternat Med* (2020) 2020:7672152. doi: 10.1155/2020/7672152
21. Liu L, Zhu X, Zhao T, Yu Y, Xue Y, Zou H. Sirt1 Ameliorates Monosodium Urate Crystal–Induced Inflammation by Altering Macrophage Polarization *via* the PI3K/Akt/STAT6 Pathway. *Rheumatology* (2019) 58:1674–83. doi: 10.1093/rheumatology/kez165
22. Martin WJ, Shaw O, Liu X, Steiger S, Harper JL. Monosodium Urate Monohydrate Crystal-Recruited Noninflammatory Monocytes Differentiate Into M1-Like Proinflammatory Macrophages in a Peritoneal Murine Model of Gout. *Arthritis Rheum* (2011) 63:1322–32. doi: 10.1002/art.30249
23. Zheng S, Zhu X, Xue Y, Zhang L, Zou H, Qiu J, et al. Role of the NLRP3 Inflammasome in the Transient Release of IL-1β Induced by Monosodium Urate Crystals in Human Fibroblast-Like Synoviocytes. *J Inflamm* (2015) 12:30. doi: 10.1186/s12950-015-0070-7
24. Chen B, Li H, Ou G, Ren L, Yang X, Zeng M. Curcumin Attenuates MSU Crystal-Induced Inflammation by Inhibiting the Degradation Of Ικbα and Blocking Mitochondrial Damage. *Arthritis Res Ther* (2019) 21:193. doi: 10.1186/s13075-019-1974-z
25. Zhang X, Liu Y, Deng G, Huang B, Kai G, Chen K, et al. A Purified Biflavonoid Extract From Selaginella Moellendorffii Alleviates Gout Arthritis *via* NLRP3/ASC/Caspase-1 Axis Suppression. *Front Pharmacol* (2021) 12:676297. doi: 10.3389/fphar.2021.676297
26. Yang QB, He YL, Zhang QB, Mi QS, Zhou JG. Downregulation of Transcription Factor T-Bet as a Protective Strategy in Monosodium Urate-Induced Gouty Inflammation. *Front Immunol* (2019) 10:1199. doi: 10.3389/fimmu.2019.01199
27. Yu Y, Yang J, Fu S, Xue Y, Liang M, Xuan D, et al. Leptin Promotes Monosodium Urate Crystal-Induced Inflammation in Human and Murine Models of Gout. *J Immunol* (2019) 202:2728–36. doi: 10.4049/jimmunol.1801097
28. Chen H, Zheng S, Wang Y, Zhu H, Liu Q, Xue Y, et al. The Effect of Resveratrol on the Recurrent Attacks of Gouty Arthritis. *Clin Rheumatol* (2016) 35:1189–95. doi: 10.1007/s10067-014-2836-3
29. Bacchi S, Palumbo P, Sponta A, Coppolino MF. Clinical Pharmacology of Non-Steroidal Anti-Inflammatory Drugs: A Review. *Antiinflamm Antiallergy Agents Med Chem* (2012) 11:52–64. doi: 10.2174/187152312803476255
30. Schjerning AM, McGettigan P, Gislason G. Cardiovascular Effects and Safety of (Non-Aspirin) NSAIDs. *Nat Rev Cardiol* (2020) 17:574–84. doi: 10.1038/s41569-020-0366-z
31. Marsico F, Paolillo S, Filardi PP. NSAIDs and Cardiovascular Risk. *J Cardiovasc Med (Hagerstown)* (2017) 18 (Suppl 1):e40–3. Special Issue on The State of the Art for the Practicing Cardiologist: The 2016 Conoscere E Curare Il Cuore (CCC) Proceedings from the CLI Foundation. doi: 10.2459/JCM.0000000000000443
32. Martinon F, Pétrilli V, Mayor A, Tardivel A, Tschopp J. Gout-Associated Uric Acid Crystals Activate the NALP3 Inflammasome. *Nature* (2006) 440:237–41. doi: 10.1038/nature04516
33. Schauer C, Janko C, Munoz LE, Zhao Y, Kienhöfer D, Frey B, et al. Aggregated Neutrophil Extracellular Traps Limit Inflammation by Degrading Cytokines and Chemokines. *Nat Med* (2014) 20:511–7. doi: 10.1038/nm.3547
34. Schorn C, Janko C, Latzko M, Chaurio R, Schett G, Herrmann M. Monosodium Urate Crystals Induce Extracellular DNA Traps in Neutrophils, Eosinophils, and Basophils But Not in Mononuclear Cells. *Front Immunol* (2012) 3:277. doi: 10.3389/fimmu.2012.00277
35. Mitroulis I, Kambas K, Chrysanthopoulou A, Skendros P, Apostolidou E, Kourtzelis I, et al. Neutrophil Extracellular Trap Formation Is Associated With IL-1β and Autophagy-Related Signaling in Gout. *PloS One* (2011) 6:e29318. doi: 10.1371/journal.pone.0029318
36. Farrera C, Fadeel B. Macrophage Clearance of Neutrophil Extracellular Traps Is a Silent Process. *J Immunol* (2013) 191:2647–56. doi: 10.4049/jimmunol.1300436
37. Hoffmann M, Fiedor E, Ptak A. 17β-Estradiol Reverses Leptin-Inducing Ovarian Cancer Cell Migration by the PI3K/Akt Signaling Pathway. *Reprod Sci* (2016) 23:1600–8. doi: 10.1177/1933719116648214
38. Martin WJ, Walton M, Harper J. Resident Macrophages Initiating and Driving Inflammation in a Monosodium Urate Monohydrate Crystal-Induced Murine Peritoneal Model of Acute Gout. *Arthritis Rheum* (2009) 60:281–9. doi: 10.1002/art.24185
39. Murray PJ. Macrophage Polarization. *Annu Rev Physiol* (2017) 79:541–66. doi: 10.1146/annurev-physiol-022516-034339
40. Fan X, Zhang H, Cheng Y, Jiang X, Zhu J, Jin T. Double Roles of Macrophages in Human Neuroimmune Diseases and Their Animal Models. *Mediat Inflammation* (2016) 2016:1–13. doi: 10.1155/2016/8489251
41. Mantovani A, Sica A, Sozzani S, Allavena P, Vecchi A, Locati M. The Chemokine System in Diverse Forms of Macrophage Activation and Polarization. *Trends Immunol* (2004) 25:677–86. doi: 10.1016/j.it.2004.09.015
42. Thapa B, Lee K. Metabolic Influence on Macrophage Polarization and Pathogenesis. *Bmb Rep* (2019) 52:360–72. doi: 10.5483/BMBRep.2019.52.6.140
43. Atri C, Guerfali FZ, Laouini D. Role of Human Macrophage Polarization in Inflammation During Infectious Diseases. *Int J Mol Sci* (2018) 19:1801. doi: 10.3390/ijms19061801
44. Funes SC, Rios M, Escobar-Vera J, Kalergis AM. Implications of Macrophage Polarization in Autoimmunity. *Immunology* (2018) 154:186–95. doi: 10.1111/imm.12910

45. Toyota K, Yamane F, Ohira T. Impacts of Methyl Farnesoate and 20-Hydroxyecdysone on Larval Mortality and Metamorphosis in the Kuruma Prawn Marsupenaeus Japonicus. *Front Endocrinol (Lausanne)* (2020) 11:475. doi: 10.3389/fendo.2020.00475
46. Tan KL, Vlisidou I, Wood W. Ecdysone Mediates the Development of Immunity in the Drosophila Embryo. *Curr Biol* (2014) 24:1145–52. doi: 10.1016/j.cub.2014.03.062
47. Kapur P, Wuttke W, Jarry H, Seidlova-Wuttke D. Beneficial Effects of Beta-Ecdysone on the Joint, Epiphyseal Cartilage Tissue and Trabecular Bone in Ovariectomized Rats. *Phytomedicine* (2010) 17:350–5. doi: 10.1016/j.phymed.2010.01.005
48. Nguyen PY, Carvalho G, Reis M, Oehmen A. A Review of the Biotransformations of Priority Pharmaceuticals in Biological Wastewater Treatment Processes. *Water Res* (2020) 188:116446. doi: 10.1016/j.watres.2020.116446
49. Kling JM, Dowling NM, Bimonte-Nelson HA, Gleason CE, Kantarci K, Manson JE, et al. Impact of Menopausal Hormone Formulations on Pituitary-Ovarian Regulatory Feedback. *Am J Physiol Regul Integr Comp Physiol* (2019) 317:R912–20. doi: 10.1152/ajpregu.00234.2019
50. Gautam NK, Verma P, Tapadia MG. Ecdysone Regulates Morphogenesis and Function of Malpighian Tubules in Drosophila Melanogaster Through EcR-B2 Isoform. *Dev Biol* (2015) 398:163–76. doi: 10.1016/j.ydbio.2014.11.003
51. Nakayama A, Matsuo H, Takada T, Ichida K, Nakamura T, Ikebuchi Y, et al. ABCG2 Is a High-Capacity Urate Transporter and Its Genetic Impairment Increases Serum Uric Acid Levels in Humans. *Nucleosides Nucleotides Nucleic Acids* (2011) 30:1091–7. doi: 10.1080/15257770.2011.633953
52. Fan Y, Li Y, Wu Y, Li L, Wang Y, Li Y. Identification of the Chemical Constituents in Simiao Wan and Rat Plasma After Oral Administration by GC-MS and LC-Ms. *Evid-Based Compl Alt* (2017) 2017:1–13. doi: 10.1155/2017/6781593

Conflict of Interest: The authors declare that the research was conducted in the absence of any commercial or financial relationships that could be construed as a potential conflict of interest.

Publisher's Note: All claims expressed in this article are solely those of the authors and do not necessarily represent those of their affiliated organizations, or those of the publisher, the editors and the reviewers. Any product that may be evaluated in this article, or claim that may be made by its manufacturer, is not guaranteed or endorsed by the publisher.

frontiers in Immunology

REVIEW
published: 14 January 2022
doi: 10.3389/fimmu.2021.811323

The Role of Advanced Imaging in Gout Management

Shuangshuang Li, Guanhua Xu, Junyu Liang, Liyan Wan, Heng Cao and Jin Lin**

Department of Rheumatology, The First Affiliated Hospital, Zhejiang University School of Medicine, Hangzhou, China

Gout is a common form of inflammatory arthritis where urate crystals deposit in joints and surrounding tissues. With the high prevalence of gout, the standardized and effective treatment of gout is very important, but the long-term treatment effect of gout is not satisfied because of the poor adherence in patients to the medicines. Recently, advanced imaging modalities, including ultrasonography (US), dual-energy computed tomography (DECT), and magnetic resonance imaging (MRI), attracted more and more attention for their role on gout as intuitive and non-invasive tools for early gout diagnosis and evaluation of therapeutic effect. This review summarized the role of US, DECT, and MRI in the management of gout from four perspectives: hyperuricemia, gout attacks, chronic gout, and gout complications described the scoring systems currently used to quantify disease severity and discussed the challenges and limitations of using these imaging tools to assess response to the gout treatment.

Keywords: ultrasonography, DECT, MRI, gout, management

OPEN ACCESS

Edited by:
Lihua Duan,
Jiangxi Provincial People's Hospital, China

Reviewed by:
Yan Yang,
University of Texas MD Anderson Cancer Center, United States
Shaolin Shi,
Nanjing University, China

****Correspondence:***
Heng Cao
caohengzju@zju.edu.cn
Jin Lin
linjinzju@zju.edu.cn
orcid.org/0000-0002-0978-0723

Specialty section:
This article was submitted to Autoimmune and Autoinflammatory Disorders, a section of the journal Frontiers in Immunology

Received: *08 November 2021*
Accepted: *21 December 2021*
Published: *14 January 2022*

Citation:
Li S, Xu G, Liang J, Wan L, Cao H and Lin J (2022) The Role of Advanced Imaging in Gout Management. Front. Immunol. 12:811323. doi: 10.3389/fimmu.2021.811323

INTRODUCTION

Gout is a chronic disease of monosodium urate (MSU) crystal deposition and is one of the most common forms of inflammatory arthritis in adults, especially men. The incidence and prevalence of gout are increasing worldwide, with recent data estimating that the prevalence of gout ranges from roughly <1% to 6.8% in Western countries and about 1.1% in China (1, 2). People with metabolic syndrome are more likely to have higher serum urate levels (3). Persistent serum urate levels (sUA, >360 μmol/l or >6 mg/dl) may lead to much MSU crystal deposition in tendons, joints, or other unusual tissues (4) and trigger acute joint inflammation (gout flares) or chronic joint inflammation (gouty arthritis and joint structural damage) (5). The typical symptoms of a gout flare are rapid painfulness, hotness, redness, and swelling in the joints (6), which are self-limiting inflammatory responses that usually disappear within 14 days. Alone or in combination, use of NSAIDs, colchicine, or corticosteroids is recommended in treating gout flares with an effective and rapid control of acute inflammatory attack. Urate-lowering therapy (ULT) is a long-term management of gout to reduce serum urate levels, which can lead to dissolution of MSU crystals deposition, reduction or prevention of gout attacks, and joint damage (7, 8). Although gout is "curable" through

Abbreviations: ACR, American College of Rheumatology; AH, asymptomatic hyperuricemia; DCs, double contour sign; DECT, dual-energy computed tomography; EULAR, European League Against Rheumatism; M1, first month; M3, third month; MRI, magnetic resonance imaging; MSU, monosodium urate; MTP1, metatarsophalangeal 1; OMERACT, Outcome Measures in Rheumatology; RAMRIS, rheumatoid arthritis magnetic resonance image scoring system; ULT, urate-lowering therapy; US, ultrasonography.

ULTs, this disease is poorly managed worldwide, because of poor adherence in gout patients to the medications (e.g., febuxostat or allopurinol) of ULTs.

MSU crystals from tophi or joint synovial fluid aspiration by microscopic detection are negatively birefringent and needle-shaped (9), which is still the gold standard in gout diagnosis, while with the rapid development of imaging techniques, particularly US, DECT, and MRI, which provide non-invasive and clear identification of MSU crystal deposition, they are considered to be a promising tool for gout diagnosis (10, 11). In 2015, the classification criteria recommended by the European League Against Rheumatism (EULAR) and the American College of Rheumatology (ACR) endorsed the US and DECT as a new and effective diagnostic tool for gout (12). What is more, these advanced imaging techniques can be used to assess the severity of gout and monitor the response to treatment in gouty patients. Although MRI is not specific enough in gout disease, it can be valuable in the assessment of soft tissue and bone damage in gout.

The main ultrasound imaging findings of gout include the double contour sign (DCs), tophus, aggregates, and erosion. These definitions were developed by the US group of Outcome Measures in Rheumatology (OMERACT) in 2015 (13). DCs are a deposit of urate on the surface of articular cartilage, forming two hyperechoic bands with the bone cortex, which are present regardless of the angle of the irradiation. Tophus refers to a large collection of hypoechoic or uneven hyperechoic MSU crystals. Aggregates are small inhomogeneous hyperechoic crystal depositions, and erosion is the discontinuity of the bone cortex and can be seen in two different vertical planes. DECT is a new imaging technique developed from conventional CT, which uses a dual-source scanner to irradiate two X-ray beams onto different materials for identification. Differences in the energy absorption curves of chemical entities are used to accurately calculate the composition of an object (14). The MSU deposits are often coded in green and can be seen in DECT images. MRI has good soft-tissue resolution and can show cartilage damage, soft tissue inflammation, and bone erosion very well. There are four main elements to the MRI assessment of gout, tophi, synovitis, bone marrow edema, and bone erosion (15). The rheumatoid arthritis magnetic resonance image scoring system (RAMRIS) is now commonly used to assess the disease progression of gout in MRI (16). This review mainly focuses on the role of US, DECT, and MRI in the management of gout.

HYPERURICEMIA

Hyperuricemia is defined as a serum uric acid level above 7 mg/dl. Most people with asymptomatic hyperuricemia (AH) do not develop gout (17), and the predictors of the transition from hyperuricemia to gout are unknown, leading us to overlook the possibility that this population may benefit from early uric acid-lowering treatment. Recent studies have shown that US and DECT imaging techniques can be used to detect MSU deposits in asymptomatic hyperuricemia. The consistency between MSU crystals and US gouty features (DCs and hyperechoic areas) in asymptomatic hyperuricemia patients was first reported in 2012, validating the role of US in the early diagnosis and detection of structural damage in AH patients (18). Metatarsophalangeal 1 (MTP1) and femoral condyle were the most common US scan sites for DCs and tophi, and a high prevalence of gouty damage in AH patients was observed (19). MSU deposits could also be detected with DECT in AH patients, but they were larger and occurred significantly more frequently in gouty patients. This suggested that a certain threshold of MSU deposition may be required during the transition from AH to gout (20). 15% of AH individuals had subclinical MSU depositions on foot or ankles by DECT detection (21). These findings highlight the important role of subclinical MSU deposition in disease progression and the need to explore the clinical significance of crystals; the use of US and DECT may provide greater insight and understanding of asymptomatic hyperuricemia.

According to the current gout classification criterion put forward by EULAR and ACR in 2015, the pain characteristics of gout are acute onset, generally reaching the maximum pain within 24 h and lasting less than 14 days, which is an episode pain (12). However, clinically, we also encounter many symptomatic hyperuricemia patients who have persistent foot pain that does not fit typical gout. Little is known about this special population. Recently, a study included 16 patients with hyperuricemia and persistent foot pain as an experimental group, compared to 15 AH individuals (22). The experimental group was given 80 mg/day with febuxostat for 3 months; the US imaging and 24-h and 7-day visual analog scores were assessed in baseline, the first month (M1), and the third month (M3) after ULTs. The results showed that sUA and foot pain scores of patients in the experimental group decreased significantly under the treatment of febuxostat. Then, the experimental group was divided into two groups based on the presence or absence of DCs; further analysis demonstrated that DC-positive patients had obviously lower 24-h and 7-day pain scores at M3, but with no significant difference of sUA levels between the two groups. These results suggested that hyperuricemia patients who have sustaining foot pain and positive US features may be the alternative gouty presentation and responsive to the ULTs, which may also be included in the gout classification criteria to identify and treat gout at an earlier stage, increasing diagnostic sensitivity and treatment effectiveness.

GOUT FLARES

Serum uric acid levels have long been considered the endpoint of conventional uric acid-lowering therapy. It was previously thought that the altered sUA concentrations were a risk factor of flares (23), and controlling serum uric acid levels could prevent gout attacks. However, this has been challenged by several studies, including those from ACR, who have argued that the correlation between targeting sUA and gout flares reduction was inadequate (24–27). In the febuxostat trial, for example, there was no significant reduction in gout attacks compared with

placebo, even when the uric acid level was controlled (28, 29). Similarly, in a 6-month randomized controlled ULT study, the frequency of gout attacks actually increased (30). Thus, there is a missing part between sUA and gout flares, and recent studies suggested that MSU crystals might be the key link between them. It has been hypothesized that the decrease in serum uric acid leads to the instability and dissolution of urate, exposing it to the autoimmune system and producing a strong immune response that leads to an outbreak of gout (23). Therefore, the volume and level of urate crystals are closely related to the onset of gout and need to be monitored continuously, which is also a good way to guide treatment to reduce uric acid.

In a follow-up observational study of 62 patients under ULTs, their MSU deposits were assessed by DECT and US, suggesting that MSU crystal burden may be a predictive risk of gout flares (31). Patients attended the visits at 0, 3, 6, and 12 months, and their knees and feet were all scanned. The study revealed that the presence and volume of urate deposits in feet measured by DECT were significantly associated with flares, rather than the number of joints bearing DCs assessed by US. The analysis of DECT evaluation displayed that for every 1-cm^3 increase in urate deposition volume in feet, the risk of gout attacks increased 2.03-fold during the first 6 months compared to the baseline. Moreover, the optimal threshold for differentiating the patients with or without gout flares was 0.81 cm^3 in this research. All these data verified the concept that urate burden was related to the risk of gout flares. Interestingly, the change in sUA levels from M0 to M6 was not obviously different among the participants undergoing or not undergoing gout flares. The role of DECT in the management of gout was supported, beyond diagnosis. It may be decisive to assess MSU burden by using DECT to identify which one was still at a high risk of gout flares when considering maintain or interruption of ULTs, especially for patients who have reached the targeted sUA level but still have urate deposition.

In the treatment of gout, a basic principle is to prevent the onset of gout in the initial stage of ULTs, but there is no consensus on how long prophylaxis drugs should be used to prevent gout attacks during ULTs. EULAR recommends at least 6 months of prophylaxis (e.g., NSAIDs or colchicine) (7), while ACR recommends that 3–6 months of prophylaxis should be followed, and screening for gout activity and continued use of anti-inflammatory drugs are needed if patients have a recurrence of gout after cessation (8). A recent study including 79 patients might shed some light on this question (32). The study was divided into two stages: the first stage was a 6-month ULTs with gout attack prophylaxis, and the second phase was 6 months of ULT maintenance therapy with stopped gout prophylaxis. Nearly half of the patients in this study had at least one episode of gout within 6 months of discontinuing their gout prophylaxis drugs; the high incidence was in line with existing research (28, 29, 33). The authors found that DCs, tophi, and sUA levels all changed significantly after treatment. Among them, DCs were the earliest indicator that changed (appear at M3). However, changes in sUA were not associated with the prevalence of gout attacks, which was consistent with other results that there was no confirmed relationship between sUA and gout flares (30, 34). Interestingly, the low rate of gout relapse was found in patients with a greater than 50% reduction in tophi volume, suggesting that changes in tophi volume could be a predictor of gout onset. These results might provide some ideas for research on the duration of gout prophylaxis and emphasize the big role of MSU crystal depositions in gout flares. It is reasonable that follow-up of MSU depositions with US and DECT can help physicians predict the onset of gout and discontinue gout prophylaxis at an appropriate time.

In addition to the four main features of US in gout mentioned above, the altered Doppler flow signal, which is unique to US, can also clearly show the inflammatory signs of an acute attack of gout. The ultrasound Doppler flow signal is more suggestive of an acute attack of gout than an assessment of the clinical presentation of the gout patient (35). It has been suggested that the ultrasound Doppler signal is more pronounced during an acute gout attack than during the intercritical phase (36). In addition, Doppler ultrasound can also indicate the responsiveness of gout patients to ULT. A study revealed that after more than 2 years of ULT, the Doppler signal was still present in a large number of gout patients, although it has been reduced to varying degrees. This finding raised reflections on the accuracy of current outcome measures and treatments (37). These data show that ultrasound Doppler signaling also played a role in the assessment of gout progression.

CHRONIC GOUT

DECT

There is growing interest in the important role of MSU deposition in the development of gout. Many studies have concluded that MSU crystals were the key pathology of gout. Instead of merely controlling serum uric acid levels, treatments that address urate crystals are truly effective. Importantly, the link between sUA and MSU crystals was weak (38), which made it difficult to assess the dynamics of MSU depositions by just measuring sUA levels. Such a view manifested the importance of monitoring MSU deposits during ULTs, and DECT was an appropriate approach. DECT has a high sensitivity in detecting even very small urate crystals and allows the testing of some special sites such as tenders, spine, blood vessels, which cannot be measured by other imaging or joint fluid aspiration (11). Furthermore, DECT allows automatic calculation of uric acid crystal volume for quantitative analysis, which is an important parameter in the outcome of the disease and can better evaluate the treatment from the starting point to the follow-up (39).

Allopurinol is the first-line drug for the treatment of gout, and DECT can visualize the therapeutic effect of allopurinol on serum uric acid levels and MSU depositions. A prospective study recruited 152 patients treated with allopurinol ≥ 300 mg/day for at least 3 months and then used DECT to assess the total number and volume of crystal deposition (40). The result showed that uric acid deposition occurred in approximately 69.1% of patients despite a mean of 5.1 years of treatment with allopurinol

300 mg/day or higher. More specifically, the presence of MSU deposition was 90% among patients with sUA ≥6.0 mg/dl and tophus and 46.9% among those with sUA <6.0 mg/dl and without obvious tophi. DECT demonstrated that the volume of the MSU crystal was greater in those with sUA ≥6.0 mg/dl, and higher crystal deposition was positively related to higher gout flares, more tophi, and worse disease activity scores in patients. In this paper, DECT detection confirmed that nearly half of the patients still had urate deposition even though the serum uric acid level had been controlled (<6.0 mg/dl), prompting us to consider whether more intensive ULTs was needed for better gout control.

Another longitudinal study of 77 patients was undertaken to assess MSU deposition depletion by DECT under the treatment of conventional ULT drugs or lifestyle (41). The first choice was allopurinol with the dose of 100 mg/day initially and gradually increased to the maximum dose of 600 mg/day if sUA was not satisfied. Participants who were intolerable to allopurinol were treated with the drug febuxostat in 80 mg/day and gradually titrated up to 120 mg/day to control the sUA level. The result showed that both the lifestyle and ULTs were useful in dissolving MSU deposits after 18 months. Urate precipitation dissipated the most in the febuxostat group, followed by the allopurinol group, and finally in the lifestyle improvement group, suggesting the better effect of febuxostat than allopurinol in MSU depletion. Moreover, it was encouraging that these data confirmed the use of lifestyle intervention on MSU decline, beyond preventing gout flares. In a word, it is necessary to observe whether urate crystals are completely relieved through DECT under long-term treatment of ULTs.

Recurrent gout attacks and chronic gout inflammation can lead to severe structural damage to the painful bones, causing great harm to patients. How to reduce bone damage in the treatment of gout is a very important and urgent issue to be addressed. A randomized controlled trial of 87 patients (dose-escalation group, n = 42, control group, n = 45) discovered a benefit of allopurinol escalation on bone damage by DECT detection (42). Patients in the dose-escalation group were initially treated with increased allopurinol to rapidly reach the targeted sUA. On the other hand, the controlled group was treated with a conventional dose of allopurinol in Year 1, followed by an increased dose of allopurinol in Year 2. The DECT data suggested that the strategy of allopurinol dose escalation prevented bone erosion compared with the control group after a 2-year treatment, although the change was small. However, the result of XR imaging did not show any differences between the two groups. These findings confirmed that gout treatment was a long-term battle. The study of structural damage in gout joints is a huge challenge, and we need advanced imaging methods such as DECT to monitor the treatment effectiveness with its better sensitivity than plain radiographs. Also, the reduction in the volume of MSU crystals was much larger compared to the small change in bone erosion, revealing a big lag between the deposition disappearance and radiographic changes. This study suggested that high levels of allopurinol might facilitate bone reconstruction in gouty joints, and other cytological studies support this concept. Allopurinol and oxypurinol drugs could promote the differentiation and development of osteoblasts and promote bone repair (43). The mean sUA level here was 0.33 mmol/l, and the results showed slight prevention of bone destruction. In contrast to the result, another research showed that serum uric acid level was undetectable under pegloticase treatment and a significant improvement in bone erosion was observed (44). Taken together, lower serum uric acid levels may be required to reverse or improve bone erosion.

Pegloticase is recommended for patients with severe intractable gout, which could cause a dramatic drop in sUA level (45). A previous study was conducted using pegloticase in 10 patients by DECT. The data demonstrated that both sUA levels and tophi were very sensitive to pegloticase, with 71.4% of tophi disappearing after a few weeks, especially in the joints, while tendon tophi were broken down more slowly (45). Similar results were found in another paper. In a patient with refractory gout, 6 months of treatment of pegloticase resulted in a significant reduction in tophi. At the same time, compared with physical measurement and US detection, DECT reflected changes in urate volume better (46). To sum up, DECT is a remarkable imaging means for a comprehensive assessment of MSU burden and longitudinal monitoring of the response to ULTs. Moreover, the state of being tophi-free can be measurable and perceptible by DECT, even for those refractory gouty patients when the right medicine is used.

In addition to ULTs, anti-inflammatory treatment should be administered at the same time, which is very beneficial for gout management. Both soft tissues and urate crystals in tophi are closely related to bone damage. Cytological studies have found that soft tissues surrounding tophi mainly contain immune cells, chemokines, cytokines, and osteoclasts, forming such a chronic inflammatory microenvironment (47, 48). Among them, mononuclear macrophages play a major role in promoting the growth and development of osteoclasts by secreting COX-2, PGE2, IL-1β, and TNF (49). Meanwhile, osteoblasts, which play a role in bone remodeling and bone repair, are significantly inhibited in their activity, function, and morphology by MSU crystals (50). A study led by conventional CT, DECT, and XR techniques showed that urate crystals and soft tissue composition of tophi were directly associated with bone destruction scores, a significant reduction in soft tissue inflammation was associated with improved bone destruction after ULTs (51). These data further intuitively confirmed the role of inflammatory soft tissues in the progression of gout disease, reflecting the value of ULTs in combination with anti-inflammatory drugs or the latest biological agent intervention. Moreover, imaging is of great value in monitoring these therapeutic effects.

US

The MSU load was identified by the OMERACT working group as one of the therapeutic targets in gout management (52), and the reduction in urate deposition can also be demonstrated by US imaging, which mainly includes four features of gout lesions. In a related study, 79 patients were treated with ULTs and underwent US monitoring of MSU deposition over a 6-month period (53).

The results showed that DCs and tophus features on US were significantly reduced during treatment. Among them, the DCs could be an early marker with an obvious change after 3 months of treatment, while tophi changed more significantly after 6 months of treatment. In line with other studies (54, 55), the reduction in urate deposition was associated with low sUA levels and was more pronounced in the group with lower serum sUA (<5 mg/dl), suggesting that lower levels of sUA were one of the effective therapeutic targets and consistent with last EULAR recommendations (7). Similarly, several other research also showed that the DCs, tophi, and aggregates decreased obviously measured by US under ULTs (55–57).

The concept of treat-to-target (T2T) is well established in many chronic diseases, including rheumatism, and the first T2T recommendations for gout were put forward by EULAR in 2016, ushering in a new era of targeted treatment for gout (7). One of the first principles is to keep the patient's serum levels below the target level throughout the whole life to eliminate urate crystal deposition. This strategy also provided some remission criteria for gout patients, but there were some limitations. For example, the proposals do not provide substantive recommendations on clinical practical issues such as the optimal target value of blood uric acid and imaging criteria for remission.

In 2020, one of the largest US studies revealed the imaging changes with a T2T approach. The study manifested an apparent crystal dissolution in 209 gout patients by adopting a T2T way in ULTs (58). The DCs were found to be the most sensitive and earliest variable marker, which was consistent with the results of other paper (53). At 12 months, nearly half of the patients had no DCs here. A reasonable explanation for the early disappearance of DCs may be that MSU deposits are in close contact with cartilage and joint fluid. During the progress of ULTs, serum uric acid levels fall rapidly, causing the reduction of the uric acid levels in joint fluid to equilibrate them with blood concentrations. They also found that MTP1 joints were the most common site of MSU depositions, and the erosion in MTP1 was highly related to the three other sonographic findings. Meanwhile, US results indicated that about 1/6 of the participants had DCs on proximal talar cartilage and distal femur and had tophi in distal patellar tendon and triceps, showing that these sites also were involved in the development of gout. This US study provided an important result that gouty patients who followed a T2T approach in ULTs in clinical practice significantly reduced the MSU crystal burden.

Another study also used OMERACT defined US gout lesions to assess MSU changes after ULTs. The study examined a number of sites in each patient, including 28 joints and 26 tendons, to better understand urate depositions (59). The results showed that MTP1 was the most prone to MSU deposition, followed by MTP2-4s and the knee joint. Importantly, they found that the most easily affected by MSU crystals were also the site of the best treatment response. Detection of so many locations by US was time-consuming, but it was meaningful to determine which sites were significant in gout diagnosis and treatment monitoring. Here, the mutual involvement and rapidly effective responsiveness to ULTs in MTP1–3s and knee joints display the possible essential of choosing these positions. Consistent with the results mentioned above, the authors also found that the changes of DCs were most sensitive, with a significant reduction even in the first 3 months of treatment. More interestingly, the study also observed obvious improvement in inflammation response through US imaging and biological markers. The results indicated that the synovitis and tenosynovitis were significantly improved; the inflammatory molecule CRP was dramatically decreased.

To date, there were still no clear criteria for which locations and at least how many areas are needed for more accurate gout diagnosis and treatment monitoring. Different groups chose different sites for imaging measures of MSU deposits. One of the groups identified the bilateral evaluation of the radiocarpal joint, two tendons (patellar tendon and triceps tendon) for aggregates, and three articular cartilages (including MTP1, second metacarpal, and talar) for DCs, having a satisfying sensitivity and specificity in gout diagnosis (60). Another group reported that the scanning of two knees and two MTP1 for DCs and aggregates was sufficient (61).

MRI

A 2-year study enrolling 314 individuals revealed the protective effects of febuxostat on the joints of patients with early gout (62). This was the first randomized controlled trial of ULTs in early gout patients to use imaging to assess the damage within the gouty joints. At baseline, there was little evidence of joint erosion, and after 2 years of observation, there were no significant changes in joint erosion or joint space narrowing in either the experimental or the control group of patients. This suggested that damage to joint structures may be a manifestation of advanced gout. Importantly, the presence of synovitis was initially detected by MRI in most subjects, and after 2 years, patients in the febuxostat group had significantly better RAMRI synovitis scores and significantly fewer acute gout attacks compared to the placebo group. The clinical significance of synovitis in gouty patients is unclear, and whether synovitis is a risk factor for gout flares or joint damage has yet to be investigated. The results of this study showed that febuxostat improved intra-articular synovitis and also reduced the frequency of acute gout flares, providing some indication of the role of synovitis in disease progression. Febuxostat not only reduced serum uric acid levels but also had a better therapeutic effect on early gouty synovitis, suggesting the need for early treatment of gout.

Uric acid deposits in the knee joint lead to restricted knee movement and can seriously affect the patient's daily life. A study has shown that ULTs can significantly reduce gout tophi deposits in the knee joint (63). The study used MRI to assess the size of gout tophi within the patient's knee joint and vernier calipers to measure the size of subcutaneous gout tophi throughout the body and continued to assess intra-articular and subcutaneous gout nodules under 18 months of ULTs. The results showed a significant improvement in knee mobility after ULTs, which also correlated positively with a reduction in intra-articular tophi. Further analysis revealed that increased knee mobility was also significantly associated with a reduction in subcutaneous tophi. Combining these data, and taking into account the relatively expensive nature of MRI, we were able to

use subcutaneous tophus nodules to assess the dissipation of gout tophi within the knee joint in order to predict and monitor improvements in knee mobility. Knee gaps were still present within the knee joint in the patients included in this study, suggesting that aggressive application with ULTs prior to irreversible knee destruction could significantly improve knee motion and avoid permanent joint damage.

In conclusion, imaging methods are well managed and monitored at all stages of gout disease progression (**Table 1**).

GOUT COMPLICATIONS

Severe gout is often accompanied by various complications, such as diabetes, obesity, cardiovascular disease, and kidney disease, especially in terms of damage to the heart and kidney organs (2).

Currently, there were many studies on the relationship between gout and coronary heart disease. It has been suggested that gout can significantly increase the incidence of coronary heart disease (64). In acute coronary syndromes, high sUA levels have been found to significantly increase the risk of coronary heart disease (65). Moreover, there were also some contradictory conclusions: one study showed no significant association between gout and myocardial infarction (66), and another suggested that urate deposition burden on knees and feet in gouty patients did not increase the risk of cardiovascular events (67). However, none of these directly indicated the cardiovascular system with gout involvement. A recent study of 59 gouty patients and 47 controls visually illustrated the MSU

TABLE 1 | The role of imaging in monitoring treatment in the different stages of gout.

Stages	Imaging modality	Management or treatment of gout		Outcome	Scanned sites	Follow-up visit	Ref.
		Experimental group	Control group				
Hyperuricemia	US	16 patients (hyperuricemia and persistent foot pain) with 80 mg/day febuxostat	15 individuals with AH	Sustaining foot pain and DCs positive patients had obviously lower pain scores under ULTs	MTP1	M1, M3	(21)
Gout flares	DECT	62 gouty patients under allopurinol/febuxostat	–	Every 1-cm^3 increase in MSU volume in feet, the risk of gout attacks increased 2.03-fold	Feet	M3, M6, M12	(30)
	US	79 individuals with a 6-month ULT and gout prophylaxis	79 individuals with continuous 6-month ULTs and stopped prophylaxis	The low rate of gout relapse was found in patients with a greater than 50% reduction in tophi volume, s	MTP1, knees	M6, M12	(31)
Chronic gout	DECT	152 patients with allopurinol ≥ 300 mg/day for a mean of 5.1 years	–	The volume of MSU crystal was greater in those with sUA ≥ 6.0 mg/dl and tophi	Hands/wrists feet/knees	Day 1 Day 28	(36)
	DECT	77 gouty patients with lifestyle improvement or allopurinol or febuxostat	–	Urate precipitation dissipated the most in the febuxostat group, followed by allopurinol group, and finally in the lifestyle improvement group	MTP1, toes Feet/ankle Soft tissues	M18	(37)
	DECT	42 patients with dose escalation of allopurinol during 2 years	45 patients with no change dose of allopurinol at Year 1 and dose escalation in Year 2	Higher levels of allopurinol benefits bone reconstruction in gout joints	Feet	Year 1, Year 2	(38)
	DECT	10 refractory gouty patients under 8 mg/day pegloticase intravenously every 2 weeks	–	sUA levels and tophi were both sensitive to pegloticase, 71.4% of tophi disappeared	Hands/wrists feet/ankles	Mean of 13.3 weeks	(41)
	DECT	A patient with refractory gout with a 6-month pegloticase	–	A significant reduction in tophi	Hands and feet	M6	(42)
	US	79 gouty patients under allopurinol/febuxostat	–	DCs and tophi features were significantly reduced	Knees and MTP1s	M3, M6	(49)
	US	209 gouty patients under allopurinol/febuxostat	–	The T2T under ULTs can reduce all MSU depositions, especially for DC	Hands/wrists feet/knees	M3, M6, M12	(54)
	US	50 gouty patients with allopurinol/benzbromarone/ febuxostat	–	A significant deduction of DC, tophus and aggregate sum scores	28 joints and 26 tendons	M3, M6	(55)
	MRI	157 early stage gouty patients with febuxostat	157 early-stage gouty patients with placebo	Patients on febuxostat had better RAMRI synovitis scores and significantly fewer acute gout attacks	Hands and feet	M6, M12 M18, M24	(58)
	MRI	26 patients with tophaceous gout and limited knee motion	–	A significant improvement in knee mobility and a reduction in intra-articular tophi	Knees and all subcutaneous nodules	M18	(59)

deposits on the coronary artery by DECT. The results showed that patients with gout had more MSU deposits on coronary arteries and were also found to have more coronary calcification (68). Urate deposits in this study were confirmed by polarizing microscopy, rather than the so-called artifacts seen in other studies.

For the renal manifestations of gout, both US and DECT can detect MSU deposition in the renal medulla of patients with severe gout (69). The former one was characterized by strong echogenicity in the renal medulla accompanied by a posterior acoustic shadow, while the latter could analyze the composition of deposits. US is commonly used to detect urolithiasis in gout, but also its usefulness in gouty nephropathy, especially its cheapness and ease to be used compared to DECT.

A large cross-sectional study also confirmed the role of US in detecting the changes in the kidney induced by gout. They found that 36% of 502 untreated gouty patients showed hyperechoic uric acid crystal deposits in the renal medulla by US, while none was observed in the 515 controls (70). Multivariate analysis found that hyperechoic patterns in the medulla were associated with gout arthritis, DC thickness, disease duration, and reduced glomerular filtration rate. These findings provided a basis for gout-induced microcrystalline nephropathy and also provided a new therapeutic target for gout.

In addition, MSU can be deposited in some unusual areas such as the ribs, spine, wrists, and lower extremity enthesopathy, causing pain to the patient. Many recent reports in the literature have found evidence of gout involvement in the spine of patients by means of DECT and MRI, as a means of identifying the cause of their pain and also allowing assessment of the efficacy of ULTs on MSU deposits in the spine and reducing unnecessary surgery (71–73). It was noted that MRI showed that some gouty patients already had significant synovitis and bone erosion at the time of the first acute gout attack, suggesting that damage to the involved joints had already occurred during the subclinical period of gout (74). Our previous study showed that the lower-extremity enthesopathy was also a location that could accumulate in gouty patients but was often overlooked, and we found that the patellar ligament, quadriceps femoris tendon, and quadriceps patellar insertion site were very likely to be deposited by MSU. Moreover, Doppler flow signals indicated acute inflammation of the quadriceps tendon (75) (**Figure 1**). The management and monitoring of gout complications are an important part of gout treatment; by using modern and advanced imaging methods, we can clearly know MSU depositions so as to better understand disease development and dynamic manifestations.

IMAGING LIMITATIONS AND CHALLENGES

Overall, imaging methods play an important role in the treatment and management of gout, but there are some limitations. Artifact is common in DECT, especially in nail beds, nose, skin, and peroneal tendons, leading to false-positive results (76, 77). A study displayed that compared to the parameter of 130 HU, adding a tin filter and setting a minimum attenuation of 150 HU could effectively reduce artifacts (78). In addition, DECT cannot effectively evaluate the internal structure of the joint including cartilage, ligament, tendon, and synovial membrane. Compared to US, DECT and MRI are relatively expensive. Moreover, the machine is not easy to move, which has limitations for patients with acute attacks. US is cheaper and more convenient than DECT or MRI. However, unlike DECT, urate deposition volume on US cannot be calculated automatically. The evaluation of crystal volume by US is related to the experience and ability of the readers. In addition, there is a large heterogeneity in the ultrasound instruments and probes used, which might affect the consistency and accuracy of image results. When we use DECT and US imaging methods to monitor the dispersion of crystal deposition under ULTs, we must take into account that DECT only shows the MSU crystal itself, whereas US fully shows the entire tophus volume, including the inflammatory tissues around the crystals, as confirmed by some histological analysis (39, 79). Therefore, the evaluation of DECT for tophi is usually smaller than US. At the same time, we should also note that the tophi often attach to the surface of the joint and the measurement of depth by US is affected by acoustic shadow, leading to the overestimation of its volume by US. On the other hand, compared to US, MRI has better visualization of deep structures and can image multiple planes for a single part, which shows disease pathology in depth.

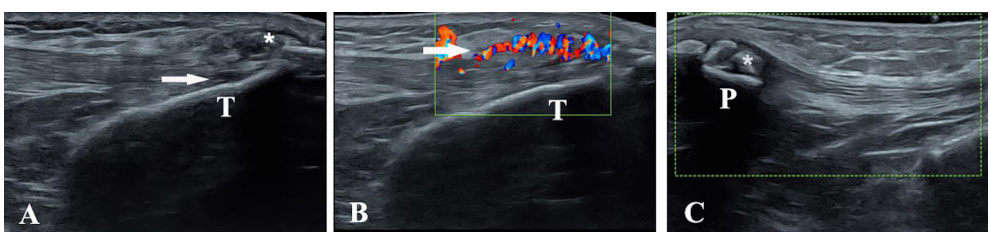

FIGURE 1 | Ultrasound evaluation in gouty patients. Longitudinal scans of the patellar ligament and the quadriceps tendon in B-mode and power Doppler ultrasound. **(A)** The asterisk shows the tophus of the patella ligament. **(B)** Doppler flow signals indicate acute inflammation of quadriceps tendon. **(C)** The asterisk shows the tophus of the quadriceps tendon.

IMAGING SCORING SYSTEMS

These advanced imaging have a certain role in evaluating the effect of ULTs, but the current studies are scattered and independent, making it difficult to combine all imaging findings. We need a suitable scoring system with good reproducibility and sensitivity to obtain standardized results. Currently, available US studies use either a binary scoring system or a semiquantitative scoring system. A binary scoring system means that a patient is defined as 1 if they have one of the US features (DCs, tophus, aggregates, or bone erosion) and 0 if they do not (59). A semiquantitative score is defined in terms of the degree to which the US features are present: 0 = none, 1 = a little, 2 = sure, and 3 = large (58). Both scoring systems were found to be sensitive to changes during treatment. However, it should be noted that both scoring methods may overlook minor lesions during follow-up.

Two related studies referred to a scoring system for DECT imaging (41, 80) and proved to be sensitive and effective. The DECT scoring system mainly consists of 4 regions: 1) MTP1 joints; 2) toes; 3) midfoot and ankle joints; and 4) soft tissues (tendons). Results were scored based on the maximum amount of MSU depositions at each site, each scored from 0 to 3 (0 = none, 1 = little dots, 2 = deposit >2 mm, 3 = fused depositions). Moreover, the ultimate score was obtained by adding the scores of the four areas, with a maximum score of 12. The inter-reader correlation coefficient (95% confidence interval) for the DECT MSU deposit score was 0.98 (0.97–0.98). This method could be used to detect the most affected areas of the crystal, and the results were highly consistent with the full-scan results and required significantly less time. Not only is it effective in distinguishing people with and without gout, but also it clearly identifies whether they are responsive to ULTs.

More research is needed to validate the above method, and in the meantime, future research should try to explore whether a more sensitive and accurate scoring system can be found.

CONCLUSIONS

Advanced imaging technologies allow us to visualize the pathological process of tissue destruction in gout, providing a new way to explore the disease *in vivo*. The use of US, DECT, and MRI is beneficial for earlier gout diagnosis and monitor of patients' response to ULTs and anti-inflammatory drug treatment. The combination of clinical manifestations, laboratory indicators, and imaging techniques can improve the understanding and adherence to treatments of gouty patients, improve their prognosis, reduce complications, and improve their quality of life. At the same time, we need to consider the challenges and limitations of using these imaging technologies. We need a better scoring system and the ultimate location of image examination to explore the optimal serum urate acid levels and the best monitoring methods for gout management.

AUTHOR CONTRIBUTIONS

SL and HC conceived of the study and its design and drafted the manuscript. GX and LW provided the gouty pictures. JYL, HC, and JL participated in its coordination and modification. All authors contributed to the article and approved the submitted version.

REFERENCES

1. Chen-Xu M, Yokose C, Rai SK, Pillinger MH, Choi HK. Contemporary Prevalence of Gout and Hyperuricemia in the United States and Decadal Trends: The National Health and Nutrition Examination Survey, 2007-2016. *Arthritis Rheumatol* (2019) 71(6):991–9. doi: 10.1002/art.40807
2. Dehlin M, Jacobsson L, Roddy E. Global Epidemiology of Gout: Prevalence, Incidence, Treatment Patterns and Risk Factors. *Nat Rev Rheumatol* (2020) 16(7):380–90. doi: 10.1038/s41584-020-0441-1
3. Choi HK, Ford ES, Li C, Curhan G. Prevalence of the Metabolic Syndrome in Patients With Gout: The Third National Health and Nutrition Examination Survey. *Arthritis Rheum* (2007) 57(1):109–15. doi: 10.1002/art.22466
4. Levin MH, Lichtenstein L, Scott HW. Pathologic Changes in Gout; Survey of Eleven Necropsied Cases. *Am J Pathol* (1956) 32(5):871–95.
5. Dalbeth N, Clark B, Gregory K, Gamble G, Sheehan T, Doyle A, et al. Mechanisms of Bone Erosion in Gout: A Quantitative Analysis Using Plain Radiography and Computed Tomography. *Ann Rheum Dis* (2009) 68 (8):1290–5. doi: 10.1136/ard.2008.094201
6. Schumacher HR. Pathology of the Synovial Membrane in Gout. Light and Electron Microscopic Studies. Interpretation of Crystals in Electron Micrographs. *Arthritis Rheum* (1975) 18(6 Suppl):771–82. doi: 10.1002/art.1780180722
7. Richette P, Doherty M, Pascual E, Barskova V, Becce F, Castaneda-Sanabria J, et al. 2016 Updated EULAR Evidence-Based Recommendations for the Management of Gout. *Ann Rheum Dis* (2017) 76(1):29–42. doi: 10.1136/annrheumdis-2016-209707
8. FitzGerald JD, Dalbeth N, Mikuls T, Brignardello-Petersen R, Guyatt G, Abeles AM, et al. 2020 American College of Rheumatology Guideline for the Management of Gout. *Arthritis Care Res (Hoboken)* (2020) 72(6):744–60. doi: 10.1002/acr.24180
9. Mandel NS, Mandel GS. Monosodium Urate Monohydrate, the Gout Culprit. *J Am Chem Soc* (1976) 98(8):2319–23. doi: 10.1021/ja00424a054
10. Ogdie A, Taylor WJ, Neogi T, Fransen J, Jansen TL, Schumacher HR, et al. Performance of Ultrasound in the Diagnosis of Gout in a Multicenter Study: Comparison With Monosodium Urate Monohydrate Crystal Analysis as the Gold Standard. *Arthritis Rheumatol* (2017) 69(2):429–38. doi: 10.1002/art.39959
11. Bongartz T, Glazebrook KN, Kavros SJ, Murthy NS, Merry SP, Franz WB3rd, et al. Dual-Energy CT for the Diagnosis of Gout: An Accuracy and Diagnostic Yield Study. *Ann Rheum Dis* (2015) 74(6):1072–7. doi: 10.1136/annrheumdis-2013-205095
12. Neogi T, Jansen TL, Dalbeth N, Fransen J, Schumacher HR, Berendsen D, et al. 2015 Gout Classification Criteria: An American College of Rheumatology/European League Against Rheumatism Collaborative Initiative. *Arthritis Rheumatol* (2015) 67(10):2557–68. doi: 10.1002/art.39254
13. Gutierrez M, Schmidt WA, Thiele RG, Keen HI, Kaeley GS, Naredo E, et al. International Consensus for Ultrasound Lesions in Gout: Results of Delphi Process and Web-Reliability Exercise. *Rheumatology (Oxford)* (2015) 54 (10):1797–805. doi: 10.1093/rheumatology/kev112
14. Choi HK, Al-Arfaj AM, Eftekhari A, Munk PL, Shojania K, Reid G, et al. Dual Energy Computed Tomography in Tophaceous Gout. *Ann Rheum Dis* (2009) 68(10):1609–12. doi: 10.1136/ard.2008.099713

15. Annemans L, Spaepen E, Gaskin M, Bonnemaire M, Malier V, Gilbert T, et al. Gout in the UK and Germany: Prevalence, Comorbidities and Management in General Practice 2000-2005. *Ann Rheum Dis* (2008) 67(7):960–6. doi: 10.1136/ard.2007.076232
16. Ostergaard M, Peterfy C, Conaghan P, McQueen F, Bird P, Ejbjerg B, et al. OMERACT Rheumatoid Arthritis Magnetic Resonance Imaging Studies. Core Set of MRI Acquisitions, Joint Pathology Definitions, and the OMERACT RA-MRI Scoring System. *J Rheumatol* (2003) 30(6):1385–6.
17. Campion EW, Glynn RJ, DeLabry LO. Asymptomatic Hyperuricemia. Risks and Consequences in the Normative Aging Study. *Am J Med* (1987) 82 (3):421–6. doi: 10.1016/0002-9343(87)90441-4
18. De Miguel E, Puig JG, Castillo C, Peiteado D, Torres RJ, Martin-Mola E. Diagnosis of Gout in Patients With Asymptomatic Hyperuricaemia: A Pilot Ultrasound Study. *Ann Rheum Dis* (2012) 71(1):157–8. doi: 10.1136/ard.2011.154997
19. Stewart S, Maxwell H, Dalbeth N. Prevalence and Discrimination of OMERACT-Defined Elementary Ultrasound Lesions of Gout in People With Asymptomatic Hyperuricaemia: A Systematic Review and Meta-Analysis. *Semin Arthritis Rheum* (2019) 49(1):62–73. doi: 10.1016/j.semarthrit.2019.01.004
20. Dalbeth N, House ME, Aati O, Tan P, Franklin C, Horne A, et al. Urate Crystal Deposition in Asymptomatic Hyperuricaemia and Symptomatic Gout: A Dual Energy CT Study. *Ann Rheum Dis* (2015) 74(5):908–11. doi: 10.1136/annrheumdis-2014-206397
21. Wang P, Smith SE, Garg R, Lu F, Wohlfahrt A, Campos A, et al. Identification of Monosodium Urate Crystal Deposits in Patients With Asymptomatic Hyperuricemia Using Dual-Energy CT. *RMD Open* (2018) 4(1):e000593. doi: 10.1136/rmdopen-2017-000593
22. Alammari YM, Gheta D, Flood RM, Boran G, Kane DJ, Mullan RH. Urate-Lowering Therapy (ULT) Reduces non-Episodic Foot Pain in Patients Who Fail to Meet ACR/EULAR 2015 Gout Classification Criteria: An Effect Predicted by Ultrasound and Potential Rationale for Reclassification. *Ann Rheum Dis* (2019) 78(4):579–80. doi: 10.1136/annrheumdis-2018-214305
23. Latourte A, Bardin T, Richette P. Prophylaxis for Acute Gout Flares After Initiation of Urate-Lowering Therapy. *Rheumatology (Oxford)* (2014) 53 (11):1920–6. doi: 10.1093/rheumatology/keu157
24. Stamp L, Morillon MB, Taylor WJ, Dalbeth N, Singh JA, Lassere M, et al. Serum Urate as Surrogate Endpoint for Flares in People With Gout: A Systematic Review and Meta-Regression Analysis. *Semin Arthritis Rheum* (2018) 48(2):293–301. doi: 10.1016/j.semarthrit.2018.02.009
25. Qaseem A, Harris RP, Forciea MAClinical Guidelines Committee of the American College of Physicians, , Denberg TD, Barry MJ, et al. Management of Acute and Recurrent Gout: A Clinical Practice Guideline From the American College of Physicians. *Ann Intern Med* (2017) 166(1):58–68. doi: 10.7326/M16-0570
26. Dalbeth N, Bardin T, Doherty M, Liote F, Richette P, Saag KG, et al. Discordant American College of Physicians and International Rheumatology Guidelines for Gout Management: Consensus Statement of the Gout, Hyperuricemia and Crystal-Associated Disease Network (G-CAN). *Nat Rev Rheumatol* (2017) 13(9):561–8. doi: 10.1038/nrrheum.2017.126
27. Kuehn BM. Chronic Disease Approaches Needed to Curb Gout's Growing Burden. *JAMA* (2018) 319(13):1307–9. doi: 10.1001/jama.2018.0547
28. Schumacher HRJr., Becker MA, Wortmann RL, Macdonald PA, Hunt B, Streit J, et al. Effects of Febuxostat Versus Allopurinol and Placebo in Reducing Serum Urate in Subjects With Hyperuricemia and Gout: A 28-Week, Phase III, Randomized, Double-Blind, Parallel-Group Trial. *Arthritis Rheum* (2008) 59(11):1540–8. doi: 10.1002/art.24209
29. Becker MA, Schumacher HR, Espinoza LR, Wells AF, MacDonald P, Lloyd E, et al. The Urate-Lowering Efficacy and Safety of Febuxostat in the Treatment of the Hyperuricemia of Gout: The CONFIRMS Trial. *Arthritis Res Ther* (2010) 12(2):R63. doi: 10.1186/ar2978
30. Becker MA, Schumacher HRJr., Wortmann RL, MacDonald PA, Eustace D, Palo WA, et al. Febuxostat Compared With Allopurinol in Patients With Hyperuricemia and Gout. *N Engl J Med* (2005) 353(23):2450–61. doi: 10.1056/NEJMoa050373
31. Pascart T, Grandjean A, Capon B, Legrand J, Namane N, Ducoulombier V, et al. Monosodium Urate Burden Assessed With Dual-Energy Computed Tomography Predicts the Risk of Flares in Gout: A 12-Month Observational Study : MSU Burden and Risk of Gout Flare. *Arthritis Res Ther* (2018) 20 (1):210. doi: 10.1186/s13075-018-1714-9
32. Ebstein E, Forien M, Norkuviene E, Richette P, Mouterde G, Daien C, et al. UltraSound Evaluation in Follow-Up of Urate-Lowering Therapy in Gout Phase 2 (USEFUL-2): Duration of Flare Prophylaxis. *Joint Bone Spine* (2020) 87(6):647–51. doi: 10.1016/j.jbspin.2020.09.014
33. Schlesinger N. Treatment of Chronic Gouty Arthritis: It is Not Just About Urate-Lowering Therapy. *Semin Arthritis Rheum* (2012) 42(2):155–65. doi: 10.1016/j.semarthrit.2012.03.010
34. Sarawate CA, Patel PA, Schumacher HR, Yang W, Brewer KK, Bakst AW. Serum Urate Levels and Gout Flares: Analysis From Managed Care Data. *J Clin Rheumatol* (2006) 12(2):61–5. doi: 10.1097/01.rhu.0000209882.50228.9f
35. Schueller-Weidekamm C, Schueller G, Aringer M, Weber M, Kainberger F. Impact of Sonography in Gouty Arthritis: Comparison With Conventional Radiography, Clinical Examination, and Laboratory Findings. *Eur J Radiol* (2007) 62(3):437–43. doi: 10.1016/j.ejrad.2006.12.005
36. Wang Q, Guo LH, Li XL, Zhao CK, Li MX, Wang L, et al. Differentiating the Acute Phase of Gout From the Intercritical Phase With Ultrasound and Quantitative Shear Wave Elastography. *Eur Radiol* (2018) 28(12):5316–27. doi: 10.1007/s00330-018-5529-5
37. Peiteado D, Villalba A, Martin-Mola E, de Miguel E. Reduction But Not Disappearance of Doppler Signal After Two Years of Treatment for Gout. Do We Need a More Intensive Treatment? *Clin Exp Rheumatol* (2015) 33(3):385–90.
38. Rajan A, Aati O, Kalluru R, Gamble GD, Horne A, Doyle AJ, et al. Lack of Change in Urate Deposition by Dual-Energy Computed Tomography Among Clinically Stable Patients With Long-Standing Tophaceous Gout: A Prospective Longitudinal Study. *Arthritis Res Ther* (2013) 15(5):R160. doi: 10.1186/ar4343
39. Dalbeth N, Aati O, Gao A, House M, Liu Q, Horne A, et al. Assessment of Tophus Size: A Comparison Between Physical Measurement Methods and Dual-Energy Computed Tomography Scanning. *J Clin Rheumatol* (2012) 18 (1):23–7. doi: 10.1097/RHU.0b013e31823e5cda
40. Dalbeth N, Nicolaou S, Baumgartner S, Hu J, Fung M, Choi HK. Presence of Monosodium Urate Crystal Deposition by Dual-Energy CT in Patients With Gout Treated With Allopurinol. *Ann Rheum Dis* (2018) 77(3):364–70. doi: 10.1136/annrheumdis-2017-212046
41. Ellmann H, Bayat S, Araujo E, Manger B, Kleyer A, Cavallaro A, et al. Effects of Conventional Uric Acid-Lowering Therapy on Monosodium Urate Crystal Deposits. *Arthritis Rheumatol* (2020) 72(1):150–6. doi: 10.1002/art.41063
42. Dalbeth N, Billington K, Doyle A, Frampton C, Tan P, Aati O, et al. Effects of Allopurinol Dose Escalation on Bone Erosion and Urate Volume in Gout: A Dual-Energy Computed Tomography Imaging Study Within a Randomized, Controlled Trial. *Arthritis Rheumatol* (2019) 71(10):1739–46. doi: 10.1002/art.40929
43. Orriss IR, Arnett TR, George J, Witham MD. Allopurinol and Oxypurinol Promote Osteoblast Differentiation and Increase Bone Formation. *Exp Cell Res* (2016) 342(2):166–74. doi: 10.1016/j.yexcr.2016.03.004
44. Dalbeth N, Doyle AJ, McQueen FM, Sundy J, Baraf HS. Exploratory Study of Radiographic Change in Patients With Tophaceous Gout Treated With Intensive Urate-Lowering Therapy. *Arthritis Care Res (Hoboken)* (2014) 66 (1):82–5. doi: 10.1002/acr.22059
45. Araujo EG, Bayat S, Petsch C, Englbrecht M, Faustini F, Kleyer A, et al. Tophus Resolution With Pegloticase: A Prospective Dual-Energy CT Study. *RMD Open* (2015) 1(1):e000075. doi: 10.1136/rmdopen-2015-000075
46. Modjinou DV, Krasnokutsky S, Gyftopoulos S, Pike VC, Karis E, Keenan RT, et al. Comparison of Dual-Energy CT, Ultrasound and Surface Measurement for Assessing Tophus Dissolution During Rapid Urate Debulking. *Clin Rheumatol* (2017) 36(9):2101–7. doi: 10.1007/s10067-017-3729-z
47. McQueen FM, Chhana A, Dalbeth N. Mechanisms of Joint Damage in Gout: Evidence From Cellular and Imaging Studies. *Nat Rev Rheumatol* (2012) 8 (3):173–81. doi: 10.1038/nrrheum.2011.207
48. Dalbeth N, Pool B, Gamble GD, Smith T, Callon KE, McQueen FM, et al. Cellular Characterization of the Gouty Tophus: A Quantitative Analysis. *Arthritis Rheum* (2010) 62(5):1549–56. doi: 10.1002/art.27356
49. Kim JH, Jin HM, Kim K, Song I, Youn BU, Matsuo K, et al. The Mechanism of Osteoclast Differentiation Induced by IL-1. *J Immunol* (2009) 183(3):1862–70. doi: 10.4049/jimmunol.0803007

50. Chhana A, Callon KE, Pool B, Naot D, Watson M, Gamble GD, et al. Monosodium Urate Monohydrate Crystals Inhibit Osteoblast Viability and Function: Implications for Development of Bone Erosion in Gout. *Ann Rheum Dis* (2011) 70(9):1684–91. doi: 10.1136/ard.2010.144774
51. Sapsford M, Gamble GD, Aati O, Knight J, Horne A, Doyle AJ, et al. Relationship of Bone Erosion With the Urate and Soft Tissue Components of the Tophus in Gout: A Dual Energy Computed Tomography Study. *Rheumatology (Oxford)* (2017) 56(1):129–33. doi: 10.1093/rheumatology/kew383
52. Schumacher HR, Taylor W, Edwards L, Grainger R, Schlesinger N, Dalbeth N, et al. Outcome Domains for Studies of Acute and Chronic Gout. *J Rheumatol* (2009) 36(10):2342–5. doi: 10.3899/jrheum.090370
53. Ebstein E, Forien M, Norkuviene E, Richette P, Mouterde G, Daien C, et al. Ultrasound Evaluation in Follow-Up of Urate-Lowering Therapy in Gout: The USEFUL Study. *Rheumatology (Oxford)* (2019) 58(3):410–7. doi: 10.1093/rheumatology/key303
54. Perez-Ruiz F, Martin I, Canteli B. Ultrasonographic Measurement of Tophi as an Outcome Measure for Chronic Gout. *J Rheumatol* (2007) 34(9):1888–93.
55. Peiteado D, Villalba A, Martin-Mola E, Balsa A, De Miguel E. Ultrasound Sensitivity to Changes in Gout: A Longitudinal Study After Two Years of Treatment. *Clin Exp Rheumatol* (2017) 35(5):746–51.
56. Ottaviani S, Gill G, Aubrun A, Palazzo E, Meyer O, Dieude P. Ultrasound in Gout: A Useful Tool for Following Urate-Lowering Therapy. *Joint Bone Spine* (2015) 82(1):42–4. doi: 10.1016/j.jbspin.2014.03.011
57. Das S, Goswami RP, Ghosh A, Ghosh P, Lahiri D, Basu K. Temporal Evolution of Urate Crystal Deposition Over Articular Cartilage After Successful Urate-Lowering Therapy in Patients With Gout: An Ultrasonographic Perspective. *Mod Rheumatol* (2017) 27(3):518–23. doi: 10.1080/14397595.2016.1214229
58. Hammer HB, Karoliussen L, Terslev L, Haavardsholm EA, Kvien TK, Uhlig T. Ultrasound Shows Rapid Reduction of Crystal Depositions During a Treat-to-Target Approach in Gout Patients: 12-Month Results From the NOR-Gout Study. *Ann Rheum Dis* (2020) 79(11):1500–5. doi: 10.1136/annrheumdis-2020-217392
59. Christiansen SN, Ostergaard M, Slot O, Keen H, Bruyn GAW, D'Agostino MA, et al. Assessing the Sensitivity to Change of the OMERACT Ultrasound Structural Gout Lesions During Urate-Lowering Therapy. *RMD Open* (2020) 6(1):e001144. doi: 10.1136/rmdopen-2019-001144
60. Naredo E, Uson J, Jimenez-Palop M, Martinez A, Vicente E, Brito E, et al. Ultrasound-Detected Musculoskeletal Urate Crystal Deposition: Which Joints and What Findings Should be Assessed for Diagnosing Gout? *Ann Rheum Dis* (2014) 73(8):1522–8. doi: 10.1136/annrheumdis-2013-203487
61. Peiteado D, De Miguel E, Villalba A, Ordonez MC, Castillo C, Martin-Mola E. Value of a Short Four-Joint Ultrasound Test for Gout Diagnosis: A Pilot Study. *Clin Exp Rheumatol* (2012) 30(6):830–7.
62. Dalbeth N, Saag KG, Palmer WE, Choi HK, Hunt B, MacDonald PA, et al. Effects of Febuxostat in Early Gout: A Randomized, Double-Blind, Placebo-Controlled Study. *Arthritis Rheumatol* (2017) 69(12):2386–95. doi: 10.1002/art.40233
63. Lu CC, Wei JC, Chang CA, Chen CM, Tsai SW, Yeh CJ. Limited Knee-Joint Range of Motion in Patients With Tophaceous Gout Improved With Medical Treatment: A 18-Months Follow Up. *Front Med (Lausanne)* (2020) 7:74. doi: 10.3389/fmed.2020.00074
64. Disveld IJM, Fransen J, Rongen GA, Kienhorst LBE, Zoakman S, Janssens H, et al. Crystal-Proven Gout and Characteristic Gout Severity Factors Are Associated With Cardiovascular Disease. *J Rheumatol* (2018) 45(6):858–63. doi: 10.3899/jrheum.170555
65. Song SH, Kwak IS, Kim YJ, Kim SJ, Lee SB, Lee DW, et al. Can Gamma-Glutamyltransferase be an Additional Marker of Arterial Stiffness? *Circ J* (2007) 71(11):1715–20. doi: 10.1253/circj.71.1715
66. Abbott RD, Brand FN, Kannel WB, Castelli WP. Gout and Coronary Heart Disease: The Framingham Study. *J Clin Epidemiol* (1988) 41(3):237–42. doi: 10.1016/0895-4356(88)90127-8
67. Pascart T, Capon B, Grandjean A, Legrand J, Namane N, Ducoulombier V, et al. The Lack of Association Between the Burden of Monosodium Urate Crystals Assessed With Dual-Energy Computed Tomography or Ultrasonography With Cardiovascular Risk in the Commonly High-Risk Gout Patient. *Arthritis Res Ther* (2018) 20(1):97. doi: 10.1186/s13075-018-1602-3
68. Klauser AS, Halpern EJ, Strobl S, Gruber J, Feuchtner G, Bellmann-Weiler R, et al. Dual-Energy Computed Tomography Detection of Cardiovascular Monosodium Urate Deposits in Patients With Gout. *JAMA Cardiol* (2019) 4(10):1019–28. doi: 10.1001/jamacardio.2019.3201
69. Bardin T, Tran KM, Nguyen QD, Sarfati M, Richette P, Vo NT, et al. Renal Medulla in Severe Gout: Typical Findings on Ultrasonography and Dual-Energy CT Study in Two Patients. *Ann Rheum Dis* (2019) 78(3):433–4. doi: 10.1136/annrheumdis-2018-214174
70. Bardin T, Nguyen QD, Tran KM, Le NH, Do MD, Richette P, et al. A Cross-Sectional Study of 502 Patients Found a Diffuse Hyperechoic Kidney Medulla Pattern in Patients With Severe Gout. *Kidney Int* (2021) 99(1):218–26. doi: 10.1016/j.kint.2020.08.024
71. Gibney B, Murray N. Dual-Energy CT of Spinal Tophaceous Gout. *Radiology* (2020) 296(2):276. doi: 10.1148/radiol.2020200816
72. Zhang T, Yang F, Li J, Pan Z. Gout of the Axial Joint-A Patient Level Systemic Review. *Semin Arthritis Rheum* (2019) 48(4):649–57. doi: 10.1016/j.semarthrit.2018.04.006
73. Toprover M, Krasnokutsky S, Pillinger MH. Gout in the Spine: Imaging, Diagnosis, and Outcomes. *Curr Rheumatol Rep* (2015) 17(12):70. doi: 10.1007/s11926-015-0547-7
74. Cimmino MA, Zampogna G, Parodi M, Andracco R, Barbieri F, Paparo F, et al. MRI Synovitis and Bone Lesions are Common in Acute Gouty Arthritis of the Wrist Even During the First Attack. *Ann Rheum Dis* (2011) 70(12):2238–9. doi: 10.1136/ard.2011.153353
75. Xu G, Lin J, Liang J, Yang Y, Ye Z, Zhu G, et al. Entheseal Involvement of the Lower Extremities in Gout: An Ultrasonographic Descriptive Observational Study. *Clin Rheumatol* (2021) 40(11):4649–57. doi: 10.1007/s10067-021-05826-0
76. Johnson TR. Dual-Energy CT: General Principles. *AJR Am J Roentgenol* (2012) 199(5 Suppl):S3–8. doi: 10.2214/AJR.12.9116
77. Glazebrook KN, Guimaraes LS, Murthy NS, Black DF, Bongartz T, Manek NJ, et al. Identification of Intraarticular and Periarticular Uric Acid Crystals With Dual-Energy CT: Initial Evaluation. *Radiology* (2011) 261(2):516–24. doi: 10.1148/radiol.11102485
78. Park EH, Yoo WH, Song YS, Byon JH, Pak J, Choi Y. Not All Green Is Tophi: The Importance of Optimizing Minimum Attenuation and Using a Tin Filter to Minimize Clumpy Artifacts on Foot and Ankle Dual-Energy CT. *AJR Am J Roentgenol* (2020) 214(6):1335–42. doi: 10.2214/AJR.19.22222
79. Pascart T, Grandjean A, Norberciak L, Ducoulombier V, Motte M, Luraschi H, et al. Ultrasonography and Dual-Energy Computed Tomography Provide Different Quantification of Urate Burden in Gout: Results From a Cross-Sectional Study. *Arthritis Res Ther* (2017) 19(1):171. doi: 10.1186/s13075-017-1381-2
80. Bayat S, Aati O, Rech J, Sapsford M, Cavallaro A, Lell M, et al. Development of a Dual-Energy Computed Tomography Scoring System for Measurement of Urate Deposition in Gout. *Arthritis Care Res (Hoboken)* (2016) 68(6):769–75. doi: 10.1002/acr.22754

Conflict of Interest: The authors declare that the research was conducted in the absence of any commercial or financial relationships that could be construed as a potential conflict of interest.

frontiers in Immunology

ORIGINAL RESEARCH
published: 18 January 2022
doi: 10.3389/fimmu.2021.798719

Identification of Inflammation-Related Biomarker Pro-ADM for Male Patients With Gout by Comprehensive Analysis

Kangli Qiu[1,2†], *Tianshu Zeng*[1,2†], *Yunfei Liao*[1,2], *Jie Min*[1,2], *Nan Zhang*[1,2], *Miaomiao Peng*[1,2], *Wen Kong*[1,2*] *and Lu-lu Chen*[1,2*]

[1] *Department of Endocrinology, Union Hospital, Tongji Medical College, Huazhong University of Science and Technology, Wuhan, China,* [2] *Hubei Provincial Clinical Research Center for Diabetes and Metabolic Disorders, Wuhan, China*

OPEN ACCESS

Edited by:
Xiaoxia Zhu,
Fudan University, China

Reviewed by:
Xiaoxiang Chen,
Shanghai JiaoTong University, China
Jinhui Tao,
University of Science and Technology of China, China

***Correspondence:**
Wen Kong
wenly-kong@163.com
Lu-lu Chen
cheria_chen@126.com

[†]*These authors have contributed equally to this work and share first authorship*

Specialty section:
This article was submitted to Autoimmune and Autoinflammatory Disorders, a section of the journal Frontiers in Immunology

Received: *20 October 2021*
Accepted: *28 December 2021*
Published: *18 January 2022*

Citation:
Qiu K, Zeng T, Liao Y, Min J, Zhang N, Peng M, Kong W and Chen L-l (2022) Identification of Inflammation-Related Biomarker Pro-ADM for Male Patients With Gout by Comprehensive Analysis. Front. Immunol. 12:798719. doi: 10.3389/fimmu.2021.798719

Objective: Gout is a local inflammatory disease caused by the deposition of monosodium urate (MSU) crystals in joints or adjacent tissues. When some gout occurs without hyperuricemia, or its clinical symptoms and signs are not typical, the diagnosis of gout will be delayed, so there is an urgent need to find a new biomarker to predict and diagnose of gout flare. Our research attempts to find the key genes and potential molecular mechanisms of gout through bioinformatics analysis, and collected general data and blood biochemical samples of patients with gout and healthy, then analyzed and compared the expression of factors regulated by key genes.

Method: GSE160170 were downloaded from GEO database for analysis. The data were normalized to identify the differentially expressed genes (DEGs), then GO and KEGG enrichment analysis were applied. Protein-protein interaction (PPI) networks and hub genes between DEGs were identified. Then collect general information and blood samples from male patients with acute gout, hyperuricemia and healthy. ELISA method was used to detect pro-ADM levels of different groups, and the data was input into SPSS statistical software for analysis.

Result: We identified 266 DEGs (179 up-regulated and 87 down-regulated) between gout patients and healthy controls. GO analysis results show that DEGs are mostly enriched in inflammatory response, growth factor activity, cytokine activity, chemokine activity, S100 protein binding and CXCR chemokine receptor binding. KEGG pathway analysis showed that DEGs are mainly related to Chemokine signaling pathway and Cytokine-cytokine receptor interaction. ADM, CXCR1, CXCR6, CXCL3, CCL3, CCL18, CCL3L3, CCL4L1, CD69, CD83, AREG, EREG, B7RP1, HBEGF, NAMPT and S100B are the most important hub genes in the PPI network. We found that the expression of pro-ADM in the gout group and hyperuricemia group was higher than that in the healthy group, and the difference was statistically significant.

Conclusion: In this study, a series of bioinformatics analyses were performed on DEGs to identify key genes and pathways related to gout. Through clinical verification, we found that pro-ADM can be used as an inflammation-related biomarker for acute attacks of gout, providing new ideas for the diagnosis and treatment of gout.

Keywords: gout, pro-ADM, comprehensive analysis, inflammation, biomarker

INTRODUCTION

Gout is a local inflammatory disease caused by the deposition of monosodium urate (MSU) crystals in joints or adjacent tissues. The pain is often described as burning, tingling or biting (1). Clinically, it can be manifested as gouty arthritis, tophi, uric acid kidney stones or gouty nephropathy. According to data reported in different studies, the global incidence rate is between 0.6-2.9/1000 person-years, and the prevalence rate is between 0.68%-3.90% in adult (2, 3). The incidence and prevalence of gout increase with age, and it is more common in men than in women. In Asia, the sex ratio of gout is about 8:1, which is much higher than in Europe and America (4–6).

The risk factors of gout include both genetic and non-genetic. Among them, hyperuricemia is the most important risk factor for the gout flare. There is a concentration-dependent relationship between serum uric acid levels and the risk of gout (7). Factors which lead to elevated uric acid are also risk factors for gout, such as alcohol, red meat, seafood, sugary drinks, diuretics and chronic kidney disease (8–10). For genetics part, 55 loci have been determined to be related to the risk of gout in the genome-wide association study (11).

The gold standard for diagnosis of gout is the presence of MSU crystals in synovial fluid or tophi under the microscope. MSU crystals are damage-related molecules that stimulate the innate immune pathway. In the pathogenesis of gout, NLRP3 inflammasome is the main way for MSU crystals to trigger cellular inflammatory response. Inflammatory cytokines, especially IL-1β, are key mediators of gout inflammation (12). A variety of regulatory pathways have been found to regulate the activity of inflammasomes and the release of IL-1β (12–15). Many studies have confirmed that the expression levels of some inflammatory factors, including IL-1β, IL-6, IL-8 and TNF-α, are significantly increased in patients with acute gout flare (16, 17), while α1antitrypsin (AAT) or some anti- Inflammatory factors such as IL-37, TGF-β, IL-10 and IL-1RA (IL1RN) are negative regulators of gout inflammation (18–21). The study by Yu Wang et al. confirmed that the serum levels of xanthine and hypoxanthine in patients with gout were significantly increased, xanthine and hypoxanthine have clinical application value in the diagnosis of gout especially in patients with normal uric acid (22). Xueshan Bai et al. found that serum CA72-4 levels are elevated in patients with frequent attacks of gout and can be used as a predictor of gout attacks (23). However, the biomarkers related to gout inflammation are still unknown, which limits the prediction of gout flare and makes atypical gout misdiagnosed or delayed in diagnosis. The basic research on the pathogenesis of gout and clinical diagnosis and treatment are still in continuous progress and exploration. Our research attempts to find the key genes and potential molecular mechanisms of gout through bioinformatics analysis, and then collect general data and blood biochemical samples of gout patients and normal patients, analyze and compare the expression of key gene regulatory factors, and verify it in the clinic, finally providive a basis for finding novel biomarkers of gout.

MATERIALS AND METHODS

Data Selection

The GSE160170 data set is downloaded from the GEO official website, and the expression matrix uses GPL21827 [HuGene-1_0-st] Affymetrix human gene 1.0 ST array [transcript (gene) version]. The data set includes six gout samples and six normal samples.

Data Processing

Evaluating the GSE160170 raw data set by using the limma R package. Our study first corrected the data, obtained the expression matrix data set required by the experiment by taking the form of a subset, and then extracted the clinical information of the corresponding sample according to the data sample of the expression matrix for subsequent sample classification, and finally performed the data on GSE160170 according to the gene ID. The normalization process eliminates the influence caused by the batch effect. Through data processing, we finally obtained normal samples (6 cases) as the control group and gout samples (6 cases) as the treat group, using $|\log2\ FC|>2$ and adjusted $p<0.05$ to identify gout-deg.

Enrichment Analysis

The database uses the org.Hs.eg.db database file on the bioconductor platform. The file contains 28 mainstream data files. We analyze the differential genes of gout. GO enrichment analysis (24) and KEGG pathway enrichment analysis (25) analyze the biological processes and key pathways that differential genes are mainly involved in. Among them, GO enrichment analysis $P<0.01$ is the selection criterion, and KEGG pathway analysis is based on $P<0.05$ for selection criteria.

Construction of PPI Network

The search tool for searching interacting genes (STRINGv-11.0, https://string-db.org/) database is an online tool for evaluating

PPI information. To evaluate the interaction relationship between DEGs, DEGs are mapped to STRING, and the interaction relationship between DEGs is screened from the protein level, and a PPI network that up-regulates and down-regulates DEGs is constructed. Then we used Cytoscape software to construct PPI network visualization. The cytohHubba plug-in was used to screen the HUB genes of the PPI network in Cytoscape, and TOP25 HUB genes were selected for analysis by using Density of Maximum Neighborhood Component (DMNC) in the local-based method and EcCentricity (EC) in the global-based method respectively.

Clinical Patient Selection

This study included 4 patients with acute gout, 6 patients with asymptomatic hyperuricemia (HUA) (no clinical manifestations of gouts, erum uric acid ≥428mol/L), and 4 healthy people (serum uric acid <428mol/L), These patients were all male and selected from the Department of Endocrinology, Union Hospital, Tongji Medical College, Huazhong University of Science and Technology. The exclusion criteria are: 1. Patients with Cushing syndrome and patients who have previously used glucocorticoids and non-steroidal anti-inflammatory drugs; 2. Patients suffering from diabetes, hypertension, tumors, liver and kidney insufficiency, acute or chronic infectious diseases, immune system diseases, cardiovascular diseases.

Enzyme-Linked Immunosorbent Assay (ELISA)

Pro-ADM levels were determined by using the human Pro-ADM ELISA kit (CSB-E14356h, CUSABIO, Wuhan, China) according to the manufacturer's instructions.

Statistical Analysis

The clinical data was analyzed by SPSS28.0 software (IBM, Armonk, NY, USA). The measurement data is represented by the mean ± standard deviation. A one-way analysis of variance (ANOVA) was used to assess the differences between the three groups. P value<0.05 is considered statistically significant.

RESULTS

Identification of Differentially Expressed Genes for Gout

We found 266 DEGs in gout patients, including 179 up-regulated genes and 87 down-regulated genes compared with the healthy control group. We drew a volcano map (**Figure 1**) and a hierarchical clustering heat map of differential genes (**Figure 2**). The results show that there is a good difference between these DEGs between the gout group and the control group. PTPRS and DCLRE1C were identified as the most up-regulated and down-regulated genes in gout patients respectively.

Functional Enrichment Analysis

We use R language to perform GO analysis of differential genes by using the org.Hs.eg.db database file on the bioconductor platform and use David (https://david.ncifcrf.gov/) online tools to perform KEGG enrichment analysis. For biological processes, molecular function and cell composition, a total of 12 GO (**Figure 3** and **Table 1**) and 23 KEGG pathways (**Figure 4**) were identified. BP mainly focuses on inflammatory response, negative regulation of cell proliferation, immune response, positive regulation of transcription from RNA polymerase II

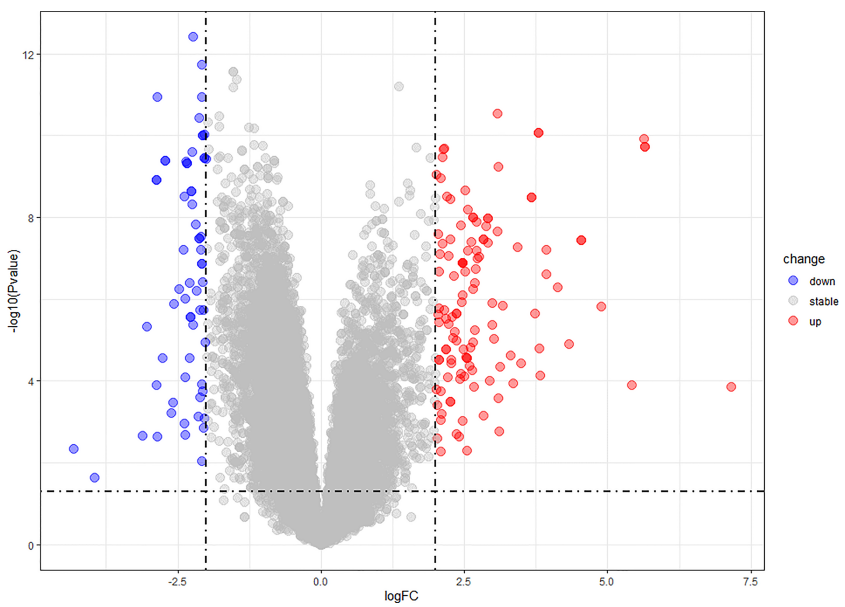

FIGURE 1 | Volcano map of DEGs.

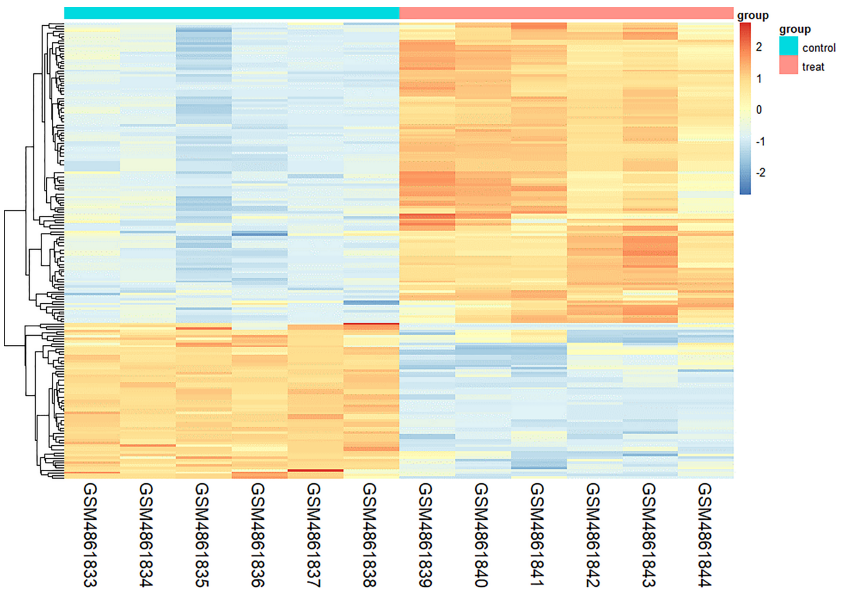

FIGURE 2 | Heat map of DEGs.

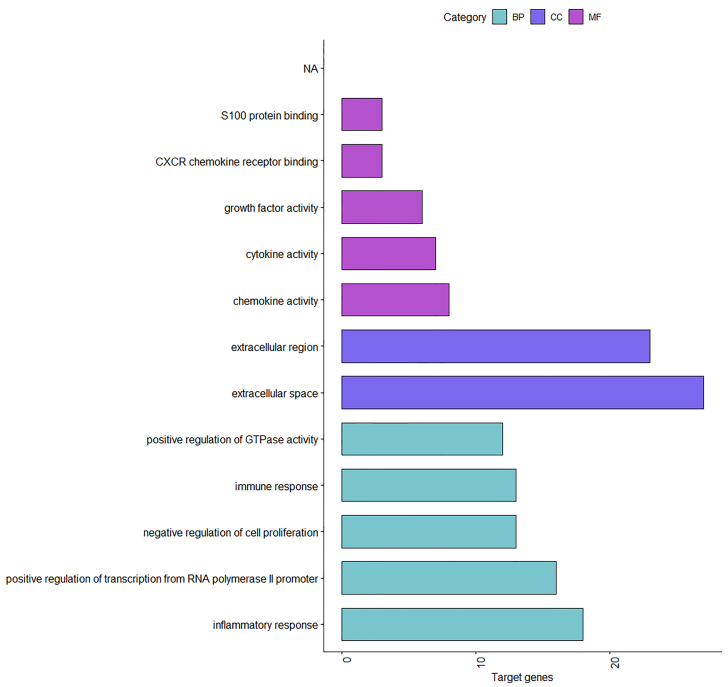

FIGURE 3 | The results of GO of DEGs.

promoter and positive regulation of GTPase activity, CC mainly focuses on extracellular space and extracellular region, MF mainly focuses on chemokine activity and cytokine activity, Growth factor activity, CXCR chemokine receptor binding and S100 protein binding. In addition, KEGG pathway analysis showed that DEGs are closely related to Salmonella infection, Chemokine signaling pathway and Cytokine-cytokine receptor interactio. We can conclude that ADM is located in the extracellular region and region, and participates in the negative regulation of cell proliferation.

TABLE 1 | The results of GO of DEGs.

Category	Term	Count	PValue	Genes
BP	inflammatory response	18	6.43E-09	CXCL8, CCL3L1, CCL4L2, TNFAIP3, CXCL1, CXCR6, LYZ, CXCL3, PTGS2, CXCL2, TNF, IL1A, IL6, CXCR1, IL1B, NFKBIZ, CCL3, CCL18
BP	positive regulation of transcription from RNA polymerase II promoter	16	0.009519	CSRNP1, LUM, NRG1, AATF, TNF, CDC73, NR4A2, IL1A, NR4A1, IL6, NR4A3, IL1B, NAMPT, MAFK, OGT, ATF3
BP	negative regulation of cell proliferation	13	6.36E-05	BTG1, CXCL8, CCL3L1, ADM, CXCL1, PTGS2, CDC73, EREG, IL1A, IL6, ADAMTS1, IL1B, FKTN
BP	immune response	13	0.000114	CXCL8, CCL4L2, CXCL1, CXCL3, SLED1, CXCL2, TNF, IL1A, IL6, RGS1, IL1B, CCL3, CCL18
BP	positive regulation of GTPase activity	12	0.004734	FARP1, PLEKHG1, ARHGEF9, CCL3L1, ADGRB3, RGS1, CCL4L2, CCL3, NRG1, CCL18, EREG, HBEGF
CC	extracellular space	27	3.06E-06	CXCL8, CCL3L1, CCL4L2, ADM, CXCL1, CXCL3, TNF, CXCL2, AREG, GPC1, NAMPT, CCL3, CCL18, PTGDS, FKTN, SLF2, EDN2, LUM, NRG1, S100B, LYZ, EREG, IL1A, IL6, IL1B, EZR, HBEGF
CC	extracellular region	23	0.002473	EDN2, CXCL8, OVCH1, CCL3L1, LUM, SPINK6, CCL4L2, ADM, CXCL1, NRG1, LYZ, CXCL3, S100B, C14ORF93, CXCL2, TNF, EREG, IL1A, IL6, IL1B, CCL3, PTGDS, HBEGF
MF	chemokine activity	8	8.05E-08	CXCL8, CCL3L1, CCL4L2, CCL3, CXCL1, CXCL3, CCL18, CXCL2
MF	cytokine activity	7	0.002241	IL1A, IL6, IL1B, NAMPT, NRG1, TNF, AREG
MF	growth factor activity	6	0.00786	IL6, CXCL1, NRG1, AREG, EREG, HBEGF
MF	CXCR chemokine receptor binding	3	0.001983	CXCL1, CXCL3, CXCL2
MF	S100 protein binding	3	0.004213	S100A1, EZR, S100B

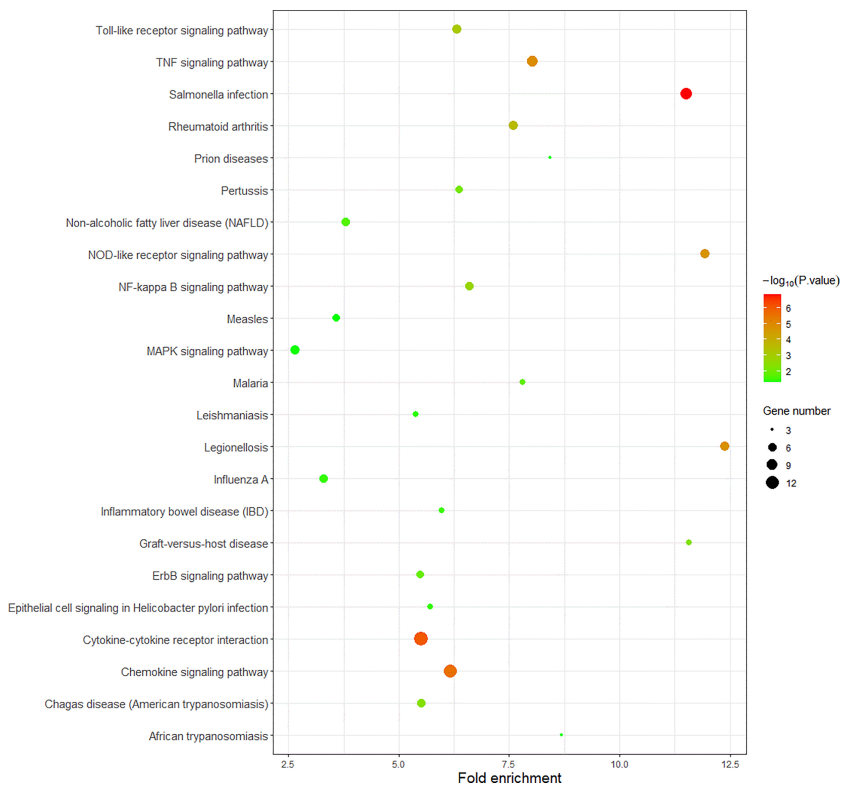

FIGURE 4 | The results of KEGG of DEGs.

PPI Network and Hub Gene Identification

We submitted DEGs to STRING database to obtain PPI data, and used Cytoscape 3.8.2 to construct a PPI network (**Figure 5**), and used two algorithms to determine the top 25 genes as key genes (**Figures 6** and **7**). We intersect the key genes of the two algorithms to obtain a total of 16 key genes, namely ADM, CXCR1, CXCR6, CXCL3, CCL3, CCL18, CCL3L3, CCL4L1, CD69, CD83, AREG, EREG, B7RP1, HBEGF, NAMPT and S100B.

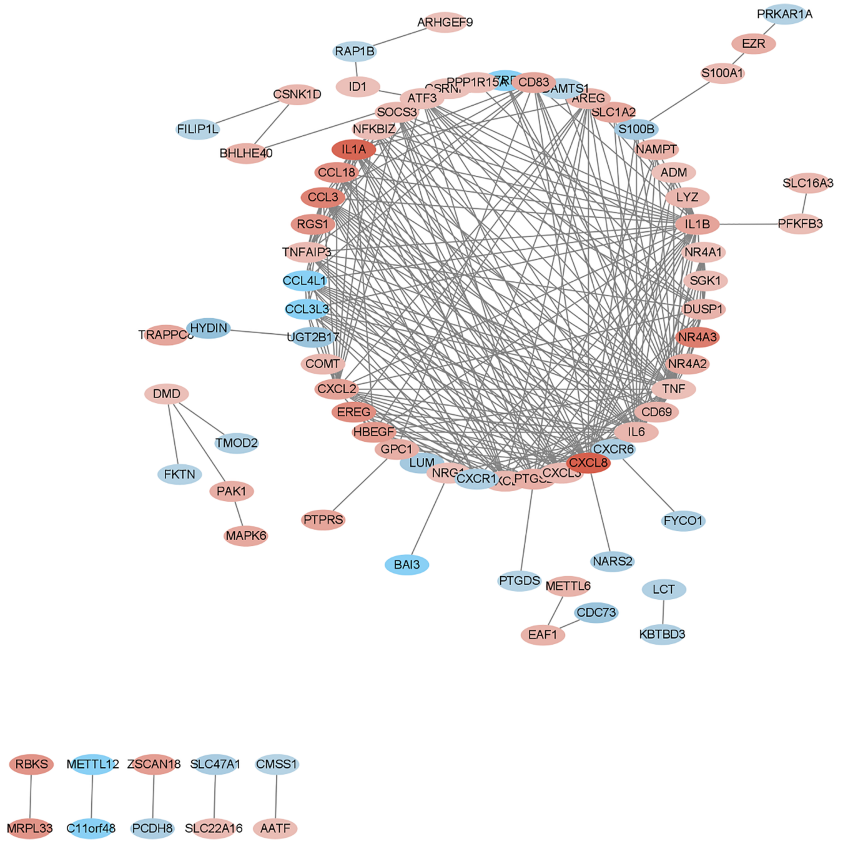

FIGURE 5 | PPI network of the DEGs.

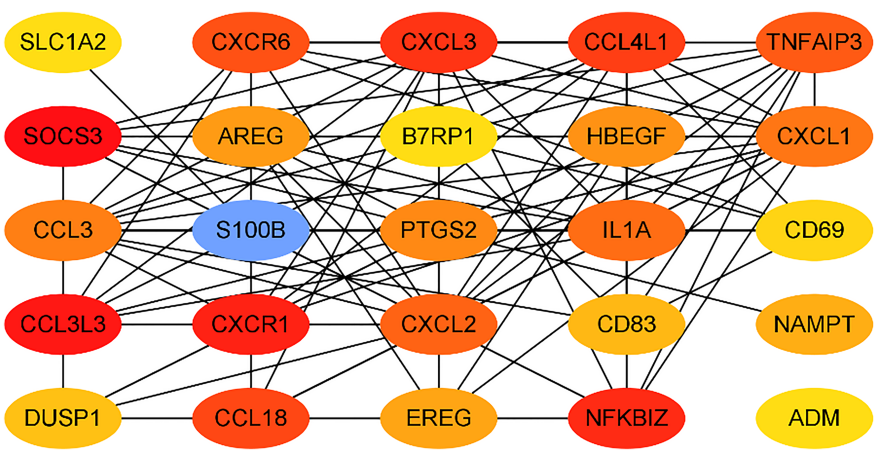

FIGURE 6 | Hub genes in the PPI network by DMNC.

Verification of Pro-ADM in Clinical Samples

Through bioinformatics methods, we found that ADM is not only an up-regulation of DEG for gout, but also highly correlated with pathways obtained by differential gene enrichment analysis, and it is also one of the hub genes in the PPI network of the DEGs. In order to verify the clinical application potential of ADM gene, ELISA method was used to detect the protein level encoded by ADM gene in clinical samples. ADM is a peptide

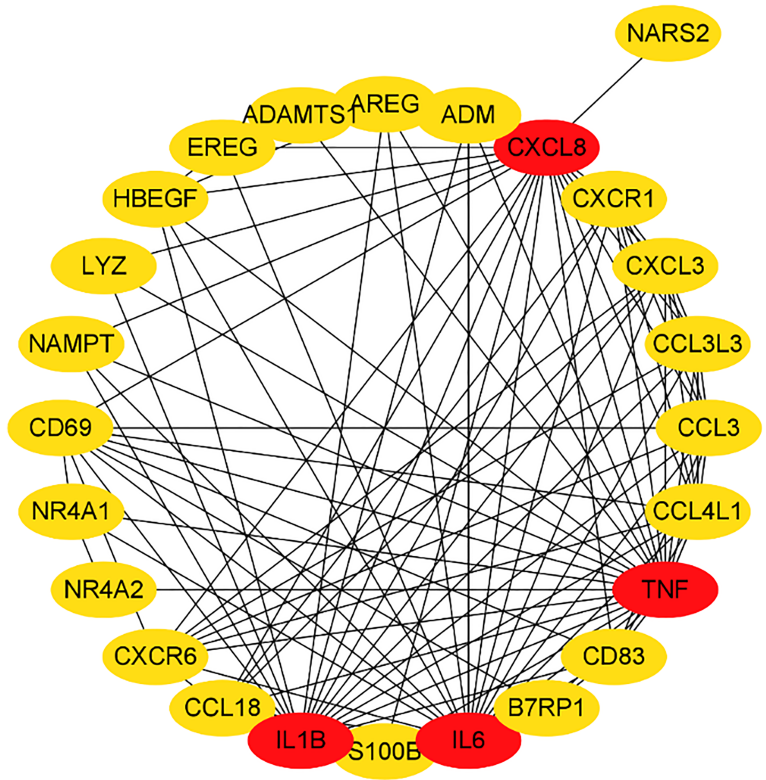

FIGURE 7 | Hub genes in the PPI network by EC.

hormone isolated from human adrenal medulla chromaffin cells and belongs to the calcitonin gene-related peptide superfamily. Due to the short half-life of ADM, pro-adrenomedullin (pro-ADM) detection is used clinically instead.

The average age of the three groups was: 34 years old in the gout group, 35 years old in the HUA group, and 44 years old in the healthy control group. There was no significant difference in age ($P > 0.05$) (**Table 2**). The blood uric acid level of the gout group and the hyperuricemia group was higher than that of the control group, and the difference was statistically significant (**Table 2**). The expression of serum pro-ADM of the acute gout group and the hyperuricemia group was higher than that of the control group, and the difference was statistically significant (**Figure 8**).

DISCUSSION

Gout is a metabolic disease that seriously endangers human health. It is caused by local inflammation caused by the deposition of monosodium urate (MSU) crystals in joints or adjacent tissues. In this study, we downloaded and analyzed data from 6 gout patients and 6 healthy controls from the GEO database. We identified a total of 266 DEGs, including 179 up-regulated DEGs and 87 down-regulated DEGs. These genes include PTPRS, SLED1, ACSL1, CXCL8, DCLRE1C, FAM217A and ADM, etc. Then we use the database to enrich and analyze these differential genes. The results show that these genes are mainly involved in immune response, inflammatory response and other processes, and are enriched in chemokine signaling pathways and cytokine-cytokine receptor interactions. Process-related genes include CXCL8, CCL3L1, ADM, CXCL1, TNF, IL1A, IL6, etc., among which ADM is highly related to these pathways. Finally, by constructing a PPI network, we took the intersection of the hub genes obtained by two algorithms, and obtained a total of 16 key genes, namely CXCR1, CXCR6, CXCL3, CCL3, CCL18, CCL3L3, CCL4L1, CD69, CD83, AREG, EREG, B7RP1, HBEGF, NAMPT, S100B and ADM.

TABLE 2 | Comparison of datas of patients in three groups (*P < 0.05 vs. control).

Indicator (median)	Gout (n = 4)	Hyperuricaemia (n = 6)	Control (n = 4)
Age (years)	34	35	44
Uric acid (μmol/L)	512.08*	505.8*	361.7
Pro-ADM (pmol/L)	5373.35 ± 1291.41*	5005.04 ± 691.23*	3331.3 ± 1370.85

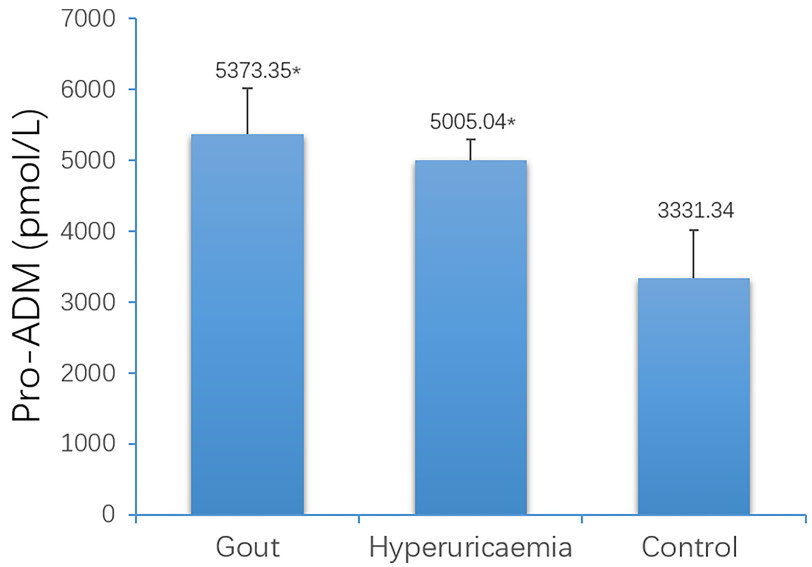

FIGURE 8 | Comparison of serum Pro-ADM levels among gout patients, hyperuricaemia patients and control (*P < 0.05 vs. control).

We analyzed these 16 genes in the next step. CXCR1, CXCR6, CXCL3, CCL3, CCL18, CCL3L3, CCL4L1 are all family members related to chemokines. The protein encoded by the CXCR1 gene is a member of the G protein-coupled receptor family and is a receptor for interleukin 8 (IL8). The combination of two leads to the activation of neutrophils (26). CXCR1 related diseases include acute pyelonephritis, cancers and human immunodeficiency virus type 1 (27), etc. related pathways include Akt signaling pathway and CCR5 pathway in macrophages. Yangang Wang et al. conducted a case-control study to investigate the relationship between the onset of gouty arthritis in Chinese Han men with CXCR1 and CXCR2 gene polymorphisms. The study found that the CXCR1 gene rs2234671 and CXCR2 gene rs1126579 in the gouty arthritis group were not related to the susceptibility of gout in Chinese men. The CXCR2 gene rs2230054 is related to the susceptibility of gout in Chinese men (28). Research by Ying Ye et al. showed that CXCR1/CXCR2 antagonist G31P can reduce the inflammatory progression of chronic uric acid nephropathy and play a role in renal protection (29). CXCR6's exclusive ligand Chemokine Ligand 16 (CCL16) is a part of the signaling pathway that regulates the migration of T lymphocytes to various peripheral tissues (lung, intestine, liver, skin and spleen red pulp), and promotes cell-cell migration. The diseases associated with CXCR6 include tumors, diabetes, respiratory diseases and immunodeficiency (30–32). Studies have found that the concentration of CXCL16 is significantly increased in the synovial fluid of patients with gout, and the migration of polymorphonuclear neutrophils in response to CXCL16 has been observed *in vitro* (33). CCL3 encodes macrophage inflammatory protein 1 α (M1P-1 α), which plays a role in inflammation by binding to CCR receptors. Related pathways include Akt signaling pathway and CCR5 pathway in macrophages (34). Studies have shown that the combination of TNF-α, GM-CSF and MSU will cause neutrophils to produce IL-8 and eliminate the release of MIP-1α, leading to the recruitment of neutrophils, which is consistent with the pathological state of gout (35). The expression of CD69-encoded protein is induced when T lymphocytes are activated, and may play a role in proliferation. Studies have found that the expression of CD69 in mucosal-associated invariant T (MAIT) cells in gout patients is increased, and it is increased by the stimulation of MSU crystals (36), and studies have suggested that allopurinol, a gout treatment drug, can attenuate the upregulation of CD69 (37)..

ADM is a peptide hormone isolated from human adrenal medulla chromaffin cells and belongs to the calcitonin gene-related peptide superfamily. ADM is mainly synthesized and secreted by vascular endothelial cells and smooth muscle cells, and mRNA is highly expressed in adrenal gland, heart, lung, kidney and other tissues. ADM can bind to CGRP receptors or its specific receptors, and exert various physiological effects through nitric oxide (NO), cyclic adenosine monophosphate (cAMP), IP3-Ca2+ or cyclic guanosine monophosphate (cGMP) pathways. ADM has a wide range of physiological effects. It has the effects of inhibiting the secretion of aldosterone, natriuretic and diuretic, inhibiting the proliferation of vascular smooth muscle, and anti-infection. ADM is closely related to diseases such as heart failure, myocardial infarction, sepsis. The plasma ADM can not only be used for the treatment of heart failure, but its elevated index is also an independent factor for the poor prognosis of chronic congestive heart failure (38). ADM can be used as an independent indicator of the prognosis of acute myocardial infarction (39). ADM can also help diagnose sepsis and assess its severity. Because ADM has a short half-life, clinically, the intermediate products that are stable when ADM is cleared in the circulation, namely adrenomedullin precursor (pro-ADM) and intermediate adrenomedullin precursor (MRpro-ADM) are used instead. ADM is generated

from the ADM precursor consisting of 185 amino acids (preproadrenomedullin) by post-translational enzymatic processing (40). ADM is processed from proadrenomedullin as glycine-extended ADM (ADM-glycine), an intermediate form of ADM. Subsequently, mature ADM is converted from ADM-glycine by enzymatic amidation (41). Another 20-amino acid peptide is also generated and called proadrenomedullin N-terminal 20 peptide (PAMP) (42, 43).The mechanisms of the increase of pro-ADM in different diseases are not completely the same, but they are all related to the physiological effects of ADM. The increase in blood volume and activation of sympathetic nerves in patients with chronic heart failure leads to an increase in plasma ADM concentration. The increased secretion of ADM can dilate blood vessels, maintain vascular integrity, inhibit the renin-angiotensin-aldosterone system, and inhibit ventricular remodeling (44). The increase in ADM in patients with infectious diseases such as sepsis is due to its bactericidal, anti-inflammatory, and immune-regulating effects (45). In addition to its own antibacterial and anti-infective effects, ADM can also bind to complement regulatory factor H and interact with it. Complement regulatory factor H prolongs the action time of ADM, and ADM accelerates the clearing of C3b (46).

As an emerging indicator of inflammation, pro-ADM has not been studied to show changes in patients with gout. We speculate that the involvement of ADM in gout may be related to the following aspects. Immune cells such as macrophages, lymphocytes, neutrophils and microglia in the body can synthesize and secrete ADM. ADM secreted by immune cells can inhibit the up-regulation of neutrophil CD11b levels and increase the content of neutrophil cAMP. Under the stimulation of bacterial mucopolysaccharide, ADM can increase IL-6 and decrease the secretion of TNF-α. Macrophages are important innate immune cells in the human body. They differentiate into different phenotypes at different stages of gout, and participate in the occurrence and alleviation of inflammation. Studies have shown that monocytes/macrophages should be considered as the main source of ADM in the circulating blood, and the secreted ADM may regulate the function of macrophages (47). In addition, TNF-α and IL-1β can enhance the synthesis and secretion of ADM (48, 49). We already know that the key step of gout attacks also include neutrophil activation leading to apoptosis inhibition and degranulation. ADM can inhibit mitochondrial-mediated apoptosis through the Akt/GSk-3β pathway, reducing the activity of caspase3, cytochrome C translocation from mitochondria to Cytoplasmic is inhibited, the mRNA and protein expression of Bcl-2 increases, and the Bcl-2/Bax ratio increases. This may also be one of the ways ADM participates in the regulation of gout. When gout affects the kidneys in the late stage, renal insufficiency and even acute and chronic renal failure may occur, manifested by symptoms such as water and sodium retention, high blood pressure, and heart failure. These symptoms can lead to increased blood volume and activation of sympathetic nerves, thereby promoting the secretion of ADM and the increase of pro- ADM levels. This theoretical speculation is consistent with the conclusion we have reached through bioinformatics methods: ADM is not only an up-regulation of DEG for gout, but also highly correlated with pathways obtained by differential gene enrichment analysis, and it is also one of the hub genes in the PPI network. Finally, through the detection of pro-ADM levels in clinical samples, we confirmed that pro-ADM is involved in gout flare. Patients with gout and hyperuricemia are relatively easy to distinguish by clinical symptoms and signs. The difficulty in clinical diagnosis of gout is that the blood uric acid level of gout patients is not necessarily elevated, so it is difficult to distinguish it from other arthralgia diseases. We also conducted DEGs analysis on rheumatoid arthritis and spondyloarthritis through bioinformatics methods. GSE134087 (rheumatoid arthritis) and GSE58667 (spondy arthritis) were downloaded from GEO database. We found that ADM is a stably expressed gene for rheumatoid arthritis and spondyloarthritis. Therefore, we believe that detecting the level of Pro-ADM is helpful for diagnosing gout, which is also the clinical significance of this study.

The main limitations of this study are that the sample size is small and all the participants are male, which may lead to the non-universal results. In future work, we will further expand the sample size and include female investigators in the study. In addition to gout, pro-ADM may also be affected by other factors. Finally, all subjects in this study are Chinese, and it is uncertain whether the results of this study can be generalized to other races. Despite these limitations, this is still the first one to study the potential biomarkers and pathogenesis of the acute attacks of gout through bioinformatics methods combined with clinical sample verification.

CONCLUSIONS

Our data provides a comprehensive DEGs bioinformatics analysis to find molecular mechanisms related to gout. We found that pro-ADM can be used as a new inflammation-related biomarker to predict and diagnose the acute attacks of gout in male patients, which provides new insights for the development of it. In the future, further experiments at the cellular and molecular levels will be needed to confirm its role in pathogenesis of gout.

DATA AVAILABILITY STATEMENT

The original contributions presented in the study are included in the article/supplementary material. Further inquiries can be directed to the corresponding authors.

ETHICS STATEMENT

The studies involving human participants were reviewed and approved by Medical Ethics Committee of Union Hospital, Tongji Medical College, Huazhong University of Science and Technology. The patients/participants provided their written informed consent to participate in this study.

AUTHOR CONTRIBUTIONS

KQ: Conceptualization, Methodology, Validation, Data curation, Writing- Original draft preparation. TZ: Conceptualization, Methodology, Supervision, Writing - Review & Editing. YL: Resources, Visualization, Validation. JM: Resources, Visualization, Software. NZ: Data Curation, Formal analysis, Resources. MP: Data Curation, Formal analysis, Investigation. WK: Funding acquisition, Writing- Reviewing and Editing. L-lC: Funding acquisition, Writing- Reviewing and Editing. All authors contributed to the article and approved the submitted version.

REFERENCES

1. Singh JA, Herbey I, Bharat A, Dinnella JE, Pullman-Mooar S, Eisen S, et al. Gout Self-Management in African American Veterans: A Qualitative Exploration of Challenges and Solutions From Patients' Perspectives. *Arthritis Care Res (Hoboken)* (2017) 69:1724–32. doi: 10.1002/acr.23202
2. Dehlin M, Drivelegka P, Sigurdardottir V, Svärd A, Jacobsson LT. Incidence and Prevalence of Gout in Western Sweden. *Arthritis Res Ther* (2016) 18:164. doi: 10.1186/s13075-016-1062-6
3. Rai SK, Aviña-Zubieta JA, McCormick N, De Vera MA, Shojania K, Sayre EC, et al. The Rising Prevalence and Incidence of Gout in British Columbia, Canada: Population-Based Trends From 2000 to 2012. *Semin Arthritis Rheumatol* (2017) 46:451–6. doi: 10.1016/j.semarthrit.2016.08.006
4. Chen-Xu M, Yokose C, Rai SK, Pillinger MH, Choi HK. Contemporary Prevalence of Gout and Hyperuricemia in the United States and Decadal Trends: The National Health and Nutrition Examination Survey, 2007-2016. *Arthritis Rheumatol* (2019) 71:991–9. doi: 10.1002/art.40807
5. Kuo CF, Grainge MJ, Mallen C, Zhang W, Doherty M. Rising Burden of Gout in the UK But Continuing Suboptimal Management: A Nationwide Population Study. *Ann Rheum Dis* (2015) 74:661–7. doi: 10.1136/annrheumdis-2013-204463
6. Kim JW, Kwak SG, Lee H, Kim SK, Choe JY, Park SH. Prevalence and Incidence of Gout in Korea: Data From the National Health Claims Database 2007-2015. *Rheumatol Int* (2017) 37:1499–506. doi: 10.1007/s00296-017-3768-4
7. Campion EW, Glynn RJ, DeLabry LO. Asymptomatic Hyperuricemia. Risks and Consequences in the Normative Aging Study. *Am J Med* (1987) 82:421–6. doi: 10.1016/0002-9343(87)90441-4
8. Bhole V, de Vera M, Rahman MM, Krishnan E, Choi H. Epidemiology of Gout in Women: Fifty-Two-Year Followup of a Prospective Cohort. *Arthritis Rheumatol* (2010) 62:1069–76. doi: 10.1002/art.27338
9. Singh JA, Reddy SG, Kundukulam J. Risk Factors for Gout and Prevention: A Systematic Review of the Literature. *Curr Opin Rheumatol* (2011) 23:192–202. doi: 10.1097/BOR.0b013e3283438e13
10. Wang W, Bhole VM, Krishnan E. Chronic Kidney Disease as a Risk Factor for Incident Gout Among Men and Women: Retrospective Cohort Study Using Data From the Framingham Heart Study. *BMJ Open* (2015) 5:e006843. doi: 10.1136/bmjopen-2014-006843
11. Tin A, Marten J, Halperin Kuhns VL, Li Y, Wuttke M, Kirsten H, et al. Target Genes, Variants, Tissues and Transcriptional Pathways Influencing Human Serum Urate Levels. *Nat Genet* (2019) 51:1459–74. doi: 10.1038/s41588-019-0504-x
12. So AK, Martinon F. Inflammation in Gout: Mechanisms and Therapeutic Targets. *Nat Rev Rheumatol* (2017) 13:639–47. doi: 10.1038/nrrheum.2017.155
13. Dalbeth N, Merriman TR, Stamp LK. Gout. *Lancet* (2016) 388:2039–52. doi: 10.1016/S0140-6736(16)00346-9
14. Dalbeth N, Gosling AL, Gaffo A, Abhishek A. Gout. *Lancet* (2021) 397:1843–55. doi: 10.1016/S0140-6736(21)00569-9
15. Hainer BL, Matheson E, Wilkes RT. Diagnosis, Treatment, and Prevention of Gout. *Am Fam Physician* (2014) 90:831–6.
16. Kienhorst LB, van Lochem E, Kievit W, Dalbeth N, Merriman ME, Phipps-Green A, et al. Gout Is a Chronic Inflammatory Disease in Which High Levels of Interleukin-8 (CXCL8), Myeloid-Related Protein 8/Myeloid-Related Protein 14 Complex, and an Altered Proteome Are Associated With Diabetes Mellitus and Cardiovascular Disease. *Arthritis Rheumatol* (2015) 67:3303–13. doi: 10.1002/art.39318
17. Popa-Nita O, Naccache PH. Crystal-Induced Neutrophil Activation. *Immunol Cell Biol* (2010) 88:32–40. doi: 10.1038/icb.2009.98
18. Ter Horst R, Jaeger M, Smeekens SP, Oosting M, Swertz MA, Li Y, et al. Host and Environmental Factors Influencing Individual Human Cytokine Responses. *Cell* (2016) 167:1111–24.e13. doi: 10.1016/j.cell.2016.10.018
19. Elliot AJ, Cross KW, Fleming DM. Seasonality and Trends in the Incidence and Prevalence of Gout in England and Wales 1994-2007. *Ann Rheum Dis* (2009) 68:1728–33. doi: 10.1136/ard.2008.096693
20. Chen YH, Hsieh SC, Chen WY, Li KJ, Wu CH, Wu PC, et al. Spontaneous Resolution of Acute Gouty Arthritis Is Associated With Rapid Induction of the Anti-Inflammatory Factors TGFβ1, IL-10 and Soluble TNF Receptors and the Intracellular Cytokine Negative Regulators CIS and SOCS3. *Ann Rheum Dis* (2011) 70:1655–63. doi: 10.1136/ard.2010.145821
21. Liu L, Xue Y, Zhu Y, Xuan D, Yang X, Liang M, et al. Interleukin 37 Limits Monosodium Urate Crystal-Induced Innate Immune Responses in Human and Murine Models of Gout. *Arthritis Res Ther* (2016) 18:268. doi: 10.1186/s13075-016-1167-y
22. Bai X, Sun M, He Y, Liu R, Cui L, Wang C, et al. Serum CA72-4 Is Specifically Elevated in Gout Patients and Predicts Flares. *Rheumatol (Oxford)* (2020) 59:2872–80. doi: 10.1093/rheumatology/keaa046
23. Ashburner M, Ball CA, Blake JA, Botstein D, Butler H, Cherry JM, et al. Gene Ontology: Tool for the Unification of Biology. *Gene Ontol Consortium Nat Genet* (2000) 25:25–9. doi: 10.1038/75556
24. Wang Y, Deng M, Deng B, Ye L, Fei X, Huang Z. Study on the Diagnosis of Gout With Xanthine and Hypoxanthine. *J Clin Lab Anal* (2019) 33:e22868. doi: 10.1002/jcla.22868
25. Kanehisa M, Goto S. KEGG: Kyoto Encyclopedia of Genes and Genomes. *Nucleic Acids Res* (2000) 28:27–30. doi: 10.1093/nar/28.1.27
26. Kharche S, Joshi M, Chattopadhyay A, Sengupta D. Conformational Plasticity and Dynamic Interactions of the N-Terminal Domain of the Chemokine Receptor CXCR1. *PloS Comput Biol* (2021) 17:e1008593. doi: 10.1371/journal.pcbi.1008593
27. Liu Q, Li A, Tian Y, Wu JD, Liu Y, Li T, et al. The CXCL8-CXCR1/2 Pathways in Cancer. *Cytokine Growth Factor Rev* (2016) 31:61–71. doi: 10.1016/j.cytogfr.2016.08.002
28. Wang Y, Wu Y, Xing Q, Chu N, Shen L, Yu X, et al. Genetic Association of Polymorphism Rs2230054 in CXCR2 Gene With Gout in Chinese Han Male Population. *Cent Eur J Immunol* (2020) 45:80–5. doi: 10.5114/ceji.2020.94702
29. Ye Y, Zhang Y, Wang B, Walana W, Wei J, Gordon JR, et al. CXCR1/CXCR2 Antagonist G31P Inhibits Nephritis in a Mouse Model of Uric Acid Nephropathy. *BioMed Pharmacother* (2018) 107:1142–50. doi: 10.1016/j.biopha.2018.07.077
30. Deng L, Chen N, Li Y, Zheng H, Lei Q. CXCR6/CXCL16 Functions as a Regulator in Metastasis and Progression of Cancer. *Biochim Biophys Acta* (2010) 1806:42–9. doi: 10.1016/j.bbcan.2010.01.004
31. La Porta CA. CXCR6: The Role of Environment in Tumor Progression. Challenges for Therapy. *Stem Cell Rev Rep* (2012) 8:1282–5. doi: 10.1007/s12015-012-9383-6
32. Limou S, Coulonges C, Herbeck JT, van Manen D, An P, Le Clerc S, et al. Multiple-Cohort Genetic Association Study Reveals CXCR6 as a New Chemokine Receptor Involved in Long-Term Nonprogression to AIDS. *J Infect Dis* (2010) 202:908–15. doi: 10.1086/655782
33. Ruth JH, Arendt MD, Amin MA, Ahmed S, Marotte H, Rabquer BJ, et al. Expression and Function of CXCL16 in a Novel Model of Gout. *Arthritis Rheumatol* (2010) 62:2536–44. doi: 10.1002/art.27518
34. Ntanasis-Stathopoulos I, Fotiou D, Terpos E. CCL3 Signaling in the Tumor Microenvironment. *Adv Exp Med Biol* (2020) 1231:13–21. doi: 10.1007/978-3-030-36667-4_2
35. Hachicha M, Naccache PH, McColl SR. Inflammatory Microcrystals Differentially Regulate the Secretion of Macrophage Inflammatory Protein 1

and Interleukin 8 by Human Neutrophils: A Possible Mechanism of Neutrophil Recruitment to Sites of Inflammation in Synovitis. *J Exp Med* (1995) 182:2019–25. doi: 10.1084/jem.182.6.2019
36. Cho YN, Jeong HS, Park KJ, Kim HS, Kim EH, Jin HM, et al. Altered Distribution and Enhanced Osteoclastogenesis of Mucosal-Associated Invariant T Cells in Gouty Arthritis. *Rheumatol (Oxford)* (2020) 59:2124–34. doi: 10.1093/rheumatology/keaa020
37. Pérez-Mazliah D, Albareda MC, Alvarez MG, Lococo B, Bertocchi GL, Petti M, et al. Allopurinol Reduces Antigen-Specific and Polyclonal Activation of Human T Cells. *Front Immunol* (2012) 3:295. doi: 10.3389/fimmu.2012.00295
38. Pousset F, Masson F, Chavirovskaia O, Isnard R, Carayon A, Golmard JL, et al. Plasma Adrenomedullin, a New Independent Predictor of Prognosis in Patients With Chronic Heart Failure. *Eur Heart J* (2000) 21:1009–14. doi: 10.1053/euhj.1999.1904
39. Nagaya N, Nishikimi T, Uematsu M, Yoshitomi Y, Miyao Y, Miyazaki S, et al. Plasma Adrenomedullin as an Indicator of Prognosis After Acute Myocardial Infarction. *Heart* (1999) 81:483–7. doi: 10.1136/hrt.81.5.483
40. Kitamura K, Sakata J, Kangawa K, Kojima M, Matsuo H, Eto T. Cloning and Characterization of cDNA Encoding a Precursor for Human Adrenomedullin. *Biochem Biophys Res Commun* (1993) 194:720–5. doi: 10.1006/bbrc.1993.1881
41. Kitamura K, Kato J, Kawamoto M, Tanaka M, Chino N, Kangawa K, et al. The Intermediate Form of Glycine-Extended Adrenomedullin Is the Major Circulating Molecular Form in Human Plasma. *Biochem Biophys Res Commun* (1998) 244:551–5. doi: 10.1006/bbrc.1998.8310
42. Kitamura K, Kangawa K, Kawamoto M, Ichiki Y, Nakamura S, Matsuo H, et al. Adrenomedullin: A Novel Hypotensive Peptide Isolated From Human Pheochromocytoma. *Biochem Biophys Res Commun* (1993) 192:553–60. doi: 10.1006/bbrc.1993.1451
43. Washimine H, Kitamura K, Ichiki Y, Yamamoto Y, Kangawa K, Matsuo H, et al. Immunoreactive Proadrenomedullin N-Terminal 20 Peptide in Human Tissue, Plasma and Urine. *Biochem Biophys Res Commun* (1994) 202:1081–7. doi: 10.1006/bbrc.1994.2039
44. Voors AA, Kremer D, Geven C, Ter Maaten JM, Struck J, Bergmann A, et al. Adrenomedullin in Heart Failure: Pathophysiology and Therapeutic Application. *Eur J Heart Fail* (2019) 21:163–71. doi: 10.1002/ejhf.1366
45. Angeletti S, Ciccozzi M, Fogolari M, Spoto S, Lo Presti A, Costantino S, et al. Procalcitonin and MR-Proadrenomedullin Combined Score in the Diagnosis and Prognosis of Systemic and Localized Bacterial Infections. *J Infect* (2016) 72:395–8. doi: 10.1016/j.jinf.2015.12.006
46. Pio R, Martinez A, Unsworth EJ, Kowalak JA, Bengoechea JA, Zipfel PF, et al. Complement Factor H Is a Serum-Binding Protein for Adrenomedullin, and the Resulting Complex Modulates the Bioactivities of Both Partners. *J Biol Chem* (2001) 276:12292–300. doi: 10.1074/jbc.M007822200
47. Kubo A, Minamino N, Isumi Y, Kangawa K, Dohi K, Matsuo H. Adrenomedullin Production Is Correlated With Differentiation in Human Leukemia Cell Lines and Peripheral Blood Monocytes. *FEBS Lett* (1998) 426:233–7. doi: 10.1016/s0014-5793(98)00349-4
48. Isumi Y, Shoji H, Sugo S, Tochimoto T, Yoshioka M, Kangawa K, et al. Regulation of Adrenomedullin Production in Rat Endothelial Cells. *Endocrinol (Philadelphia)* (1998) 139:838–46. doi: 10.1210/endo.139.3.5789
49. Sugo S, Minamino N, Shoji H, Kangawa K, Kitamura K, Eto T, et al. Interleukin-1, Tumor Necrosis Factor and Lipopolysaccharide Additively Stimulate Production of Adrenomedullin in Vascular Smooth Muscle Cells. *Biochem Biophys Res Commun* (1995) 207:25–32. doi: 10.1006/bbrc.1995.1148

Conflict of Interest: The authors declare that the research was conducted in the absence of any commercial or financial relationships that could be construed as a potential conflict of interest.

Publisher's Note: All claims expressed in this article are solely those of the authors and do not necessarily represent those of their affiliated organizations, or those of the publisher, the editors and the reviewers. Any product that may be evaluated in this article, or claim that may be made by its manufacturer, is not guaranteed or endorsed by the publisher.

frontiers in Immunology

ORIGINAL RESEARCH
published: 07 February 2022
doi: 10.3389/fimmu.2021.791983

Prevalence of Hyperuricemia Among Chinese Adults: Findings From Two Nationally Representative Cross-Sectional Surveys in 2015–16 and 2018–19

Mei Zhang[1†], Xiaoxia Zhu[2†], Jing Wu[1], Zhengjing Huang[1], Zhenping Zhao[1], Xiao Zhang[1], Yu Xue[2], Weiguo Wan[2], Chun Li[1], Wenrong Zhang[1], Linhong Wang[1], Maigeng Zhou[1], Hejian Zou[2*] and Limin Wang[1*]*

[1] National Center for Chronic and Noncommunicable Disease Control and Prevention, Chinese Center for Disease Control and Prevention, Beijing, China, [2] Division of Rheumatology, Huashan Hospital, Fudan University, Shanghai, China

Objective: To determine the nationwide prevalence of hyperuricemia in China and evaluate its trends and associated risk factors.

Methods: Using a multi-stage, stratified, cluster-randomized sampling design, two cross-sectional surveys (representative of national and provincial information) were conducted in 31 provinces (autonomous regions and municipalities) in mainland China, with 166, 861 Chinese adults in 2015–16 and 168, 351 in 2018–19. Serum uric acid (SUA) levels of all participants were measured after a >10-hour overnight fast. Hyperuricemia (HUA) was defined when SUA was >420 μmol/L. Prevalence estimates were weighted to represent the total population considering the complex sampling design. Multivariable logistic regression models was used to estimate factors associated with HUA.

Results: The overall hyperuricemia prevalence in the Chinese adult population was 11.1% (95% confidence interval 10.3% to 11.8%) in 2015–16 and 14.0% (13.1% to 14.8%) in 2018–19; an alarming rise was observed in the three years. Hyperuricemia was more common in men with 19.3% (17.9% to 20.7%) in 2015–16 and 24.4% (23.0% to 25.8%) in 2018–19, although the prevalence also escalated from 2.8% (2.5% to 3.0%) in 2015–16 to 3.6% (3.2% to 4.0%) in 2018–19 in women. The hyperuricemia risk factors include the urban culture, settlement in the East, Zhuang descent, high education, heavy or frequent beer drinking, high red meat intake, physical inactivity, high body mass index, central obesity, hypertension, hyperlipidemia, and low glomerular filtration rate.

Conclusion: The estimated hyperuricemia prevalence among Chinese adults was 14.0% in 2018-19; significant escalating trends were observed between 2015-16 and 2018-19.

Keywords: hypeuricemia, prevalence, trends, Chinese, gout

OPEN ACCESS

Edited by:
Huji Xu,
Tsinghua University, China

Reviewed by:
Beatriz Tejera Segura,
Insular University Hospital of Gran Canaria, Spain
James Cheng-Chung Wei,
Chung Shan Medical University Hospital, Taiwan

****Correspondence:***
Limin Wang
wanglimin@ncncd.chinacdc.cn
Hejian Zou
hjzou@fudan.edu.cn
Maigeng Zhou
zhoumaigeng@ncncd.chinacdc.cn

[†]These authors have contributed equally to this work

Specialty section:
This article was submitted to Autoimmune and Autoinflammatory Disorders, a section of the journal Frontiers in Immunology

Received: *09 October 2021*
Accepted: *31 December 2021*
Published: *07 February 2022*

Citation:
Zhang M, Zhu X, Wu J, Huang Z, Zhao Z, Zhang X, Xue Y, Wan W, Li C, Zhang W, Wang L, Zhou M, Zou H and Wang L (2022) Prevalence of Hyperuricemia Among Chinese Adults: Findings From Two Nationally Representative Cross-Sectional Surveys in 2015–16 and 2018–19. Front. Immunol. 12:791983. doi: 10.3389/fimmu.2021.791983

INTRODUCTION

Hyperuricemia (HUA) has gradually become an important worldwide public health issue (1). HUA is critically involved in the development of gout (2), and elevated serum uric acid (SUA) is associated with increased risks of onset and progression of chronic kidney disease, end-stage kidney disease (3, 4), cardiovascular events, and death (5, 6). People with high SUA have shown an increased risk of readmission for heart failure and longer hospital stays (7). A national health and nutrition examination survey in the United States revealed similar mortality risks for HUA and diabetes (8).

The prevalence of HUA among Chinese adults in 2009–2010 was 8.4% (9). Miao et al. reported a significantly higher HUA prevalence (18.32% in men; 8.56% in women) in coastal cities in 2008 (10), and a recent study showed HUA prevalence of 11.3% (20.7% in men; 5.6% in women) in the eastern Chinese population (21 cities from the five provinces of Shanghai, Zhejiang, Jiangsu, Anhui, and Jiangxi) in 2014-15 (11). According to a recent meta-analysis, the HUA prevalence has been increasing steadily in China in the past few decades (12). However, large-scale national population-based data is lacking in China.

In this study, data from two representative surveys, presenting national and provincial data, conducted from 2015–16 and 2018–19, were researched to determine the nationwide prevalence of HUA in China and evaluate its trends and associated risk factors.

METHODS

Study Population

The Chinese Chronic and Risk Factor Surveillance (CCDRFS) is the national system that conducts health-related surveys on Chinese adults regarding chronic and noncommunicable diseases and their risk factors. Established in 2004, CCDRFS has conducted six field surveys so far; four in 2004, 2007, 2010, and 2013 and the other two, the most recent ones, in 2015 and 2018 within the Disease Surveillance Points (DSPs) system covered 31 province (autonomous regions and municipalities) (**Supplementary 1** and **Supplementary Figure 1**). Since CCDRFS 2013, 298 surveillance counties/districts were randomly selected from the DSPs system (13, 14). These surveys were designed to represent both national and provincial data. The target population included adults aged 18 years and above and living in mainland China. The residents who met the following inclusion criteria were included: aged 18 years or older; having lived in the address for more than 6 months in the past 12 months; not pregnant; not having a serious health condition or illness that prevents from participating, including intellectual disability or language disorder. The ethical review committee of the Chinese Center for Disease Control and Prevention (China CDC) approved the CCDRFS 2015 (approval number 201519-B) and that of the National Center for Chronic and Noncommunicable Disease Control and Prevention, China CDC approved the CCDRFS 2018 (approval number 201819). All participants of the CCDRFS study consented in writing.

Sampling Methods

The CCDRFS 2015 and CCDRFS 2018 used a complex multi-stage cluster sampling method to select eligible participants within every surveillance district/county for every survey. First, three townships or subdistrict were selected using the systematic sampling method. Second, two administrative villages or communities were selected using the same sampling technique as in each chosen township/subdistrict. Third, each administrative village or community was divided into several residential quarters, each with nearly 60 households. Finally, 45 households from one residential quarter were selected to be the target households. The selected households and eligible family members were invited to participate in the survey. Both of two surveys started on Auguest and by June of the next year. In total, 82 995 of the 87 086 households in 2015–16 and 83 902 of the 89 689 households in 2018–19 completed the survey, giving a 94.4% family response rate. Of 389 617 eligible participants, 374 630 completed the interview, giving an individual response rate of 96.2%. **Figure 1** shows the detailed sampling frames.

Data Collection

Each field survey started in August of the survey year, with most interviews and exams finished in the same year. All remaining visits were completed by June of the next year. In both surveys, a householder or adult who knew the details of the household well was interviewed using a questionnaire. The economic information of the household and basic information of all family members (e.g., birth date, sex, and name) were collected. Participants who met the inclusion criteria were given individual questionnaires to obtain detailed information on demographic characteristics, lifestyle factors, and the history of chronic diseases. Smoking status was obtained using the Global Adult Tobacco Survey questionnaire. The Global Physical Activity Questionnaire was used to assess physical activity. Dietary behavior in the preceding 12 months was evaluated using a food frequency questionnaire. The participants were also invited to a community health service station for measuring physical attributes and collecting biological samples. Weight and height were measured using a standard protocol, and body mass index (BMI) was calculated by dividing the weight in kilograms by the square of height in meters. Waist circumference was measured in the standing position, midway between the lower edge of the costal arch and upper edge of the iliac crest. Systolic and diastolic blood pressures were measured three times, with one-minute intervals in between, using an electronic sphygmomanometer (HBP-1300; OMRON Healthcare Product Development Dalian Co., Ltd., Dalian, China) after the participants had rested for 5 minutes in a seated position. Therefore, each parameter was recorded three times and the average of the last two readings was used for data analysis. Blood samples were collected in the morning, after an overnight fast of ≥10 hours. In 2018-19, an oral glucose tolerance test (OGTT) was also performed; the participants without a self-reported history of diabetes were given a standard 75 g glucose solution, and plasma glucose levels were measured at 0 and 2 hours after its administration. Besides, in 2018-19, the participants were asked to collect samples of their first-morning urine at home and submit them to the interviewers when they

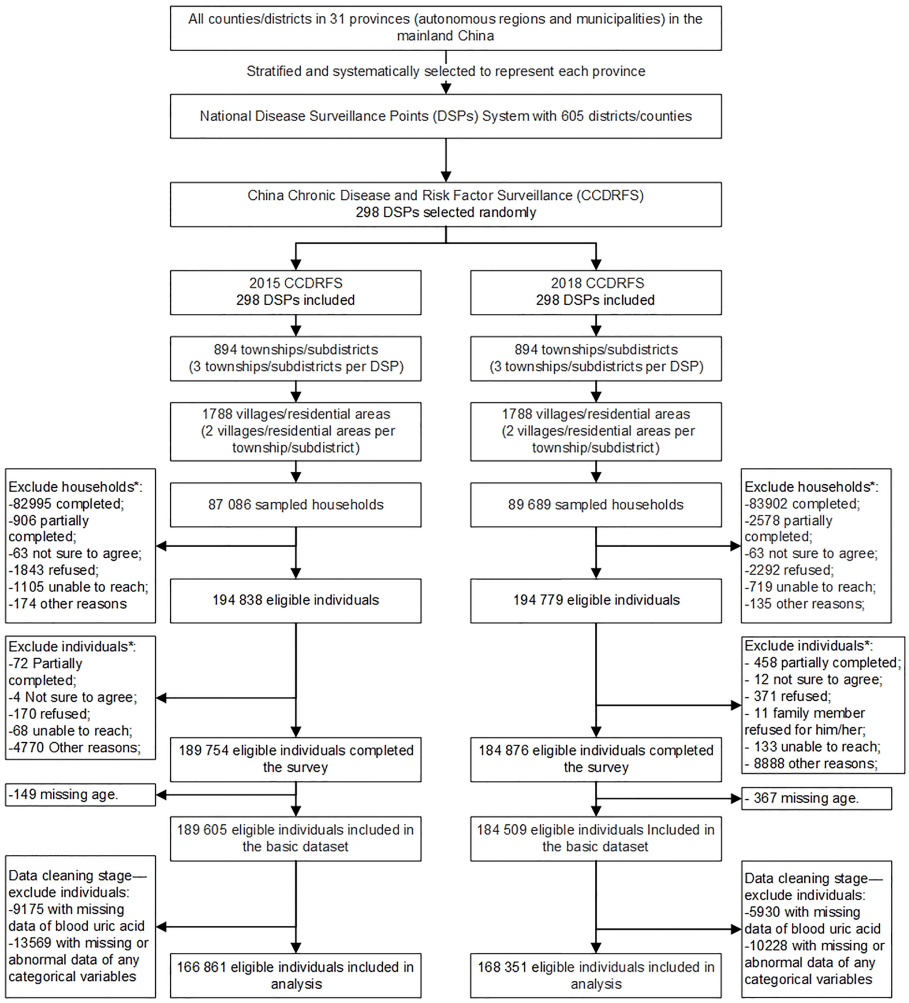

FIGURE 1 | Flow diagram of study sample.

arrived at the health service station. After pretreatment at the health service station, the plasma, serum, and urine samples were transported at 4°C within 2 h of pretreatment to the laboratories of the local Centers for Disease Control and Prevention (CDCs), and stored in a deep freezer or dry ice at −20 or −80°C, respectively. Plasma glucose was detected within 48 h after sample collection. Within one month of collection, all serum and urine samples frozen at −80°C with dry ice were shipped by air to the central laboratories. The uric acid, total cholesterol (TC), triglycerides (TG), and creatinine in serum, and creatinine and microalbumin in urine, were tested using an automatic biochemical analyzer. **Supplementary Table 1** shows the details of the methods and equipment used in the two surveys to test for biochemical indicators. Trained interviewers from the local CDCs carried out all the interviews and measurements and collected biochemical samples. All local labs were certified for quality before the analysis, and the quality was maintained and validated through daily quality checks. The central labs were certified by the College of American Pathologists and followed stringent quality control procedures for all tests.

Definition of HUA and Related Factors

Given that the level at which uricemia becomes abnormal is still disputed, we have defined HUA according to the commonly used cut-off point of 420 μmol/L, for both men and women. Besides, for HUA in women, we exclusively used a sex-specific cut-off of 360 μmol/L (9). The participants were categorized into six groups based on age: 18–29, 30–39, 40–49, 50–59, 60–69, and ≥70 years. The neighborhood committees and villages were considered as urban and rural areas, respectively. According to the geographical location, the 31 provinces (autonomous regions and municipalities) were classified into three regions: the East, Middle, and the West (**Supplementary Figure 1**). Participants were divided into the following groups based on educational attainment: those who finished primary school or less, those who finished secondary school, those who finished high school, and

those who finished college or above. Seven ethnic groups were presented: Han, Hui, Manchu, Tibetan, Uighur, Zhuang, and others (including 50 ethnic minority groups). Household per capita income was classified into four groups with tertile, and participants who refused to provide or did not know the income was categorized as a separate group. Participants who were smoking during the survey period were defined as smokers. Male participants who drank pure alcohol ≥25 g/d and female participants who drank pure alcohol ≥15 g/d were defined as heavy drinkers (15). Insufficient intake of vegetables and fruits and physical inactivity were identified based on WHO definitions (16). According to standard WHO criteria, overweight was defined by a BMI of 25.0 to 29.9 kg/m^2, and obesity by a BMI of 30.0 kg/m^2 or higher. Having a waist circumference of 90 cm or more in men and 85 cm or more in women was defined as central obesity. Hypertension was diagnosed when the systolic blood pressure was ≥140 mmHg, diastolic blood pressure was ≥90 mmHg, or the participants were taking medications for the treatment of high blood pressure during the survey period (17). High total cholesterol (TC) was defined by TC ≥ 6.22 mmol/L and high low-density lipoprotein cholesterol (LDL-C) was defined by LDL-C ≥ 4.14 mmol/L (18). Among participants without a self-reported diabetes history before the survey, those with fasting blood glucose ≥7.0 mmol/L or/and OGTT glucose ≥11.1 mmol/L were regarded as participants with newly diagnosed diabetes, and those with fasting blood glucose in the range of 6.1–6.9 mmol/L or/and OGTT glucose in the range of 7.8–11.0 mmol/L were regarded as prediabetic (19). The estimated glomerular filtration rate (eGFR) was considered low when the eGFR was <60 ml/min*1·73m^2. Albuminuria was defined as urine microprotein/creatinine >30 mg/g (20).

Statistical Analysis

We excluded 24 313 participants with missing or abnormal values for demographic or socio-economic characteristics and 15105 participants with missing or abnormal blood uric acid data. Therefore, a total of 335 212 individuals (166 861 from CCDRFS 2015 and 168 351 from CCDRFS 2018) were included in this analysis. We described the sample size of the study population and the general characteristics of Chinese adults aged 18 years and above. All estimates, including those of prevalence, proportions, and means, were adjusted for age based on China's 2010 census released by the National Bureau of Statistics. Logistic regression models were used to study the linear trends in the prevalence of hyperuricemia over the survey years. The chi-square test was used to compare prevalence estimates between groups (e.g., divided based on residential status, smoking history, and hypertension history), and logistic regression models were used to examine the trends of ordered categorical variables (e.g., age, education attainment, and income). Based on mixed data from two surveys, survey, multiariable logistic regression was used to examine the association of the odds of hyperuricemia with potential risk factors, including demographic characteristics, behaviro habits, and chronic conditions. Taylor series linearization method with a finite population correction was used to estimate standard errors (SE), accounting for the complex sampling design. All tests were two-sided, and a P-value < 0.05 was considered statistically significant. All analyses were performed using SAS 9.4 (SAS Institute, Inc., Cary, North Carolina, USA). Choropleth maps were generated using the R software (version 3.6.1).

Role of the Funding Source

The funding bodies had no role in the study design, data collection, data analysis, data interpretation, or manuscript preparation. All of the authors had full access to all the data in the study and the corresponding authors accept final responsibility to submit for publication.

RESULTS

The general characteristics of the study population and distribution of potential risk factors are shown in **Table 1**. A total of 166,861 and 168,351 adults were included in the surveys of 2015–16 and 2018–19, respectively. The weighted mean age was 43.9 (SD 16.0) years in the 2015–16 survey and 43.7 (SD 16.1) in the 2018–19 survey. Compared to those in 2015–16, the adults in 2018–19 were better educated, earned a higher income, consumed red meat more commonly, were physically inactive, and had higher TC and TG levels.

In 2018–19, the weighted prevalence of HUA was 14.0% (95% CI, 13.1–14.8%) in Chinese adults, with a higher estimate in men (24.4% [95% CI, 23.0–25.8%]) than in women (3.6% [95% CI, 3.2–4.0%]) (P<0·001). Significant age-based differences were also observed. The prevalence was the highest at 32.3% in the 18–29 years old group and then decreased with age; the lowest was at 17.0% in men in the 60–69 years old group. However, in women, the prevalence decreased in the childbearing age and increased after menopause. Besides, the prevalence increased with education and income; it was 19.0% in adults who had high education (finished college or above) and 16.9% in those with the highest income. Comparing the major ethnic groups, the HUA prevalence was the highest in Zhuang (17.1% [95% CI, 14.3–20.0%] and the lowest in Uighur (2.1% [95% CI, 0.6–3.0%]). The prevalence also differed significantly based on geography and human settlement; it was higher in the urban areas, Eastern China, and the coastal provinces (**Table 2** and **Figure 2**). And the prevalence was also higher in participants with specific health-related risk factors (e.g., smoking, heavy drinking, high red meat intake, physical inactivity, overweight or obesity, etc.; **Table 3**).

Between 2015–16 and 2018–19, the HUA prevalence had increased by 2.9% (95% CI, 2.5–3.3%, P<0.05). The increase was higher in men, younger people (18-29 and 30-39 years old), the best educated (those who finished college or above), urban adults, and those living in Eastern China (all P <0.05). Compared to 2015–16, the HUA prevalence increased in 2018–19 in the Han (P <0.05) and Manchu (P <0.05) groups, while no significant changes were observed in the other ethnic groups (**Table 2**). Furthermore, the prevalence increased more rapidly between the two periods in adults with health-related risk factors, including smoking, heavy drinking, high red meat intake,

TABLE 1 | General Characteristics of Samples in Two Surveys*.

	Men		Women		Overall	
	2015-16 (n = 77480)	2018-19 (n = 74184)	2015-16 (n = 89381)	2018-19 (n = 94167)	2015-16 (n = 166861)	2018-19 (n = 168351)
Age group (years), *n (%)*						
18-29	6356 (8.2)	3707 (5.0)	8045 (9.0)	5025 (5.3)	14401 (8.6)	8732 (5.2)
30-39	8834 (11.4)	6743 (9.1)	11114 (12.4)	9838 (10.4)	19948 (12.0)	16581 (9.8)
40-49	16420 (21.2)	12666 (17.1)	20403 (22.8)	17767 (18.9)	36823 (22.1)	30433 (18.1)
50-59	18762 (24.2)	18850 (25.4)	22182 (24.8)	25618 (27.2)	40944 (24.5)	44468 (26.4)
60-69	18056 (23.3)	21104 (28.4)	19166 (21.4)	24662 (26.2)	37222 (22.3)	45766 (27.2)
≥70	9052 (11.7)	11114 (15.0)	8471 (9.5)	11257 (12.0)	17523 (10.5)	22371 (13.3)
Urban, *n (%)*	30677 (39.6)	28859 (38.9)	37731 (42.2)	39727 (42.2)	68408 (41.0)	68586 (40.7)
Location, *n (%)*						
East	29115 (37.6)	27534 (37.1)	33888 (37.9)	35811 (38.0)	63003 (37.8)	63345 (37.6)
Middle	22718 (29.3)	20984 (28.3)	25969 (29.1)	27193 (28.9)	48687 (29.2)	48177 (28.6)
West	25647 (33.1)	25666 (34.6)	29524 (33.0)	31163 (33.1)	55171 (33.1)	56829 (33.8)
Education, *n (%)*						
Primary school or less	32173 (41.5)	30915 (41.7)	49609 (55.5)	52840 (56.1)	81782 (49.0)	83755 (49.8)
Secondary school	27514 (35.5)	26516 (35.7)	23506 (26.3)	24528 (26.0)	51020 (30.6)	51044 (30.3)
High school	11794 (15.2)	11409 (15.4)	9821 (11.0)	10511 (11.2)	21615 (13.0)	21920 (13.0)
College or higher	5999 (7.7)	5344 (7.2)	6445 (7.2)	6288 (6.7)	12444 (7.5)	11632 (6.9)
Ethnicity, *n (%)*						
Han	68607 (92.4)	65275 (88.0)	78915 (88.3)	82805 (87.9)	147522 (88.4)	148080 (88.0)
Hui	987 (0.5)	1075 (1.4)	1228 (1.4)	1366 (1.5)	2215 (1.3)	2441 (1.4)
Manchu	979 (1.2)	974 (1.3)	1141 (1.3)	1304 (1.4)	2120 (1.3)	2278 (1.4)
Tibetan	1012 (1.3)	1397 (1.9)	1342 (1.5)	1627 (1.7)	2354 (1.4)	3024 (1.8)
Uighur	1119 (1.4)	903 (1.2)	1091 (1.2)	1174 (1.2)	2210 (1.3)	2077 (1.2)
Zhuang	748 (1.0)	917 (1.2)	955 (1.1)	1311 (1.4)	1703 (1.0)	2228 (1.3)
Others	4028 (5.2)	3643 (4.9)	4709 (5.3)	4580 (4.9)	8737 (5.2)	8223 (4.9)
Income per capita (CNY), *n (%)*						
Q1 (<¥6000)	17204 (22.2)	14681 (19.8)	18418 (20.6)	17164 (18.2)	35622 (21.3)	31845 (18.9)
Q2 (¥6000-11999)	15549 (20.1)	13329 (18.0)	17750 (19.9)	16104 (17.1)	33299 (20.0)	29433 (17.5)
Q3 (¥12000-23999)	17491 (22.6)	15050 (20.3)	20558 (23.0)	19323 (20.5)	38049 (22.8)	34373 (20.4)
Q4 (≥¥24000)	14521 (18.7)	15673 (21.1)	17253 (19.3)	20471 (21.7)	31774 (19.0)	36144 (21.5)
Refused/Don't know	12715 (16.4)	15451 (20.8)	15402 (17.2)	21105 (22.4)	28117 (16.9)	36556 (21.7)
Current smoking, *n (%)*	40884 (52.8)	37841 (51.0)	2642 (3.0)	2627 (2.8)	43526 (26.1)	40468 (24.0)
Heavy drinking, *n (%)*	15745 (20.3)	13172 (17.8)	4231 (4.7)	1327 (1.4)	19976 (12.0)	14499 (8.6)
Beer drinking, *n (%)*						
Never	53902 (69.6)	57113 (77.0)	82836 (92.7)	88517 (94.0)	136738 (81.9)	145630 (86.5)
At least once a year	13779 (17.8)	9683 (13.1)	5386 (6.0)	4614 (4.9)	19165 (11.5)	14297 (8.5)
At least once a week	9799 (12.6)	7388 (10.0)	1159 (1.3)	1036 (1.1)	10958 (6.6)	8424 (5.0)
Fruit/vegetable intake <400g/d, *n (%)*	42127 (54.4)	35319 (47.6)	48289 (54.0)	43688 (46.4)	90416 (54.2)	79007 (46.9)
Red meat intake ≥ 100g/d, *n (%)*	23561 (30.4)	31229 (42.1)	18777 (21.0)	29353 (31.2)	42338 (25.4)	60582 (36.0)
Physical inactivity (<150min/w), *n (%)*	15670 (20.2)	16276 (21.9)	14654 (16.4)	16683 (17.7)	30324 (18.2)	32959 (19.6)
BMI group (kg/m^2), *n (%)*						
<18.5	2720 (3.5)	2164 (2.9)	3470 (3.9)	2819 (3.0)	6190 (3.7)	4983 (3.0)
18.5-24.9	45399 (58.6)	41001 (55.3)	51300 (57.4)	51418 (54.6)	96699 (58.0)	92419 (54.9)
25.0-29.9	25087 (32.4)	26228 (35.4)	28466 (31.8)	32685 (34.7)	53553 (32.1)	58913 (35.0)
≥30.0	4274 (5.5)	4791 (6.5)	6145 (6.9)	7245 (7.7)	10419 (6.2)	12036 (7.1)
Central obesity, *n (%)*	23410 (30.2)	27369 (36.9)	30794 (34.5)	39639 (42.1)	54204 (32.5)	67008 (39.8)
Hypertension, *n (%)*	32309 (41.7)	32429 (43.7)	33928 (38.0)	37145 (39.4)	66237 (39.7)	69574 (41.3)
High TC, *n (%)*	5077 (6.6)	6819 (9.2)	7537 (8.4)	11331 (12.0)	12614 (7.6)	18150 (10.8)
High TG, *n (%)*	13743 (17.7)	15288 (20.6)	12316 (13.8)	16696 (17.7)	26059 (15.6)	31984 (19.0)
Glycemia status, *n (%)*						
Normal	NA	42288 (58.7)	NA	56177 (62.1)	NA	98465 (60.6)
Prediabetes	NA	16772 (23.3)	NA	19501 (21.6)	NA	36273 (22.3)
Newly diagnosed diabetes	NA	7799 (10.8)	NA	7778 (8.6)	NA	15577 (9.6)
Diagnosed diabetes	NA	5148 (7.1)	NA	7000 (7.7)	NA	12148 (7.5)
Low eGFR, *n (%)*	NA	3073 (4.3)	NA	3528 (3.9)	NA	6601 (4.1)
Albuminuria, *n (%)*	NA	5999 (8.3)	NA	8582 (9.5)	NA	14581 (9.0)

**Percentages may not sum to 100 due to rounding. NA, data not available; BMI, body mass index; TC, total cholesterol; TG, triglycerides; eGFR, estimated glomerular filtration rate. ¥ 100, £11; €13; $15.5.*

TABLE 2 | Prevalence of hyperuricemia among adult in mainland China by characteristics, 2015-16 and 2018-19*.

Characteristics	Prevalence, % (95%CI)								
	Men			Women[$]			Overall		
	2015-16	2018-19	Changes of prevalence, 2018-19 vs 2015-16	2015-16	2018-19	Changes of prevalence, 2018-19 vs 2015-16	2015-16	2018-19	Changes of prevalence, 2018-19 vs 2015-16
Overall	19.3 (17.9,20.7)	24.4 (23.0,25.8)	5.1 (4.4,5.8)[†]	2.8 (2.5,3.0)[‡]	3.6 (3.2,4.0)[†]	0.8 (0.6,1.1)[†]	11.1 (10.3,11.8)	14.0 (13.1,14.8)	2.9 (2.5,3.3)[†]
Age group (years)									
18-29	23.9 (21.7,26.1)	32.3 (29.4,35.3)	8.4 (6.7,10.1)[†]	2.7 (2.2,3.1)	4.2 (3.2,5.2)	1.5 (0.9,2.1)[†]	13.4 (12.2,14.6)	18.0 (16.1,19.8)	4.6 (3.7,5.6)[†]
30-39	20.6 (19.1,22.1)	28.4 (26.0,30.7)	7.8 (6.6,8.9)[†]	1.7 (1.3,2.0)	2.3 (1.8,2.9)	0.7 (0.3,1.0)	11.3 (10.4,12.1)	15.5 (14.2,16.9)	4.3 (3.6,4.9)[†]
40-49	18.6 (16.1,21.1)	21.4 (20.0,22.9)	2.8 (1.5,4.1)[†]	2.1 (1.7,2.5)	2.2 (1.9,2.5)	0.1 (-0.2,0.3)	10.4 (9.0,11.7)	11.8 (11.1,12.5)	1.4 (0.7,2.1)
50-59	15.4 (14.4,16.5)	18.1 (17.0,19.3)	2.7 (1.9,3.5)[†]	2.8 (2.5,3.1)	3.7 (3.2,4.1)	0.9 (0.6,1.2)[†]	9.2 (8.6,9.7)	10.9 (10.2,11.6)	1.8 (1.3,2.2)[†]
60-69	15.0 (13.9,16.0)	17.0 (15.9,18.0)	2.0 (1.2,2.7)[†]	4.0 (3.5,4.4)	4.4 (4.0,4.8)	0.4 (0.1,0.7)	9.5 (8.9,10.2)	10.7 (10.1,11.4)	1.2 (0.7,1.7)[†]
≥70	17.0 (15.3,18.7)	19.5 (18.2,20.7)	2.4 (1.3,3.5)[†]	6.3 (5.5,7.2)	8.0 (7.0,9.1)	1.7 (0.9,2.4)[†]	11.3 (10.2,12.4)	13.4 (12.4,14.4)	2.1 (1.2,2.9)[†]
P for trend	<0.0001	<0.0001		<0.0001	<0.0001		<0.0001	<0.0001	
Residence									
Urban	22.5 (20.4,24.6)	28.1 (26.1,30.2)	5.7 (4.6,6.8)[†]	2.9 (2.6,3.3)	4.1 (3.4,4.7)	1.1 (0.7,1.5)[†]	12.8 (11.7,13.9)	16.1 (14.8,17.3)	3.3 (2.7,3.9)[†]
Rural	16.0 (15.1,16.9)	20.4 (19.1,21.8)	4.4 (3.7,5.2)[†]	2.6 (2.3,2.9)	3.1 (2.8,3.5)	0.5 (0.3,0.8)[†]	9.3 (8.7,9.8)	11.7 (10.9,12.5)	2.4 (2.0,2.9)[†]
P for difference	<0.0001	<0.0001		0.1316	0.0099		<0.0001	<0.0001	
Location									
East	21.5 (18.9,24.1)	29.6 (27.0,32.2)	8.1 (7.0,9.3)[†]	2.8 (2.5,3.1)	4.8 (4.0,5.6)	2.0 (1.6,2.5)[†]	12.2 (10.8,13.6)	17.1 (15.5,18.8)	5.0 (4.3,5.6)[†]
Middle	16.3 (14.7,17.9)	18.4 (17.0,19.8)	2.1 (1.2,3.0)[†]	2.6 (2.2,3.0)	2.6 (2.2,3.0)	0.0 (-0.2,0.3)	9.4 (8.5,10.2)	10.4 (9.7,11.2)	1.0 (0.5,1.5)[†]
West	19.5 (17.9,21.1)	23.1 (21.2,25.0)	3.6 (2.4,4.8)[†]	3.0 (2.4,3.6)	2.8 (2.4,3.3)	-0.2 (-0.5,0.2)	11.4 (10.4,12.3)	13.0 (12.0,14.1)	1.7 (1.1,2.3)[†]
P for difference	<0.0001	<0.0001		0.4642	<0.0001		<0.0001	<0.0001	
Education									
Primary school or less	15.8 (14.7,16.8)	18.1 (16.9,19.3)	2.4 (1.6,3.2)[†]	3.2 (2.9,3.5)	3.8 (3.4,4.2)	0.6 (0.4,0.8)[†]	8.4 (7.8,8.9)	9.6 (9.0,10.2)	1.3 (0.9,1.6)[†]
Secondary school	18.1 (16.5,19.8)	21.4 (19.9,22.8)	3.2 (2.3,4.2)[†]	2.3 (1.9,2.7)	3.4 (2.9,4.0)	1.1 (0.8,1.5)[†]	11.1 (10.2,12.0)	13.3 (12.4,14.2)	2.3 (1.7,2.8)[†]
High school	22.7 (19.4,26.0)	29.1 (26.3,32.0)	6.4 (4.9,7.9)[†]	2.5 (2.0,3.0)	3.7 (2.9,4.5)	1.2 (0.7,1.7)[†]	14.3 (12.2,16.4)	18.1 (16.3,19.9)	3.8 (2.8,4.8)[†]
College or higher	24.8 (22.7,26.9)	34.9 (32.1,37.7)	10.1 (8.3,11.9)[†]	2.7 (2.0,3.5)	3.4 (2.3,4.5)	0.6 (-0.1,1.4)	14.0 (12.9,15.1)	19.0 (17.3,20.6)	4.9 (3.8,6.0)[†]
P for trend	<0.0001	<0.0001		0.0781	0.4927		<0.0001	<0.0001	
Ethnicity									
Han	19.1 (17.6,20.6)	24.7 (23.2,26.2)	5.6 (4.8,6.3)[†]	2.7 (2.5,3.0)	3.6 (3.2,4.0)	0.9 (0.6,1.1)[†]	11.0 (10.2,11.8)	14.1 (13.2,15.0)	3.1 (2.7,3.6)[†]
Hui	17.3 (12.4,22.2)	18.1 (8.9,27.4)	0.8 (-4.1,5.7)	3.7 (1.2,6.1)	1.7 (0.6,2.8)	-2.0 (-3.4,-0.5)	9.8 (7.4,12.2)	9.2 (4.7,13.7)	-0.6 (-3.0,1.8)
Manchu	17.2 (13.3,21.1)	19.2 (16.3,22.1)	2.1 (-0.6,4.8)	4.1 (2.5,5.8)	7.5 (4.1,10.9)	3.4 (1.3,5.5)	10.3 (8.4,12.3)	13.5 (11.5,15.5)	3.1 (1.6,4.7)[†]
Tibetan	27.6 (11.7,43.5)	23.4 (19.2,27.7)	-4.1 (-13.1,4.9)	3.5 (1.6,5.3)	1.8 (0.2,3.5)	-1.6 (-2.8,-0.4)	13.9 (5.8,22.0)	12.4 (9.7,15.1)	-1.5 (-5.7,2.6)
Uighur	5.0 (3.5,6.6)	4.0 (1.3,6.6)	-1.0 (-2.6,0.6)	0.3 (0.0,0.8)	0.2 (0.0,0.4)	-0.2 (-0.5,0.2)	2.8 (1.8,3.8)	2.1 (0.6,3.6)	- 0.7 (-1.7,0.3)
Zhuang	28.4 (24.0,32.9)	32.2 (23.7,40.7)	3.8 (-1.4,8.9)	8.0 (6.0,9.9)	4.5 (2.0,7.0)	-3.5 (-5.3,-1.8)[†]	17.1 (14.3,20.0)	17.1 (12.7,21.5)	0.0 (-2.6,2.5)
Others	26.3 (23.5,29.1)	24.7 (20.8,28.5)	-1.6 (-3.8,0.6)	2.9 (1.8,4.0)	3.0 (2.1,3.8)	0.1 (-0.5,0.6)	14.4 (12.9,16.0)	13.3 (11.3,15.4)	-1.1 (-2.1,-0.2)
P for difference	<0.0001	<0.0001		<0.0001	<0.0001		<0.0001	<0.0001	

(Continued)

TABLE 2 | Continued

Characteristics	Prevalence, % (95%CI)								
	Men			Women[§]			Overall		
	2015-16	2018-19	Changes of prevalence, 2018-19 vs 2015-16	2015-16	2018-19	Changes of prevalence, 2018-19 vs 2015-16	2015-16	2018-19	Changes of prevalence, 2018-19 vs 2015-16
Income per capita (CNY)									
Q1 (¥<6000)	15.1 (13.8,16.3)	17.4 (15.6,19.1)	2.3 (1.2,3.4)[†]	2.7 (2.3,3.2)	2.9 (2.4,3.5)	0.2 (- 0.2,0.6)	9.0 (8.3,9.6)	10.2 (9.3,11.2)	1.3 (0.7,1.9)[†]
Q2 (¥6000-11999)	16.4 (15.0,17.7)	20.5 (18.2,22.8)	4.1 (2.7,5.6)[†]	2.7 (2.3,3.2)	3.2 (2.5,3.8)	0.5 (0.1,0.9)	9.5 (8.8,10.3)	11.9 (10.6,13.2)	2.4 (1.6,3.2)[†]
Q3 (¥12000-23999)	19.5 (18.1,20.9)	25.9 (23.7,28.0)	6.4 (5.1,7.6)[†]	2.6 (2.3,3.0)	4.0 (3.3,4.7)	1.4 (0.9,1.8)[†]	11.2 (10.4,12.0)	14.8 (13.5,16.1)	3.7 (2.9,4.4)[†]
Q4 (≥¥24000)	24.6 (21.9,27.2)	29.6 (27.1,32.1)	5.0 (4.0,6.0)[†]	2.8 (2.5,3.1)	4.1 (3.3,4.8)	1.3 (0.9,1.7)[†]	13.9 (12.4,15.4)	16.9 (15.3,18.5)	3.0 (2.5,3.6)[†]
Refused/Don't know [‡]	19.6 (17.4,21.8)	25.1 (22.5,27.6)	5.4 (3.7,7.2)[†]	3.0 (2.5,3.6)	3.5 (2.9,4.1)	0.4 (0.0,0.8)	11.1 (10.0,12.2)	13.9 (12.5,15.3)	2.8 (1.9,3.7)[†]
P for trend	<0.0001	<0.0001		0.9119	0.0060		<0.0001	<0.0001	

**Data are presented incorporating sample weights and adjusted for clusters and strata of the complex sample design of CCDRFS. [†]P values for changes from 2015-16 to 2018-19 are <0.05. [‡]Participants who answered "I don't know or I don't want to tell you" are not included in the trend test. [§]P values for difference between men and women are <0.05. 95% CI=95% confidence interval. NA, data not available. ¥ 100= £11/€13/$15.5.*

physical inactivity, BMI ≥25 kg/m^2, central obesity, high TC and TG levels (all P <0.05, **Table 3**). The estimated HUA prevalence in women increased from 9.6 to 11.5% between 2015–16 and 2018–19, when HUA was defined as SUA >360 μmol/L (**Supplementary Table 3**).

We further estimated the mean levels of SUA. From 2015–16 to 2018–19, the mean levels of SUA among Chinese adults increased from 310.0 μmol/L (95% CI 306.6– 313.4 μmol/L) to 320.8 μmol/L (95% CI 317.8–323.9 μmol/L, P<0.0001), with a higher increase observed in men (**Supplementary Table 2**). It reached 387.3 μmol/L (95% CI 379.7–394.9 μmol/L) in men aged 18–29 years in 2018–19 (**Supplementary Table 4**). Furthermore, the percentage with severely high SUA levels increased notably; 15.3% had SUA values >540 μmol/L and 5.3% had SUA values >600 μmol/L. Severely high SUA levels were more common in the urban residences, and the adults with younger age or higher education (**Supplementary Table 5**).

The risk factors for HUA were evaluated using data combined from the two surveys (**Figure 3**). Factors that were significantly associated with HUA include age between 18 and 29 years or above 70 years, urban residency, location in East, Zhuang descent, high income, red meat intake >100 g/d, physical inactivity, high BMI, central obesity, hypertension, and high TC and TG levels. In addition, Tibetan descent, age 30–39 years, heavy alcohol/beer drinking at least once a week, and high educational qualification were risk factors of HUA in men. Smoking was inversely correlated with HUA in men. Based on the 2018–19 data, prediabetes, diabetes, low eGFR, and albuminuria were notable risk factors associated with HUA.

DISCUSSION

This nationwide study estimated that approximately 14.0% of Chinese adults (18 years or older) had HUA in 2018–19, among them 15.2% had an SUA value >540 μmol/L and 5.3% had an SUA value >600 μmol/L. HUA prevalence had significantly increased in three years from 11.1% in 2015–16 to 14.0% in 2018–19. In the national survey in 2009–10, the overall HUA prevalence in Chinese adults was 8.4% (9). The sustained increase in the prevalence of HUA in the past decade indicates that HUA has reached warning levels in the general Chinese population.

The HUA prevalence in China is similar to that in developed countries. A national survey in Japan reported an HUA prevalence of 13.4% in 2016–17 (21), while national research in the United States (US) reported HUA prevalences of 14.6% in 2015–16 and 15.9% in 2007–08, suggesting that the HUA prevalence in the US was stable over the past decade (22). However, the HUA prevalence is steadily growing in China, attributed to its booming economy and large-scale urbanization (23). Economic development has brought about lifestyle changes that have increased the prevalence of metabolic diseases, such as HUA, obesity, diabetes, and hypertension (24). Moreover, increased red meat intake, physical inactivity, higher BMI, and central obesity were observed in 2018–19 compared to that in 2015–16.

HUA appears to be more common in men. A prevalence of 24.7% in men and 5.2% in women was reported in the US in 2015–16 (22). Our values were similar to these, with a prevalence of 24.4% in men and 3.6% in women in 2018–19 in China. The lower HUA prevalence and SUA levels in women may be hormonal, attributed to the effects of estrogen, or their lifestyles (25, 26). HUA prevalence in women in China was reported to be 7.0% in a national survey in 2009–10 with HUA defined as SUA>360 μmol/L. This percentage rose to 11.5% in 2018–19, when HUA was defined to be SUA >360 μmol/L in our survey; 7.9% of Chinese women had SUA levels between 360 and 420 μmol/L. However, it is inappropriate to classify women with

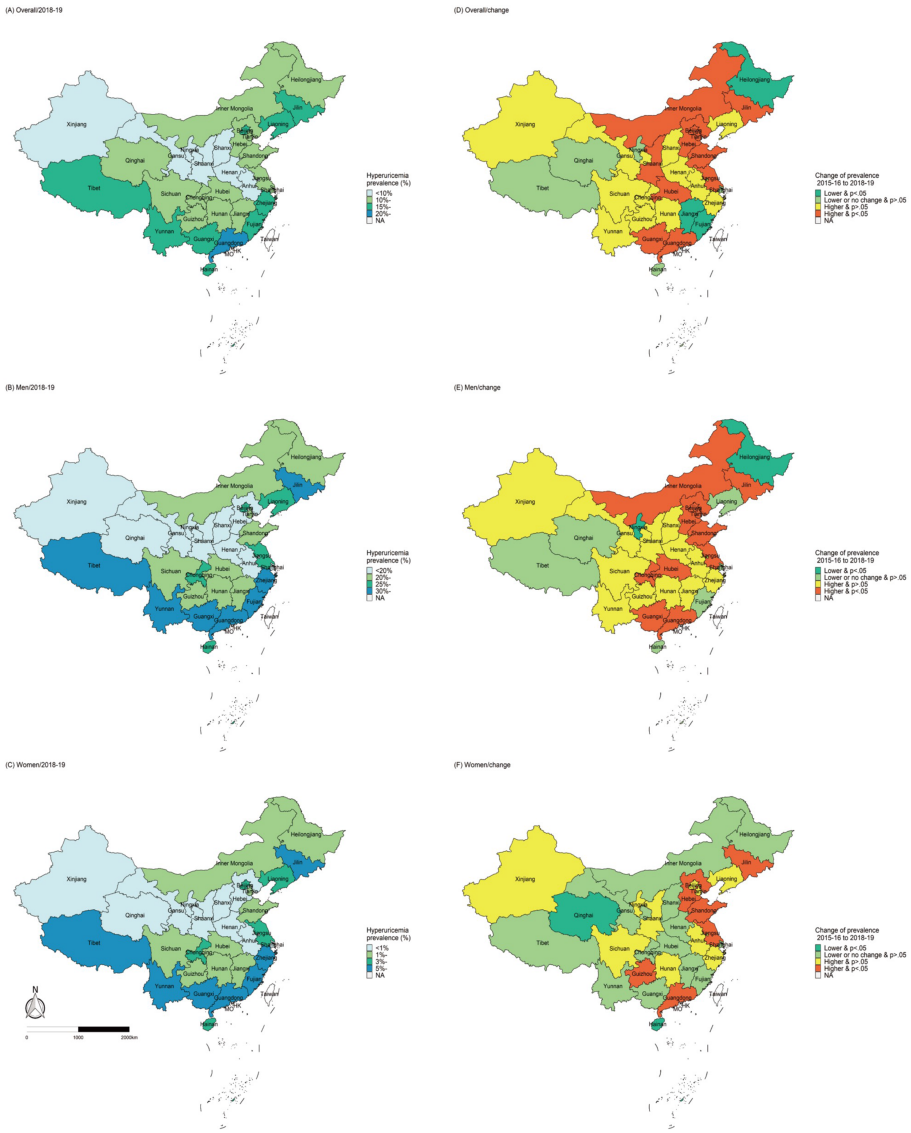

FIGURE 2 | Geographic distribution of hyperuricemia prevalence in 2018–19 and changes from 2015–16 to 2018–19.

SUA levels of 360–420 μmol/L as positive for HUA because there is lacking of definited evidence that SUA levels >360 μmol/L in women are beyond the saturation level in blood and cause possible pathological injury. In this study, we have defined HUA with an SUA level >420 μmol/L, regardless of sex (27, 28), although research has shown that the SUA threshold for all-cause mortality was 320 μmol/L in men and 280 μmol/L in women in Italian cohorts (29). Above all, The prevalence of HUA in Chinese women has been rising steadily in the past decade, and the female population with SUA levels of 360–420 μmol/L may be at a high risk of developing HUA.

The risk factors for HUA were evaluated in this study. Age (18–29 or >70 years), urban culture, geographical location (settlers in the East), high education, Zhuang descent, heavy drinking or frequent beer drinking, high red meat intake, physical inactivity, high BMI or central obesity, hypertension, hyperlipidemia, prediabetes, diabetes, and low eGFR were risk factors for HUA. We observed a significantly high prevalence amongst young people aged 18-29 years old in China, which may be a result of unhealthy lifestyles, including high-stress levels at work, the habit of eating out, physical inactivity, and high-fructose intake (7, 26, 30–32). Recent research has shown that HUA occurs earlier than other metabolic disorders, including hypertension, hypertriglyceridemia, and diabetes mellitus, suggesting that HUA may play an upstream role in cardio-metabolic disease development (33). HUA has been confirmed to be an independent risk factor for metabolic disorders, and in our research the metabolic disorders, including obesity, hypertension, hyperlipidemia, and diabetes, have shown associations with HUA.

TABLE 3 | Prevalence of hyperuricemia among adults in mainland China by risk factors and major chronic diseases, 2015-16 and 2018-19*.

Characteristics	Prevalence, 95% CI								
	Men			Women			Overall		
	2015-16	2018-19	Changes of prevalence, 2018-19 vs 2015-16	2015-16	2018-19	Changes of prevalence, 2018-19 vs 2015-16	2015-16	2018-19	Changes of Prevalence, 2018-19 vs 2015-16
Current smoking									
Yes	18.4 (17.2,19.7)	22.7 (21.3,24.1)	4.3(3.5,5.0)†	3.7 (2.7,4.7)	3.7 (2.7,4.7)	0.0(-0.7,1.0)	17.9 (16.7,19.0)	21.9 (20.6,23.3)	4.1(3.4,4.8)†
No	20.3 (18.5,22.1)	26.2 (24.2,28.1)	5.9(4.9,6.8)†	2.8 (2.5,3.0)	3.6 (3.2,4.0)	0.9(0.6,0.0)†	8.5 (7.9,9.2)	13.0 (12.2,13.8)	2.7(2.3,3.1)†
P for difference	0.0047	<0.0001		0.0436	0.8691		<0.0001	<0.0001	
Heavy drinking									
Yes	22.5 (19.5,25.6)	26.2 (24.2,28.2)	3.7(2.0,5.4)†	3.4 (2.5,4.2)	5.5 (3.5,7.5)	2.2(1.0,0.1)	18.5 (16.2,20.7)	24.8 (23.0,26.6)	6.3(5.0,7.7)†
No	18.5 (17.4,19.7)	24.1 (22.7,25.6)	5.6(4.9,6.3)†	2.7 (2.5,3.0)	3.6 (3.2,4.0)	0.9(0.6,0.0)†	10.0 (9.4,10.6)	13.0 (12.2,13.8)	3.0(2.6,3.4)†
P for difference	<0.0001	<0.0001		0.1588	0.0309		<0.0001	<0.0001	
Beer drinking									
Never	17.9 (17.0,18.9)	23.0 (21.6,24.4)	5.1(4.3,5.9)†	2.8 (2.6,3.1)	3.7 (3.3,4.1)	0.9(0.6,1.1)†	9.0 (8.5,9.4)	11.9 (11.1,12.6)	2.9(2.4,3.3)†
At least once/ year	20.5 (17.9,23.1)	26.0 (23.5,28.5)	5.5(4.2,6.9)†	2.0 (1.5,2.6)	2.8 (2.0,3.5)	0.7(0.2,1.2)	15.6 (13.6,17.6)	19.3 (17.4,21.1)	3.7(2.7,4.6)†
At least once/ week	23.1 (19.9,26.2)	29.2 (26.7,31.8)	6.2(4.4,7.9)†	4.7 (2.1,7.2)	3.7 (2.1,5.3)	-1.0(-2.6,0.6)	21.5 (18.5,24.4)	27.1 (24.8,29.4)	5.6(4.0,7.3)†
P for trend	<0.0001	<0.0001		0.9621	0.1290		<0.0001	<0.0001	
Fruit & vegetable intake <400g/d									
Yes	18.8 (17.6,20.0)	25.1 (22.8,27.4)	6.3(5.2,7.4)†	2.9 (2.6,3.3)	3.3 (3.0,3.7)	0.4(0.2,0.7)	11.0 (10.2,11.7)	14.4 (13.1,15.7)	3.4(2.8,4.1)†
No	19.9 (18.1,21.7)	23.9 (22.6,25.1)	4.0(3.1,4.9)†	2.6 (2.4,2.9)	3.8 (3.3,4.3)	1.2(0.9,1.5)†	11.2 (10.3,12.1)	13.6 (12.9,14.4)	2.4(2.0,2.9)†
P for difference	0.1026	0.33		0.1077	0.1112		0.5070	0.2584	
Red meat intake >100g/d									
Yes	23.2 (21.7,24.7)	29.2 (27.3,31.1)	6.0(5.2,6.8)†	2.9 (2.6,3.3)	4.7 (3.8,5.5)	1.7(1.1,2.2)†	15.3 (14.4,16.2)	19.0 (17.6,20.5)	3.7(3.1,4.4)†
No	17.3 (16.0,18.7)	19.8 (18.3,21.3)	2.5(1.5,3.5)†	2.6 (2.4,2.9)	3.0 (2.7,3.4)	0.3(0.1,0.5)	10.7 (9.9,11.5)	13.3 (12.4,14.1)	0.9(0.4,1.4)
P for difference	<0.0001	<0.0001		0.2911	<0.0001		<0.0001	<0.0001	
Physical inactivity (<150min/w)									
Yes	20.0 (18.5,21.6)	26.1 (24.0,28.2)	6.1(4.9,7.3)†	3.0 (2.5,3.6)	4.6 (3.8,5.3)	0.7(0.4,1.0)†	12.5 (11.5,13.4)	16.4 (15.0,17.7)	3.9(3.1,4.7)†
No	19.1 (17.5,20.8)	23.9 (22.4,25.3)	4.8(4.0,5.5)†	2.7 (2.5,2.9)	3.4 (3.0,3.8)	1.3(0.9,1.8)†	10.7 (9.9,11.5)	13.3 (12.4,14.1)	2.6(2.2,3.0)†
P for difference	0.3864	0.0349		0.0372	0.0021		0.0018	<0.0001	
BMI group (kg/m^2)									
<18.5	9.8 (7.2,12.3)	17.5 (11.1,23.8)	7.7(3.5,11.9)	1.4 (0.9,1.8)	0.8 (0.4,1.2)	-0.6(-0.9,-0.2)	5.2 (4.1,6.4)	8.4 (5.0,11.8)	3.2(1.1,5.3)
18.5-24.9	14.6 (12.8,16.4)	17.6 (16.3,18.9)	3.0(2.1,3.8)†	1.9 (1.6,2.1)	2.4 (2.1,2.7)	0.5(0.3,0.7)†	8.0 (7.1,9.0)	9.5 (8.8,10.2)	1.4(1.0,1.8)†
25.0-29.9	25.4 (23.7,27.2)	29.8 (28.0,31.5)	4.3(3.3,5.4)†	3.6 (3.1,4.0)	5.0 (4.3,5.8)	1.5(1.0,1.9)†	15.4 (14.3,16.4)	18.5 (17.4,19.7)	3.2(2.5,3.8)†
≥30.0	35.8 (33.3,38.2)	46.9 (43.0,50.7)	11.1(8.7,13.5)†	9.1 (7.8,10.4)	10.0 (8.1,11.8)	0.9(-0.3,2.1)	22.6 (21.3,24.0)	30.1 (27.4,32.9)	7.5(5.9,9.1)†
P for trend	<0.0001	<0.0001		<0.0001	<0.0001		<0.0001	<0.0001	
Central obesity									
Yes	27.4 (25.6,29.1)	33.4 (31.5,35.3)	6.0(4.9,7.2)†	5.0 (4.6,5.5)	6.1 (5.4,6.9)	1.1(0.7,1.6)†	16.5 (15.5,17.5)	20.5 (19.2,21.8)	4.0(3.3,4.7)†
No	15.9 (14.3,17.4)	19.1 (17.6,20.7)	3.3(2.5,4.0)†	1.9 (1.6,2.1)	2.4 (2.0,2.7)	0.5(0.3,0.7)†	8.8 (8.0,9.6)	10.5 (9.6,11.3)	1.6(1.2,2.0)†

(Continued)

TABLE 3 | Continued

Characteristics	Prevalence, 95% CI								
	Men			Women			Overall		
	2015-16	2018-19	Changes of prevalence, 2018-19 vs 2015-16	2015-16	2018-19	Changes of prevalence, 2018-19 vs 2015-16	2015-16	2018-19	Changes of Prevalence, 2018-19 vs 2015-16
P for difference	<0.0001	<0.0001		<0.0001	<0.0001		<0.0001	<0.0001	
Hypertension									
Yes	22.1 (20.7,23.5)	27.0 (25.5,28.5)	4.9(3.9,5.8)†	4.8 (4.3,5.3)	6.3 (5.5,7.0)	1.5(1.0,1.9)†	14.2 (13.3,15.0)	17.8 (16.8,18.8)	3.6(3.0,4.3)†
No	18.0 (16.4,19.7)	23.3 (21.7,24.9)	5.3(4.5,6.1)†	2.0 (1.8,2.3)	2.8 (2.4,3.2)	0.7(0.5,1.0)†	10.6 (9.9,11.4)	12.5 (11.6,13.5)	2.7(2.3,3.1)†
P for difference	<0.0001	<0.0001		<0.0001	<0.0001		<0.0001	<0.0001	
Diabetes status									
Normal	NA	24.1 (22.5,25.7)	NA	NA	2.6 (2.3,3.0)	NA	NA	12.9 (12.0,13.8)	NA
Prediabetes	NA	26.9 (24.9,29.0)	NA	NA	5.6 (4.7,6.5)	NA	NA	17.2 (15.8,18.5)	NA
Diabetes without treatment	NA	26.0 (23.6,28.4)	NA	NA	7.3 (6.2,8.4)	NA	NA	18.2 (16.6,19.7)	NA
Diabetes treated	NA	16.8 (14.3,19.4)	NA	NA	6.9 (5.9,8.0)	NA	NA	11.7 (10.1,13.2)	NA
P for difference		<0.0001			<0.0001			<0.0001	
Low eGFR									
Yes	NA	52.6 (49.3,56.0)	NA	NA	25.3 (22.6,28.0)	NA	NA	38.0 (35.7,40.3)	NA
No	NA	23.8 (22.4,25.3)	NA	NA	3.1 (2.7,3.4)	NA	NA	13.4 (12.6,14.3)	NA
P for difference		<0.0001			<0.0001			<0.0001	
Albuminuria									
Yes	NA	31.4 (28.7,34.1)	NA	NA	6.8 (5.9,7.7)	NA	NA	18.5 (16.8,20.2)	NA
No	NA	23.9 (22.6,25.3)	NA	NA	3.4 (3.0,3.8)	NA	NA	13.8 (12.9,14.6)	NA
P for difference		<0.0001			<0.0001			<0.0001	
High TC									
Yes	30.3 (27.3,33.2)	36.2 (32.4,39.9)	5.9(4.1,7.7)†	6.5 (5.4,7.6)	8.9 (7.1,10.7)	2.4(1.2,3.5)†	17.9 (16.5,19.2)	22.7 (20.4,25.1)	4.9(3.7,6.0)†
No	18.7 (17.3,20.0)	23.3 (22.0,24.7)	4.7(3.9,5.4)†	2.5 (2.3,2.8)	3.1 (2.8,3.5)	0.6(0.4,0.8)†	10.6 (9.9,11.4)	13.2 (12.4,13.9)	2.5(2.1,2.9)†
P for difference	<0.0001	<0.0001		<0.0001	<0.0001		<0.0001	<0.0001	
High TG									
Yes	34.1 (32.3,35.9)	40.7 (38.4,43.1)	6.6(5.2,8.0)†	8.5 (7.4,9.6)	8.8 (7.7,9.8)	0.3(-0.5,1.1)	24.6 (23.4,25.8)	29.3 (27.4,31.1)	4.6(3.6,5.7)†
No	15.9 (14.3,17.5)	19.4 (18.1,20.7)	3.5(2.7,4.2)†	2.1 (1.9,2.2)	2.8 (2.5,3.2)	0.8(0.5,1.0)†	8.7 (7.9,9.5)	10.5 (9.8,11.3)	1.8(1.5,2.2)†
P for difference	<0.0001	<0.0001		<0.0001	<0.0001		<0.0001	<0.0001	

**Data are presented incorporating sample weights and adjusted for clusters and strata of the complex sample design of CCDRFS. †P values for changes from 2015-16 to 2018-19 are <0.05. 95% CI, 95% confidence interval. NA, data not available; BMI, body mass index; TC, total cholesterol; TG, triglycerides; eGFR, estimated glomerular filtration rate.*

Eastern China has a relatively higher prevalence of metabolic diseases than the rest of the country (34, 35). A regional survey of the eastern Chinese population from January 2014 to December 2015 sh2owed an HUA prevalence of 11.3% (11). Our results showed that the prevalence, which was 12.2% in 2015–16, ascended to 17.1% in 2018–19. It may be attributed to the developed economy (36) and abundant seafood consumption in the coastal areas (10).

We observed notable differences in HUA prevalence among different ethnicities in China. The prevalence was 14.1% in the Han, as high as 17.1% in the Zhuang, as low as 2.1% in the Uighur in 2018–19. The mean SUA level was also strikingly lower in the Uighur than in the other ethnic group. These ethnic variations of HUA prevalence may be associated with their different lifestyles. A recent survey in Xinjiang reported a similarly low HUA prevalence in the Uighur community (37), and correlated it with the low alcohol intake in Uighur. However, apart from lifestyles, genetic backgrounds may potentially influence the HUA prevalence among the different ethnic groups.

To our knowledge, the CCDRFS is the only surveillance that provide both national and preovincial representative information on chronic diseases and risk factors, including uric acid level in China. Standardized survey instruments, consistent

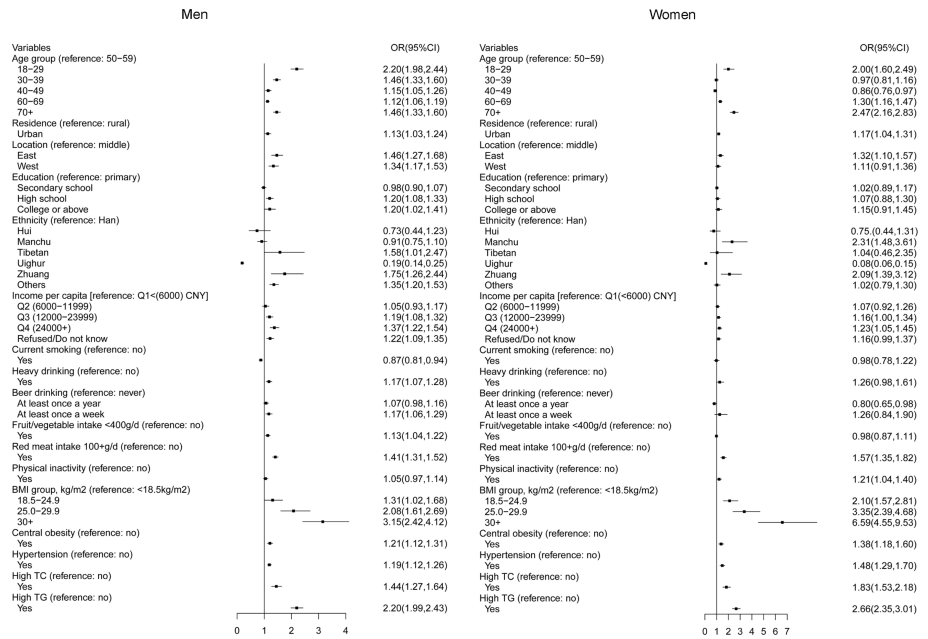

FIGURE 3 | Risk factors associated with hyperuricemia among adults in mainland China.

sampling method, high participants acceptance rate, and quality control protocol guarantee the reliablitly and comparability of the results over the years. Espeicially, all blood samples were tested for uric acid by standard option process in the central laboratory, which provide us high quality data. Nevertheless, two limitations should be considered when interpreting the study results. First, women and rural people were overly sampled in this study. To control this, all results were weighted by the Chinese population distribution. Second, it was a cross-sectional survey, which hampered the study's ability to determine the causal relationship between risk factors and hyperuricemia development.

In conclusion, from the two large-scale national surveys, we observed an HUA prevalence of 14.0% in the Chinese population (approximately 19.19 million individuals) in 2018–19. The prevalence has been constantly increasing, with the younger generation being affected more. These findings indicate the importance of HUA as a public health problem in China.

DATA AVAILABILITY STATEMENT

The datasets presented in this article are not readily available because individual participant data in our study will not be made available publicly. Requests to access the datasets should be directed to LW, jianceshi@ncncd.chinacdc.cn.

ETHICS STATEMENT

The studies involving human participants were reviewed and approved by the ethical review committee of the Chinese Center for Disease Control and Prevention (China CDC) and the ethical review committee of the National Center for Chronic and Noncommunicable Disease Control and Prevention, China CDC. The patients/participants provided their written informed consent to participate in this study.

AUTHOR CONTRIBUTIONS

LMW, MGZ, JW, and MZ had full access to all the data in the study and take responsibility for the integrity of the data and accuracy of the data analysis. MGZ, LMW, HZ, MZ, and XXZ conceived and designed the study. All authors acquired, or interpreted the data. MZ and XXZ drafted the manuscript. LMW, HZ, and MGZ critically revised the manuscript for intellectual content. MZ statistically analyzed the data. ZZ and XZ verified the underlying data. MZ and LMW obtained funding. JW, MGZ, and LHW provided administrative, technical, or material support. MGZ, HZ, and LMW supervised the study. All authors contributed to the article and approved the submitted version.

FUNDING

The surveillance was funded by the Chinese Central Government (Key Project of Public Health Program). This study was supported by the National Key R&D Program of China (grant numbers 2018YFC1311702 and 2018YFC1311706).

ACKNOWLEDGMENTS

We would like to thank the participants, project staff, and diligent provincial and local staff of the CDCs for their participation and contributions.

SUPPLEMENTARY MATERIAL

The Supplementary Material for this article can be found online at: https://www.frontiersin.org/articles/10.3389/fimmu.2021.791983/full#supplementary-material

REFERENCES

1. Dehlin M, Jacobsson L, Roddy E. Global Epidemiology of Gout: Prevalence, Incidence, Treatment Patterns and Risk Factors. *Nat Rev Rheumatol* (2020) 16(7):380–90. doi: 10.1038/s41584-020-0441-1
2. Choi HK, Mount DB, Reginato AM. Pathogenesis of Gout. *Ann Intern Med* (2005) 143(7):499–516. doi: 10.7326/0003-4819-143-7-200510040-00009
3. Badve SV, Brown F, Hawley CM, Johnson DW, Kanellis J, Rangan GK, et al. Challenges of Conducting a Trial of Uric-Acid-Lowering Therapy in CKD. *Nat Rev Nephrol* (2011) 7(5):295–300. doi: 10.1038/nrneph.2010.186
4. Jalal DI, Chonchol M, Chen W, Targher G. Uric Acid as a Target of Therapy in CKD. *Am J Kidney Dis* (2013) 61(1):134–46. doi: 10.1053/j.ajkd.2012.07.021
5. Puddu PE, Bilancio G, Terradura Vagnarelli O, Lombardi C, Mancini M, Zanchetti A, et al. Serum Uric Acid and Egfr_CKDEPI Differently Predict Long-Term Cardiovascular Events and All Causes of Deaths in a Residential Cohort. *Int J Cardiol* (2014) 171(3):361–7. doi: 10.1016/j.ijcard.2013.12.029
6. Otaki Y, Watanabe T, Konta T, Watanabe M, Asahi K, Yamagata K, et al. Impact of Hyperuricemia on Mortality Related to Aortic Diseases: A 3.8-Year Nationwide Community-Based Cohort Study. *Sci Rep* (2020) 10(1):14281. doi: 10.1038/s41598-020-71301-6
7. Stamp LK, Frampton C, Drake J, Doughty RN, Troughton RW, Richards AM. Associations of Gout and Baseline Serum Urate Level With Cardiovascular Outcomes: Analysis of the Coronary Disease Cohort Study. *Arthritis Rheumatol* (2019) 71(10):1733–8. doi: 10.1002/art.41007
8. Chen PH, Chen YW, Liu WJ, Hsu SW, Chen CH, Lee CL. Approximate Mortality Risks Between Hyperuricemia and Diabetes in the United States. *J Clin Med* (2019) 8(12):2127. doi: 10.3390/jcm8122127
9. Liu H, Zhang XM, Wang YL, Liu BC. Prevalence of Hyperuricemia Among Chinese Adults: A National Cross-Sectional Survey Using Multistage, Stratified Sampling. *J Nephrol* (2014) 27(6):653–8. doi: 10.1007/s40620-014-0082-z
10. Miao Z, Li C, Chen Y, Zhao S, Wang Y, Wang Z, et al. Dietary and Lifestyle Changes Associated With High Prevalence of Hyperuricemia and Gout in the Shandong Coastal Cities of Eastern China. *J Rheumatol* (2008) 35(9):1859–64.
11. Han B, Wang N, Chen Y, Li Q, Zhu C, Chen Y, et al. Prevalence of Hyperuricaemia in an Eastern Chinese Population: A Cross-Sectional Study. *BMJ Open* (2020) 10(5):e035614. doi: 10.1136/bmjopen-2019-035614
12. Li Y, Shen Z, Zhu B, Zhang H, Zhang X, Ding X. Demographic, Regional and Temporal Trends of Hyperuricemia Epidemics in Mainland China From 2000 to 2019: A Systematic Review and Meta-Analysis. *Glob Health Action* (2021) 14(1):1874652. doi: 10.1080/16549716.2021.1874652
13. Liu S, Wu X, Lopez AD, Wang L, Cai Y, Page A, et al. An Integrated National Mortality Surveillance System for Death Registration and Mortality Surveillance, China. *Bull World Health Organ* (2016) 94(1):46–57. doi: 10.2471/BLT.15.153148
14. Zhang M, Wang L, Wu J, Huang Z, Zhang X, Li C, et al. Data Resource Profile: China Chronic Disease and Risk Factor Surveillance (CCDRFS). *Int J Epidemiol* (2021) 15:dyab255. doi: 10.1093/ije/dyab255
15. Chinese Nutrition Society. *The Chinese Dietary Guidelines*. Beijing: People's Medical Publishing House (2016). (in Chinese).
16. World Health Orgnization. *Global Action Plan for the Prevention and Control of Noncommunicable Diseases 2013-2020*. Genva: World Health Orgnization (2013).
17. Liu LS. Writing Group of 2010 Chinese Guidelines for the Management of Hypertension. 2010 Chinese Guidelines for the Management of Hypertension. *Zhonghua Xin Xue Guan Bing Za Zhi* (2011) 39:579–615. (in Chinese).
18. Joint Committee on Revision of guidelines for prevention and treatment of dyslipidemia in Chinese adults. Chinese Guideline for the Management of Dyslipidemia in Adults. *Zhonghua Xin Xue Guan Bing Za Zhi* (2016) 44(10):833–53. (in Chinese). doi: 10.11909/j.issn.1671-5411.2018.01.011
19. American Diabetes Association. Dignosis and Classification of Diabetes Mellitus. *Diabetes Care* (2010) 33(suppl 1):S62–9. doi: 10.2337/dc10-S062
20. National Kidney Foundation. K/DOQI Clinical Practice Guidelines for Chronic Kidney Disease: Evaluation, Classification, and Stratification. *Am J Kidney Dis* (2002) 39(2 Suppl 1):S1–266.
21. Koto R, Nakajima A, Horiuchi H, Yamanaka H. Real-World Treatment of Gout and Asymptomatic Hyperuricemia: A Cross-Sectional Study of Japanese Health Insurance Claims Data. *Mod Rheumatol* (2021) 31(1):261–9. doi: 10.1080/14397595.2020.1784556
22. Chen-Xu M, Yokose C, Rai SK, Pillinger MH, Choi HK. Contemporary Prevalence of Gout and Hyperuricemia in the United States and Decadal Trends: The National Health and Nutrition Examination Survey, 2007-2016. *Arthritis Rheumatol* (2019) 71(6):991–9. doi: 10.1002/art.40807
23. China National Bureau of statistics. *Statistical Communiqué of China on 2018 National Economic and Social Development* (2019). Available at: http://www.stats.gov.cn/tjsj/zxfb/201902/t20190228_1651265.html (Accessed 20 August, 2021).
24. Rhee SY, Kim C, Shin DW, Steinhubl SR. Present and Future of Digital Health in Diabetes and Metabolic Disease. *Diabetes Metab J* (2020) 44(6):819–27. doi: 10.4093/dmj.2020.0088
25. Cho SK, Winkler CA, Lee SJ, Chang Y, Ryu S. The Prevalence of Hyperuricemia Sharply Increases From the Late Menopausal Transition Stage in Middle-Aged Women. *J Clin Med* (2019) 8(3):296. doi: 10.3390/jcm8030296
26. Liu L, Lou S, Xu K, Meng Z, Zhang Q, Song K. Relationship Between Lifestyle Choices and Hyperuricemia in Chinese Men and Women. *Clin Rheumatol* (2013) 32(2):233–9. doi: 10.1007/s10067-012-2108-z
27. Multi-Disciplinary Expert Task Force on Hyperuricemia and Its Related Diseases. Chinese Multi-Disciplinary Consensus on the Diagnosis and Treatment of Hyperuricemia and its Related Diseases. *Chin Med J (Engl)* (2017) 130(20):2473–88. doi: 10.4103/0366-6999.216416
28. FitzGerald JD, Dalbeth N, Mikuls T, Brignardello Petersen R, Guyatt G, Abeles AM, et al. 2020 American College of Rheumatology Guideline for the Management of Gout. *Arthritis Rheumatol* (2020) 72(6):879–95. doi: 10.1002/art.41247
29. Virdis A, Masi S, Casiglia E, Tikhonoff V, Cicero AFG, Ungar A, et al. Identification of the Uric Acid Thresholds Predicting an Increased Total and Cardiovascular Mortality Over 20 Years. *Hypertension* (2020) 75(2):302–8. doi: 10.1161/HYPERTENSIONAHA.119.13643
30. Ebrahimpour-Koujan S, Saneei P, Larijani B, Esmaillzadeh A. Consumption of Sugar Sweetened Beverages and Dietary Fructose in Relation to Risk of Gout and Hyperuricemia: A Systematic Review and Meta-Analysis. *Crit Rev Food Sci Nutr* (2020) 60(1):1–10. doi: 10.1080/10408398.2018.1503155
31. Kono S, Shinchi K, Imanishi K, Honjo S, Todoroki I. Behavioural and Biological Correlates of Serum Uric Acid: A Study of Self-Defence Officials in Japan. *Int J Epidemiol* (1994) 23(3):517–22. doi: 10.1093/ije/23.3.517
32. Nakanishi N, Tatara K, Nakamura K, Suzuki K. Risk Factors for the Incidence of Hyperuricaemia: A 6-Year Longitudinal Study of Middle-Aged Japanese Men. *Int J Epidemiol* (1999) 28(5):888–93. doi: 10.1093/ije/28.5.888
33. Chiang KM, Tsay YC, Vincent Ng TC, Yang HC, Huang YT, Chen CH, et al. Is Hyperuricemia, an Early-Onset Metabolic Disorder, Causally Associated With Cardiovascular Disease Events in Han Chinese? *J Clin Med* (2019) 8(8):1202. doi: 10.3390/jcm8081202
34. Song Y, Zhang X, Zhang H, Yang Q, Zhang S, Zhang Y, et al. Prevalence of Diabetes and Prediabetes in Adults From a Third-Tier City in Eastern China: A Cross-Sectional Study. *Diabetes Ther* (2019) 10(4):1473–85. doi: 10.1007/s13300-019-0655-x
35. Liu J, Zhao D, Liu Q, Liu J, Sun J, Smith SC Jr, et al. Prevalence, Awareness, and Treatment of Hypercholesterolemia Among Inpatients With Acute

Coronary Syndrome in China. *Zhonghua Xin Xue Guan Bing Za Zhi* (2009) 37 (5):449–53. doi: 10.3760/cma.j.issn.0253-3758.2009.05.017
36. China National Bureau of statistics. *Statistical Communiqué of China on 2018 National Economic* (2019). Available at: http://www.stats.gov.cn/tjsj/zxfb/201911/t20191119_1710340.html (Accessed 20 August, 2021). Available from.
37. Liu F, Du GL, Song N, Ma YT, Li XM, Gao XM, et al. Hyperuricemia and its Association With Adiposity and Dyslipidemia in Northwest China: Results From Cardiovascular Risk Survey in Xinjiang (CRS 2008-2012). *Lipids Health Dis* (2020) 19(1):58. doi: 10.1186/s12944-020-01211-z

Conflict of Interest: The authors declare that the research was conducted in the absence of any commercial or financial relationships that could be construed as a potential conflict of interest.

Publisher's Note: All claims expressed in this article are solely those of the authors and do not necessarily represent those of their affiliated organizations, or those of the publisher, the editors and the reviewers. Any product that may be evaluated in this article, or claim that may be made by its manufacturer, is not guaranteed or endorsed by the publisher.

frontiers in Immunology

MINI REVIEW
published: 24 February 2022
doi: 10.3389/fimmu.2022.845684

The Role of the Intestine in the Development of Hyperuricemia

Hui Yin[1,2†], *Na Liu*[1,2†] *and Jie Chen*[1,2*]

[1] Department of Rheumatology and Clinical Immunology, Jiangxi Provincial People's Hospital, The First Hospital of Nanchang Medical College, Nanchang, China, [2] Department of Rheumatology and Clinical Immunology, Jiangxi Provincial People's Hospital Affiliated to Nanchang University, Nanchang, China

Gout is a common inflammatory arthritis caused by the deposition of sodium urate crystals in the joints. Hyperuricemia is the fundamental factor of gout. The onset of hyperuricemia is related to purine metabolism disorders or uric acid excretion disorders. Current studies have shown that the intestine is an important potential organ for the excretion of uric acid outside the kidneys. The excretion of uric acid of gut is mainly achieved through the action of uric acid transporters and the catabolism of intestinal flora, which plays an important role in the body's uric acid balance. Here we reviewed the effects of intestinal uric acid transporters and intestinal flora on uric acid excretion, and provide new ideas for the treatment of hyperuricemia and gout.

Keywords: gout, hyperuricemia, ABCG2, SLC2A9, intestinal flora

OPEN ACCESS

Edited by:
Xiaoxia Zhu,
Fudan University, China

Reviewed by:
Zhu Chen,
University of Science and Technology of China, China
Jinhui Tao,
University of Science and Technology of China, China

***Correspondence:**
Jie Chen
jiechen86213@163.com

†These authors have contributed equally in this work

Specialty section:
This article was submitted to Autoimmune and Autoinflammatory Disorders, a section of the journal Frontiers in Immunology

Received: *30 December 2021*
Accepted: *31 January 2022*
Published: *24 February 2022*

Citation:
Yin H, Liu N and Chen J (2022) The Role of the Intestine in the Development of Hyperuricemia. Front. Immunol. 13:845684. doi: 10.3389/fimmu.2022.845684

INTRODUCTION

Gouty arthritis is an inflammatory disease caused by the deposition of sodium urate crystals in and around the joints caused by long-term hyperuricemia (1). Uric acid is the final product of human purine metabolism. Uric acid in the human body maintains a dynamic balance under the action of the liver, kidneys and intestines. When the balance is lost, the serum uric acid level will increase (2). Hyperuricemia (>6.8mg/dL) is the main cause of gout and a risk factor for cardiovascular disease, kidney disease, metabolic syndrome and other diseases (3–6). Under physiological conditions, two thirds of uric acid is excreted from the kidneys and one third is excreted through the intestines (7). Hyperuricemia was divided into overproduction of uric acid and insufficient excretion (8, 9). In recent years, the hypothesis of "kidney overload" is increasingly recognized, suggesting that the types of hyperuricemia should be changed to renal excretion disorders and renal overload types, which including insufficient extrarenal excretion and excessive uric acid production (10). The extrarenal excretion of uric acid is mainly achieved through the intestinal tract. The current uric acid lowering drugs mainly include three categories: inhibiting the production of uric acid, promoting the dissolution of uric acid, and promoting the excretion of uric acid in the kidneys (11). Several drugs can inhibit the production of uric acid, such as allopurinol, febuxostat, and topiroxostat. Allopurinol reduces the synthesis of uric acid by inhibiting xanthine oxidase. However, allopurinol hypersensitivity syndrome (AHS), in which allopurinol has a fatal risk, warrants attention, and the incidence of AHS is higher in Asians, especially Han people (12). As a non-purine xanthine oxidase inhibitor, febuxostat is better than allopurinol in inhibiting the production of uric acid. However, it has been reported that febuxostat can increase the mortality of cardiovascular events in patients with gout. Other adverse reactions include muscle pain, elevated liver enzymes, etc. (11, 13).

Recombinant uricase that promote the dissolution of uric acid, such as rasburicase, pegloticase, and pegloticase have a higher probability of infusion-related reactions such as rash, headache, and dyspnea (14, 15). Benzbromarone, probenecid, and lesinurad can promote the excretion of uric acid in the kidney. Benzbromarone inhibits the reabsorption of uric acid in the renal tubules to achieve the purpose of lowering uric acid, which can lead to the formation of uric acid kidney stones and liver toxicity (16). Probenecid and lesinurad reduces uric acid reabsorption by inhibiting the activity of renal uric acid transporter, but adverse reactions may occur in various systems (17). A clinical trial has shown that lesinurad monotherapy treats increased serum creatinine and the occurrence of renal-related adverse events (18). At present, the target of drugs for promoting uric acid excretion is mainly concentrated in the kidneys, which will increase the burden on the kidneys, especially for patients with chronic kidney disease. As the largest organ of the human body, the intestine has a huge potential for uric acid excretion, and it is hoped that it will become a safer and more effective target organ for lowering uric acid drugs. This article reviews the metabolic pathways of uric acid in the intestines and the possible therapeutic targets derived therefrom.

METABOLIC PATHWAY OF URIC ACID

Uric acid is mainly synthesized in the liver, and a small amount is produced in the small intestine. It is the final product of human purine metabolism. Purine nucleotides generate adenosine, inosine and guanosine under the action of adenosine deaminase, adenosine is deaminated to form inosine, and inosine and guanosine are further converted into hypoxanthine and guanine, hypoxanthine Purine forms xanthine under the action of xanthine oxidase, and guanine deaminates to form xanthine. Xanthine is oxidized again by xanthine oxidase and finally produces uric acid (**Figure 1**) (19, 20). In most mammals, uricase can oxidatively degrade uric acid into the soluble compound allantoin. In the process of human evolution, the gene encoding uricase has undergone inactivation mutations, resulting in a lack of uricase (21). It has been shown that two-thirds of the uric acid in the human body is excreted from the kidneys, one-third is excreted from the intestines and bile, and the proportion of uric acid excreted by bile is very small. The kidney regulates the excretion of uric acid through the reabsorption and secretion of proximal tubules, and this process is mainly achieved through uric acid transporters (22, 23). Uric acid transporter dysfunction plays an important role in the pathogenesis of hyperuricemia. Genome-wide association studies (GWAS) found that many genes related to hyperuricemia and gout. The genes encoding proteins referred to as uric acid transporter (24, 25), including URAT1, OAT4 and SLC2A9 that mediate the reabsorption of uric acid, and transporters such as ABCG2, OAT1, OAT2, OAT3, and MRP4 that mediate the secretion of uric acid (**Figure 2**) (26).

THE EFFECT OF INTESTINAL URIC ACID TRANSPORTERS ON LEVEL OF URIC ACID

The blood uric acid concentration is related to a variety of transporter-encoding genes. Among them, the uric acid transporter in intestinal epithelial cells transports uric acid from the blood to the intestinal lumen, which involves the participation of multiple transporters, mainly ABCG2 and SLC2A9 (27).

ABCG2

ABCG2, also known as breast cancer resistance protein (BCRP), containing 1 transmembrane domain and 1 ATP binding domain. ABCG2 gene is located at the gout susceptibility site of chromosome 4q (28), and expressed on the apical membrane of cells in various tissues such as the intestine, liver and kidneys

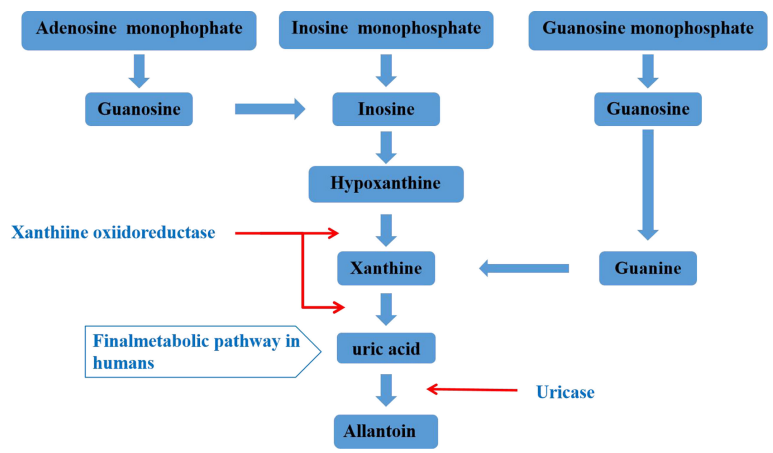

FIGURE 1 | Metabolism of uric acid.

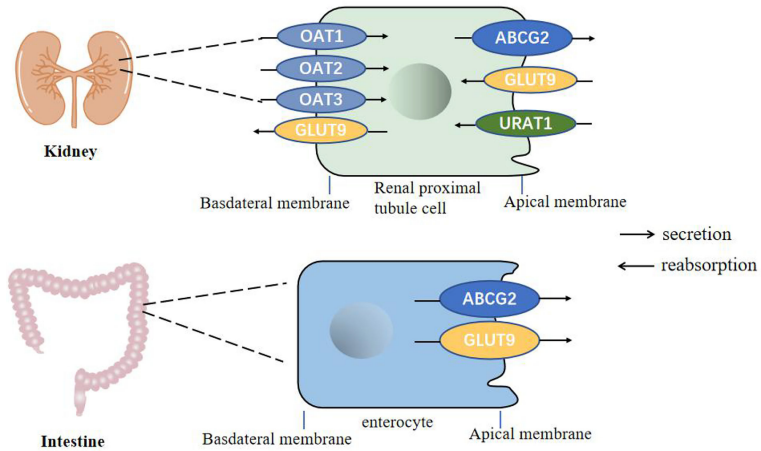

FIGURE 2 | Urate transporters in the kidneys and intestine in humans. GLUT9 and URAT1 on the proximal tubule cells mediate renal urate reabsorption, while GLUT9 on the enterocytes mediate urate excretion in the intestine. ABCG2 is involved in urate export in both the intestine and the kidney. OAT1, OAT2 and OAT3 are present on the basolateral membrane of renal proximal tubule cells and mediates urate secretion.

(29, 30). ABCG2 is a high-volume uric acid transporter. More and more studies have found that ABCG2 plays an important role in intestinal uric acid excretion and the pathogenesis of hyperuricemia. The dysfunction of ABCG2 reduces the excretion of uric acid in the intestinal tract, resulting in increased blood uric acid levels.

Dehghan et al. first proposed the correlation between the ABCG2 gene and uric acid level and gout (31). It has been found that the uric acid content was significantly reduced by 75.5% in ABCG2 expressed oocytes when compared with the control (32). Consistently, the serum uric acid level is increased in ABCG2 gene knockout mice in a established a hyperuricemia mouse model by using the urinase inhibitor potassium oxonate. Interestingly, the intestinal uric acid clearance rate is significantly reduced, while the renal uric acid excretion compensatoryly increases (10). To explore the distribution of uric acid in the body, a mouse model of hyperuricemia with 14 C-labeled uric acid was established. The results showed that the expression of uric acid in the intestine was second only to that in the kidney, and ABCG2 transporter inhibitor elacridar can significantly reduce the clearance rate of uric acid in the intestine (33). The above data show that inhibiting ABCG2 expression can reduce the excretion of uric acid in the intestine, confirming that intestinal ABCG2 dysfunction is one of the pathogenesis of hyperuricemia.

The expression of ABCG2 is regulated by a variety of transcription factors and hormones, and the mechanism is still unclear. Previous study has shown that toll-like recepter 4 (TLR4)-NLRP3(NOD-,LRRand pyrin domain-containing 3) inflammasome and phosphatidylinositol 3-kinase protein kinase B (PI3K/Akt) signaling pathway up-regulates the expression of ABCG2 through PDZK1 on the HT-29 and Caco-2 cells membrane (34, 35). Consistently, ABCG2 gene mutation has the greatest impact on human serum uric acid levels through affecting its protein expression level and uric acid transport efficiency. Q141K and Q126K are the two variants of ABCG2 that cause hyperuricemia (36). The Q141K variant causes a 54% reduction in ABCG2 uric acid excretion, and the latter almost loses its transport function (37). Targeted drugs for ABCG2 mutations have been reported, Woodward et al. found histone deacetylase (HDAC) inhibitor, namely 4-phenylbutyric acid, can correct the conformation of 141K ABCG2 mutant protein and restore its function (38). Uric acid-lowering drugs for ABCG2 dysfunction are expected to become a new treatment direction.

SLC2A9

The SLC2A9 gene is located on human chromosome 4p and encodes glucose transporter 9 (GULT9), which is expressed in the liver, kidney, small intestine and chondrocytes. A large number of studies have found that SLC2A9 has a strong correlation with uric acid levels (39). SLC2A9 is a voltage-dependent high-volume uric acid transporter, which is involved in the reabsorption of uric acid (40, 41). The genetic variation of the SLC2A9 locus is quite complex. Many other SNPs that are closely related to gout, such as rs4447863, rs737267, rs13129697, rs6449213, rs1014290, rs6449213, rs737267, and rs16890979 (31, 39). A meta-analysis showed that rs3733591 may be a protective SNP in the Caucasian population, while it is a cause for the Asian population (42). Therefore, SLC2A9 mutations may mediate the onset of gout and can become a target for the treatment of gout.

It has shown that SLC2A9 is abundantly expressed in intestinal epithelial cells, especially jejunum and ileum, and is mainly located on the top and basolateral membrane of intestinal epithelial cells, which suggests that SLC2A9 may also mediate the excretion of uric acid from the intestine. Actually, the intestinal cell-specific SLC2A9 gene knock-out mice had elevated serum urate levels, and the mice lacking the SLC2A9 gene were prone to metabolic syndrome (high uric acid, hypertension, hyperglycemia, hyperlipidemia), indicating that SLC2A9 mediates the excretion

of uric acid from the intestine (43). However, the mechanism of uric acid metabolism mediated by SLC2A9 in the intestinal tract needs to be further studied.

Studies have shown that the expression of nuclear factor receptor HNF4α can up-regulate the expression of SLC2A9 (44). Peroxisome proliferator-activated receptor PPARγ is a ligand-regulated transcription factor that participates in various pathophysiological processes, including metabolism, inflammation, and tumorigenesis (45). It was also found that the activation of PPARγ can induce the expression of SLC2A9 in the ileum and jejunum. However, the specific regulation mechanism of SLC2A9 in intestinal uric acid excretion needs further study.

Other Intestinal Uric Acid Transporters

In addition, other intestinal uric acid transporters are also involved in the regulation of serum uric acid levels. A Meta-analysis pointed out that SLC16A9 is related to human serum uric acid concentration (46). It was found that the common rs2242206 mutation of SLC16A9 increased the risk of renal non-low excretion overload hyperuricemia, suggesting that SLC16A9 plays a role in intestinal uric acid excretion (47). Besides, SLC17A4 protein exists in the apical membrane of small intestinal epithelial cells and transports various organic anions including urate, confirming that SLC17A4 is related to serum uric acid levels (48).

THE INFLUENCE OF INTESTINAL FLORA ON URIC ACID AND GOUT

Intestinal microbes are composed of various microorganisms such as bacteria, fungi and viruses in the intestine. At least 100 trillion bacteria in the intestinal microecosystem live in the human intestines. They participate in host metabolism, immune regulation, and maintenance of internal environment homeostasis, etc. (49–51). Increasing evidences show that there are differences in the distribution of intestinal flora between gout patients and healthy people (52, 53). Studies have found that supplementing probiotics can improve uric acid levels. It is promising that probiotics may become a new direction for the treatment of gout and hyperuricemia (54–57). Current research suggests that the impact of intestinal flora on gout is mainly achieved through the following three aspects: participation in purine metabolism and decomposition of uric acid to reduce uric acid levels; metabolites produced by intestinal flora promote the excretion of uric acid (**Figure 3**); participation in immune-inflammatory regulation of gout.

Intestinal Flora Is Involved in the Catabolism of Uric Acid

It has been shown that intestinal bacteria can decompose uric acid (58). In addition to the intestinal flora participating in the biosynthesis of various substances including essential amino acids, some symbiotic bacteria in the intestine, such as lactobacillus and pseudomonas, which can express uricase, allantoicase, and allantoinase participating in the breakdown of uric acid (59, 60). Under the action of the flora, the uric acid in the intestines eventually produces oxalate and glycine, which provide carbon and nitrogen to the body (61, 62). Lactic acid bacteria isolated from sauerkraut exert the ability to degrade inosine and guanosine, the two key intermediates of purine metabolism. In addition, gavage of specific strains could effectively reduce the serum uric acid level in hyperuricemia rats (63).

Metabolites of the Intestinal Flora Promote the Excretion of Uric Acid

The intestinal flora can produce some small molecular metabolites that affect host metabolisms, such as short-chain fatty acids (SCFAs), taurine, succinic acid, lipopolysaccharide, acetic acid, butyric acid, and propionic acid (64, 65). It has shown that the types and numbers of the intestinal flora of gout patients and healthy people are significantly different through the 16S rRNA sequencing (66). Further study showed that butyrate-producing bacteria in gout patients decreased by metagenomic analysis, indicating that butyrate may promote intestinal uric acid excretion (67). Besides, a study also showed that the content

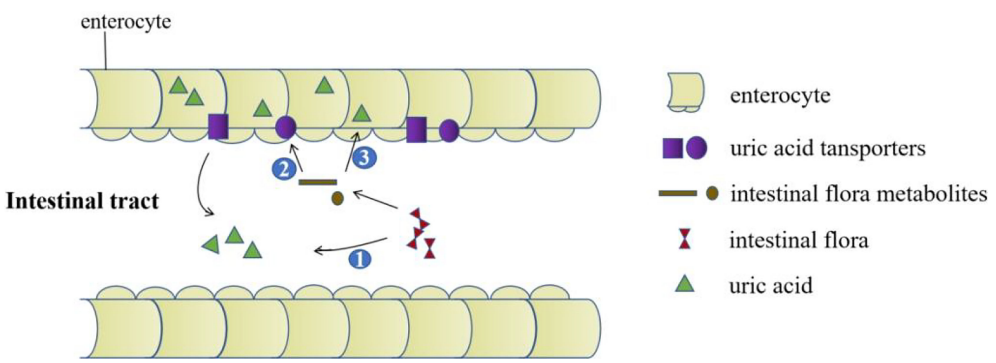

FIGURE 3 | The role of the intestinal tract in uric acid excretion. The intestinal flora decomposes the uric acid directly. Intestinal flora metabolites upregulate the expression of uric acid transporters. Metabolites produced by intestinal flora promote the excretion of uric acid by providing energy for intestinal epithelial cells.

of glucose, acetic acid, butyric acid in the stool of patients with gout is different from that of the control group (53), and these metabolites are involved in energy metabolism (68, 69), which can provide energy for intestinal epithelial cells and participate in the excretion of uric acid.

Regulation of Gut Microbiota Metabolites in the Gout Inflammation

As a metabolite of intestinal flora, SCFAs can regulate the function of intestinal epithelial cells, alleviate inflammation and maintain intestinal mucosa homeostasis (70). Previous study showed that the intake of dietary fiber will increase SCFAs and regulate related immune responses (71). Interestingly, high-fiber dietary feeding alleviates the inflammatory response induced by monosodium urate (MSU) through SCFAs production (72). Consistently, a clinical research observation also found that increasing intake of dietary fiber can reduce the symptoms of gout (73). It is currently believed that SCFAs mainly exert their biological effects through the activation of G-protein-coupled receptors (GPCRs) GPR41, GPR43, and GPR109α in intestinal epithelial cells (74, 75). Another intestinal metabolite butyrate also exerts anti-inflammatory effect through GPR43 and GPR109α on macrophages (76, 77). In addition, as an HDAC inhibitor, butyrate can inhibit the acetylation of a variety of proteins in the NF-κB signaling pathway family, thereby reducing IL-1β, IL-2, IL-6, TNFα, and other pro-inflammatory factor releases (78, 79). Furthermore, Angélica et al. found that acetic acid induces caspase-dependent neutrophil apoptosis by inhibiting the NF-κB pathway and promotes the production of IL-10, TGF-β, and annexin A1 to alleviate the inflammatory response (72). These studies suggest that intestinal products also play an important role in the regulation of gout inflammation resulted from the macrophage and neutrophil activation.

CROSSTALK BETWEEN INTESTINE FLORA AND URIC ACID TRANSPORTERS

It has shown that intestinal flora has a regulatory effect on expression of uric acid transporters. Anserine, a natural carnosine derivative, shows an anti-hyperuricaemic effect, which was closely associated with an increasing abundance of clostridium and lactobacillus in the gut. Importantly, anserine-mediated regulation of uric acid transporters ABCG2, URAT1, and GLUT9 is dependent on intestinal flora (80). In addition, intestinal ABCG2 expression was significantly suppressed by gingko biloba leaf extract (GLE) administration, which is closely related to decreased populations of proteobacteria and deferribacteres at the phylum level. It is worth noting that GLE treatment did not affect ABCG2 expression, but treatment with the lysates of GLE-treated mouse stool significantly suppressed ABCG2 expression. These findings reveal a role for intestinal flora in regulating ABCG2 expression (81). Not only does the intestinal flora plays an important role in intestinal immune homeostasis, studies have also shown it can regulate uric acid transporters through its metabolites. In SCFAs treated rats, the expression and function of intestinal ABCG2 were increased. Similar results were also observed in mouse primary enterocytes and Caco-2 cells treated with SCFAs (82). These findings showed that microbiota has a regulatory effect on expression of uric acid transporters.

In keeping with *in vitro* and animal studies, data from large-scale metagenome genome-wide association studies (mgGWAS) for the oral microbiome revealed unequivocal human genetic loci associated with the oral microbiome, including uric acid transporter SLC2A9. SLC2A9 showed a strong correlation with species-level clusters belonging to oribacterium and lanchnoanaerobaculum in tongue dorsum samples (83). A previous study reported that oral cavity and stool bacteria overlapped in more than 45% of subjects (84). Interestingly, the tongue dorsum microbiota related gene SLC2A9 was correlated with the abundance of Bifidobacterium animalis in the gut (83). These results demonstrated that gut microbial diversity also has an impact on uric acid transporters.

SUMMARY

Currently uric acid lowering drugs are mainly achieved through the kidneys, while the intestine is the second largest uric acid excretion organ. The decrease in intestinal uric acid excretion will increase the burden on the kidneys. At present, the intestinal excretion of uric acid has been used as a new direction for the treatment of gout and hyperuricemia, which can avoid side effects such as aggravating kidney damage and urinary tract stone formation. In summary, there is a bright prospect for drug and gut microbiota research targeting intestinal uric acid transporters to treat hyperuricemia and gout (**Figure 3**). However, there are scarce studies about the association between intestinal flora and uric acid transporters, and the specific mechanism of the interaction between these need to be further elucidated.

AUTHOR CONTRIBUTIONS

HY, NL, and JC reviewed the literature and wrote the first draft. HY and JC reviewed the literature and finalized the manuscript. All authors have read and approved the final manuscript.

ACKNOWLEDGMENTS

JiangXi Provincial Natural Science Foundation of China (20202ACBL206011), Interdisciplinary Innovation Team, Frontier Science Key Research Project of Jiangxi Provincial People's Hospital (19-008), Long-term (Youth) Project for Leading Innovative Talents in Jiangxi Province for JC (jxsq2019101061), Jiangxi Provincial Clinical Research Center for Rheumatic and Immunologic Diseases (20192BCD42005), Jiangxi Province Medical Leading Discipline Construction Project (Rheumatology), and Provincial and municipal joint construction projects of medical disciplines in Jiangxi Province (Rheumatology).

REFERENCES

1. Richette P, Bardin T. Gout. *Lancet* (2010) 375:318–28. doi: 10.1016/S0140-6736(09)60883-7
2. Maiuolo J, Oppedisano F, Gratteri S, Muscoli C, Mollace V. Regulation of Uric Acid Metabolism and Excretion. *Int J Cardiol* (2016) 213:8–14. doi: 10.1016/j.ijcard.2015.08.109
3. Dalbeth N, Merriman TR, Stamp LK. Gout. *Lancet* (2016) 388:2039–52. doi: 10.1016/S0140-6736(16)00346-9
4. Lv S, Liu W, Zhou Y, Liu Y, Shi D, Zhao Y, et al. Hyperuricemia and Severity of Coronary Artery Disease: An Observational Study in Adults 35 Years of Age and Younger With Acute Coronary Syndrome. *Cardiol J* (2019) 26:275–82. doi: 10.5603/CJ.a2018.0022
5. Chang CC, Wu CH, Liu LK, Chou RH, Kuo CS, Huang PH, et al. Association Between Serum Uric Acid and Cardiovascular Risk in Nonhypertensive and Nondiabetic Individuals: The Taiwan I-Lan Longitudinal Aging Study. *Sci Rep* (2018) 8:5234. doi: 10.1038/s41598-018-22997-0
6. Stamp LK, Chapman PT. Gout and Its Comorbidities: Implications for Therapy. *Rheumatology* (2013) 52:34–44. doi: 10.1093/rheumatology/kes211
7. Sorensen LB. Role of the Intestinal Tract in the Elimination of Uric Acid. *Arthritis Rheum* (1965) 8:694–706. doi: 10.1002/art.1780080429
8. Boss GR, Seegmiller JE. Hyperuricemia and Gout. Classification, Complications and Management. *N Engl J Med* (1979) 300:1459–68. doi: 10.1056/NEJM197906283002604
9. Yamauchi T, Ueda T. Primary Hyperuricemia Due to Decreased Renal Uric Acid Excretion. *Nihon Rinsho* (2008) 66:679–81.
10. Ichida K, Matsuo H, Takada T, Nakayama A, Murakami K, Shimizu T, et al. Decreased Extra-Renal Urate Excretion Is a Common Cause of Hyperuricemia. *Nat Commun* (2012) 3:764. doi: 10.1038/ncomms1756
11. Strilchuk L, Fogacci F, Cicero AF. Safety and Tolerability of Available Urate-Lowering Drugs: A Critical Review. *Expert Opin Drug Saf* (2019) 18:261–71. doi: 10.1080/14740338.2019.1594771
12. Cao ZH, Wei ZY, Zhu QY, Zhang JY, Yang L, Qin SY, et al. HLA-B*58:01 Allele Is Associated With Augmented Risk for Both Mild and Severe Cutaneous Adverse Reactions Induced by Allopurinol in Han Chinese. *Pharmacogenomics* (2012) 13:1193–201. doi: 10.2217/pgs.12.89
13. White WB, Saag KG, Becker MA, Borer JS, Gorelick PB, Whelton A, et al. Cardiovascular Safety of Febuxostat or Allopurinol in Patients With Gout. *N Engl J Med* (2018) 378:1200–10. doi: 10.1056/NEJMoa1710895
14. Becker MA, Baraf HS, Yood RA, Dillon A, Vazquez-Mellado J, Ottery FD, et al. Long-Term Safety of Pegloticase in Chronic Gout Refractory to Conventional Treatment. *Ann Rheum Dis* (2013) 72:1469–74. doi: 10.1136/annrheumdis-2012-201795
15. Pui CH. Rasburicase: A Potent Uricolytic Agent. *Expert Opin Pharmacother* (2002) 3:433–42. doi: 10.1517/14656566.3.4.433
16. Tausche AK, Jansen TL, Schroder HE, Bornstein SR, Aringer M, Muller-Ladner U. Gout–current Diagnosis and Treatment. *Dtsch Arztebl Int* (2009) 106:549–55. doi: 10.3238/arztebl.2009.0549
17. Boger WP, Strickland SC. Probenecid (Benemid); Its Uses and Side-Effects in 2,502 Patients. *AMA Arch Intern Med* (1955) 95:83–92. doi: 10.1001/archinte.1955.00250070099012
18. Tausche A-K, Alten R, Dalbeth N, Kopicko J, Fung M, Adler S, et al. Lesinurad Monotherapy in Gout Patients Intolerant to a Xanthine Oxidase Inhibitor: A 6 Month Phase 3 Clinical Trial and Extension Study. *Rheumatology* (2017) 56:2170–8. doi: 10.1093/rheumatology/kex350
19. Alvarez-Lario B, Macarron-Vicente J. Uric Acid and Evolution. *Rheumatol (Oxford)* (2010) 49:2010–5. doi: 10.1093/rheumatology/keq204
20. Keenan RT. The Biology of Urate. *Semin Arthritis Rheum* (2020) 50:S2–S10. doi: 10.1016/j.semarthrit.2020.04.007
21. Wu XW, Lee CC, Muzny DM, Caskey CT. Urate Oxidase: Primary Structure and Evolutionary Implications. *Proc Natl Acad Sci USA* (1989) 86:9412–6. doi: 10.1073/pnas.86.23.9412
22. Lipkowitz MS. Regulation of Uric Acid Excretion by the Kidney. *Curr Rheumatol Rep* (2012) 14:179–88. doi: 10.1007/s11926-012-0240-z
23. Fathallah-Shaykh SA, Cramer MT. Uric Acid and the Kidney. *Pediatr Nephrol* (2014) 29:999–1008. doi: 10.1007/s00467-013-2549-x
24. Li C, Li Z, Liu S, Wang C, Han L, Cui L, et al. Genome-Wide Association Analysis Identifies Three New Risk Loci for Gout Arthritis in Han Chinese. *Nat Commun* (2015) 6:7041. doi: 10.1038/ncomms8041
25. Kottgen A, Albrecht E, Teumer A, Vitart V, Krumsiek J, Hundertmark C, et al. Genome-Wide Association Analyses Identify 18 New Loci Associated With Serum Urate Concentrations. *Nat Genet* (2013) 45:145–54. doi: 10.1038/ng.2500
26. Major TJ, Dalbeth N, Stahl EA, Merriman TR. An Update on the Genetics of Hyperuricaemia and Gout. *Nat Rev Rheumatol* (2018) 14:341–53. doi: 10.1038/s41584-018-0004-x
27. Xu X, Li C, Zhou P, Jiang T. Uric Acid Transporters Hiding in the Intestine. *Pharm Biol* (2016) 54:3151–5. doi: 10.1080/13880209.2016.1195847
28. Matsuo H, Takada T, Ichida K, Nakamura T, Nakayama A, Ikebuchi Y, et al. Common Defects of ABCG2, a High-Capacity Urate Exporter, Cause Gout: A Function-Based Genetic Analysis in a Japanese Population. *Sci Transl Med* (2009) 1:5ra11. doi: 10.1126/scitranslmed.3000237
29. Huls M, Brown CDA, Windass AS, Sayer R, van den Heuvel JJMW, Heemskerk S, et al. The Breast Cancer Resistance Protein Transporter ABCG2 Is Expressed in the Human Kidney Proximal Tubule Apical Membrane. *Kidney Int* (2008) 73:220–5. doi: 10.1038/sj.ki.5002645
30. Maliepaard M, Scheffer GL, Faneyte IF, van Gastelen MA, Pijnenborg A, Schinkel AH, et al. Subcellular Localization and Distribution of the Breast Cancer Resistance Protein Transporter in Normal Human Tissues. *Cancer Res* (2001) 61:3458–64.
31. Dehghan A, Köttgen A, Yang Q, Hwang S-J, Kao WHL, Rivadeneira F, et al. Association of Three Genetic Loci With Uric Acid Concentration and Risk of Gout: A Genome-Wide Association Study. *Lancet* (2008) 372:1953–61. doi: 10.1016/S0140-6736(08)61343-4
32. Woodward OM, Kottgen A, Coresh J, Boerwinkle E, Guggino WB, Kottgen M. Identification of a Urate Transporter, ABCG2, With a Common Functional Polymorphism Causing Gout. *Proc Natl Acad Sci USA* (2009) 106:10338–42. doi: 10.1073/pnas.0901249106
33. Hosomi A, Nakanishi T, Fujita T, Tamai I. Extra-Renal Elimination of Uric Acid *via* Intestinal Efflux Transporter BCRP/Abcg2. *PloS One* (2012) 7:e30456. doi: 10.1371/journal.pone.0030456
34. Chen M, Lu X, Lu C, Shen N, Jiang Y, Chen M, et al. Soluble Uric Acid Increases PDZK1 and ABCG2 Expression in Human Intestinal Cell Lines *via* the TLR4-NLRP3 Inflammasome and PI3K/Akt Signaling Pathway. *Arthritis Res Ther* (2018) 20:20. doi: 10.1186/s13075-018-1512-4
35. Shimizu T, Sugiura T, Wakayama T, Kijima A, Nakamichi N, Iseki S, et al. PDZK1 Regulates Breast Cancer Resistance Protein in Small Intestine. *Drug Metab Dispos* (2011) 39:2148–54. doi: 10.1124/dmd.111.040295
36. Kondo C, Suzuki H, Itoda M, Ozawa S, Sawada J, Kobayashi D, et al. Functional Analysis of SNPs Variants of BCRP/Abcg2. *Pharm Res* (2004) 21:1895–903. doi: 10.1023/B:PHAM.0000045245.21637.d4
37. Nakamura M, Fujita K, Toyoda Y, Takada T, Hasegawa H, Ichida K. Investigation of the Transport of Xanthine Dehydrogenase Inhibitors by the Urate Transporter ABCG2. *Drug Metab Pharmacokinet* (2018) 33:77–81. doi: 10.1016/j.dmpk.2017.11.002
38. Woodward OM, Tukaye DN, Cui J, Greenwell P, Constantoulakis LM, Parker BS, et al. Gout-Causing Q141K Mutation in ABCG2 Leads to Instability of the Nucleotide-Binding Domain and can be Corrected With Small Molecules. *Proc Natl Acad Sci USA* (2013) 110:5223–8. doi: 10.1073/pnas.1214530110
39. Vitart V, Rudan I, Hayward C, Gray NK, Floyd J, Palmer CN, et al. SLC2A9 Is a Newly Identified Urate Transporter Influencing Serum Urate Concentration, Urate Excretion and Gout. *Nat Genet* (2008) 40:437–42. doi: 10.1038/ng.106
40. Merriman TR. An Update on the Genetic Architecture of Hyperuricemia and Gout. *Arthritis Res Ther* (2015) 17:98. doi: 10.1186/s13075-015-0609-2
41. Caulfield MJ, Munroe PB, O'Neill D, Witkowska K, Charchar FJ, Doblado M, et al. SLC2A9 Is a High-Capacity Urate Transporter in Humans. *PloS Med* (2008) 5:e197. doi: 10.1371/journal.pmed.0050197
42. Zhang X, Yang X, Wang M, Li X, Xia Q, Xu S, et al. Association Between SLC2A9 (GLUT9) Gene Polymorphisms and Gout Susceptibility: An Updated Meta-Analysis. *Rheumatol Int* (2016) 36:1157–65. doi: 10.1007/s00296-016-3503-6
43. DeBosch BJ, Kluth O, Fujiwara H, Schurmann A, Moley K. Early-Onset Metabolic Syndrome in Mice Lacking the Intestinal Uric Acid Transporter SLC2A9. *Nat Commun* (2014) 5:4642. doi: 10.1038/ncomms5642
44. Prestin K, Wolf S, Feldtmann R, Hussner J, Geissler I, Rimmbach C, et al. Transcriptional Regulation of Urate Transportosome Member SLC2A9 by

Nuclear Receptor HNF4alpha. *Am J Physiol Renal Physiol* (2014) 307:F1041–51. doi: 10.1152/ajprenal.00640.2013
45. Berger J, Moller DE. The Mechanisms of Action of PPARs. *Annu Rev Med* (2002) 53:409–35. doi: 10.1146/annurev.med.53.082901.104018
46. Phipps-Green AJ, Merriman ME, Topless R, Altaf S, Montgomery GW, Franklin C, et al. Twenty-Eight Loci That Influence Serum Urate Levels: Analysis of Association With Gout. *Ann Rheum Dis* (2016) 75:124–30. doi: 10.1136/annrheumdis-2014-205877
47. Nakayama A, Matsuo H, Shimizu T, Ogata H, Takada Y, Nakashima H, et al. A Common Missense Variant of Monocarboxylate Transporter 9 (MCT9/SLC16A9) Gene Is Associated With Renal Overload Gout, But Not With All Gout Susceptibility. *Hum Cell* (2013) 26:133–6. doi: 10.1007/s13577-013-0073-8
48. Togawa N, Miyaji T, Izawa S, Omote H, Moriyama Y. A Na+-Phosphate Cotransporter Homologue (SLC17A4 Protein) Is an Intestinal Organic Anion Exporter. *Am J Physiol Cell Physiol* (2012) 302:C1652–60. doi: 10.1152/ajpcell.00015.2012
49. H.M.P.R.N.C. Integrative. The Integrative Human Microbiome Project. *Nature* (2019) 569:641–8. doi: 10.1038/s41586-019-1238-8
50. Hall JA, Bouladoux N, Sun CM, Wohlfert EA, Blank RB, Zhu Q, et al. Commensal DNA Limits Regulatory T Cell Conversion and Is a Natural Adjuvant of Intestinal Immune Responses. *Immunity* (2008) 29:637–49. doi: 10.1016/j.immuni.2008.08.009
51. Pickard JM, Zeng MY, Caruso R, Nunez G. Gut Microbiota: Role in Pathogen Colonization, Immune Responses, and Inflammatory Disease. *Immunol Rev* (2017) 279:70–89. doi: 10.1111/imr.12567
52. Xing SC, Meng DM, Chen Y, Jiang G, Liu XS, Li N, et al. Study on the Diversity of Bacteroides and Clostridium in Patients With Primary Gout. *Cell Biochem Biophys* (2015) 71:707–15. doi: 10.1007/s12013-014-0253-5
53. Shao T, Shao L, Li H, Xie Z, He Z, Wen C. Combined Signature of the Fecal Microbiome and Metabolome in Patients With Gout. *Front Microbiol* (2017) 8:268. doi: 10.3389/fmicb.2017.00268
54. Szulinska M, Loniewski I, van Hemert S, Sobieska M, Bogdanski P. Dose-Dependent Effects of Multispecies Probiotic Supplementation on the Lipopolysaccharide (LPS) Level and Cardiometabolic Profile in Obese Postmenopausal Women: A 12-Week Randomized Clinical Trial. *Nutrients* (2018) 10:773–85. doi: 10.3390/nu10060773
55. Wang J, Chen Y, Zhong H, Chen F, Regenstein J, Hu X, et al. The Gut Microbiota as a Target to Control Hyperuricemia Pathogenesis: Potential Mechanisms and Therapeutic Strategies. *Crit Rev Food Sci Nutr* (2021) 22:1–11. doi: 10.1080/10408398.2021.1874287
56. García-Arroyo FE, Gonzaga G, Muñoz-Jiménez I, Blas-Marron MG, Silverio O, Tapia E, et al. Probiotic Supplements Prevented Oxonic Acid-Induced Hyperuricemia and Renal Damage. *PloS One* (2018) 13:e0202901. doi: 10.1371/journal.pone.0202901
57. Lin X, Shao T, Huang L, Wen X, Wang M, Wen C, et al. Simiao Decoction Alleviates Gouty Arthritis by Modulating Proinflammatory Cytokines and the Gut Ecosystem. *Front Pharmacol* (2020) 11:955. doi: 10.3389/fphar.2020.00955
58. Buzard J, Bishop C, Talbott JH. Recovery in Humans of Intravenously Injected Isotopic Uric Acid. *J Biol Chem* (1952) 196:179–84. doi: 10.1016/S0021-9258(18)55717-3
59. Crane JK. Role of Host Xanthine Oxidase in Infection Due to Enteropathogenic and Shiga-Toxigenic Escherichia Coli. *Gut Microbes* (2013) 4:388–91. doi: 10.4161/gmic.25584
60. Yun Y, Yin H, Gao Z, Li Y, Gao T, Duan J, et al. Intestinal Tract Is an Important Organ for Lowering Serum Uric Acid in Rats. *PloS One* (2017) 12:e0190194. doi: 10.1371/journal.pone.0190194
61. Mendez-Salazar EO, Martinez-Nava GA. Uric Acid Extrarenal Excretion: The Gut Microbiome as an Evident Yet Understated Factor in Gout Development. *Rheumatol Int* (2021). doi: 10.1007/s00296-021-05007-x
62. Ramazzina I, Costa R, Cendron L, Berni R, Peracchi A, Zanotti G, et al. An Aminotransferase Branch Point Connects Purine Catabolism to Amino Acid Recycling. *Nat Chem Biol* (2010) 6:801–6. doi: 10.1038/nchembio.445
63. Li M, Yang D, Mei L, Yuan L, Xie A, Yuan J. Screening and Characterization of Purine Nucleoside Degrading Lactic Acid Bacteria Isolated From Chinese Sauerkraut and Evaluation of the Serum Uric Acid Lowering Effect in Hyperuricemic Rats. *PloS One* (2014) 9:e105577. doi: 10.1371/journal.pone.0105577
64. Samuel BS, Shaito A, Motoike T, Rey FE, Backhed F, Manchester JK, et al. Effects of the Gut Microbiota on Host Adiposity Are Modulated by the Short-Chain Fatty-Acid Binding G Protein-Coupled Receptor, Gpr41. *Proc Natl Acad Sci USA* (2008) 105:16767–72. doi: 10.1073/pnas.0808567105
65. Hsu YJ, Chiu CC, Li YP, Huang WC, Huang YT, Huang CC, et al. Effect of Intestinal Microbiota on Exercise Performance in Mice. *J Strength Cond Res* (2015) 29:552–8. doi: 10.1519/JSC.0000000000000644
66. Guo Z, Zhang J, Wang Z, Ang KY, Huang S, Hou Q, et al. Intestinal Microbiota Distinguish Gout Patients From Healthy Humans. *Sci Rep* (2016) 6:20602. doi: 10.1038/srep20602
67. Chu Y, Sun S, Huang Y, Gao Q, Xie X, Wang P, et al. Metagenomic Analysis Revealed the Potential Role of Gut Microbiome in Gout. *NPJ Biofilms Microbiomes* (2021) 7:66. doi: 10.1038/s41522-021-00235-2
68. Nieuwdorp M, Gilijamse PW, Pai N, Kaplan LM. Role of the Microbiome in Energy Regulation and Metabolism. *Gastroenterology* (2014) 146:1525–33. doi: 10.1053/j.gastro.2014.02.008
69. Tremaroli V, Backhed F. Functional Interactions Between the Gut Microbiota and Host Metabolism. *Nature* (2012) 489:242–9. doi: 10.1038/nature11552
70. Macia L, Tan J, Vieira AT, Leach K, Stanley D, Luong S, et al. Metabolite-Sensing Receptors GPR43 and GPR109A Facilitate Dietary Fibre-Induced Gut Homeostasis Through Regulation of the Inflammasome. *Nat Commun* (2015) 6:6734. doi: 10.1038/ncomms7734
71. Kim M, Qie Y, Park J, Kim CH. Gut Microbial Metabolites Fuel Host Antibody Responses. *Cell Host Microbe* (2016) 20:202–14. doi: 10.1016/j.chom.2016.07.001
72. Vieira AT, Galvao I, Macia LM, Sernaglia EM, Vinolo MA, Garcia CC, et al. Dietary Fiber and the Short-Chain Fatty Acid Acetate Promote Resolution of Neutrophilic Inflammation in a Model of Gout in Mice. *J Leukoc Biol* (2017) 101:275–84. doi: 10.1189/jlb.3A1015-453RRR
73. Lyu LC, Hsu CY, Yeh CY, Lee MS, Huang SH, Chen CL. A Case-Control Study of the Association of Diet and Obesity With Gout in Taiwan. *Am J Clin Nutr* (2003) 78:690–701. doi: 10.1093/ajcn/78.4.690
74. Tan J, McKenzie C, Potamitis M, Thorburn AN, Mackay CR, Macia L. The Role of Short-Chain Fatty Acids in Health and Disease. *Adv Immunol* (2014) 121:91–119. doi: 10.1016/B978-0-12-800100-4.00003-9
75. Sun M, Wu W, Liu Z, Cong Y. Microbiota Metabolite Short Chain Fatty Acids, GPCR, and Inflammatory Bowel Diseases. *J Gastroenterol* (2017) 52:1–8. doi: 10.1007/s00535-016-1242-9
76. Furusawa Y, Obata Y, Fukuda S, Endo TA, Nakato G, Takahashi D, et al. Commensal Microbe-Derived Butyrate Induces the Differentiation of Colonic Regulatory T Cells. *Nature* (2013) 504:446–50. doi: 10.1038/nature12721
77. Singh N, Gurav A, Sivaprakasam S, Brady E, Padia R, Shi H, et al. Activation of Gpr109a, Receptor for Niacin and the Commensal Metabolite Butyrate, Suppresses Colonic Inflammation and Carcinogenesis. *Immunity* (2014) 40:128–39. doi: 10.1016/j.immuni.2013.12.007
78. Vinolo MA, Rodrigues HG, Hatanaka E, Sato FT, Sampaio SC, Curi R. Suppressive Effect of Short-Chain Fatty Acids on Production of Proinflammatory Mediators by Neutrophils. *J Nutr Biochem* (2011) 22:849–55. doi: 10.1016/j.jnutbio.2010.07.009
79. Puertollano E, Kolida S, Yaqoob P. Biological Significance of Short-Chain Fatty Acid Metabolism by the Intestinal Microbiome. *Curr Opin Clin Nutr Metab Care* (2014) 17:139–44. doi: 10.1097/MCO.0000000000000025
80. Han J, Wang Z, Lu C, Zhou J, Li Y, Ming T, et al. The Gut Microbiota Mediates the Protective Effects of Anserine Supplementation on Hyperuricaemia and Associated Renal Inflammation. *Food Funct* (2021) 12:9030–42. doi: 10.1039/D1FO01884A
81. Kim JK, Choi MS, Kim JY, Yu JS, Seo JI, Yoo HH, et al. Ginkgo Biloba Leaf Extract Suppresses Intestinal Human Breast Cancer Resistance Protein Expression in Mice: Correlation With Gut Microbiota. *BioMed Pharmacother* (2021) 140:111712. doi: 10.1016/j.biopha.2021.111712
82. Xie QS, Zhang JX, Liu M, Liu PH, Wang ZJ, Zhu L, et al. Short-Chain Fatty Acids Exert Opposite Effects on the Expression and Function of P-Glycoprotein and Breast Cancer Resistance Protein in Rat Intestine. *Acta Pharmacol Sin* (2021) 42:470–81. doi: 10.1038/s41401-020-0402-x

83. Liu X, Tong X, Zhu J, Tian L, Jie Z, Zou Y, et al. Metagenome-Genome-Wide Association Studies Reveal Human Genetic Impact on the Oral Microbiome. *Cell Discov* (2021) 7:117. doi: 10.1038/s41421-021-00356-0
84. Segata N, Haake SK, Mannon P, Lemon KP, Waldron L, Gevers D, et al. Composition of the Adult Digestive Tract Bacterial Microbiome Based on Seven Mouth Surfaces, Tonsils, Throat and Stool Samples. *Genome Biol* (2012) 13:R42. doi: 10.1186/gb-2012-13-6-r42

Conflict of Interest: The authors declare that the research was conducted in the absence of any commercial or financial relationships that could be construed as a potential conflict of interest.

Publisher's Note: All claims expressed in this article are solely those of the authors and do not necessarily represent those of their affiliated organizations, or those of the publisher, the editors and the reviewers. Any product that may be evaluated in this article, or claim that may be made by its manufacturer, is not guaranteed or endorsed by the publisher.

Advantages of publishing in Frontiers

OPEN ACCESS
Articles are free to read for greatest visibility and readership

FAST PUBLICATION
Around 90 days from submission to decision

HIGH QUALITY PEER-REVIEW
Rigorous, collaborative, and constructive peer-review

TRANSPARENT PEER-REVIEW
Editors and reviewers acknowledged by name on published articles

Frontiers
Avenue du Tribunal-Fédéral 34
1005 Lausanne | Switzerland

Visit us: www.frontiersin.org
Contact us: frontiersin.org/about/contact

REPRODUCIBILITY OF RESEARCH
Support open data and methods to enhance research reproducibility

DIGITAL PUBLISHING
Articles designed for optimal readership across devices

FOLLOW US
@frontiersin

IMPACT METRICS
Advanced article metrics track visibility across digital media

EXTENSIVE PROMOTION
Marketing and promotion of impactful research

LOOP RESEARCH NETWORK
Our network increases your article's readership